

LATE HOLOCENE STRATIGRAPHIC HISTORY OF THE
GULF OF AQABA COASTAL PLAIN, JORDAN

A THESIS IN
Environmental and Urban Geosciences

Presented to the Faculty of
the University of Missouri – Kansas City in partial fulfillment
of the requirements for the degree

Master of Science

By

Janet E. Smith

B.S. Geology, University of Missouri – Kansas City, 2015
B.A. Communication, University of Arkansas, 1999

Kansas City, Missouri
2020

© 2020
Janet Smith

ALL RIGHTS RESERVED

LATE HOLOCENE STRATIGRAPHIC HISTORY OF THE
GULF OF AQABA COASTAL PLAIN, JORDAN

Janet E. Smith, Candidate for the Master of Science Degree
University of Missouri-Kansas City, 2020

ABSTRACT

Construction of the lower tidal lagoon at the Ayla Oasis Development in Aqaba, Jordan provided a unique opportunity to study the 3-D architecture of coastal plain sediment of the northern Gulf of Aqaba. Previous studies of sediment cores had identified a mid-Holocene transgression and a late Holocene regression. In this study, one cross-section of buried structures adjacent to the archaeological site of Tel el-Kheleifeh (8th-4th C. BCE) and two stratigraphic columns of 7 m-high outcrops that extended to a depth of 3.2 m below sea level were described and sampled for grain-size, SEM, and radiocarbon age analyses. The base of the section contains subtidal and beach sand and cobble gravel containing abundant shells and coral fragments. Three vertically stacked beachrock layers that developed in the intertidal zone indicate a rising sea level. The uppermost beachrock is found at an elevation of 1.3 m above present sea level and is constrained to be younger than 3.5 ka based on radiocarbon dating of shells. Raised reef, wave-cut notches, and other sea level indicators across the Gulf of Aqaba and northern Red Sea attest to a mid-Holocene highstand. A down-cutting event that eroded the beach sediment and is marked by an irregular unconformity and channels cut to depths below modern sea level. The channels are filled with a blue-gray gravel and sand with abundant rip-up clasts, terrestrial organic material, cross-bedding and convolute bedding which denote high flow velocities and rapid sedimentation. Radiocarbon dating of sediment above the channel constraint its age to before 3.1 ka. As rapid sea level change is not supported by

regional evidence, the erosion and deposition of blue-gray channels are interpreted to represent inundation and drawdown of the sea by a tsunami. Similar erosion and deposition in low-lying areas has been documented in tsunamis in Sumatra, Chili, and the Kuril Islands.

APPROVAL PAGE

The faculty listed below, appointed by the Dean of the College of Arts and Sciences, have examined a thesis titled “Late Holocene Stratigraphic History of the Gulf of Aqaba Coastal Plain, Jordan” presented by Janet Smith, candidate for the Master of Science degree, and certify that in their opinion it is worthy of acceptance.

Supervisory Committee

Tina M. Niemi, Ph.D., Committee Chair
Department of Earth and Environmental Sciences

Alison H. Graettinger, Ph.D.,
Department of Earth and Environmental Sciences

James B. Murowchick, Ph.D.
Department of Earth and Environmental Sciences

TABLE OF CONTENTS

ABSTRACT	iii
LIST OF ILLUSTRATIONS	viii
LIST OF TABLES	ix
ACKNOWLEDGEMENTS	x
CHAPTER	
1. INTRODUCTION	1
2. REGIONAL ENVIRONMENTAL SETTING	8
3. METHODS	14
Fieldwork	14
XRD	16
SEM/EDS	16
Grain Size	16
Radiocarbon	17
4. RESULTS	20
Stratigraphic Sections	20
Facies Model	23
Buried Archaeological Structures	31
Age Control and Elevation	35
5. DISCUSSION	38
Tell el-Kheleifeh	38
Sea Level Highstand	39

Blue-gray Channels.....	43
6. CONCLUSION	46
REFERENCES	47
APPENDIX	
A. SAMPLE METADATA	53
B. WEIGHED GRAIN-SIZE FRACTIONS	58
C. GRAIN-SIZE ANALYSES USING GRADISTAT SOFTWARE	101
D. RADIOCARBON CALIBRATION DATA.....	147
E. XRD, SEM, EDS DATA	156
VITA.....	177

LIST OF ILLUSTRATIONS

Figure 1: Map of the Aqaba, Jordan showing the location of archaeological sites	1
Figure 2: Photographs of the archaeological sites in Aqaba	2
Figure 3: Google Earth image showing location of the Ayla Oasis development site from 2010	5
Figure 4: Dead Sea Transform	8
Figure 5: Geologic map of the Aqaba-Eilat region.....	10
Figure 6: Location of stratigraphic sections described in this study plotted on a 2012 Google Earth image	14
Figure 7: Photographs of the AO-2 section location	15
Figure 8: Stratigraphic Section AO-2	21
Figure 9: Stratigraphic Section AO-3	22
Figure 10: Facies Model	28
Figure 11: Beachrock exposed in the Ayla Oasis outcrop, hand specimens, and thin sections	25
Figure 12: Coral and shell fragments found in the intertidal zone section of AO-2	26
Figure 13: Details of the channel exposed at the AO-2 outcrop	29
Figure 14: Convolute beds and terrestrial organic matter at the AO-3 outcrop.....	30
Figure 15: Photographs of buried walls near Tell el-Kheleifeh exposed in the Ayla Oasis lagoon construction in August 2010	32
Figure 16: Section drawing of the TK-4 buried structure	34
Figure 17: Holocene sea level curve for the Gulf of Aqaba and Northern Red Sea	41

LIST OF TABLES

Table 1: Radiocarbon results from the Ayla Oasis exposures	18
Table 2: Recalibration of the radiocarbon data from the Brückner (1999) study near Tel el-Kheleifeh	19
Table 3: Holocene higher-than-present sea level indicators along the Gulf of Aqaba and northern Red Sea	43

ACKNOWLEDGEMENTS

Thank you to Dr. Tina Niemi, who through her endless patience, words of encouragement, and critique have taught me what it means to become a scientist. Tina's enthusiasm for field work, dedication to supporting literature, and asking questions from every angle has shown me that science isn't necessarily the end result, but rather the pursuit because the answers are always changing based on what is learned in the process of discovery.

Thank you to the members of my committee Dr. James Murowchick, and Dr. Alison Graettinger for their availability and support and assistance in the lab. Thank you as well to Dr. Jejung Lee for his assistance and advice in the classroom. Thank you as well to Megan Medley for her calming and caring communication.

Field research for this project was conducted under an excavation and survey permit granted from the Jordanian Department of Antiquities (DoA) to Dr. Tina Niemi as part of the Wadi 'Arabah Earthquake Project. We thank Dr. Fawwaz al-Khraysheh, past director of the DoA, and Dr. Sawsan Fakhri, past head of the Aqaba Office of the DoA for supporting this project. A special thanks to UMKC students, Abdelrahman Abueladas, Alivia Alison, Julie Galloway (Hopkinson), and John Rucker, for assistance in the field. Dr. Abueladas, Head of the Department of Surveying and Geomatics Engineering at Al-Balqa Applied University in Al-Salt, Jordan, shared borehole data and maps that were very useful.

A special thanks to Dr. Christopher Hein from the Virginia Institute of Marine Sciences for sharing his spreadsheet on locations along the Gulf of Aqaba and the Red Sea with higher-than-present sea level data. Dr. Thomas Felis from the Center for Marine Environmental Sciences at the University of Bremen in Bremen, Germany, provided additional information on the 2.9 ka coral reef in Jordan from his publication (Felis et al., 2004).

Thank you to Dr. Kathleen Roy and Mr. John D. Martin for bridging the gap between English and German by providing and translating a paper essential to this thesis.

And thank you to my daughter Grace Smith whose experience with paleontology led to her assistance in identifying a variety of shells found in the sediment by teaching me about shell taphonomy, color and morphology.

Thank you to my family who have supported me throughout this endeavor from the moment I told them I wanted to go back to school I had their love and support. I wish my mother and my grandmother had lived to see me defend this thesis and graduate.

Lastly, thank you to my late grandfather, Van Bettis for teaching me about rocks and minerals when I was little back home in Arkansas. My grandfather not only took me on many adventures around the state to look at and learn about rocks, but we spent many successful hours in his backyard hunting for crystals.

CHAPTER 1

INTRODUCTION

Aqaba, Jordan, located on the north shore of the Gulf of Aqaba, is the only port for the nation and is a vibrant tourist destination and essential for commerce and trade in the region. The location of the city at the head of the gulf has been at the nexus of trade between Africa, Asia, and the Mediterranean via land and sea routes for millennia. The long cultural history is preserved in the records at archaeological tells (artificial mounds) and the extant Aqaba Castle located at various sites across Aqaba (Figures 1 and 2).

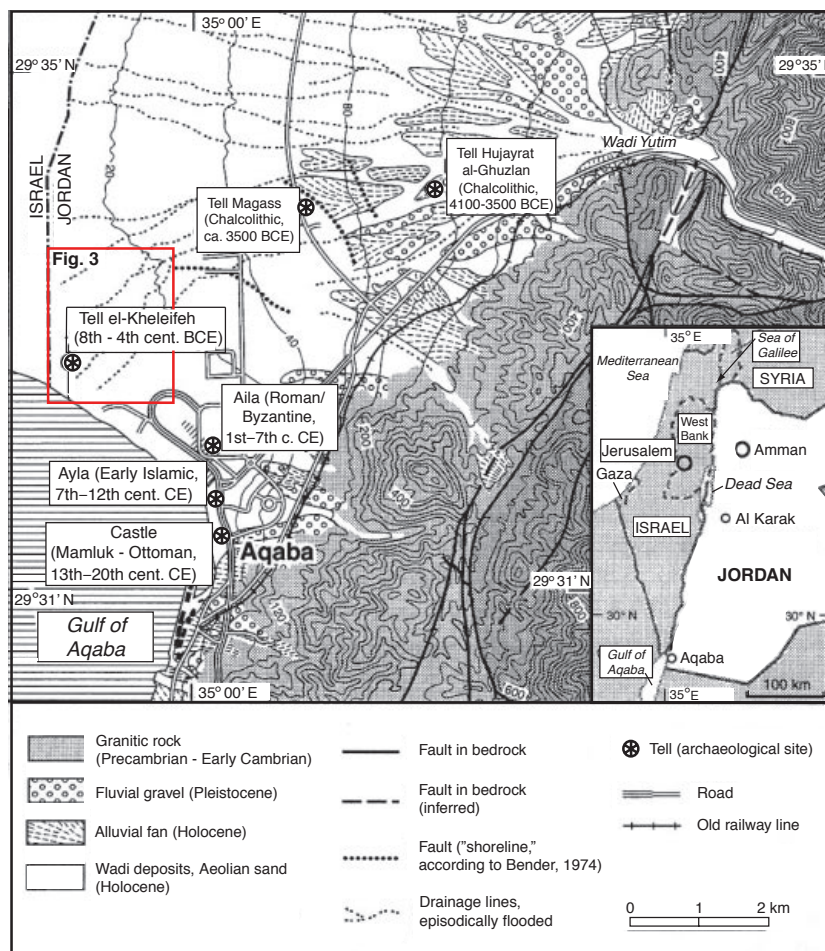


Figure 1: Map of Aqaba, Jordan showing the location of archaeological sites. Red rectangle outlines the area of the Ayla Oasis development shown in Figure 3. Modified after Brückner (1999) and Alison and Niemi (2010).

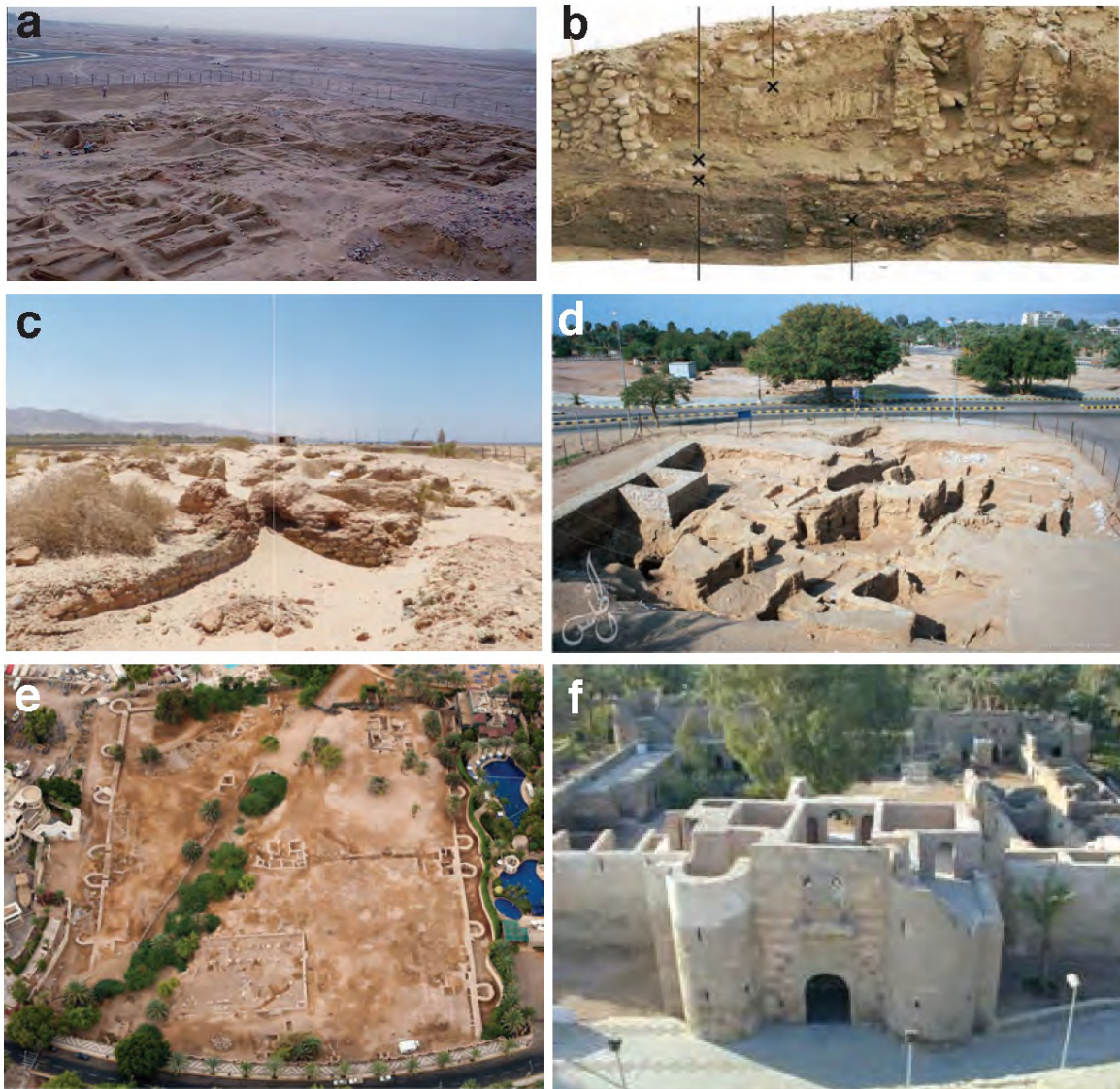


Figure 2: Photographs of the archaeological sites in Aqaba. a) Aerial photograph of the Chalcolithic site of Tell Hujayrat al-Ghuzlan (Klimscha, 2013). b) The road was cut through Tell Magass exposing a 6-m-high cross section of the Chalcolithic mound (Notroff et al., 2014). c) A photograph of Tell el-Kheleifeh viewed toward the southeast shows sand dunes infilling the site excavated in 1938-1940 by Nelson Glueck (Pratico, 1993). d) Nabataean/Roman to Byzantine Aila (1st – 7th Century CE) excavated by S. Thomas Parker (North Carolina State University) from 1994-2002 exposed a 3rd century mudbrick church (Parker, 1997). Photograph from Atlas Tours. e) Aerial view of the fortified Islamic city of Ayla showing the outline of the city wall with towers (Kennedy, 2014) was excavated by Donald Whitcomb (Oriental Institute, Chicago) from 1986-1999 and Kristoffer Damsgaard (University of Copenhagen) from 2009-2010. f) Oblique aerial photograph of the Mamluk to Ottoman Aqaba castle excavated by Johnny De Meulemeester and Reem Al Shqour (University of Ghent) (Al Shqour, 2019).

The earliest occupation of Aqaba is seen at the Chalcolithic-aged (5th to 4th millennium BCE) Tell Magass and Tell Hujayrat al-Ghuzlan located 4.2 km and 5.3 km from the shoreline, respectively, at an elevation >100 m on an alluvial fan (Khalil and Schmidt, 2009; Klimscha, 2013; Notroff et al., 2014). The late Iron Age (8th and 4th centuries BCE) site of Tell el-Kheleifeh is located 500 m north of the shoreline in the middle of the valley (Pratico, 1993). The Nabatean port city of Aila, established in the 1st century CE and extending to the Byzantine period (4th century CE), is located approximately 200 m from the modern shore of the Gulf and about 2 km southeast of Tell el-Kheleifeh. Farther southeast is the walled Islamic city of Ayla (7th - 12th century CE) (Whitcomb, 1994) and Castle or Khan (13th – 20th century CE; Al Shqour, 2019). This scattered pattern of archeological site distribution is unusual as most settlements in antiquity in the Near East have built large tells at one site over many centuries.

The archaeological site of Tell el-Kheleifeh is of particular interest as it is adjacent to the stratigraphic data examined in this paper. Tell el-Kheleifeh was first surveyed by German architect and historian Fritz Frank in 1934 (Pratico, 1993). Frank speculated the tell was the ancient port city of King Solomon known in the Bible as Ezion-Geber. Nelson Glueck, an American archaeologist excavated the site in three seasons between 1938-1940. Glueck identified five periods of occupation between the 10th and 5th centuries BCE. He also agreed with Frank the tell was the port city of Ezion-Geber (Pratico, 1993). Additional analyses of Glueck's excavation archival materials and pottery sherds determined the site to be too young to have been occupied by King Solomon (Pratico, 1993) as Solomon lived around 950 BCE and the pottery dates were between the 8th and 4th centuries BCE. Tel el-Kheleifeh is located along the international border between Israel and Jordan at the western edge on the Ayla Oasis Development about 500 m from the modern shoreline.

The modern city of Aqaba has experienced extensive growth from the 1990s to today. Population in the mid-1990s was around 60,000. According to the Oxford Business Group's 2018 report, as of 2018, the population had reached nearly 180,000. The city has a land area of approximately 375 km² (Ghazal, 2016) with 24 km of coastline. Expansion towards the south includes the building of a new port. In 2001, the Aqaba Special Economic Zone Authority (ASEZA) took over administration of the city. ASEZA decreased local taxes and made the city a duty-free zone as a way to attract tourists. The vision of ASEZA is to grow Aqaba into a major tourist destination as well as increase industry and trade, and heighten environmental awareness by establishing offshore nature preserves. Aqaba has no cap on foreign investment. As of 2017, the city had over \$20 billion invested with \$10 billion invested in tourism and the port. ASEZA projects the population to reach 200,000 by the end of 2020.

As part of the urban revitalization, the Ayla Oasis Development is a residential and tourist area located along the westernmost edge of the city of Aqaba (Figure 3). The Ayla Oasis Development covers an area of 4.3 km² with a narrow sea frontage along the Gulf of Aqaba located west of the Jordanian Royal Palace (Manasrah, 2015). Construction began in 2008 and infrastructure was completed in 2014. Hotels and the golf course opened in 2018. The Ayla Oasis Development added 17 km of "coastline" to the city with the creation of three lagoons (Al-Rshaidat et al., 2020). The lower lagoon is connected directly to the gulf by a 235-m-wide opening and is tidally dominated at present sea level. Water depth in the lower tidal lagoon is about 10 m deep. Water is pumped up to the middle and upper lagoons which have surface elevations of 3 m above mean sea level (asl) and 6 masl, respectively. The water depth in the middle and upper lagoons is approximately 2 m. The lagoons were flooded in May 2012 (Al-Rshaidat et al., 2020).

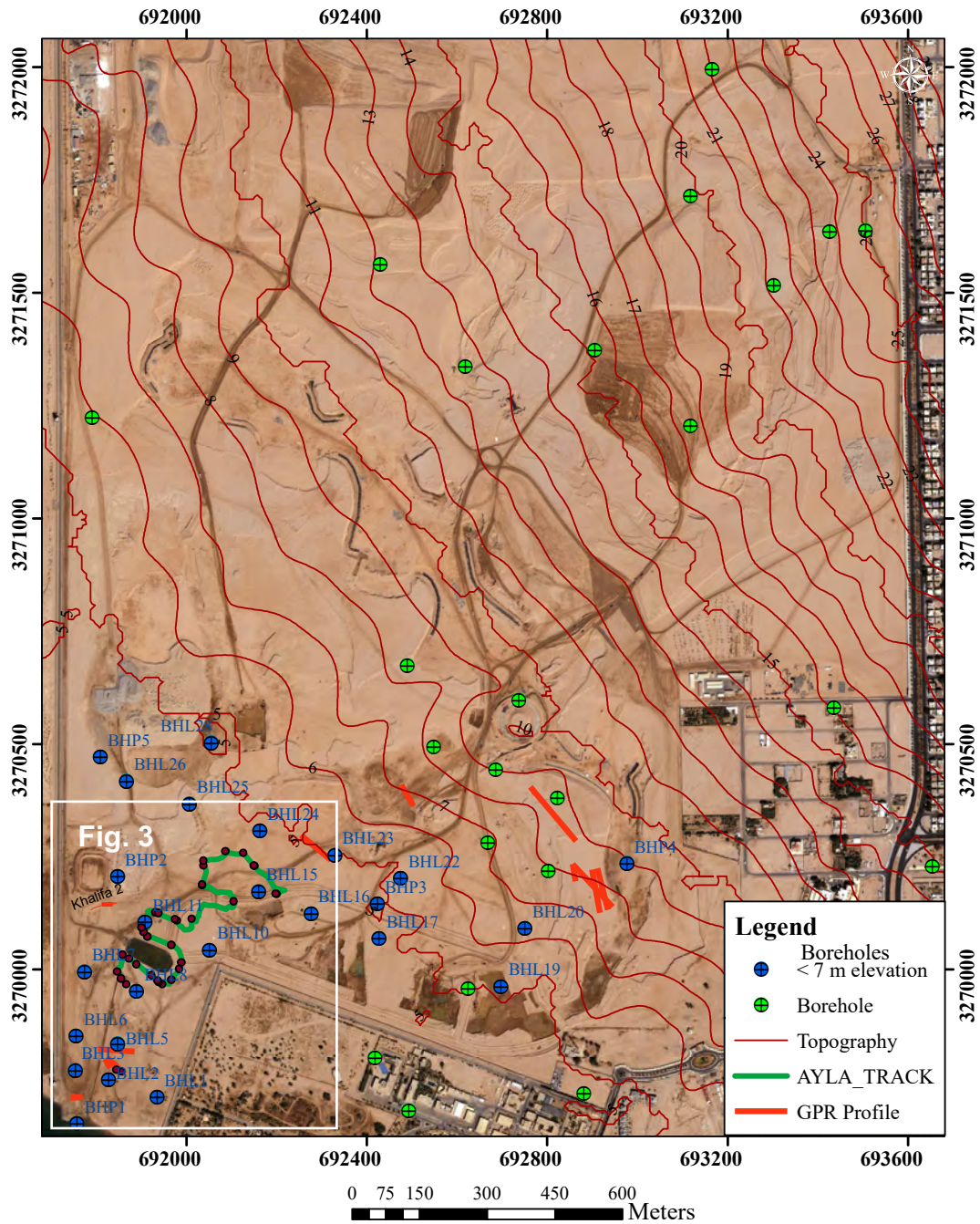


Figure 3: Google Earth map of the Ayla Oasis development site from 2010 showing the early stages of construction. Topographic contours and borehole locations are from consulting reports by the Arab Center for Engineering Studies in Amman, Jordan. Green line with red dot waypoints is a GPS track of the wall surveyed in February 2010.

The construction of the lower tidal lagoon at the Ayla Oasis development involved excavation below sea level and below the water table. A series of dewatering wells were installed across the site in order to create dry excavation conditions and provided a unique opportunity to study the 3-D architecture of the stratigraphy exposed along the lagoon construction site. This study examines the stratigraphic sections and field relationships of sediment collected at the Ayla Oasis construction site during February 2010 when the floor of the lagoon was at about -3 m below sea level (bsl). Furthermore, during July-August 2010, the lagoon construction exposed buried structures adjacent to the Late Iron Age (8th and 4th centuries BCE; Pratico, 1993) archaeological site of Tel el-Kheleifeh. These outcrops were documented and provide insight into paleoenvironmental conditions at this important site.

Two previous studies have presented paleoenvironmental data for the Aqaba coastal plain of the Gulf of Aqaba based on borehole data (Brückner, 1999; Alison and Niemi, 2010). Brückner (1999) collected five sediment cores from about 350 m to 700 m inland from the coastline corresponding to surface elevation between 3 and 5 m asl. These cores were extracted along a transect from the coast to Tel el-Kheleifeh and beyond. From these data, Brückner (1999) interpreted a marine transgression followed by a regression. At around 6.2 ka, the shoreline was 600 m inland from its current position and by 3.7 ka the shoreline had moved to 270 m inland based on Brückner (1999). Alison and Niemi (2010) interpret marine deposits at 5 mbsl changing to brackish water to freshwater conditions at 2-3 mbsl around 6 ka based on freshwater ostracod identification from cores in Aqaba, followed by a regression. Neither study discusses the possibility of a higher-than-present sea level.

The excavation of the Ayla Oasis's lower tidal lagoon construction site exposed sediment to -3 m bsl at the time of the field study in 2010. The outcrops showed several blueish-

colored, mostly gravel- and sand-filled channels cutting through intertidal marine deposits. The channels have never been exposed or previously described, and their interpretation is the subject of this thesis. Furthermore, the stratigraphic section of TK-4 is close to Tell el-Kheleifeh was mapped and shows clear stratigraphic relationships between the blue-gray channel and later stratigraphy.

In this study, two stratigraphic columns and a stratigraphic section were described and sampled in the field in 2010 and over 2000 m of subsurface outcrop exposed in the construction site walls were examined and photographed. Grain-size, XRD, and SEM analyses provide additional insight to the changes in the coastal environment of the Aqaba region. The previously documented transgressive sequence appears to extend to higher-than-present sea levels and the regressive sequence is punctuated by a down-cutting erosional event that extends below modern sea level.

CHAPTER 2

REGIONAL ENVIRONMENTAL SETTING

Aqaba, Jordan lies on the northern shore of the Gulf of Aqaba at the southern end of the Wadi 'Arabah valley (Figure 4).

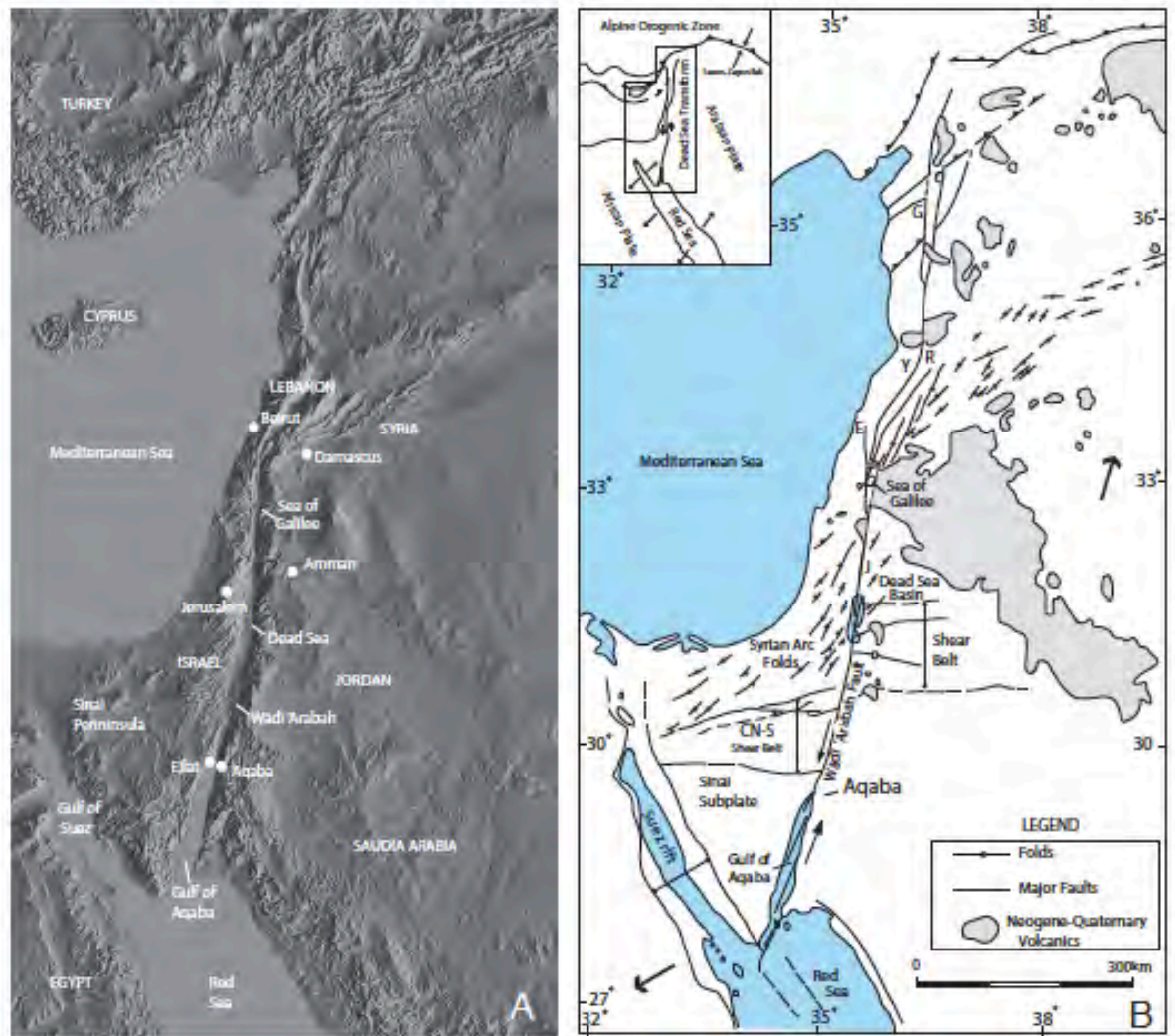


Figure 4: Dead Sea Transform (After Niemi, 2014)

The Gulf of Aqaba is roughly 180 km long and is the northeastern branch of the Red Sea. The Straits of Tiran mark the boundary between the gulf and the Red Sea to the south and restricts circulation between the two water bodies. The low influx of freshwater into the gulf results in

high temperatures, increased salinity, and increased evaporation rates (e.g. Morcos, 1970). The tidal range at the north end of the gulf near the city of Aqaba is less than a meter. In the Gulf of Aqaba, coral reefs only grow along the west and eastern shores (e.g. Al-Rifaiy and Cherif, 1988; Bouchon et al., 1981; Friedman, 1965; Shaked et al., 2004). The water depth of the gulf exceeds 1500 m. The Aqaba fault system underneath the gulf forms a steep escarpment and narrow shelf adjacent to the eastern shore of the gulf (Tibor et al., 2010; Hartman et al., 2014).

Wadi ‘Arabah and the region, including Aqaba, is a hyperarid environment and receives less than 50 mm of rainfall annually (Aqaba Meteorological Station, 1955-1985). Rainfall in Aqaba occurs primarily during the months between November and March and is sporadic. Two separate weather systems supply the region with precipitation. One is the mid-latitude cyclone known as the Cyprus Low which brings moisture from the Mediterranean Sea. The other weather system is the Red Sea trough which is an extension of the tropical monsoon season which occurs to the south (Black et al., 2011). These two systems also bring precipitation north of Aqaba to the Jordanian Plateau and farther north.

Wadi ‘Arabah valley is a NE-trending, linear valley formed along the Dead Sea Transform fault (DST). The valley extends from the Gulf of Aqaba to the Dead Sea. The wadi (ephemeral stream) drains southwestward into the gulf from a divide 80 km north of Aqaba. The valley floor is comprised of mudflats and alluvial fan deposits which are Pleistocene to Holocene in age (Figure 5). Drainage into Wadi ‘Arabah comes from the mountains that flank the valley. The mountains to the east have a higher elevation up to 1200 m compared to the mountain range to the west that have elevations of approximately 600 m. The largest drainage system in the southern ‘Arabah valley is the Wadi Yutim which has a drainage basin originating at the eastern plateau.

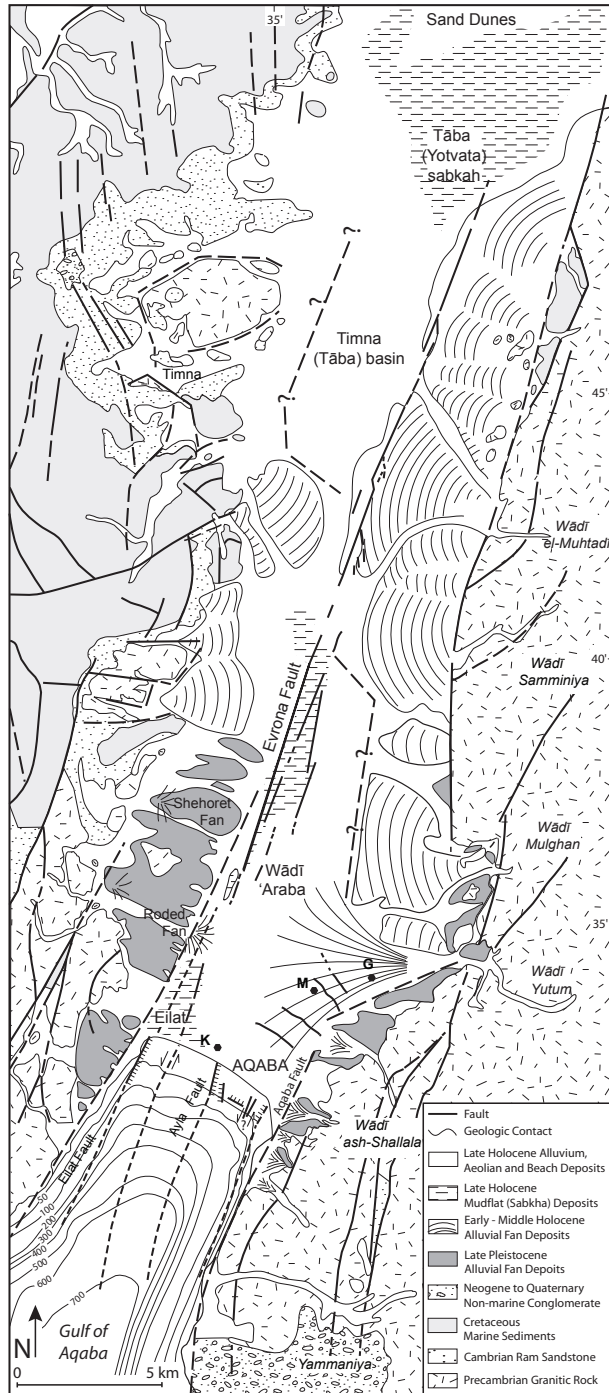


Figure 5: Geologic map of the Aqaba-Eilat region (After Niemi, 2014).

The catchment of the basin is approximately 4500 km². The city of Aqaba is largely built on the alluvial fans of Wadi Yutim. The basin is prone to flash flood events due to higher annual precipitation on the Jordan plateau to the east.

The Gulf of Aqaba and Wadi ‘Arabah formed along the Dead Sea Transform Fault (DST) that extends from the gulf and eastern Turkey (Figures 1 and 4). The DST is a sinistral transform plate boundary system which separates the Sinai subplate from the Arabian plate (Freund et al., 1970). A component of divergence has down-dropped a rift valley along normal faults that parallel the DST and uplift of the flanking mountains (Garfunkel, 1981). A series of pullapart basins along the Gulf of Aqaba, Dead Sea, and the Sea of Galilee were created between *en echelon*, left-stepping strike-slip faults (Figure 4) (e.g. Ben-Avraham et al., 1979; Ben-Avraham, 1985).

A cumulative, left-lateral offset of 105 km along the DST juxtaposes various bedrock (e.g. Freund et al., 1970). The mountains to the east are much older than those to the west of the valley (Figure 5). Eastern mountains are Precambrian to Cambrian in age. Western mountains are of Cretaceous age. East of Aqaba and extending 50 km northeast the mountains are comprised of Precambrian igneous rocks of the Aqaba Granite Complex (Rashdan, 1988). The rocks are a composition of granite, monzogranite, granodiorite, and quartz diorite (Ibrahim and McCourt, 1995; Jarrar et al., 2003). Felsite dikes crosscut the granite. An unconformity caps this sequence. Over the crystalline bedrock is a series of Cambrian arkosic sandstones and conglomerates. These rocks transition to Cambrian quartzose sandstones to Silurian Nubian Sandstone. The Nubian Sandstone outcrops 50 km NE of Aqaba. To the west the elevations are lower than the mountains to the east. The rocks west of Aqaba are composed of

Cretaceous sandstones, limestones, and dolomites. The limestone is fossiliferous and interbedded with chert, shale, and phosphate.

The Evrona fault is the active strike-slip fault mapped along the western side of the northern Gulf of Aqaba that extends onshore into Eilat (Kanari et al., 2020). A slip rate for the Evrona fault of 2.3-3.4 mm/yr was calculated from seismic reflection data of an offset coral reef front on the shelf (Makowsky et al. 2008, Hartman et al., 2014). In Eilat, near the Shehoret fan, and Taba Sabkha (Figure 5), paleoseismic data show that the Evrona fault ruptured in the historic earthquake of 1068 CE (Amit et al., 2002; Klinger et al., 2015; Kanari et al., 2020; Zilberman et al., 2005). Guidoboni and Comastri (2005) and Ambraseys (2009) describe the historical earthquake of 1068 CE as being devastating. One contemporary account states that “its inhabitants all perished except for 12 persons who had gone fishing at sea” (Guidoboni and Comastri, 2005, p. 53). Another historical reference refers to the destruction of the city by a “withdrawal and return to the sea” as described by Ibn al-Jauzi, an author from the 12th century (Ambraseys, 2009, p. 274). Whitcomb (1994) excavated portions of the fortified wall city of Islamic Ayla and found evidence for earthquakes in the 8th and 11th centuries CE.

Along the eastern side of the Gulf of Aqaba, Tibor et al. (2010) and Hartman et al. (2014) map the steep drop forming the narrow shelf to the deeper basin as the Aqaba fault (Figure 5). Slip rate estimates of the presumed normal fault is 0.4 ± 0.1 mm/yr. The offshore Aqaba fault comes onshore beneath the city of Aqaba, although its exact position is largely unknown. Motion from the Aqaba fault appears to fan out into a horsetail splay of a series of northwest-striking cross faults (Niemi and Smith, 1999; Slater and Niemi, 2003; Mansoor et al., 2004). The cross faults have ruptured in earthquakes which displaced archaeological structures between the 2nd and 7th centuries CE (Thomas et al., 2007).

The Nuweiba earthquake was the largest seismic event along the DST in the 20th century and occurred in 1995 (Shamir et al., 2003). The earthquake ruptured a fault under the Gulf of Aqaba and structural damage occurred in Aqaba and neighboring city, Eilat in Israel. The epicenter was near the Egyptian city of Nuweiba, and was felt as far as Lebanon and Syria. Evidence for liquefaction, differential settling, and apparently a small tsunami in Aqaba and Eilat were documented (Wust, 1997).

CHAPTER 3

METHODS

Field Work

Along the Ayla Oasis lagoon construction site in February and August of 2010 over 2 km of sediment to a depth of >3 mbsl were surveyed. One cross-section (TK 4) of exposed and buried walls and two stratigraphic columns (AO-2 and AO-3) were drawn, described, and sampled. A buried structure at AO-1 was determined to be modern and not discussed in this thesis. Figure 6 shows the location of the sections. A log of the samples is given in Appendix A. Figure 7 shows the outcrop of AO-2.

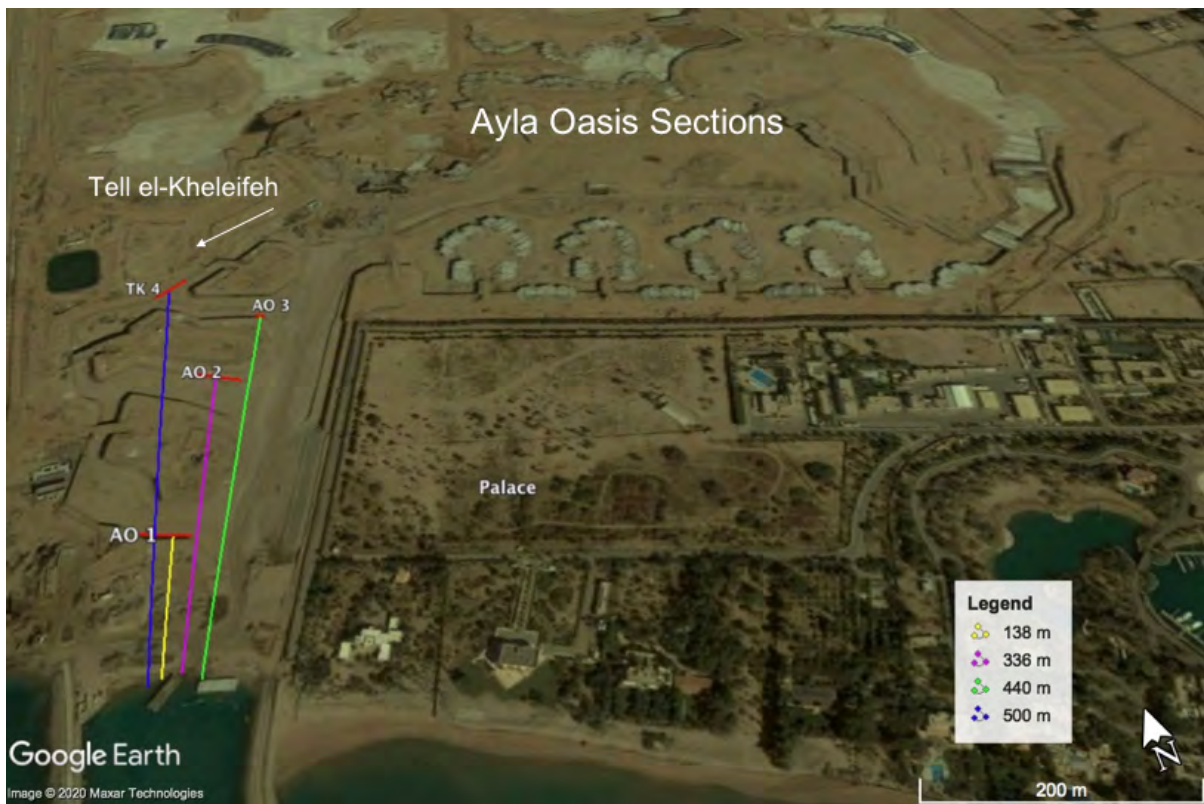


Figure 6: Location of stratigraphic sections described in this study plotted on a 2011 Google Earth image. The distance from the shoreline to each site is given in the legend.

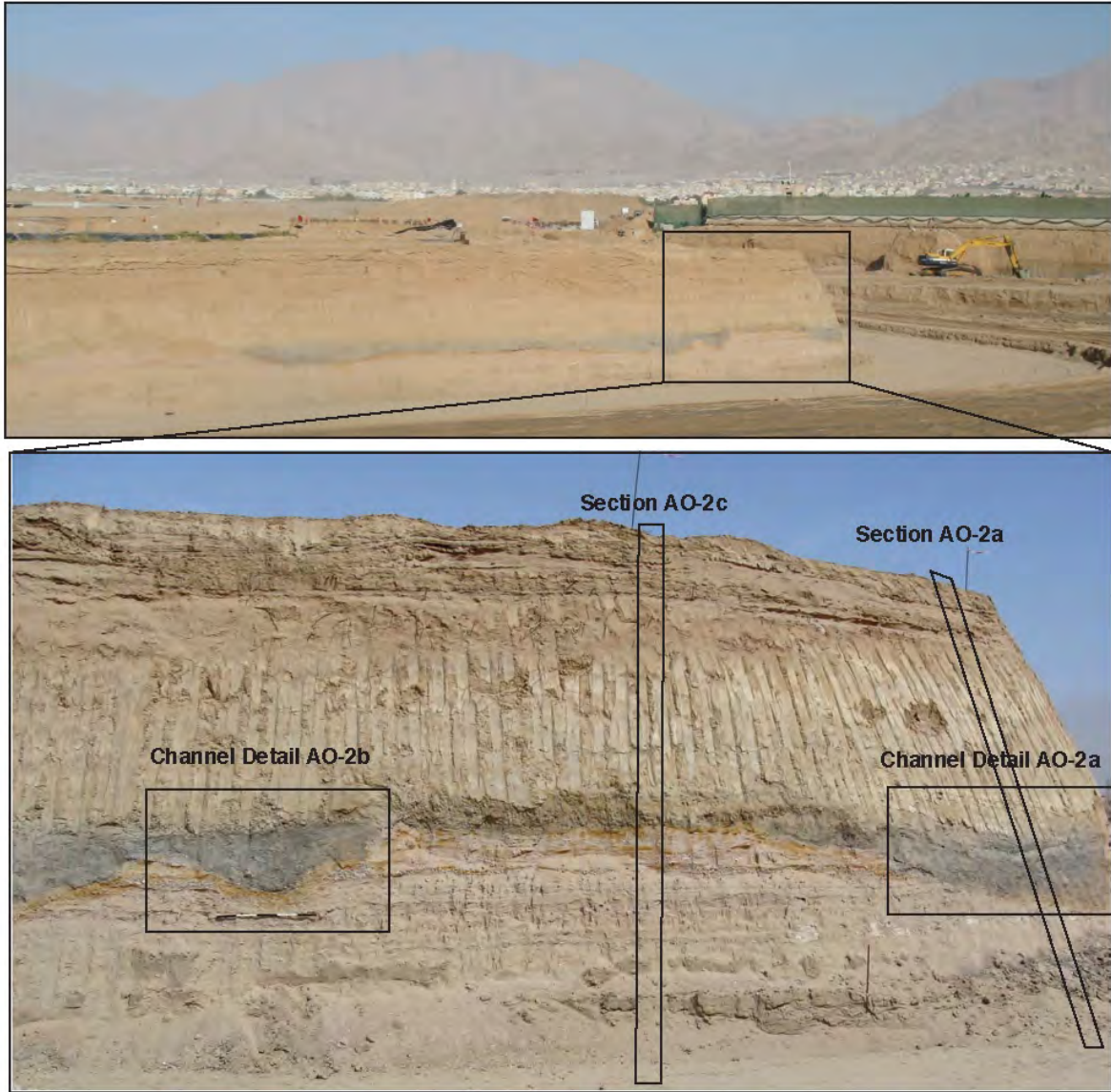


Figure 7: Photographs of the AO-2 section location 338 m from the shoreline. See Figure 6 for map location.

In the field, a surveyor from the Ayla Oasis Development company reported that the depth of the lagoon (i.e. the base of AO-2 and AO-3 sections) was being excavated to 3.2 mbsl. This datum indicates that the surface elevation at the AO-2 and AO-3 site is at 3.8 m or around 4 masl. This is a reasonable estimation given the topographic map and drill core elevations and proximity to the Jordanian Royal Palace Property boundary (Figure 3).

XRD, SEM, EDS

Samples from several units (Appendix A) were analyzed by powder X-ray diffraction (XRD). The samples were finely ground and homogenized. The untreated mounts were analyzed on a Rigaku Miniflex automated diffractometer. The samples were scanned from 5-40° 2θ , 0.05 step width, 3/s step using CoK α radiation with 1.7902 Å Fe filter. Patterns were processed using MDI Jade software.

Scanning electron microscope (SEM) analysis was conducted for sample TK-4-13. The bulk sample was mounted, carbon coated and analyzed with a Tescan VEGA 3 LMU scanning electron microscope with a Bruker Quantax EDS system. EDS (Energy Dispersive spectroscopy) was used to identify key minerals in the sample. SEM images were taken for sample AO-2 unit 6. (See Appendix E)

Grain-Size Analysis

Four sections AO-1, AO-2, AO-3, and TK-4 at the Ayla Oasis development were analyzed. There were 42 total sediment samples collected across the four exposures. The bulk sediment samples were weighed and then rinsed with a sodium hexametaphosphate solution to disaggregate compaction. Organic material was skimmed from the top of the submerged sample and collected for analysis. The samples were oven-dried for 24 hours, and weighed again to determine moisture loss.

The samples range in size from clay to coarse sand. A total of 8 pans (7 sieves plus the pan) at one phi intervals (Appendix B) were used to determine the percentage of each grain-size fraction ranging from granules to <53 microns. The sediment was sieved by shaker for 10 minutes. Each grain-size fraction was weighed and recorded in a table (See Appendix B).

Statistical analysis parameters for the grain sizes was determined by the Gradistat program, version 8 (Blott and Pye, 2001). The Microsoft Excel worksheet and graphic program for the Gradistat program was developed by Blott (2010). Weights for each grain-size fraction was entered into the worksheet. Grain-size mathematical calculations are described using the Method of Moments in Microsoft Visual Basic programming language (Appendix C).

Radiocarbon Dating

Three wood and one charcoal samples were sent to the Center for Accelerator Mass Spectrometry (CAMS) at the Lawrence Livermore National Laboratory for radiocarbon age analyses. These samples were collected from within the blue-gray channel fill and from the sand unit that caps it. As the production of radiocarbon in the atmosphere has fluctuated over time, radiocarbon ages need to be calibrated to adjust them to calendar ages (BCE/CE) or to years before present (cal BP) with present given as 1950 CE. We utilized the CALIB 7.10 radiocarbon calibration program to calibrate the terrestrial carbon sample ages utilizing the Intcal13 radiocarbon curve. Results are reported in Table 1.

Table 1: Radiocarbon Results from the Ayla Oasis Exposures

CAMS No.	Sample No.	Material	Depth	Elevation	$\delta^{13}\text{C}$	fraction Modern	D^{14}C
163766	AO-2-15	wood	4.6 m	-0.8 m	-25	0.6831 ± 0.0025	-316.9 ± 2.5
163767	AO-2-18	charcoal	4.2 m	-0.2-0.6 m	-25	0.6941 ± 0.0026	-305.9 ± 2.6
163768	AO-3-1	wood	3.6 m	0.3-0.5 m	-25	0.6472 ± 0.0023	-352.8 ± 2.3
163769	AO-7b-1	wood	~ 4.5 m	NA	-25	0.4924 ± 0.0018	-507.6 ± 1.8

CAMS No.	Sample No.	^{14}C age	Calibrated age (2σ)	Median Probability	Calendar age (2σ)
163766	AO-2-15	3060 ± 30	3181-3359 cal BP	3278 cal BP	1410-1232 BCE
163767	AO-2-18	2935 ± 30	2979-3173 cal BP	3092 cal BP	1224-1030 BCE
163768	AO-3-1	3495 ± 30	3609-3826 cal BP	3688 cal BP	1877-1660 BCE
163769	AO-7b-1	5690 ± 30	6406-6549 cal BP	6468 cal BP	4600-4457 BCE

- 1) $\delta^{13}\text{C}$ values are the assumed values according to Stuiver and Polach (1977) when given without decimal places. Values measured for the material itself are given with a single decimal place.
- 2) The quoted age is in radiocarbon years using the Libby half-life of 5568 years and following the conventions of Stuiver and Polach (1977).
- 3) Radiocarbon concentration is given as fraction Modern, D^{14}C , and conventional radiocarbon age.
- 4) Sample preparation backgrounds have been subtracted, based on measurements of samples of ^{14}C -free coal. Backgrounds were scaled relative to sample size.
- 5) The CALIB 7.10 program with the IntCal13 radiocarbon curve was used to calibrate radiocarbon ages.

C-14 ages of shells presented in Brückner (1999) were also calibrated. Because of the storage of old carbon in the ocean, radiocarbon dating of shells or other marine material will yield an age several hundred years older than the actual age. Therefore, a marine reservoir correction must be made. The average global ocean correction is given as 400 yr (Stuiver and Braziunas, 1993). However, basins restricted from the global ocean and changes to seawater circulation cause the region marine reservoir to vary from the global value. Delta R (ΔR) is given as the difference of the region reservoir to the average global ocean reservoir correction. In the marine reservoir correction database for the program CALIB (Stuiver and Reimer, 1993), the regional ΔR for the Gulf of Aqaba in Aqaba is 224 ± 35 yr or 121 ± 30 yr based on analyses of modern *Porites* coral presented in Felis et al. (2004). The weighted mean value for

these data yields a ΔR of 165 ± 72 yr. Brückner (1999) used the global marine reservoir correction of 402 yrs. for adjustment of radiocarbon analyses of shells sampled from boreholes near Tel el-Kheleifeh. Given that the Gulf of Aqaba reservoir correction data were not available to Brückner (1999), we have re-calibrated his Beta Analytic C-14 ages using the CALIB 7.10 program with the Marine-13 radiocarbon curve and a ΔR of 165 ± 72 yr (Table 2).

Table 2: Recalibration of the radiocarbon data from the Brückner (1999) study near Tel el-Kheleifeh

Beta No.	Sample No.	Material	Depth	Elev.	$^{12}\text{C}/^{13}\text{C}$ ratio	^{14}C	Calibrated age (2σ)	Median Probability	Calendar age (2σ)
121046	AQ 5/11F	<i>Codakia</i> shell	5.1 m	-1.4	3.1	3740 ± 50	3249-3687 cal BP	3472 cal BP	1738-1300 BCE
121047	AQ 6/15F	shell	7.7 m	-2.6	3.4	6200 ± 50	6268-6665 cal BP	6459 cal BP	4717-4319 BCE

- 1) The CALIB 7.10 program with the Marine13 radiocarbon curve and a ΔR of 165 ± 72 yrs. was used to calibrate radiocarbon ages.

CHAPTER 4

RESULTS

Stratigraphic Sections

Two stratigraphic columns (AO-2 and AO-3), located 336 and 440 m from the shoreline, respectively, were measured and described (Figures 8 and 9). Section AO-2 is 7 m in height, and has 14 units. Unit 14 marks the base of the section which contains pinkish sand with pebbles, shells, and sand dollars. Unit 13 is beachrock approximately 22 cm thick, but is broken into a disjointed layer. Unit 12 contains parallel inclined interbeds of sand and pebbles. Marine gastropods, clam shells, and coral fragments were found in Unit 12. Unit 11 is the base of the channel and contains blue-gray sand with rip-up clasts. Unit 10 is iron stained at the top with slightly cemented gray sand and denotes fill in the channel sequence. Unit 9 overlies a channel sequence and is interbedded sandy and silty clay. Units 6, 7, and 8 are all distinct units of sand, silt, and clay with some units indurated and some units containing calcium carbonate nodules. Unit 5 contains sand with calcium carbonate nodules and appears to mark the base of the pedogenic unit. Unit 4 has cobbles at the top with loose and broken roots in fine sand. Unit 2 is layers of light brown silty clay and Unit 3 is cross-stratified and bioturbated medium to fine sandy soil. The top of the section, Unit 1, is brown sand and in places is construction fill from the excavation of lagoons.

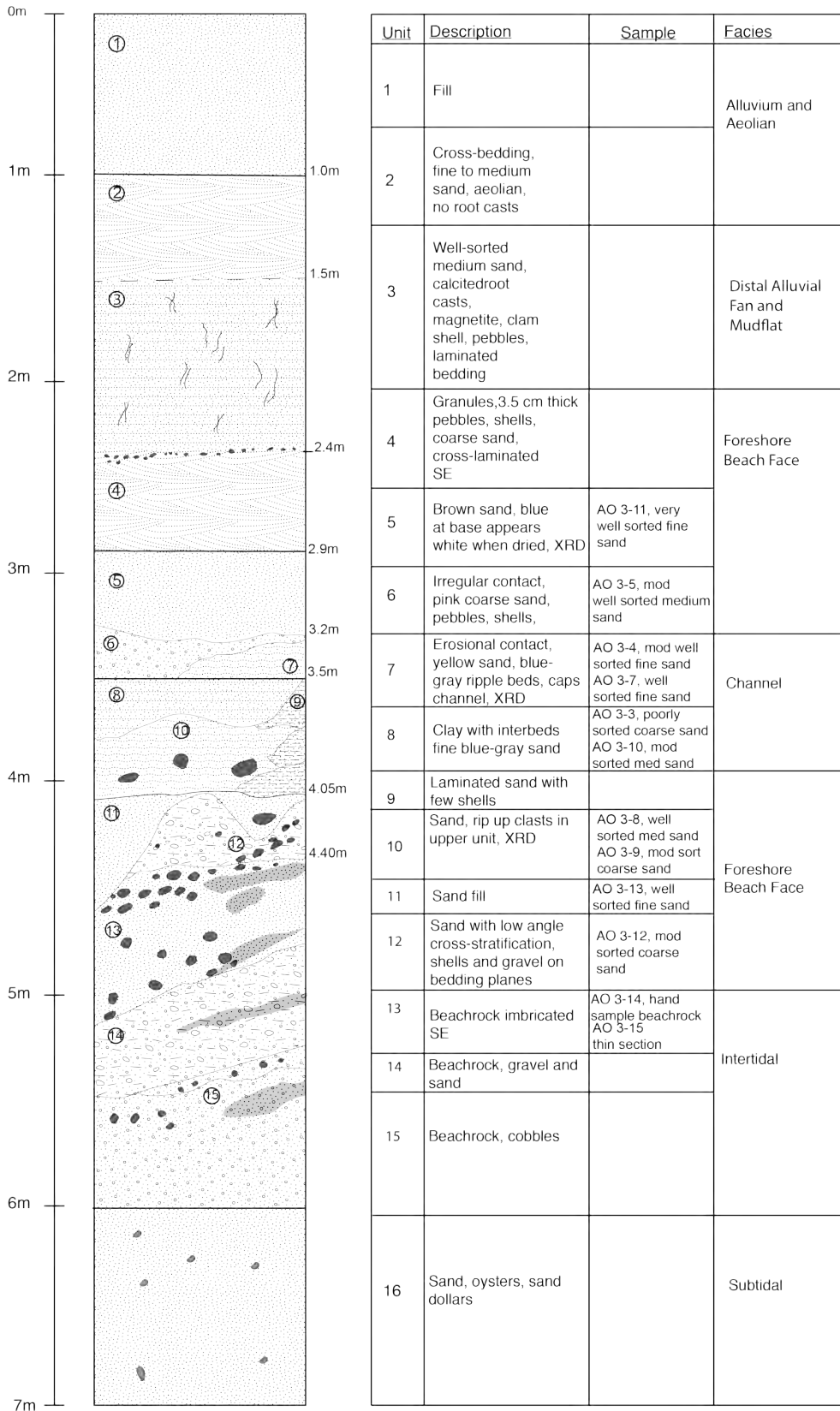


Figure 8: Stratigraphic section AO-2

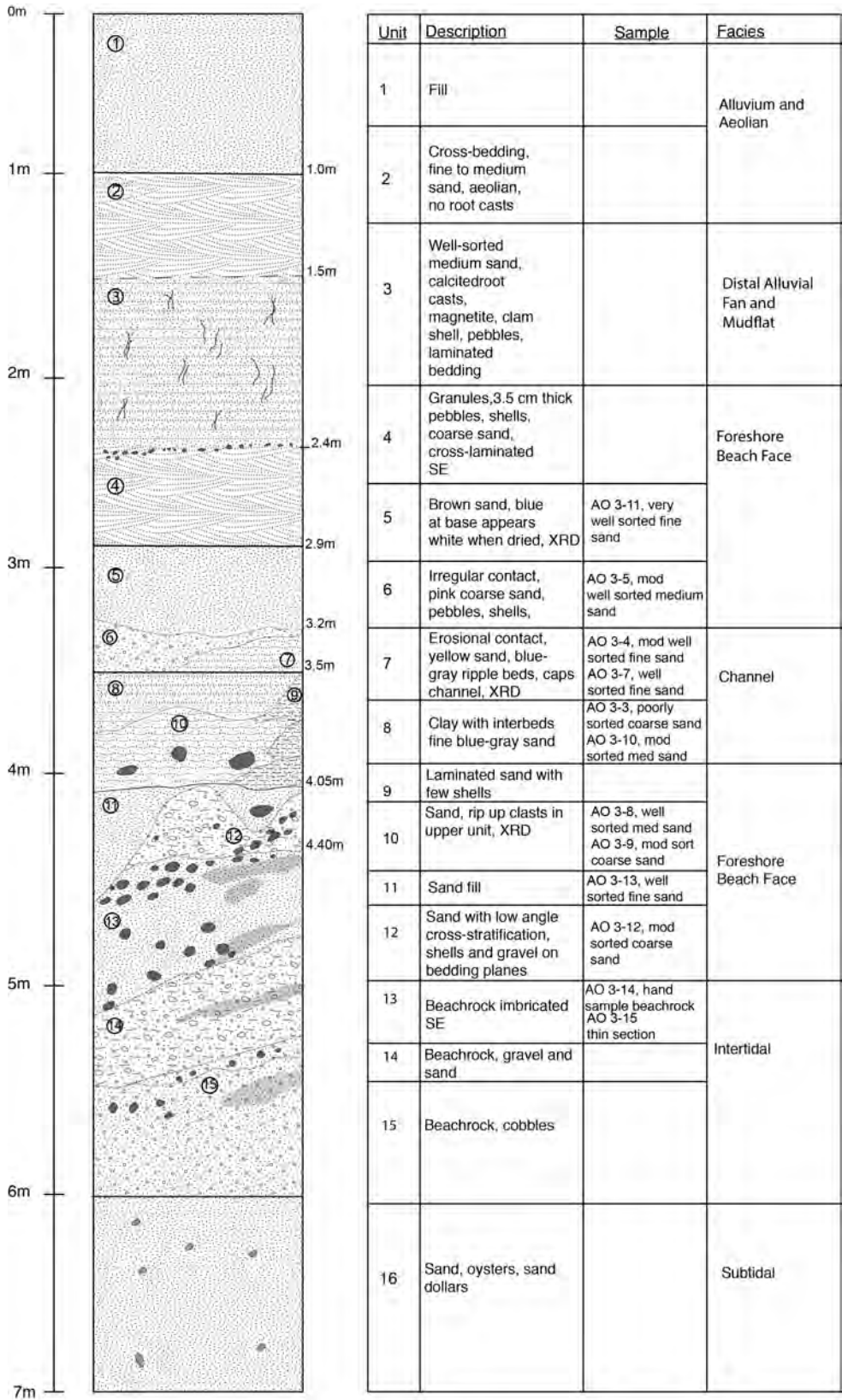


Figure 9: Stratigraphic section AO-3

Section AO-3 contains 16 units, and is also 7 m in height. The base of the section is unit 16 which is bioturbated sand with sand dollars and oysters. Unit 15 is beachrock encrusted with worm snails and oysters. Unit 14 is beachrock with gravel, sand, shells, and coral fragments. Unit 13 contains beachrock pieces imbricated to the southeast and 3 layers of beachrock. Unit 12 is sand with low-angle cross-stratification containing shells and gravel. Unit 11 is a well-sorted sand fill with convoluted bedding marking the base of the channel, and channel margin trends N10°E. Unit 10 is sand with rip up clasts in the upper channel fill unit. Unit 9 is in the channel and is laminated sand with shells. Unit 8 is blue-gray sand interbedded with clay and is above the channel sequence. Unit 7 is yellow sand at the top overlying blue-gray ripple beds below. Unit 6 denotes an irregular contact and contains pink coarse sand, pebbles and shells. Unit 5 is brown, well-sorted fine sand. Unit 4 is cross-laminated coarse sand trending to the southeast, and contains pebbles. Unit 3 is laminated sand beds with calcite root casts and pebbles. Unit 2 is fine aeolian sand which is cross bedded. The top of section AO-3 is Unit 1 is construction fill from the excavation of the Ayla Oasis Development.

A section referred to as AO-1 is a buried structure and was also sampled and photographed in the field. Grain-size analysis was run on the samples. The top of the structure infilling contained modern debris and was determined to be a modern well. Grain size data is provided in the appendix, but further discussion of the structure is not included in this thesis.

Facies Model

The stratigraphy from the AO-2 and AO-3 stratigraphic section and observations from other outcrops in the tidal lagoon construction site was used to divide the sedimentary units

into six different facies: 1) subtidal, 2) beachrock, 3) foreshore, 4) channel, 5) distal alluvial fan/mudflat, and 6) aeolian and alluvium

The oldest exposed horizon is defined as subtidal facies. The layer is partially exposed, and it begins at a depth of 6 m from the surface. This layer is characterized by bioturbated grayish pink sand with pebbles. The well-sorted, fine-grained sand is mesokurtic with symmetrical skew with unimodal distribution. Fauna includes sand dollars and oysters.

Overlying the subtidal zone is a cemented intertidal unit characterized by beachrock (Figure 11). This zone is indicative of the upper shoreface where seawater mixes with freshwater in the swash zone. Beachrock forms in seawater high in calcium carbonate where it mixes with the freshwater lens from groundwater flowing seaward. The water becomes supersaturated with carbonate as carbon dioxide is released resulting in precipitation of carbonate which forms the cement. This layer in the AO-2 section measured 22 cm in thickness and was broken into a disjointed unit. In the AO-3 section, three distinct levels of beachrock were documented. The vertical stacking of the beachrock indicates rising sea level. Encrusting oyster shells (*Spondylus spinosus*) were noted on some cobbles. Encrustation of the worm snails, *Vermetidae* were found on the surface of a beachrock fragment. Thin section analysis shows the beachrock consists of moderately sorted, sub-angular clasts composed of quartz and plagioclase grains, granitic lithic clasts, and some bioclasts. At least one bioclast can be identified as foraminifera (*Rotaliina*). Primary fabric-selective porosity leads to the formation of acicular aragonite crystals forming isopachous growth on the grains in the beachrock. The crystals are arranged perpendicular to the grain surfaces. A micritic envelope encompassing the grains is indicative of microbial activity prior to cementation. The shape and orientation of

the aragonite cement is also indicative of the upper shoreface (Scholl and Ulmer-Scholle, 2003).

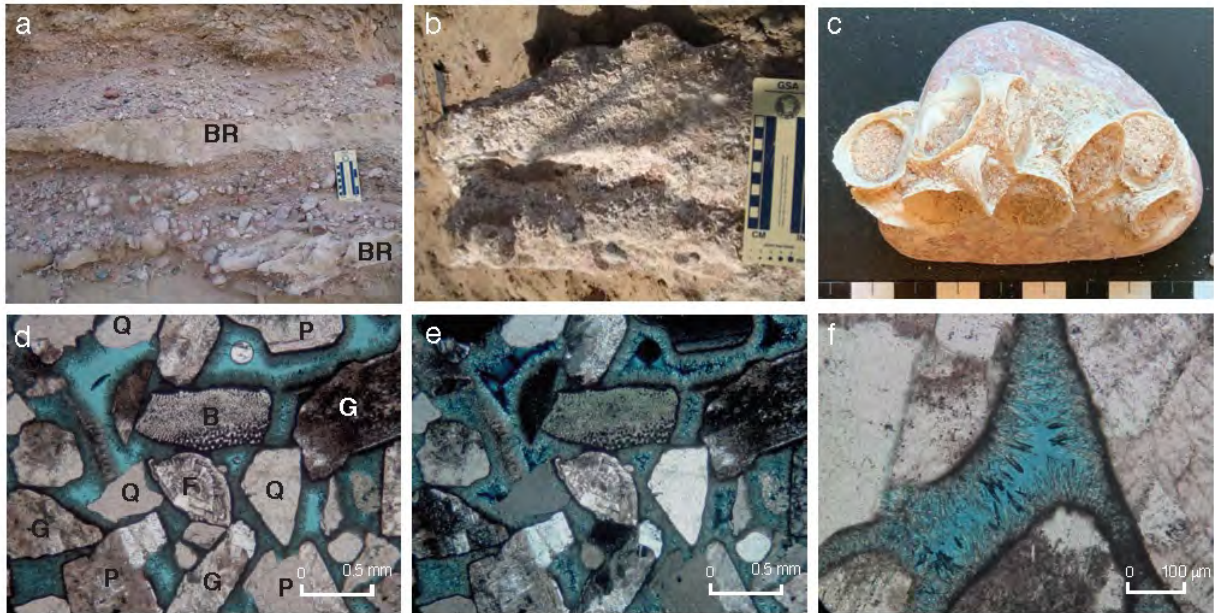


Figure 11: Beachrock exposed in the Ayla Oasis outcrop, hand specimens, and thin sections. a) Photograph of outcrop near section AO-3 showing two levels of beachrock (BR) formation. Scale is 10 cm. b) The surface of a dislodged block of beachrock showing the encrustation of Vermetidae worm snails on the surface. Scale is 10 cm. c) Granite clast from below the cobble unit under the upper beach rock in section AO-3 showing encrustation of the *Spondylus spinosus* oysters. Scale in centimeters. d) Photomicrograph of the beachrock showing the angular coarse sand in plane light. Sand is composed of quartz (Q), plagioclase feldspar (P), and granitic rock fragments and is classified as a feldspathic lithic arenite. Two bioclasts can be identified as a *Rotaliina foraminifera* (F) and a coral? bioclast (B). e) Photomicrograph of the beachrock shown in (d) in polarized light. f) Detailed photomicrograph of the grain boundary of the beachrock showing acicular aragonite cement typical of the marine intertidal zone (Scholl and Ulmer-Scholle, 2003). Note the micritic coating of the clasts.

Overlying the beachrock facies in the intertidal zone is the beachface measuring just over a meter in thickness and designated the foreshore facies. The foreshore facies is within the swash zone and is characterized by high energy wave activity. The swash zone sometimes cements and sometimes does not. The beachface may also move to higher elevations during a storm. This unit consists of moderately well-sorted medium to coarse grained pinkish brown to pale brown sand with platykurtic coarse skewness which dips gently seaward between 2 and 5 degrees. Wave activity in the swash zone reworks the sediment resulting in the well-sorted nature of the grains. An 85-cm-thick bed of sand, pebbles, and cobbles has gently southwest inclined, parallel bedding, and is capped by cross-bedded sand. A variety of marine shells were found in the foreshore facies corresponding to the intertidal zone from section AO-2 (Figure 12).



Figure 12: Coral and shell fragments found in the intertidal zone section of AO-2. a) *Porites cylindrica* (Dana, 1846), b) *Dosinia anus* (Philippi, 1848), c) *Venus foveolata* (Sowerby, 1853), d) *Lambis Lambis* (Linnaeus, 1758), e) *Cerithium Thericium Lutosum* (Adams, 1845), f) *Cantharus fumosus* (Dillwyn, 1817), g) *Polinices tumidus* (Swanson, 1840), h) *Trochus maculatus* (Linnaeus, 1758) Scale bar = 1cm. Shell identification is based on similarities to mollusk fossils from the Farasan Island in the southern Red Sea, Saudi Arabia (Bantan and Abu-Zied, 2014).

The shells found in the foreshore facies are all marine animals found in shallow water depths of 5 m. *Porites cylindrica* (Dana, 1846), commonly referred to as a “stony coral”, is a species common in mid-latitude waters. Its habitat includes lagoons and back-reef margins. *Dosinia anus* (Philippi, 1848) and *Venus foveolata* (Sowerby, 1853) are marine clams found in shallow waters with sandy substrate. *Lambis Lambis* (Linnaeus, 1758), is a marine animal, commonly known as a spider conch, found in the warmer waters of the Indo-Pacific. Its habitat includes reef flats with shallow water depths of 5 m. *Cerithium Thericium Lutosum* (Adams, 1845), is a common marine snail with a habitat of very shallow water. *Cantharus fumosus* (Dillwyn, 1817), *Polinices tumidus* (Swanson, 1840), and *Trochus maculatus* (Linnaeus, 1758) are shallow water marine snails commonly found in the Red Sea as throughout the Indo-Pacific. The bivalve shells were found disarticulated, with some abrasion visible. Disarticulation can indicate depositional energy of sediment (El-Sorogy, 2015). Since the shells were disarticulated and given the lack of abrasion on the shells they were likely carried by high energy and subsequently buried by rapid sediment deposition. The beachrock and uncemented beach facies denote the intertidal zone climbing higher in elevation with rising sea level thus moving the beachface farther inland in a transgression. The top of the foreshore facies sediment is capped by an erosional unconformity with irregular relief.

Sporadically across the outcrop are channels filled with a distinct blue-gray sediment (Figures 7 and 10) that was labelled the “blue channels” in the field and are designated as the channel facies.

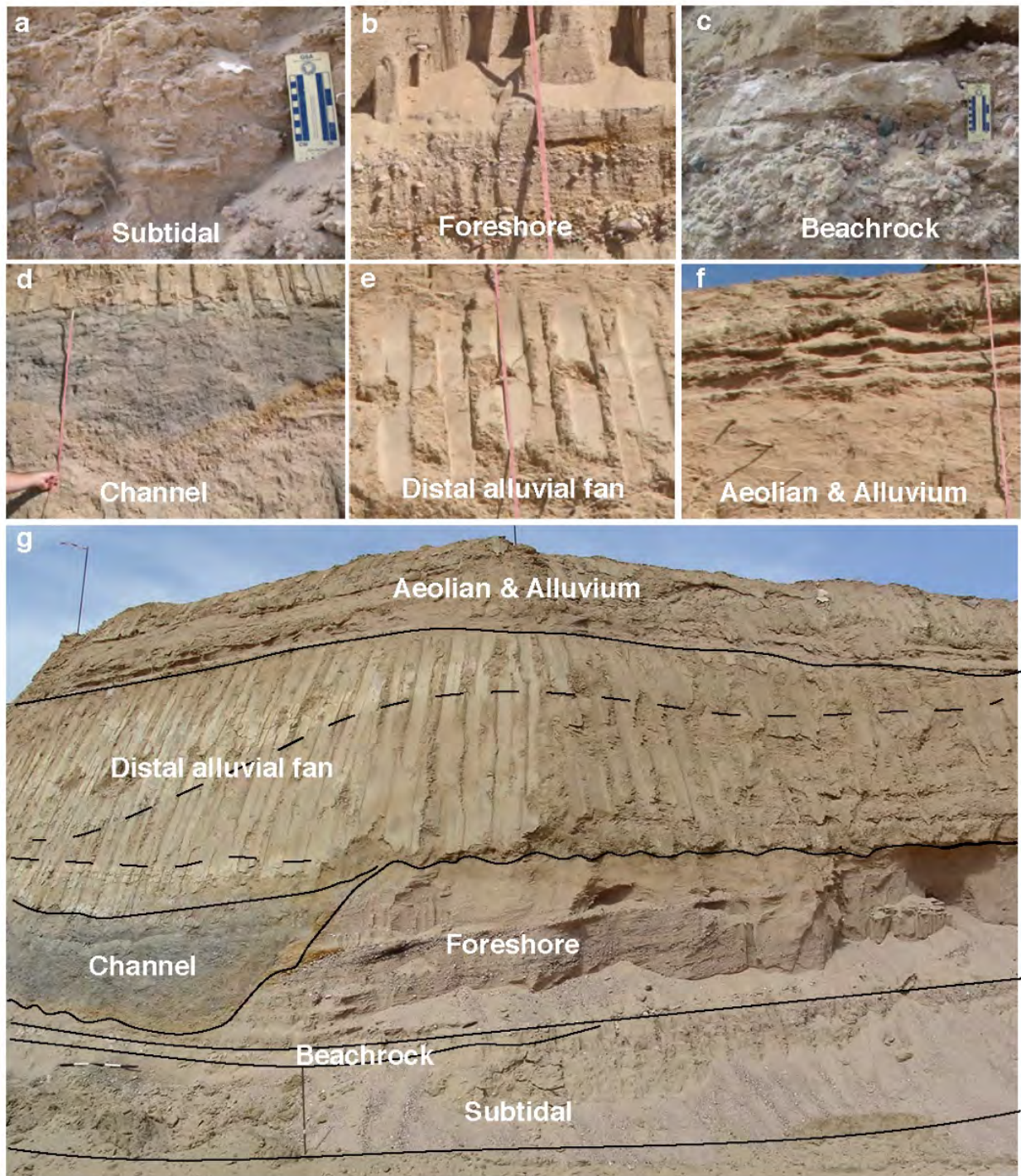


Figure 10: Facies model

The base of the channels cut below present sea level. The erosion at the base of the channel connects with the irregular unconformity at the top of the foreshore facies and they appear to be genetically linked. The channel-fill thickness varies but in places is >1.5 m. Sediment within the channels ranges in color from dark gray at the bottom to grayish brown. The basal layer of the channels has abundant organic-rich material such as roots and wood fragments. Grain size of the sediment is sometimes well-sorted, coarse-to-medium sands. In other places, the channel is filled with sandy gravel that is either structureless or has cross-bedding (Figure 13).

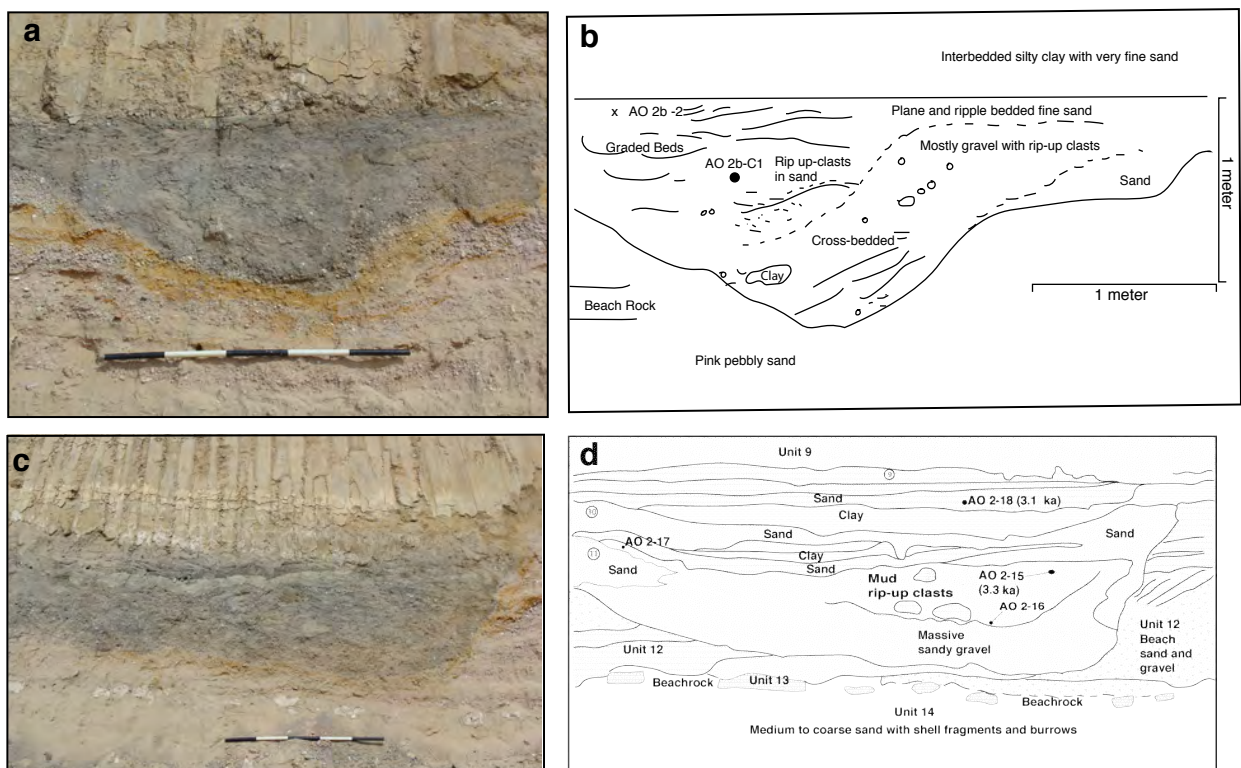


Figure 13: Details of the channel exposed at the AO-2 outcrop.

Rip-up clasts in the channel fill are abundant and composed of mud or fine sand (materials that are uncommon in the foreshore facies). Convolute beds of sand sometimes make up the basal layer of the channel (Figure 14). The middle layer sometimes contains *Cerithium* gastropods, but woody fragments are abundant. Capping the channel sequences are ripple beds, graded beds, and some plane-bedded sand with organic material in the ripple lag denoting a lowering of flow velocity. Soft-sediment deformation seen as convolute bedding and fluid-escape structures (Figure 14) suggests rapid deposition of water-laden sediment.

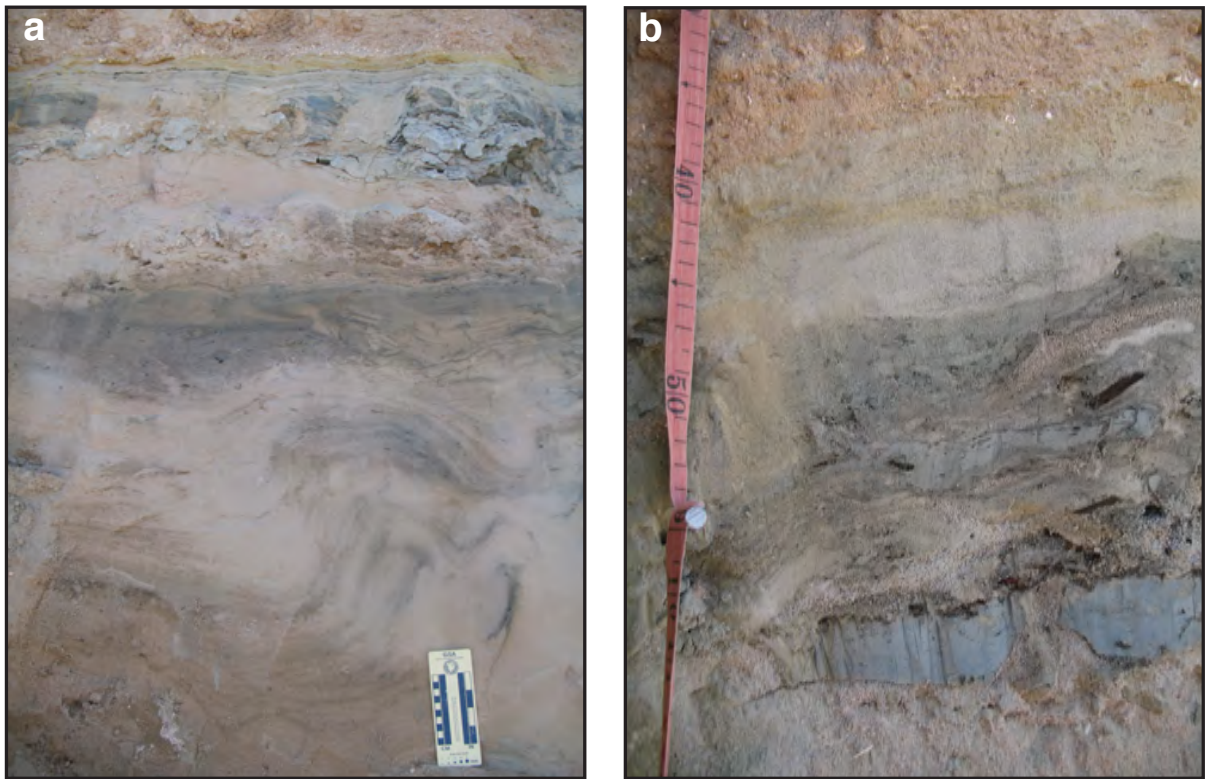


Figure 14: Convolute beds and terrestrial organic matter at the AO-3 outcrop

A distinct change in sedimentation is marked by distal alluvial fan and mudflat facies that overlies either the channel facies or the foreshore facies. The top of the channels are filled with yellow to yellowish brown layers of very well-sorted fine sand with alternating mud layers. The sediment of the distal alluvial fan and mud flat facies range in thickness between 2 to 3 m. The layers consist of interbedded sandy silt with clay directly above the channels to indurated sandy silt in the upper layers of the unit. Carbonate nodules and broken roots are also found in the layers. The sediment is moderately well-sorted fine sand. The top of the fan layer is marked with fine sand, cobbles, and loose roots.

The upper approximately 1 m of section contains ripple bedded and cross-bedded fine to medium sand that is interbedded with mud. The mud sometimes fills ripple swales and has mudcracks. This layer in other places is missing and artificial fill takes its place. The uppermost part of the section was designated as the aeolian and alluvium facies.

Buried Archaeological Structures

According to Pratico (1993), the elevation of the top of Tell el-Kheleifeh was measured as 6.83 masl and the 1938-1940 excavations by Nelson Glueck extended to a maximum depth of 4.37 masl. Therefore, the elevation of the land surface at the time of the founding of the settlement was approximately 2.5 masl. The distance from the shoreline to the southern edge of the tell is today about 500 m. Today, the distance from the shoreline to land at approximately 2.5 mbsl is approximately 200 m inland. These calculations suggest that Tel el-Kheleifeh was closer to the shoreline when it was occupied, perhaps a distance of 200 m.

Buried anthropogenic structures were found at the lagoon construction in August 2010 just south of the Tell el-Kheleifeh archaeological site (Figure 15). The map location of Tell el-

Kheleifeh is shown on figures 3 and 6. There are four structures exposed across the outcrop labelled TK-1, TK-2, TK-3, and TK-4.

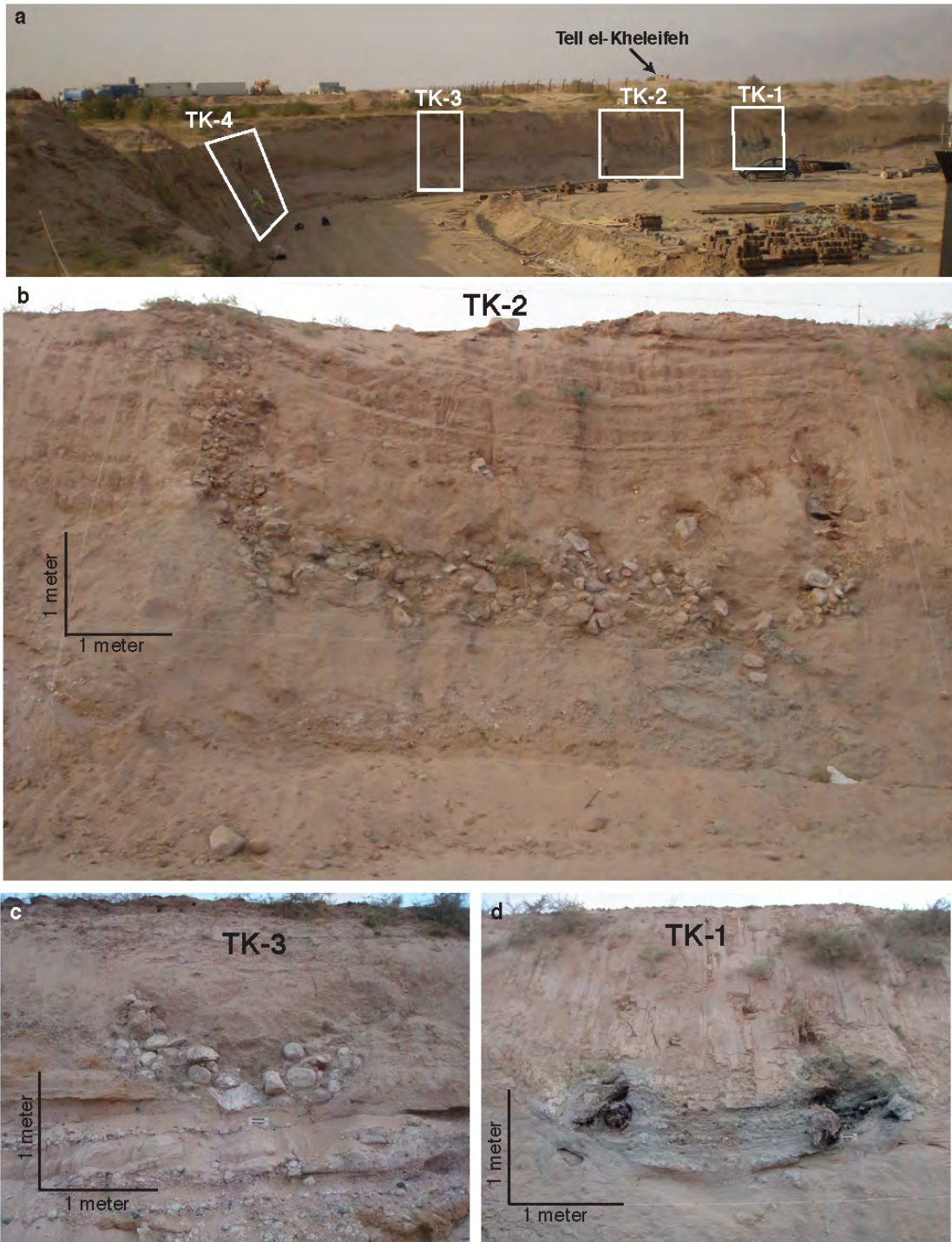


Figure 15: Photographs of buried walls near Tell el-Kheleifeh exposed in the Ayla Oasis lagoon construction in August 2010.

These structures appear to be walls, some with floors or rubble. The purpose of the structures is unknown. The top of the TK-1 structure is approximately 2 m below the surface and is just over 3 m wide. There are no walls at TK-1. There are two trees which appear to be palm trees lying down horizontally. There is a blue-gray sediment in between the trees that is composed of sandy gravel with abundant rip-up clasts interbedded with sand. There is no base to this feature. The feature is channel shaped and cuts into the pink foreshore beach facies. This outcrop may be equivalent to the channel facies exposed at sections AO-2 and AO-3.

The structure at TK-2 is 7 m wide. The top of the wall on the right is buried approximately 1.5 m below the surface. The wall on the left appears to extend to the ground surface, has a foundation trench that appears higher in elevation, and is likely younger than the wall on the right. The wall on the right is associated with a boulder and cobble rubble horizon that extends 7 m horizontally and is at least 1 m thick. Additional walls may be in this section as seen from boulders that are higher in the fill. The fill of TK-2 is pale brown sand with exposed cobbles which is structureless. Above the boulders the infill dips away from the wall on the left and bows into the center of the structure. Under the structure is beachrock overlying sand and pebbles of the foreshore facies.

TK-3 is a smaller structure measuring 2 m across with what appears to be two walls and a floor. The top of each wall structure is approximately a meter below the surface, and floor at its center is at a depth of 2 m. The structure is overlying beachrock and foreshore facies sediment.

The structure and units for TK-4 are outlined in Figure 16 with a corresponding image from the field. The outcrop measures 5.5 m in height. The top of each wall of the TK-4 structure

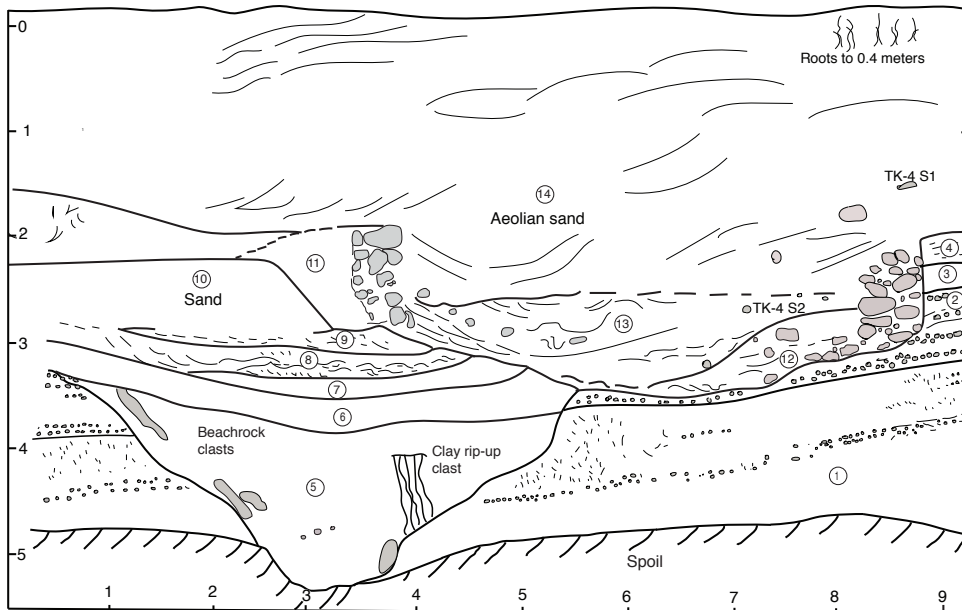


Figure 16: Section drawing of the TK-4 buried structure

is approximately 2 m below the surface and buried by aeolian sands of Unit 14. The walls are about 1 m in height and about 4 m apart. Boulders and cobbles in the wall are composed of granite, coral fragments, and beachrock blocks. The fill in between the walls is about 1.5 m at the center. The lower units in the fill (Units 12 and 13) show evidence of water flow including

cross stratification, ripple beds, and convolute bedding. The structure has no apparent floor and is sitting on top of the subtidal and foreshore facies (Unit 1) which is pink sand interbedded with pebbles, beachrock facies (Unit 3) and the channel facies (Units 5-8).

Beneath the TK-4 structure an erosional channel of blue-gray sediment cuts into the foreshore beach facies. The depth of the base of the channel is approximately 2.5 m which is evidence for erosion below current sea level. The eastern wall was built up against beachrock as indicated in Unit 2 (Figure 16). Given a ground surface elevation of 4 masl, the elevation of the beachrock in Unit 2 is 1.3 masl. The foundation trench (Unit 11) of the western wall was cut into the alluvial fan sediment of Unit 10. The top of Unit 10 is likely the land surface at the time of the walled structure at 2.4 masl as noted by the oxidation of this horizon and root casts.

Age Control and Elevation

The results for the radiocarbon analysis from the blue-gray channel and sediment overlying it are given in (Table 1). The sample labeled AO-2-18 was charcoal collected from a depth of 4.2 m from the surface which corresponds to an elevation of -0.2 to -0.6 mbsl, and is above the channel sequence. The calibrated age range for this sample is 2979-3173 cal BP with a median age of 3092 cal BP. This date of 3.1 ka likely caps the event that created the channels. The other sample from AO-2-15 was a wood fragment taken from a depth of 4.6 m which corresponds to an elevation of -0.8 mbsl. The sample was collected from the channel sequence at the AO-2 location. The age range for the sample is 3181-3359 with a median age of 3278 cal BP (i.e. 3.3 ka). The AO-3 sample was also a wood fragment collected at a depth of 3.6 m which corresponds to an elevation around sea level, and is within the channel sequence. The age range is 3609-3826 cal BP with a median age of 3688 cal BP (i.e. 3.7 ka).

The AO-7b sample from within the channel has a mean age of 6.5 ka and is older than the 3.3 ka age from the same channel fill and may be inherited age. These data indicate that the channel likely formed after 3.3 ka and before 3.1 ka.

Surface level for the Ayla Oasis Development prior to excavation for the artificial lagoons was 4 masl at the TK-4, AO-2, and AO-3 sites. The base of the excavation was -3.2 mbsl. The exposures measured 7 m. The channel sequence downcuts through the foreshore sediment to various depths up to 2.5 m. This places the base of the channel and the depth of erosion below modern sea level.

A survey of the outcrop at the Ayla Oasis tidal lagoon site (waypoint track in Figure 3) showed that the foreshore facies extended 700 m inland from the shoreline. The highest elevation of the beachrock was measured in the TK-4 section where it was mapped at 2.7 m below the ground surface. Given that the elevation of the TK-4 site is 4 masl, the beachrock marks a highstand of sea level at +1.3 m. The beachrock was not directly dated but must be older than the channel that cross cuts it which is dated to 3.3 ka. Furthermore, Brückner (1999) radiocarbon dated a *Codakia* (clam) shell (sample AQ-5) that was collected from a depth of 5.1 m in a borehole located at approximately 340 m from the shoreline which corresponds to 1.4 mbsl. The recalibrated ages using the Gulf of Aqaba ΔR correction (Table 2) yield a mean probability of 3472 cal BP (i.e. 3.5 ka). The TK-4 beachrock which lies at a higher elevation denoting the sea had transgressed farther inland, must be younger than 3.5 ka.

Brückner (1999) also radiocarbon dated a shell (sample AQ-6) from the marine deposits collected from a depth of 7.7 m in a borehole located approximately 600 m from the shoreline. This corresponds to an elevation of 2.6 mbsl. The shell was dated to the age range 6268-6665 cal BP with a median age of 6459 cal BP (6.5 ka). As the shell was collected from

the subtidal facies which has an assemblage of shells indicating a water depth of 5 m, these data suggest that sea level at 6.5 ka may have already been higher-than-present. We recalibrated his ages using the ΔR correction (Table 2).

CHAPTER 5

DISCUSSION

Tell el-Kheleifeh

The age-old question of the location of the Biblical port city of Ezion-Geber remains a mystery despite the assumptions of Frank and Glueck. Pratico (1993) all but confirmed that the ruins of Tell el-Kheleifeh are not Ezion-Geber by re-calibrating the ages of pottery samples collected during Glueck's excavation of the Tell. Bruckner (1999) questioned more the location of tell along the coastline of Aqaba. He speculated ports associated with the ancient settlement are more likely along the eastern coast of Aqaba. Bruckner (1999) surmised that if the Tell was actually the port of Ezion-Geber, given its location of 550 m from the modern coastline, then the shore must have been closer to the Tell in order for the settlement to have been a port. As well, Bruckner (1999) reasoned climate must have been warmer and wetter in order for trees to grow that were suitable to build ships belonging to the port. This is interesting to note with respect to the two overturned trees found in the outcrop at TK-1, although the buried trees appear to have been palm trees.

Bruckner (1999) collected samples from six boreholes that extend from 3 masl to 5 masl elevation along a 700 m transect from the coastline to 100 m north of the archaeological site of Tell el-Kheleifeh. Depths of the cores ranged from 6 m to 9.75 m. From the core data, Bruckner (1999) interpreted a marine transgression at 6 ka with regressive sequences and change to alluvial conditions after 3.5 ka.

Sea Level Highstand

Outcrops at the sites AO-2, AO-3, and TK-4 sites in the wall of the lower tidal lagoon construction site at the Ayla Oasis development provided a 3-D exposure of the strata architecture that had never been seen. We define a sequence that includes a lower subtidal facies overlain by beachrock and foreshore facies that were deposited in the intertidal zone. Overlying these beach sediments is an enigmatic unconformity that shows an erosional down-cutting event that extended below present sea level followed by a rapid infilling of the erosional channels. Overlying the erosional event, there is little evidence of continued beachface deposition. Stratigraphically above the channels are layers that include mudflat deposits, distal alluvial fan deposits, and sand dunes.

Our study of the Ayla Oasis tidal lagoon outcrops shows that *in situ* beachrock at the TK-4 site located 500 m inland from the modern shoreline lies at an elevation of 1.3 masl. Mauz et al., (2015) investigated beachrock outcrops along the coast of the Mediterranean Sea and argued that beachrock formation is a reliable indicator for relative sea level change because of the limited geographic locations of coral reefs and of the non-linear growth rate of coral colonies (Montaggioni, 2005). The rapid lithification of beachrock which occurs in decades preserves evidence of the intertidal zone (Hopley, 1986).

Al-Ramadan (2014) studied beachrock from the Gulf of Aqaba and discerned its formation begins with organic processes. He notes that micrite envelopes are around the siliciclastic grains in the Gulf of Aqaba beachrock. The micrite envelopes are microcrystals of high-magnesium calcite (HMC), and Al-Ramadan (2014) suggests the envelopes are the result of boring activity by algae whose decay created anaerobic conditions which led to the carbonate precipitation. The beachrock samples in Al-Ramadan's study also contain acicular

aragonite cement growing perpendicular to the micritic envelopes which he notes are formed through evaporation of seawater during low tides (e.g., Stoddart and Cann, 1965; Hanor, 1978). The beachrock sample from Ayla Oasis has micritic envelopes around the grains with acicular aragonite cement growing perpendicular to the envelopes. Al-Ramadan (2014) draws a conclusion that beachrock cementation is organic by linking algal activity and micritic coatings on the grains. While beachrock formation is fairly rapid, the presence of algae points to the water level at a consistent elevation for a period of time to allow the algae to grow. Given the beachrock at our location has the same features as the beachrock in the Al-Ramadan (2013) study it is likely conditions which lead to algal growth were favorable in the intertidal zone at Ayla Oasis.

At the Ayla Oasis, vertical succession of at least three beachrock layers indicates an aggrading beachface likely due to rising sea level. The highest position of beachrock at the Ayla Oasis outcrops reflects the maximum transgression and is found at 1.3 masl. Bruckner (1999) did not report beachrock in his borehole sediment, and he attributed marine sediments he found above modern sea level to be storm deposits only. In the coring study of Allison and Niemi (2010), a 6 ka marine transgression is overlain with regressive sequences (lagoons, backshore lake, alluvium, and dunes) capped by anthropogenic deposits. The data were not interpreted as evidence for higher-than-present sea level even though marine foraminifera was found in a layer above sea level. This points more to the limitations of methodology as elevation is difficult to record in a coring campaign and the point source data of cores cannot match the newly excavated continuous outcrop of the subsurface.

There is a growing body of evidence that the Gulf of Aqaba and the northern Red Sea had higher-than-present sea level based on elevated coral reefs, elevated wave-cut notches, and

beachrock (Figure 17). Hein et al. (2011) discussed coastal morphology along the Red Sea at the site of Mersa at the Wadi Gawasis in Egypt, and the relationship of those changes with sea level fluctuation, changing climate, and sediment deposition. Their research leads them to conclude a 0.5 to 2 masl at 5 ka was linked to melt after the last glacial maximum and isostatic rebound. Hein et al. (2011) tracked changes in sea level with data from features along the Red Sea Coast. The beachrock from the TK-4 site is included on the curve (Figure 17).

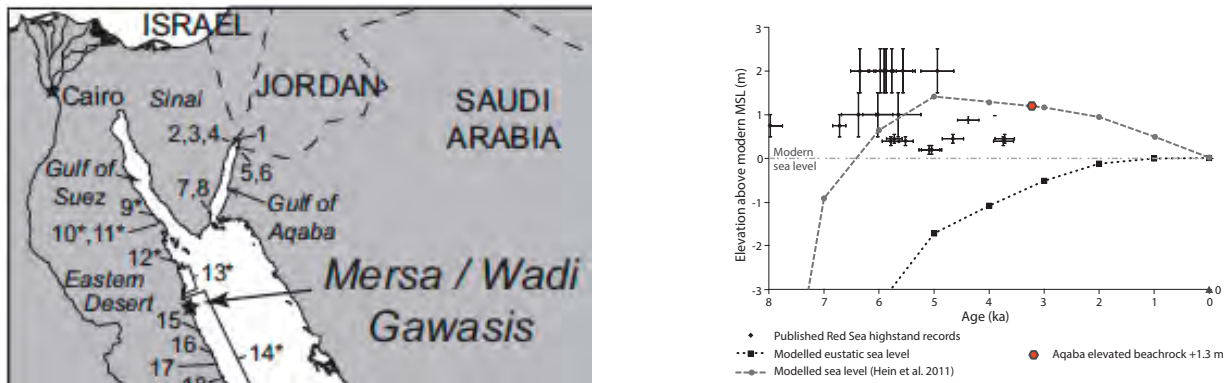


Figure 17: Holocene sea level curve for the Gulf of Aqaba and Northern Red Sea (Hein et al. 2011). See Table 3 for locations of sites.

Other research conducted in the area which points to higher-than-present sea level looked at elevated and buried coral reefs in the Gulf of Aqaba. Al-Rifaiy and Cherif (1988) studied a sequence of fossilized reefs south of Aqaba along the border between Jordan and Saudi Arabia. Their investigation led them to interpret seven terraces of fossil reef units, all above modern sea level, with the most recent unit at the shore and is partially submerged. The terraces vary in height between 1 and 10 m and rise inland by approximately 30 m. Al-Rifaiy and Cherif (1988) determined the terraces were built over three cycles with a 4th cycle of current modern reef growth. The modern reef overlies the submerged terrace. One terrace they studied is located 1-2 masl, and interpreted to be mid-Holocene. They did not use radiocarbon

dating on the organics found in their research, but correlated it to an elevated reef in Eilat (Friedmann, 1965). The elevation however corresponds to beachrock found 1.3 masl at TK-4. They concluded the cycles were determined by changes in eustatic sea level by glacial and interglacial periods in the late Pleistocene. However, they also surmised coastal erosion and tectonic activity to be a factor in reef burial and regrowth.

Shaked et al. (2004) discussed buried coral reefs as proxies for climate and sea level change. They studied a late Holocene reef under the Interuniversity Marine Lab in Eilat, Israel on the Gulf of Aqaba. The buried reef was found under siliciclastic sediments. Pristine preservation of the reef suggested rapid deposition of sediment. Shaked et al (2004) excavated further under the buried reef to discover two distinct periods of growth and destruction of the reef. Their study of the buried reefs suggested a history of a reef developing ca 5 ka at approximately 1 masl. The most recent age from radiometric dating of corals from the buried reef revealed a date of 2.3 ka. Shaked et al. (2004) concluded an earthquake occurred 2300 years ago and buried the reef. These and other studies along the Gulf of Aqaba and the northern Red Sea (Table 3) supports higher-than-present sea level in the mid-Holocene.

Table 3: Holocene higher-than-present sea level indicators along the Gulf of Aqaba and northern Red Sea (Data from Hein et al., 2011)

Site ID	Site Name	North Lat.	East Long.	Sea Level Marker	Elevation Above Modern MSL	Reported Radiocarbon Age (BP)	Calibrated (1 sigma) Radiocarbon Age OR U/Th Age (BP)	Citation
1	Eilat, Israel, Gulf of Aqaba	29° 32'	34° 57'	Coral terrace	-1 m to 1 m	4770 ± 140	4827 ± 211	Friedman, 1965
2	Eilat, Israel, Gulf of Aqaba	29° 31'	34° 56'	Emergent reef terrace	2 m	4450 - 5750	4423 - 6017	Moustafa et al., 2000
3	Eilat, Israel, Gulf of Aqaba	29° 31'	34° 56'	Coral terrace	1 m	N/A	5380 ± 50	Shaked et al., 2004
4	Eilat, Israel, Gulf of Aqaba	29° 31'	34° 56'	Coral terrace	1 m	N/A	4960 ± 50	Shaked et al., 2004
5	Jordanian Coast of Gulf of Aqaba	29° 27'	34° 58'	Reef Terrace	0.45 - 0.55 m	5570 - 6210	5774 - 6480	Dullo and Montaggioni, 1998
6	Jordanian Coast of Gulf of Aqaba	29° 27'	34° 58'	Reef Terrace	1 - 2 m	Interpreted as mid-Holocene	N/A	Al-Kifaiy and Cherif, 1988; Bouchon et al., 1981
7	Umm-Sid Reef, Esh-Shaura El-Manqata, Egypt	28° 13'	34° 26'	Reef Terrace	0.5 m	Range of dates: 2500 - 6800 (mean 4885)	N/A	Gvirtzman et al., 1992; Gvirtzman, 1994
8	Umm-Sid Reef, Maria Schroeder Wreck, Egypt	28° 11'	34° 27'	Reef Terrace	0.5 m	Range of dates: 5300 - 6500 (mean 5800)	N/A	Gvirtzman et al., 1992; Gvirtzman, 1994
9	Ras Shukeir, Egypt	28° 08'	33° 14'	Coral terrace	1 m	5420 ± 350	5655 ± 410	Plaziat et al., 1998
10	Ras Dib, Egypt	28° 01'	33° 24'	Coral terrace	2 m	5740 ± 360	5978 ± 395	Plaziat et al., 1998
11	Ras Dib, Egypt	28° 01'	33° 24'	Coral terrace	2 m	5550 ± 380	5773 ± 428	Plaziat et al., 1998
12	Gebel Abu Shaar, Egypt	27° 18'	33° 45'	Shell middens	2 m	5365 - 6075	5572 - 6352	Plaziat et al., 1998
13	Hurghada, Safaga, Giftun Islands, Egypt	26° 45' to 27° 13'	33° 58' to 33° 51'	Reef terrace	0.2 - 0.45 m	3930 - 5580	3721 - 5792	Dullo and Montaggioni, 1998
14	Safaga to Ras Banas, Egypt	23° 56' to 26° 43'	35° 29' to 33° 56'	Erosional terrace	1 m	5390 - 6410	5615 - 6713	Plaziat et al., 1998

Blue-Gray Channels

The unique aspect of the transgressive and regressive sequence of the Ayla Oasis exposure is the presence of an erosional down-cutting event and subsequent rapid channel infilling that marks the boundary between subtidal and beach sediment and the overlying alluvium and aeolian sediment. The channel erosion cuts to depths that are below modern sea level. In only a few locations, beach sediment is seen above the channel deposits. The data suggest that either sea level rapidly fell below present and rose back up around 3.2 ka, or another mechanism needs to be explored to explain the features. One mechanism that can cause extensive erosion and rapid deposition within channels is a tsunami.

Given the location of the channels found at Ayla Oasis, the distance to the shore could have been closer given the channel sequences cut into the foreshore beach face. This supports evidence sea level was higher-than-present. Sediments found within the erosional channels are congruent with fast-moving water. The color of the sediment in the channels is gray to grayish-blue or dark brown. Sedimentary structures found within the channels include rip-up clasts, cross beds, pebbles, cobbles, and convoluted beds (soft sediment deposition – rapid dewatering – static liquefaction). Massive beds of pebbly sand, rip-up clasts, and soft-sediment deformation structures point towards a possible flood event or tsunami.

Dawson and Stewart (2007) discuss characteristics of tsunami deposit beds in a tectonically active margin. Those features include an erosional base and rip-up clasts. Uimitsu et al. (2006) discuss the modern tsunami at Sumatra and the features created by the flow. They note the color of the deposits ranges from white to green to dark gray based on the thickness of the tsunami deposits. They also describe erosional swales created near the beach ridges filled with chaotic tsunami deposits.

Simms et al. (2017) discuss an erosional feature identified in a GPR survey and coring campaign conducted along the Cascadia subduction zone in Northern California. The erosional features are described as cutting to a depth of 1.5 m. Simms et al. (2017) also note an abundance of organic material within the erosional feature and that the erosion extended approximately 110 m inland.

All of the channel-fill sediment at the Ayla Oasis exposures show an abundance of terrestrial vegetation. The blue-gray channels at Ayla Oasis share similar features with modern tsunami deposits along active tectonic margins such as the Chilean coast, Indonesia, and ancient buried features in the Cascadia Subduction Zone. The bedforms and organic material,

color, and sediment size of the channels at Ayla Oasis suggest evidence of tsunami which likely occurred between 3.3 ka and 3.1 ka. The sediment above the blue channels include mudflats and distal alluvial fans, and sand dunes indicating a regression of the shoreline.

CHAPTER 6

CONCLUSION

Investigating the sediment and interpreting the facies at AO-2, AO-3, and TK-4 outcrops at Ayla Oasis points to two conclusions. First, beachrock exposed at the TK-4 site is 1.3 m higher than present sea level. Radiocarbon dates from shells below the beachrock and the channel sequence that incised through the beachrock and constrain the age of the beachrock to be younger than 3.5 and older than 3.3 ka. This is significant due to the location of the exposure and its proximity to the archaeological site of Tell el-Kheleifeh, and could possibly lead to a reinterpretation of the purpose of the Tell and its importance in history. Second, the erosional event which led to the formation of the channels marks a boundary between the foreshore facies and distal alluvial deposits. The sedimentary structures and within the channels such as convoluted beds, cross-beds, rip-up clasts, and abundant organic material suggest an event with flow velocity strong enough to downcut 1-2 m through beach deposits followed by rapid infilling. As sea level is not likely to regionally change rapidly, the erosional event is more likely evidence for a local tsunami. Age of sediment in the channel and overlying the channel constrain the event to be between 3.3 ka and 3.1 ka. Since the Gulf of Aqaba and the city of Aqaba lie on an active tectonic plate boundary, the impact of a tsunami stemming from an earthquake could have a significant effect on the inhabitants of the region. Given Aqaba's projected growth over the next decade, the need for increased awareness of tsunami potential in the Gulf of Aqaba is evident.

REFERENCES

- Al Shqour, R., 2019. *The Aqaba Khans and the Origin of Khans in Jordan: An Archaeological Approach*. Piscataway, NJ: Gorgias Press. 558p.
- Al-Rifa'iy, I. and Cherif. O., 1988. The fossil coral reefs of al-Aqaba, Jordan. *Facies*, 18(1), 219-29.
- Al-Ramadan, K., 2014. Diagenesis of Holocene beachrocks: a comparative study between the Arabian Gulf and the Gulf of Aqaba, Saudi Arabia. *Arab Journal of Geosciences*, 7, 4933–4942.
- Al-Rshaidat, M.M.D.; Segonds-Pichon, A., and Salem, M., 2020. Chlorophyll-nutrient relationships of an artificial inland lagoon equipped with seawater replenishment system in the northern Red Sea (Gulf of Aqaba). *Journal of Marine Science and Engineering*, 8, 147. doi:10.3390/jmse8030147
- Allison, J. and Niemi, T., 2010. Paleoenvironmental reconstruction of Holocene coastal sediments adjacent to archaeological ruins in Aqaba, Jordan. *Geoarchaeology: An International Journal*, 25(5), 602-625.
- Ambraseys, N., 2009. *Earthquakes in the Mediterranean and Middle East: A multidisciplinary study of seismicity up to 1900*. Cambridge: Cambridge University Press.
- Amit, R.; Zilberman, E.; Enzel, Y., and Porat, N., 2002. Paleoseismic evidence for time dependency of seismic response on a fault system in the southern Arava Valley, Dead Sea rift, Israel. *Geological Society of America Bulletin*, 114, 192-206.
- Aqaba Special Economic Zone Authority Website. <http://aseza.jo>.
- Bantan, R. and Abu-Zied, R., 2014. Sediment characteristics and molluscan fossils of the Farasan Islands shores, southern Red Sea, Saudi Arabia. *Arab Journal of Geosciences*, 7, 773-787.
- Ben-Avraham, Z., 1985. Structural framework of the Gulf of Elat (Aqaba), northern Red Sea. *Journal of Geophysical Research*, 90(B1), 1703-726.
- Ben-Avraham, Z.; Almagor, G., and Garfunkel, Z., 1979. Sediments and structure of the Gulf of Elat (Aqaba), northern Red Sea. *Sedimentary Geology*, 23, 239-267.
- Black, E.; Hoskins, C.; Slingo, J., and Brayshaw, D., 2011. The present-day climate of the Middle East. In: Mithen, S., and Black, E. (eds.), *Water, Life and Civilisation: Climate, Environment and Society in the Jordan Valley*. Cambridge: Cambridge University, pp. 13-24.

Blott, S.J. and Pye, K., 2001. GRADISTAT: A grain size distribution and statistics package for the analysis of unconsolidated sediments. *Earth Surface Processes and Landforms*, 26, 1237-1248.

Bouchon, C.; Jaubert, J.; Montaggioni, L., and Pichon, M. 1981. Morphology and evolution of the coral reefs of the Jordanian coast of the Gulf of Aqaba (Red Sea). *Proceedings of the Fourth International Coral Reef Symposium*, (Manila, the Philippeans), volume 1.

Brückner, H., 1999. Palaogeographische kustenforschung am Golf von Aqaba im bereich des Tell el-Kheleifeh, Jordanien, *Frankfurter Geowissenschaften Arbeiten*, serie D, Band 25, 25-41.

Dawson, A.G. and Stewart, I., 2007. Tsunami deposits in the geologic record. *Sedimentary Geology*, 200, 166-183.

El-Sorogy, A.S., 2015. Taphonomic processes of some intertidal gastropod and bivalve shells from northern Red Sea coast, Egypt. *Pakistan Journal of Zoology*, 47(5), 1287-1296.

Felis, T.; Lohmann, G.; Kuhnert, H.; Lorenz, S.J.; Scholz, D.; Patzold, J.; Al-Rousan, S.A., and Al-Moghrabi, S.M., 2004. Increased seasonality in Middle East temperatures during the last interglacial period. *Nature*, 429, 164-168.

Freund, R.; Zak, I.; Garfunkel, Z.; Goldberg, M.; Weissbrod, T., and Derin, B., 1970. The shear along the Dead Sea right. *Philosophical Transactions of the Royal Society*. London, 267, 105-127.

Friedman, G.M., 1965. A fossil shoreline reef in the Gulf of Elat (Aqaba). *Israeli Journal of Earth Sciences*, 14, 86-90.

Friedman, G.M., 1968. Geology and geochemistry of reefs, carbonate sediments and waters, Gulf of Aqaba (Elat), Red Sea. *Journal of Sedimentary Petrology*, 38(3), 895-919.

Ghazal, M., 2016. Population stands around 10.24 million, including 2.9 million guests. *The Jordan Times*, The Jordan News.

Galloway, J., 2011. Late Holocene paleoclimate reconstruction of the northern Gulf of Aqaba using foraminifera as a proxy. Kansas City, Missouri: University of Missouri-Kansas City, Master's thesis, 75p.

Goodman Tchernov, B.G.; Katz, T.; Shaked, Y.; Qupty, N.; Kanari, M.; Niemi, T., and Agnon, A., 2016. Offshore evidence for an undocumented tsunami event in the low risk Gulf of Aqaba-Eilat, Northern Red Sea, *Plos One*, doi: 10.1371/journal.pone.0145802.

Guidoboni, E. and Comastri, A., 2005. *Catalogue of earthquakes and tsunamis in the Mediterranean area from the 11th to the 15th century*. Istituto Nazionale di Geofisica e Vulcanologia, Rome

Hanor, J.S., 1978. Precipitation of beachrock cements: mixing of marine and meteoric waters vs. CO₂-degassing. *Journal of Sedimentary Petrology*, 48, 489–501.

Hartman, G.; Niemi, T.; Ben-Avraham, Z.; Tibor, G.; Al-Zoubi, A.; Al-Ruzouq, R., and Makovsky, Y., 2015. Distinct relict fringing reefs in the northern shelf of the Gulf of Elat/Aqaba: Markers of Quaternary eustatic and climatic episodes. *Sedimentology*, doi:10.1111/sed 12179.

Hartman, G.; Niemi, T.; Tibor, G.; Ben-Avraham, Z.; Al-Zoubi, A.; Makovsky, Y.; Akawwi, E.; Abueladas, A., and Al-Ruzouq, R., 2014. Quaternary tectonic evolution of the Northern Gulf of Elat/Aqaba along the Dead Sea Transform. *Journal of Geophysical Research*, 119, doi:10.1002/2013JB010879.

Hein, C.; Fitzgerald, D.; Milne, G.; Bard, K., and Fattovich, R., 2011. Evolution of a Pharaonic harbor on the Red Sea: Implications for coastal response to changes in sea level and climate. *Geology*, 39(7), 687-690.

Hopley, D., 1986. Beachrock as a sea-level indicator. In: Van de Plassche, O. (Ed.), *Sea-level Research: A Manual for the Collection and Evaluation of Data*. Geo Books, Norwich, pp. 157–173.

Ibrahim, K.M. and McCourt, W.J., 1995. Neoproterozoic granitic magmatism and tectonic evolution of the northern Arabian Shield: evidence from southwest Jordan. *Journal of African Earth Sciences*, 20(2), 103-118.

Jarrar, G.; Stern, R.J.; Saffarini, G., and Al-Zubi, H., 2003. Late- and post-orogenic Neoproterozoic intrusions of Jordan: implications for crustal growth in the northernmost segment of the East African Orogen. *Precambrian Research*, 123, 295–319.

Kanari, M., Niemi, T.M., Ben-Avraham, Z., Freislander, U., Tibor, G., Goodman-Tchernov, B.N., Wechsler, N., Abueladas, A., Al-Zoubi, A., Marco, S., and Basson, U., 2020. Seismic potential of the Dead Sea Fault in the northern Gulf of Aqaba-Elat: New evidence from liquefaction, seismic reflection, and paleoseismic data. *Tectonophysics*.

Kennedy, D., 2014. APAAME: Aerial photographic Archive for Archaeology in the Middle East. <http://www.apaame.org/2014/10/flights-20141019-20-aqaba-trip.html>.

Khalil, L. and Schmidt, K., 2009. Prehistoric Aqaba I. *Orient-Archaeologia Band 23*. Rahden/Westfalen, Germany: Verlag Marie Leidorf, 443p.

Klimscha, F., 2013. Innovations in Chalcolithic metallurgy in the Southern Levant during the 5th and 4th Millennium BC. Copper-production at Tall Hujayrat al-Ghuzlan and Tall al-Magass, Aqaba Area, Jordan. In: Burmeister, S., Hanse, S. Kunst, M. and Müller-Scheeßel, N. (eds.), *Metal Matters: Innovative Technologies and Social Change in Prehistory and Antiquity*: Rahden/Westf. Leidorf, pp. 31-63.

Klinger, Y.; Le Béon, M., and Al-Qaryouti, M., 2015. 5000 yr of paleoseismicity along the southern Dead Sea Fault. *Geophysical Journal International*, 202, 313–327.

Makovsky, Y.; Wunch, A.; Ariely, R.; Shaked, Y.; Rivlin, A.; Shemesh, A.; Ben-Avraham, Z., Agnon, A., 2008. Quaternary transform kinematics constrained by sequence stratigraphy and submerged coastline features: The Gulf of Aqaba. *Earth Planetary Science Letters*, 271, 109–122.

Manasrah, R., 2015. Physical properties and exchange system of seawater in Ayla lagoons in the northern Gulf of Aqaba, Red Sea. *Fresenius Environmental Bulletin*, 24(4), 1232-1249.

Mansoor, N.; Niemi, T., and Misra, A., 2004. A GIS-based assessment of liquefaction potential of the city of Aqaba, Jordan. *Environmental and Engineering Geoscience*, 10(4), 297-320.

Mauz, B.; Vacchi, M.; Green, A.; Hoffmann, G., and Cooper, A., 2015. A tool for reconstructing relative sea level in the far-field. *Marine Geology*, 362, 1-16.

Montaggioni, L.F., 2005. History of Indo-Pacific coral reef systems since the last glaciation: development patterns and controlling factors. *Earth Science Reviews*, 71, 1–75.

Morcos, S.A., 1970. Physical and Chemical Oceanography of the Red Sea. *Oceanography of Marine Biology Annual Review*, 8, 73-202.

Niemi, T., 2014. Regional environmental setting, seismic history, and natural resources of Aqaba, Jordan. In: Parker, S.T. and Smith, A.M (eds.), *The Roman Aqaba Project Final Report: Volume 1, The Regional Environment and the Regional Survey*. Boston: Archaeological Reports 19, American School of Oriental Research, pp. 33-80.

Niemi, T. and Smith II, A., 1999. Initial results of the Southeastern Wadi Araba, Jordan Geoarchaeological Study: Implications for Shifts in Late Quaternary Aridity. *Geoarchaeology*, 14(8), 791-820.

Notroff, J.; Schmidt, K.; Siegel, U., and Khalil, L., 2014. Reconstructing networks, linking spaces—the view from the Aqaba region (Jordan). *Levant*, 46(2), 249-267.

Oxford Business Group, 2018. Aqaba. *The Report: Jordan*. Oxford, England.

Parker, S.T., 1997. Preliminary report on the 1994 season of the Roman Aqaba Project. *Bulletin of the American School of Oriental Research*, 305, 19-44.

Pratico, G., 2003. *Nelson Glueck's 1938-1940 Excavations at Tell El-Kheleifeh: A Reappraisal*. Atlanta, Georgia: Scholars Press. 223p.

Rashdan, M., 1988. *The Regional Geology of the Aqaba-Wadi Araba Area, Map Sheets 3049 III, 2949 II, Bulletin, 7*. Amman: Ministry of Energy and Mineral Resources, Natural Resources Authority, Geology Directorate.

Reimer, P.J.; Bard, E.; Bayliss, A.; Beck, J.W.; Blackwell, P.G.; Bronk-Ramsey, C.; Buck, C.E.; Cheng, H.; Edwards, R.L.; Friedrich, M.; Grootes, P.M.; Guilderson, T.P.; Haflidason, H.; Hajdas, I.; Hatté, C.; Heaton, T.J.; Hogg, A.G.; Hughen, K.A.; Kaiser, K.F.; Kromer, B.; Manning, S.W.; Niu, M.; Reimer, R.W.; Richards, D.A.; Scott, E.M.; Southon, J.R.; Turney, C.S.M., and van der Plicht, J., 2010. IntCal13 and MARINE13 radiocarbon age calibration curves 0-50000 years cal BP. *Radiocarbon* 55(4). doi:10.2458/azu_js_rc.55.16947.

Scholl and Ulmer-Scholle, 2003. *A color guide to the petrography of carbonate rocks: grains, textures, porosity, diagenesis*. Tulsa, Oklahoma: The American Association of Petroleum Geologists. *AAPG Memoir* 77.

Shaked, Y.; Agnon, A.; Lazar, B.; Marcio, S.; Avner, U., and Stein, M., 2004. Large earthquakes kill coral reefs at the north-west Gulf of Aqaba. *Terra Nova*, 16, 133-38.

Shamir, G.; Baer, G., and Hofstetter, A., 2003. Three-dimensional elastic earthquake modelling based on integrated seismological and InSar data: the Mw = 7.2 Nuweiba Earthquake, Gulf of Elat/Aqaba 1995 November. *International Journal of Geophysics*, 154, 731-744.

Simms, A.R.; DeWitt, R.; Zurbuchen, J., and Vaughan, P., 2017. Coastal erosion and recovery from a Cascadia subduction zone earthquake. *Marine Geology*, 392, 30-40.

Slater, L. and Niemi, T., 2003. Ground-penetrating radar investigation of active faults along the Dead Sea Transform and implications for seismic hazards within the city of Aqaba, Jordan. *Tectophysics*, 368, 33-50.

Stoddart, D.R., Cann, J.R., 1965. Nature and origin of beach rock. *Journal of Sedimentary Petrology*, 35, 243–247.

Stuiver, M. and Braziunas, T. F., 1993. Modeling atmospheric 14C influences and 14C ages of marine samples to 10,000 BC. *Radiocarbon*, 35, 137-189.

Stuiver, M. and Reimer, P.J., 1993. Extended 14C data base and revised CALIB 3.0 14C age calibration program. *Radiocarbon*, 35, 215-230.

Tibor, G., T. Niemi, Z. Ben-Avraham, A. Al-Zoubi, R. Sade, J. Hall, G. Hartman, E. Akawi, A. Abueladas, and R. Al-Ruzouq (2010), Active tectonic morphology and submarine deformation of the northern Gulf of Eilat/Aqaba from analyses of multibeam data, *Geo Mar. Lett.*, 30, 561–573.

Thomas, R.; Niemi, T., and Parker, S.T., 2007. Structural Damage from Earthquakes in the second-ninth centuries at the archaeological site of Aila in Aqaba, Jordan. *Bulletin of the American School of Oriental Research*, 346, 59-77.

Umitsu, M.; Tanavud, C., and Patanakanog, B., 2007. Effects of landforms on tsunami flow in the plains of Banda Aceh, Indonesia, and Nam Khem, Thailand. *Marine Geology*, 242, 141-153.

Wentworth, C., 1922. A Scale of Grade and Class Terms for Clastic Sediments. *The Journal of Geology*, 30(5), 377-392.

Whitcomb, D., 1994, *Ayla: Art and Industry in the Islamic port of Aqaba*. Chicago, IL: Special Publications, Oriental Institute of the University of Chicago.

Wust, H., 1997. *The November 22, 1995 Nuweiba earthquake, Gulf of Elat (Aqaba). Post-Seismic Analysis of Failure Features and Seismic Hazard Implications*. Jerusalem, Israel: Geological Survey of Israel Report GSI 3-97.

Zilberman, E.; Amit, R.; Porat, N.; Enzel, Y., and Avner, U., 2005. Surface ruptures induced by the devastating 1068 AD earthquake in the southern Arava valley, Dead Sea Rift, Israel. *Tectonophysics* 408, 79–99. <https://doi.org/DOI: 10.1016/j.tecto.2005.05.030>

APPENDIX A
Sample Metadata

AO - 1

Location: 29 32'35" N, 34 58'47" E

<u>Sample #</u>	<u>Unit</u>	<u>Munsell Color</u>	<u>Grain Size</u>	<u>Parameters</u>	<u>Field Notes & Lab Analysis</u>
AO-1 6	10		C-14 Sample		Charcoal, Sample not processed
AO-1 8	10	10 YR 4/4 Dark yellowish brown	Moderately well sorted fine sand	Unimodal, Fine Skew, Platykurtic	Above channel, clay layer
AO-1 3	4	5 YR 6/3 Light reddish brown	Moderately well sorted medium sand	Trimodal, Coarse Skew, Platykurtic	Outside wall B, parallel to channel black sediment "very fine sand", shells
AO-1 5	18	7.5 YR 7/4 Pink	Well sorted fine sand	Unimodal, Fine Skew, Very Leptokurtic	Outside wall A, shells in sand layer
AO-1 4	31	10 YR 4/4 Dark yellowish brown	Poorly sorted medium sand	Bimodal, Very Fine Skew, Very Platykurtic	Top of channel, clay
AO-1 13	22	10 YR 5/4 Yellowish brown	Moderately well sorted fine sand	Bimodal, Coarse Skew, Very Leptokurtic	In Channel
AO-1 2	20	10 YR 5/2 Grayish brown	Very well sorted fine sand	Unimodal, Symmetrical, Platykurtic	In channel, gastropod shells
AO-1 1	19		C-14 Sample		Charcoal, Sample not processed
AO-1 11	19	7.5 YR 4/1 Dark gray	Well sorted fine sand	Unimodal, Symmetrical, Leptokurtic	In channel top unit 19, carbon layer, gastropod shell, woody fragments, XRD
AO-1 12	19	7.5 YR 4/1 Dark gray	Moderately well sorted fine sand	Unimodal, Coarse skew, Leptokurtic	In channel roots from unit 19, XRD
AO-1 9	1	10 YR 6/3 Pale brown	Well sorted fine sand	Unimodal, Coarse Skew, Mesokurtic	Below channel, pink sand
AO-1 10	26	10 YR 6/3 Pale brown	Well sorted medium sand	Unimodal, Coarse Skew, Mesokurtic	Below channel
AO-1 7	27	5 YR 6/2 Pinkish gray	Well sorted fine sand	Unimodal, Symmetrical, Mesokurtic	Base of unit, blue sand with shells

AO - 2

Location: 29 32' 40" N, 34 58' 51" E

Sample #	Unit	Depth (m)	Munsell Color	Grain Size	Parameters	Field Notes & Lab Analysis
AO-2 4	4	1.3	10 YR 5/6 Yellowish brown	Moderately well sorted fine sand	Unimodal, Coarse Skew, Mesokurtic	Highly weathered granitic cobbles, top of unit possible soil horizon, modern roots, top of unit reddish in color, fine sand, no evident bedding
AO-2 5	5	2.18	7.5 YR 6/4 Light brown	Well sorted fine sand	Unimodal, Fine Skew, Platykurtic	Fine sand indurate with calcite, base of pedogenic unit (4&5) possible BK horizon
AO-2 6	6	2.67	10 YR 7/3 Very pale brown	Very well sorted very fine sand	Unimodal, Symmetrical, Leptokurtic	Sandy-silty-clay, carbonate nodules & root casts
AO-2 7	7	2.85	10 YR 6/4 Light yellowish brown	Moderately well sorted fine sand	Bimodal, Fine Skew, Leptokurtic	Sandy silt, indurated
AO-2 8	8	3.25	10 YR 6/4 Light yellowish brown	Moderately well sorted fine sand	Bimodal, Fine Skew, Leptokurtic	XRD, Fine sand, carbonate nodules
AO-2 9	9	3.6	10 YR 6/4 Light yellowish brown	Moderately well sorted fine sand	Bimodal, Coarse Skew Mesokurtic	Interbedded sand/silt/clay
AO-2 10	10	4.05	7.5 YR 7/2 Pinkish Gray	Moderately well sorted fine sand	Unimodal, Symmetrical, Leptokurtic	Top of channel, gray coarse sand slightly cemented, top of unit iron oxide stain
AO-2 18	10	4.2		C-14 Sample		Charcoal
AO-2 15	11	4.6		C-14 Sample		Wood fragment
AO-2 12a	12	5.2	7.5 YR 5/4 Brown	Moderately sorted coarse sand	Bimodal, Very Fine Skew, Mesokurtic	Below channel, Rip up clasts, coarse sand, bluish gray
AO-2 12b	12	5.4	7.5 YR 5/4 Brown	Moderately sorted medium sand	Bimodal, Coarse Skew Platykurtic	85cm thick parallel inclined bedding, interbedded sand & pebbles, slightly indurated vertical root casts, iron staining at top of unit with sand waves & cross-bedding, clams, gastropod shells.
No Sample				Beachrock		Beachrock 22cm thick broken in disjointed layer (unit sampled at section AO 3)

AO - 3

Location: 29 32'43" N, 34 58' 53" E

Sample #	Unit	Depth (m)	Munsell Color	Grain Size	Parameters	Field Notes & Lab Analysis
AO-3 16	11	3.2		C-14 Sample		Sample not run
AO-3 11	5	3.2	Very pale brown	Well sorted very fine sand	Unimodal, Coarse Skew, Mesokurtic	Brown, irregular structure, blue at base rises north, XRD
AO-3 5	6	3.35	Reddish brown	Moderately well sorted medium sand	Unimodal, Fine Skew, Leptokurtic	Irregular contact, pink coarse sand, loose pebbles, shells (concave up clams, disarticulated below shells)
AO-3 4	7	3.4	Yellow	Moderately well sorted fine sand	Bimodal, Symmetrical, Very Leptokurtic	Erosional contact yellow sand
AO-3 7	7	3.5	Grayish brown	Well sorted fine sand	Bimodal, Fine Skew, Very Leptokurtic	In channel, blue-gray ripple bedded sand, caps channel sequence, XRD
AO-3 3	8	3.55	Gray	Poorly sorted coarse sand	Bimodal, Very Fine Skew, Very Platykurtic	In channel, XRD
AO-3 1	8	3.6		C-14 Sample		Wood fragment
AO-3 10	8	3.64	Grayish brown	Moderately well sorted fine sand	Bimodal, Fine Skew, Leptokurtic	In channel, fine blue sand interbedded with clay, XRD
AO-3 8	10	3.95	Light brown	Well sorted medium sand	Unimodal, Symmetrical, Mesokurtic	XRD, Sand with rip up clasts upper part of unit
AO-3 9	10	3.9	Light yellowish brown	Moderately sorted coarse sand	Bimodal, Very Fine Skew, Platykurtic	Rip up clasts upper unit
AO-3 13	11	4.3	Yellowish brown	Well sorted fine sand	Unimodal, Symmetrical, Leptokurtic	Sand
AO-3 12	12	4.5	Pale brown	Moderately sorted coarse sand	Bimodal, Fine Skew, Very Platykurtic	Rip up clasts at channel base
AO 3-14	14	4.5		Beachrock with oysters (photo)		
AO-3 15	15	7.45		Beachrock thin section		

TK - 4

Location: 29 32'46" N, 34 58'50" E

Ground Elevation 4masl

Base of Channel 1.5m below present sea level

<u>Sample #</u>	<u>Unit</u>	<u>Depth (m)</u>	<u>Munsell Color</u>	<u>Grain Size</u>	<u>Parameters</u>	<u>Field Notes & Lab Analysis</u>
TK-4 S1	14	1.7m				Pottery Sherd - Sample not run
TK-4 14	14	2.0	7.5 YR 6/4 Light brown	Moderately well sorted fine sand	Unimodal, Symmetrical, Very Leptokurtic	Top of Unit
TK-4 11	11	2.3	7.5 YR 6/3 Light brown	Poorly sorted coarse sand	Polymodal, Very Fine Skew, Platykurtic	Above layer 9, next to layer 10, touches wall A
TK-4 3	3	2.5	7.5 YR 6/3 Light brown	Moderately sorted fine sand	Trimodal, Coarse Skew, Leptokurtic	Above layer 2, outside wall B
TK-4 S2	13	2.7m				Pottery Sherd - Sample not run
TK-4 2	2	2.7	7.5 YR 7/4 Pink	Moderately sorted fine sand	Bimodal, Coarse Skew, Mesokurtic	Above beachrock, outside wall B, sand with shells and pebbles
TK-4 10	10	2.8	7.5 YR 6/3 Light brown	Well sorted fine sand	Unimodal, Coarse Skew, Leptokurtic	Above layer 9, outside wall A
TK-4 13	13	3.0	10 YR 5/1 Gray	Well sorted fine sand	Unimodal, Symmetrical, Leptokurtic	Channel inside wall above pink sand, XRD, SEM/EDS, blue-gray sediment with concretions and pyrite framboids
TK-4 9	9	3.2	7.5 YR 7/3 Pink	Moderately sorted coarse sand	Bimodal, Very Fine Skew, Platykurtic	Above channel outside wall A
TK-4 12	12	3.3	7.5 YR 7/4 Pink	Moderately well sorted fine sand	Bimodal, Symmetrical, Very Leptokurtic	Base of channel inside wall
TK-4 8	8	3.5	7.5 YR 7/4 Pink	Moderately well sorted fine sand	Unimodal, Coarse Skew, Leptokurtic	Above channel outside wall A
TK-4 6	6	3.8				Radiocarbon sample
TK-4 5a	5	4.5	10 YR 7/3 Very pale brown	Poorly sorted very fine sand	Trimodal, Very Coarse Skew, Very Platykurtic	Above beachrock
TK-4 1	1	4.5	7.5 YR 8/4 Pink	Moderately sorted fine sand	Bimodal, Very Coarse Skew, Mesokurtic	Base of Unit, Pink sand capped by beachrock

APPENDIX B

Grain Size Logs

Sample Number: AO-1 9, Unit 1
 Raw Mass (g): 173.10
 Dried Mass (g): 173
 Field Notes and Descriptors: Pink Sand

Sieve Number	Diameter (mm)	Mass of Empty Sieve (g)	Mass of Sieve + Soil Retained (g)	Soil Retained (g)	Percent Retained	Grain Size
10	2	479	480	1	0.58%	Lg Grains
18	1	361	365	4	2.31%	VC Sand
30	0.60	307	315	8	4.62%	Coarse Sand
60	0.25	283	336	53	30.64%	Med Sand
100	0.15	265	353	88	50.87%	Fine Sand
230	0.075	345	358	13	7.51%	VF Sand
270	0.053	344	345	1	0.58%	Silt
Pan	0.038	360	360	0	0.00%	Clay

Sample Number: AO-1 3, Layer 4

Raw Mass (g): 65.65

Dried Mass (g): 65

Field Notes and Descriptors: Shells, Black VF Sand XRD

			Mass of			
Sieve	Diameter	Mass of Empty	Sieve + Soil	Soil	Percent	Grain
Number	(mm)	Sieve (g)	Retained (g)	Retained (g)	Retained	Size
10	2	479	485	6	9.23%	Lg Grains
18	1	361	367	6	9.23%	VC Sand
30	0.60	307	324	17	26.15%	Coarse Sand
60	0.25	283	293	10	15.38%	Med Sand
100	0.15	265	289	24	39.92%	Fine Sand
230	0.075	345	346	1	1.54%	VF Sand
270	0.053	344	344	0	0.00%	Silt
Pan	0.038	360	361	1	1.54%	Clay

Sample Number: AO-1 8, Unit10

Raw Mass (g): 387

Dried Mass (g): 387

Field Description and Notes: Blue Clay

Sieve Number	Diameter (mm)	Mass of Empty Sieve (g)	Mass of Sieve + Soil Retained (g)	Soil Retained (g)	Percent Retained	Grain Size
10	2	479	0	0	0.00%	Lg Grains
18	1	361	0	0	0.00%	VC Sand
30	0.60	307	0	0	0.00%	Coarse Sand
60	0.25	283	0	0	0.00%	Med Sand
100	0.15	265	361	96	24.81%	Fine Sand
230	0.075	345	500	156	40.31%	VF Sand
270	0.053	344	409	165	16.80%	Silt
Pan	0.038	360	430	70	18.09%	Clay

Sample Number: AO-1 5-1, Unit18

Raw Mass (g): 28.61

Dried Mass (g): 28

Field Description and Notes: Shells

			Mass of			
Sieve	Diameter	Mass of Empty	Sieve + Soil	Soil	Percent	Grain
Number	(mm)	Sieve (g)	Retained (g)	Retained (g)	Retained	Size
10	2	479	480	1	3.57%	Lg Grains
18	1	361	361	0	0.00%	VC Sand
30	0.60	307	307	0	0.00%	Coarse Sand
60	0.25	283	285	2	7.14%	Med Sand
100	0.15	265	283	18	64.30%	Fine Sand
230	0.075	345	350	5	17.85%	VF Sand
270	0.053	344	346	2	7.14%	Silt
Pan	0.038	360	360	0	0.00%	Clay

Sample Number: AO-1 11, Carbon top of unit 19

Raw Mass (g): 95.16

Dried Mass (g): 95

Field Descriptors and Notes: XRD, Aquatic gastropod shell, wood (or plant) fragments

			Mass of			
Sieve	Diameter	Mass of Empty	Sieve + Soil	Soil	Percent	Grain
Number	(mm)	Sieve (g)	Retained (g)	Retained (g)	Retained	Size
10	2	479	479	0	0.00%	Lg Grains
18	1	361	362	1	1.05%	VC Sand
30	0.60	307	311	4	4.21%	Coarse Sand
60	0.25	283	297	14	14.73%	Med Sand
100	0.15	265	316	51	53.68%	Fine Sand
230	0.075	345	367	22	23.16%	VF Sand
270	0.053	344	346	2	2.11%	Silt
Pan	0.038	360	361	1	1.05%	Clay

Sample Number: AO-1 12, roots from Unit 19
 Raw Mass (g): 58
 Dried Mass (g): 58
 Field Descriptors and Notes: XRD, Bark/Wood, Granules

			Mass of			
Sieve	Diameter	Mass of Empty	Sieve + Soil	Soil	Percent	Grain
Number	(mm)	Sieve (g)	Retained (g)	Retained (g)	Retained	Size
10	2	479	480	1	1.72%	Lg Grains
18	1	361	363	2	3.45%	VC Sand
30	0.60	307	308	1	1.72%	Coarse Sand
60	0.25	283	293	10	17.24%	Med Sand
100	0.15	265	298	24	41.38%	Fine Sand
230	0.075	345	363	18	31.03%	VF Sand
270	0.053	344	345	1	1.72%	Silt
Pan	0.038	360	361	1	1.72%	Clay

Sample Number: AO-1 2, Unit20

Raw Mass (g): 5.57

Dried Mass (g): 5.55

Descriptors: Gastropod Shells

			Mass of			
Sieve	Diameter	Mass of Empty	Sieve + Soil	Soil	Percent	Grain
Number	(mm)	Sieve (g)	Retained (g)	Retained (g)	Retained	Size
10	2	479	479	0	0.00%	Lg Grains
18	1	361	361	0	0.00%	VC Sand
30	0.60	307	307	0	0.00%	Coarse Sand
60	0.25	283	283	0	0.00%	Med Sand
100	0.15	265	265	0	0.00%	Fine Sand
230	0.075	345	350	5.55	100.00%	VF Sand
270	0.053	344	340	0	0.00%	Silt
Pan	0.038	360	360	0	0.00%	Clay

Sample Number: AO-1 13, Unit 22

Raw Mass (g): 245

Dried Mass (g): 245

Descriptors:

			Mass of			
Sieve	Diameter	Mass of Empty	Sieve + Soil	Soil	Percent	Grain
Number	(mm)	Sieve (g)	Retained (g)	Retained (g)	Retained	Size
10	2	479	500	21	8.57%	Lg Grains
18	1	361	364	3	1.22%	VC Sand
30	0.60	307	310	3	1.22%	Coarse Sand
60	0.25	283	342	59	24.08%	Med Sand
100	0.15	265	378	113	46.12%	Fine Sand
230	0.075	345	388	43	17.55%	VF Sand
270	0.053	344	346	2	0.82%	Silt
Pan	0.038	360	361	1	0.41%	Clay

Sample Number: AO 1-10, Unit 26

Raw Mass (g): 198.27

Dried Mass (g): 198

Descriptors: Pink Sand

			Mass of			
Sieve	Diameter	Mass of Empty	Sieve + Soil	Soil	Percent	Grain
Number	(mm)	Sieve (g)	Retained (g)	Retained (g)	Retained	Size
10	2	479	481	2	1.01%	Lg Grains
18	1	361	368	7	3.54%	VC Sand
30	0.60	307	318	11	5.56%	Coarse Sand
60	0.25	283	370	87	43.94%	Med Sand
100	0.15	265	347	82	41.41%	Fine Sand
230	0.075	345	354	9	4.54%	VF Sand
270	0.053	344	344	0	0.00%	Silt
Pan	0.038	360	360	0	0.00%	Clay

Sample Number: AO-1 7, Unit21

Raw Mass (g): 127.23

Dried Mass (g): 126

Descriptors: Blue Sand, Large Shell

			Mass of			
Sieve	Diameter	Mass of Empty	Sieve + Soil	Soil	Percent	Grain
Number	(mm)	Sieve (g)	Retained (g)	Retained (g)	Retained	Size
10	2	479	480	1	0.79%	Lg Grains
18	1	361	362	1	0.79%	VC Sand
30	0.60	307	310	3	2.38%	Coarse Sand
60	0.25	283	318	35	27.78%	Med Sand
100	0.15	265	331	66	52.38%	Fine Sand
230	0.075	345	363	18	14.29%	VF Sand
270	0.053	344	345	1	0.79%	Silt
Pan	0.038	360	361	1	0.79%	Clay

Sample Number: AO-1 4, Unit31

Raw Mass (g): 45

Dried Mass (g): 45

Descriptors: Clay Sample

			Mass of			
Sieve	Diameter	Mass of Empty	Sieve + Soil	Soil	Percent	Grain
Number	(mm)	Sieve (g)	Retained (g)	Retained (g)	Retained	Size
10	2	479	0	0	0.00%	Lg Grains
18	1	361	0	0	0.00%	VC Sand
30	0.60	307	320	12	26.67%	Coarse Sand
60	0.25	283	303	18	40.00%	Med Sand
100	0.15	265	0	0	0.00%	Fine Sand
230	0.075	345	0	0	0.00%	VF Sand
270	0.053	344	0	0	0.00%	Silt
Pan	0.038	360	375	15	33.33%	Clay

Sample Number: AO Sect 2, Unit 4

Raw Mass (g): 98

Dried Mass (g): 97

Descriptors:

			Mass of			
Sieve	Diameter	Mass of Empty	Sieve + Soil	Soil	Percent	Grain
Number	(mm)	Sieve (g)	Retained (g)	Retained (g)	Retained	Size
10	2	479	481	2	2.06%	Lg Grains
18	1	361	365	4	4.12%	VC Sand
30	0.60	307	318	11	11.34%	Coarse Sand
60	0.25	283	304	21	21.65%	Med Sand
100	0.15	265	286	21	21.65%	Fine Sand
230	0.075	345	377	32	32.99%	VF Sand
270	0.053	344	346	2	2.06%	Silt
Pan	0.038	360	364	4	4.12%	Clay

Sample Number: AO 2, Unit 5

Raw Mass (g): 27

Dried Mass (g): 27

Descriptors:

			Mass of			
Sieve	Diameter	Mass of Empty	Sieve + Soil	Soil	Percent	Grain
Number	(mm)	Sieve (g)	Retained (g)	Retained (g)	Retained	Size
10	2	479	479	0	0.00%	Lg Grains
18	1	361	361	0	0.00%	VC Sand
30	0.60	307	307	0	0.00%	Coarse Sand
60	0.25	283	284	1	3.70%	Med Sand
100	0.15	265	280	15	55.55%	Fine Sand
230	0.075	345	354	9	33.33%	VF Sand
270	0.053	344	346	2	7.40%	Silt
Pan	0.038	360	360	0	0.00%	Clay

Sample Number: AO Sect 2, Unit 6

Raw Mass (g): 425

Dried Mass (g): 385

Descriptors:

			Mass of			
Sieve	Diameter	Mass of Empty	Sieve + Soil	Soil	Percent	Grain
Number	(mm)	Sieve (g)	Retained (g)	Retained (g)	Retained	Size
10	2	479	479	0	0.00%	Lg Grains
18	1	361	361	0	0.00%	VC Sand
30	0.60	307	307	0	0.00%	Coarse Sand
60	0.25	283	283	0	0.00%	Med Sand
100	0.15	265	317	52	13.51%	Fine Sand
230	0.075	345	610	266	69.10%	VF Sand
270	0.053	344	395	51	13.25%	Silt
Pan	0.038	360	376	16	4.15%	Clay

Sample Number: AO Sect 2, Unit 7

Raw Mass (g): 124

Dried Mass (g): 124

Descriptors: Limestone (Rounded), Wood or Grass

			Mass of			
Sieve	Diameter	Mass of Empty	Sieve + Soil	Soil	Percent	Grain
Number	(mm)	Sieve (g)	Retained (g)	Retained (g)	Retained	Size
10	2	479	479	0	0.00%	Lg Grains
18	1	361	361	0	0.00%	VC Sand
30	0.60	307	313	6	4.84%	Coarse Sand
60	0.25	283	298	15	12.10%	Med Sand
100	0.15	265	314	49	39.52%	Fine Sand
230	0.075	345	347	37	29.84%	VF Sand
270	0.053	344	347	3	2.42%	Silt
Pan	0.038	360	374	14	11.29%	Clay

Sample Number: AO 2-8, Unit 8

Raw Mass (g): 96

Dried Mass (g): 96

Descriptors: XRD Black Sand

			Mass of			
Sieve	Diameter	Mass of Empty	Sieve + Soil	Soil	Percent	Grain
Number	(mm)	Sieve (g)	Retained (g)	Retained (g)	Retained	Size
10	2	479	479	0	0.00%	Lg Grains
18	1	361	362	1	1.04%	VC Sand
30	0.60	307	310	3	3.13%	Coarse Sand
60	0.25	283	287	4	4.17%	Med Sand
100	0.15	265	303	38	39.58%	Fine Sand
230	0.075	345	383	38	39.58%	VF Sand
270	0.053	344	346	2	2.08%	Silt
Pan	0.038	360	370	10	10.42%	Clay

Sample Number: AO Sect 2, Unit 9 (3.7m)

Raw Mass (g): 66

Dried Mass (g): 66

Descriptors: XRD

			Mass of			
Sieve	Diameter	Mass of Empty	Sieve + Soil	Soil	Percent	Grain
Number	(mm)	Sieve (g)	Retained (g)	Retained (g)	Retained	Size
10	2	479	480	1	1.52%	Lg Grains
18	1	361	365	4	6.06%	VC Sand
30	0.60	307	313	6	9.09%	Coarse Sand
60	0.25	283	292	9	13.64%	Med Sand
100	0.15	265	277	12	18.18%	Fine Sand
230	0.075	345	365	20	30.30%	VF Sand
270	0.053	344	348	4	6.06%	Silt
Pan	0.038	360	370	10	15.15%	Clay

Sample Number: AO Sect 2, Unit 10

Raw Mass (g): 78.70

Dried Mass (g): 78

Descriptors: Wood Fragment

			Mass of			
Sieve	Diameter	Mass of Empty	Sieve + Soil	Soil	Percent	Grain
Number	(mm)	Sieve (g)	Retained (g)	Retained (g)	Retained	Size
10	2	479	480	1	1.28%	Lg Grains
18	1	361	364	3	3.85%	VC Sand
30	0.60	307	313	6	7.69%	Coarse Sand
60	0.25	283	306	23	29.49%	Med Sand
100	0.15	265	294	29	37.18%	Fine Sand
230	0.075	345	356	11	14.10%	VF Sand
270	0.053	344	345	1	1.28%	Silt
Pan	0.038	360	364	4	5.13%	Clay

Sample Number: AO 2-12a

Raw Mass (g): 154

Dried Mass (g): 154

Descriptors: Unit 12, Black Stain

			Mass of			
Sieve	Diameter	Mass of Empty	Sieve + Soil	Soil	Percent	Grain
Number	(mm)	Sieve (g)	Retained (g)	Retained (g)	Retained	Size
10	2	479	573	94	61.03%	Lg Grains
18	1	361	379	18	11.69%	VC Sand
30	0.60	307	319	12	7.79%	Coarse Sand
60	0.25	283	290	7	4.54%	Med Sand
100	0.15	265	284	19	12.34%	Fine Sand
230	0.075	345	348	3	1.95%	VF Sand
270	0.053	344	344	0	0.00%	Silt
Pan	0.038	360	361	1	0.650%	Clay

Sample Number: AO 2-12b

Raw Mass (g): 133

Descriptors: Large shells, coral, granite pebbles

Sieve Number	Diameter (mm)	Mass of Empty Sieve (g)	Mass of Sieve + Soil Retained (g)	Soil Retained (g)	Percent Retained	Grain Size
10	2	479	537	58	43.61%	Lg Grains
18	1	361	362	1	0.75%	VC Sand
30	0.60	307	369	61	45.86%	Coarse Sand
60	0.25	283	295	10	7.52%	Med Sand
100	0.15	265	266	1	0.75%	Fine Sand
230	0.075	345	346	1	0.75%	VF Sand
270	0.053	344	345	1	0.75%	Silt
Pan	0.038	360	0	0	0.000%	Clay

Sample Number: AO 3-11

Raw Mass (g): 259

Dried Mass (g): 256

Descriptors: Brown Clay, XRD

			Mass of			
Sieve	Diameter	Mass of Empty	Sieve + Soil	Soil	Percent	Grain
Number	(mm)	Sieve (g)	Retained (g)	Retained (g)	Retained	Size
10	2	479	479	0	0.00%	Lg Grains
18	1	361	361	0	0.00%	VC Sand
30	0.60	307	307	0	0.00%	Coarse Sand
60	0.25	283	288	5	1.95%	Med Sand
100	0.15	265	302	37	14.45%	Fine Sand
230	0.075	345	408	63	24.61%	VF Sand
270	0.053	344	469	125	48.83%	Silt
Pan	0.038	360	386	26	10.15%	Clay

Sample Number: AO 3-5

Raw Mass (g): 196

Dried Mass (g): 195

Descriptors:

			Mass of			
Sieve	Diameter	Mass of Empty	Sieve + Soil	Soil	Percent	Grain
Number	(mm)	Sieve (g)	Retained (g)	Retained (g)	Retained	Size
10	2	479	491	12	6.15%	Lg Grains
18	1	361	418	57	29.23%	VC Sand
30	0.60	307	395	88	45.13%	Coarse Sand
60	0.25	283	301	18	9.23%	Med Sand
100	0.15	265	280	15	7.69%	Fine Sand
230	0.075	345	350	5	2.56%	VF Sand
270	0.053	344	344	0	0.00%	Silt
Pan	0.038	360	360	0	0.00%	Clay

Sample Number: AO 3-4

Raw Mass (g): 348

Dried Mass (g): 213

Descriptors:

			Mass of			
Sieve	Diameter	Mass of Empty	Sieve + Soil	Soil	Percent	Grain
Number	(mm)	Sieve (g)	Retained (g)	Retained (g)	Retained	Size
10	2	479	483	4	1.88%	Lg Grains
18	1	361	363	2	0.94%	VC Sand
30	0.60	307	309	2	0.94%	Coarse Sand
60	0.25	283	290	7	3.29%	Med Sand
100	0.15	265	312	47	22.06%	Fine Sand
230	0.075	345	466	121	56.81%	VF Sand
270	0.053	344	354	10	4.69%	Silt
Pan	0.038	360	380	20	9.39%	Clay

Sample Number: AO 3-7, Sect 7

Raw Mass (g): 461

Dried Mass (g): 458

Descriptors: XRD, Snail Shells & Fragments, Wood Fragments

			Mass of			
Sieve	Diameter	Mass of Empty	Sieve + Soil	Soil	Percent	Grain
Number	(mm)	Sieve (g)	Retained (g)	Retained (g)	Retained	Size
10	2	479	480	1	0.22%	Lg Grains
18	1	361	363	2	0.44%	VC Sand
30	0.60	307	311	4	0.87%	Coarse Sand
60	0.25	283	294	11	2.40%	Med Sand
100	0.15	265	298	33	7.21%	Fine Sand
230	0.075	345	677	332	72.49%	VF Sand
270	0.053	344	354	10	2.18%	Silt
Pan	0.038	360	425	65	14.19%	Clay

Sample Number: AO 3-10, unit 8

Raw Mass (g): 80

Dried Mass (g): 80

Descriptors: Blue Sand

			Mass of			
Sieve	Diameter	Mass of Empty	Sieve + Soil	Soil	Percent	Grain
Number	(mm)	Sieve (g)	Retained (g)	Retained (g)	Retained	Size
10	2	479	479	0	0.00%	Lg Grains
18	1	361	362	<1	0.00%	VC Sand
30	0.60	307	308	<1	0.00%	Coarse Sand
60	0.25	283	283	<1	0.00%	Med Sand
100	0.15	265	291	26	32.09%	Fine Sand
230	0.075	345	383	38	46.91%	VF Sand
270	0.053	344	349	5	6.17%	Silt
Pan	0.038	360	372	12	14.81%	Clay

Sample Number: AO 3-3, Unit 8

Raw Mass (g): 637

Dried Mass (g): 636

Descriptors: XRD

			Mass of			
Sieve	Diameter	Mass of Empty	Sieve + Soil	Soil	Percent	Grain
Number	(mm)	Sieve (g)	Retained (g)	Retained (g)	Retained	Size
10	2	479	650	171	26.89%	Lg Grains
18	1	361	485	124	19.50%	VC Sand
30	0.60	307	371	64	10.06%	Coarse Sand
60	0.25	283	320	37	5.82%	Med Sand
100	0.15	265	332	67	10.53%	Fine Sand
230	0.075	345	432	87	13.68%	VF Sand
270	0.053	344	397	53	8.33%	Silt
Pan	0.038	360	393	33	5.19%	Clay

Sample Number: AO 3-12, Base Channel

Raw Mass (g): 154

Dried Mass (g): 153

Descriptors: Granite Pebbles

			Mass of			
Sieve	Diameter	Mass of Empty	Sieve + Soil	Soil	Percent	Grain
Number	(mm)	Sieve (g)	Retained (g)	Retained (g)	Retained	Size
10	2	479	522	43	28.10%	Lg Grains
18	1	361	384	23	15.03%	VC Sand
30	0.60	307	322	15	4.66%	Coarse Sand
60	0.25	283	296	13	8.49%	Med Sand
100	0.15	265	307	42	27.45%	Fine Sand
230	0.075	345	357	12	3.36%	VF Sand
270	0.053	344	349	5	1.43%	Silt
Pan	0.038	360	360	0	0.00%	Clay

Sample Number: AO 3-8, Unit 10

Raw Mass (g): 330

Dried Mass (g): 330

Descriptors: Clam Shell Fragment

			Mass of			
Sieve	Diameter	Mass of Empty	Sieve + Soil	Soil	Percent	Grain
Number	(mm)	Sieve (g)	Retained (g)	Retained (g)	Retained	Size
10	2	479	483	4	1.21%	Lg Grains
18	1	361	372	11	3.33%	VC Sand
30	0.60	307	326	19	5.76%	Coarse Sand
60	0.25	283	461	178	53.94%	Med Sand
100	0.15	265	373	108	32.73%	Fine Sand
230	0.075	345	354	9	2.73%	VF Sand
270	0.053	344	345	0	0.30%	Silt
Pan	0.038	360	361	<1	0.00%	Clay

Sample Number: AO 3-9, Unit 10

Raw Mass (g): 283

Dried Mass (g): 283

Descriptors:

			Mass of			
Sieve	Diameter	Mass of Empty	Sieve + Soil	Soil	Percent	Grain
Number	(mm)	Sieve (g)	Retained (g)	Retained (g)	Retained	Size
10	2	479	594	115	40.63%	Lg Grains
18	1	361	424	63	22.26%	VC Sand
30	0.60	307	337	30	10.60%	Coarse Sand
60	0.25	283	302	19	6.70%	Med Sand
100	0.15	265	295	30	10.60%	Fine Sand
230	0.075	345	360	15	5.30%	VF Sand
270	0.053	344	352	8	2.82%	Silt
Pan	0.038	360	363	3	1.06%	Clay

Sample Number: AO 3-13, Unit 11

Raw Mass (g): 270

Dried Mass (g): 270

Descriptors:

			Mass of			
Sieve	Diameter	Mass of Empty	Sieve + Soil	Soil	Percent	Grain
Number	(mm)	Sieve (g)	Retained (g)	Retained (g)	Retained	Size
10	2	479	479	0	0.00%	Lg Grains
18	1	361	362	1	0.37%	VC Sand
30	0.60	307	310	3	1.10%	Coarse Sand
60	0.25	283	350	67	24.80%	Med Sand
100	0.15	265	416	151	55.93%	Fine Sand
230	0.075	345	385	40	14.90%	VF Sand
270	0.053	344	346	2	0.74%	Silt
Pan	0.038	360	366	6	2.22%	Clay

Sample Number: TK 4-1

Raw Mass (g): 20

Dried Mass (g): 20

Descriptors: shells & coral mass 167g (removed prior to sorting)

			Mass of			
Sieve	Diameter	Mass of Empty	Sieve + Soil	Soil	Percent	Grain
Number	(mm)	Sieve (g)	Retained (g)	Retained (g)	Retained %	Size
20	0.85	57	58.67	1.67	8.35	Lg Grains
30	0.60	56.75	59.47	2.72	13.60	VC Sand
40	0.42	55.5	56.47	0.97	4.85	Coarse Sand
60	0.25	53.2	57.93	2.73	13.65	Med Sand
100	0.15	53	63.87	10.87	54.35	Fine Sand
230	0.063	51.7	52.63	0.93	4.65	VF Sand
Pan	0.038	65.76	65.87	0.11	0.55	Clay

Sample Number: TK 4-2

Raw Mass (g): 4.84

Dried Mass (g): 4.84

Descriptors: shells & coral mass 55g (removed prior to sorting)

			Mass of			
Sieve	Diameter	Mass of Empty	Sieve + Soil	Soil	Percent	Grain
Number	(mm)	Sieve (g)	Retained (g)	Retained (g)	Retained	Size
20	0.85	57	57.4	0.27	5.58%	Lg Grains
30	0.60	56.75	57.59	0.84	17.35%	VC Sand
40	0.42	55.5	55.82	0.32	6.61%	Coarse Sand
60	0.25	53.2	55.76	0.56	11.57%	Med Sand
100	0.15	53	55.14	2.01	41.53%	Fine Sand
230	0.063	51.7	52.24	0.54	11.16%	VF Sand
Pan	0.038	65.5	65.8	0.3	6.20%	Clay

Sample Number: TK 4-3

Raw Mass (g): 108

Dried Mass (g): 108

Descriptors:

			Mass of			
Sieve	Diameter	Mass of Empty	Sieve + Soil	Soil	Percent	Grain
Number	(mm)	Sieve (g)	Retained (g)	Retained (g)	Retained	Size
20	0.85	338	348	10	9.26%	Lg Grains
30	0.60	307	317	10	9.26%	VC Sand
40	0.42	299	316	17	15.74%	Coarse Sand
60	0.25	283	292	9	8.33%	Med Sand
100	0.15	265	308	43	39.81%	Fine Sand
230	0.063	248	261	13	12.04%	VF Sand
Pan	0.038	361	367	6	5.56%	Clay

Sample Number: TK 4-4

Raw Mass (g): 176

Dried Mass (g): 176

Descriptors:

			Mass of			
Sieve	Diameter	Mass of Empty	Sieve + Soil	Soil	Percent	Grain
Number	(mm)	Sieve (g)	Retained (g)	Retained (g)	Retained	Size
20	0.85	338	387	49	27.84%	Lg Grains
30	0.60	307	324	17	9.66%	VC Sand
40	0.42	299	314	15	8.52%	Coarse Sand
60	0.25	283	295	12	6.82%	Med Sand
100	0.15	265	305	40	22.73%	Fine Sand
230	0.063	248	277	29	16.48%	VF Sand
Pan	0.038	361	375	14	7.95%	Clay

Sample Number: TK 4-5A

Raw Mass (g): 20

Dried Mass (g): 20

Descriptors:

			Mass of			
Sieve	Diameter	Mass of Empty	Sieve + Soil	Soil	Percent	Grain
Number	(mm)	Sieve (g)	Retained (g)	Retained (g)	Retained	Size
20	0.85	338	342	4	20.00%	Lg Grains
30	0.60	307	308	1	5.00%	VC Sand
40	0.42	299	300	1	5.00%	Coarse Sand
60	0.25	283	284	1	5.00%	Med Sand
100	0.15	265	267	2	10.00%	Fine Sand
230	0.063	248	251	3	15.00%	VF Sand
Pan	0.038	361	369	8	40.00%	Clay

Sample Number: TK 4-8

Raw Mass (g): 67

Dried Mass (g): 67

Descriptors:

			Mass of			
Sieve	Diameter	Mass of Empty	Sieve + Soil	Soil	Percent	Grain
Number	(mm)	Sieve (g)	Retained (g)	Retained (g)	Retained	Size
20	0.85	338	339	1.8	2.69%	Lg Grains
30	0.60	307	309	2.2	3.28%	VC Sand
40	0.42	299	304	5	7.46%	Coarse Sand
60	0.25	283	301	18	26.86%	Med Sand
100	0.15	265	300	35	52.24%	Fine Sand
230	0.063	248	251	3	4.48%	VF Sand
Pan	0.038	361	363	2	2.99%	Clay

Sample Number: TK 4-9

Raw Mass (g): 74

Dried Mass (g): 74

Descriptors:

			Mass of			
Sieve	Diameter	Mass of Empty	Sieve + Soil	Soil	Percent	Grain
Number	(mm)	Sieve (g)	Retained (g)	Retained (g)	Retained	Size
20	0.85	338	380	42	56.76%	Lg Grains
30	0.60	307	314	7	9.46%	VC Sand
40	0.42	299	304	5	6.76%	Coarse Sand
60	0.25	283	285	2	2.70%	Med Sand
100	0.15	265	273	8	13.51%	Fine Sand
230	0.063	248	255	7	9.46%	VF Sand
Pan	0.038	361	361	0.99	1.35%	Clay

Sample Number: TK 4-10

Raw Mass (g): 50

Dried Mass (g): 50

Descriptors:

			Mass of			
Sieve	Diameter	Mass of Empty	Sieve + Soil	Soil	Percent	Grain
Number	(mm)	Sieve (g)	Retained (g)	Retained (g)	Retained	Size
20	0.85	338	339	1	2.00%	Lg Grains
30	0.60	307	308	1	2.00%	VC Sand
40	0.42	299	304	5	10.00%	Coarse Sand
60	0.25	283	297	14	28.00%	Med Sand
100	0.15	265	290	25	50.00%	Fine Sand
230	0.063	248	251	3	6.00%	VF Sand
Pan	0.038	361	362	1	2.00%	Clay

Sample Number: TK 4-11

Raw Mass (g): 82

Dried Mass (g): 82

Descriptors:

			Mass of			
Sieve	Diameter	Mass of Empty	Sieve + Soil	Soil	Percent	Grain
Number	(mm)	Sieve (g)	Retained (g)	Retained (g)	Retained	Size
20	0.85	338	377	39	47.56%	Lg Grains
30	0.60	307	314	7	8.54%	VC Sand
40	0.42	299	306	7	8.54%	Coarse Sand
60	0.25	283	287	4	4.88%	Med Sand
100	0.15	265	277	12	14.63%	Fine Sand
230	0.063	248	254	6	7.32%	VF Sand
Pan	0.038	361	368	7	8.54%	Clay

Sample Number: TK 4-12

Raw Mass (g): 105

Dried Mass (g): 105

Descriptors:

Sieve Number	Diameter (mm)	Mass of Empty Sieve (g)	Mass of Sieve + Soil Retained (g)	Soil Retained (g)	Percent Retained	Grain Size
20	0.85	338	340	2	1.90%	Lg Grains
30	0.60	307	309	2	1.90%	VC Sand
40	0.42	299	302	3	2.86%	Coarse Sand
60	0.25	283	285	2	1.90%	Med Sand
100	0.15	265	303	38	36.19%	Fine Sand
230	0.063	248	293	45	42.86%	VF Sand
Pan	0.038	361	374	13	12.38%	Clay

Sample Number: TK 4-13
 Raw Mass (g): 190
 Dried Mass (g): 190
 Descriptors: XRD, quartz concretions & calcite and aragonite with framboids (pyrite spheres), SEM Report

			Mass of			
Sieve	Diameter	Mass of Empty	Sieve + Soil	Soil	Percent	Grain
Number	(mm)	Sieve (g)	Retained (g)	Retained (g)	Retained	Size
20	0.85	338	340	2	1.05%	Lg Grains
30	0.60	307	308	1	0.53%	VC Sand
40	0.42	299	302	3	1.58%	Coarse Sand
60	0.25	283	290	7	3.68%	Med Sand
100	0.15	265	334	69	36.32%	Fine Sand
230	0.063	248	315	97	51.05%	VF Sand
Pan	0.038	361	372	11	5.79%	Clay

Sample Number: TK 4-14

Raw Mass (g): 39

Dried Mass (g): 39

Descriptors:

			Mass of			
Sieve	Diameter	Mass of Empty	Sieve + Soil	Soil	Percent	Grain
Number	(mm)	Sieve (g)	Retained (g)	Retained (g)	Retained	Size
20	0.85	338	339	1	2.56%	Lg Grains
30	0.60	307	308	1	2.56%	VC Sand
40	0.42	299	301	2	5.13%	Coarse Sand
60	0.25	283	287	4	10.26%	Med Sand
100	0.15	265	281	16	41.03%	Fine Sand
230	0.063	248	261	13	33.33%	VF Sand
Pan	0.038	361	363	2	5.13%	Clay

APPENDIX C

Grain Size Analysis Calculations and Statistics

Method of Moments Statistical Calculation Equations

Statistical formulae used in the calculation of grain size parameters, and suggested descriptive terminology. f is the frequency in percent; m is the mid-point of each class interval in metric (m_m) or phi (m_f) units; P_x and f_x are grain diameters, in metric or phi units respectively, at the cumulative percentile value of x .

(a) Arithmetic Method of Moments

Mean	Standard Deviation	Skewness	Kurtosis
$\bar{x}_a = \frac{\sum f_m}{100}$	$S_a = \sqrt{\frac{\sum f(m_m - \bar{x}_a)^2}{100}}$	$Sk_a = \frac{\sum f(m_m - \bar{x}_a)^3}{100S_a^3}$	$K_a = \frac{\sum f(m_m - \bar{x}_a)^4}{100S_a^4}$

(b) Geometric Method of Moments

Mean	Standard Deviation	Skewness	Kurtosis
$x_g = \exp \frac{\sum f \ln m_m}{100}$	$S_g = \exp \sqrt{\frac{\sum f(\ln m_m - \ln x_g)^2}{100}}$	$Sk_g = \frac{\sum f(\ln m_m - \ln x_g)^3}{100 \ln S_g^3}$	$K_g = \frac{\sum f(\ln m_m - \ln x_g)^4}{100 \ln S_g^4}$

Sorting (S_g)	Skewness (Sk_g)	Kurtosis (K_g)
Very well sorted	< 1.27	Very fine skewed < -1.30
Well sorted	1.27 – 1.41	Fine skewed -1.30 – -0.43
Moderately well sorted	1.41 – 1.62	Symmetrical -0.43 – +0.43
Moderately sorted	1.62 – 2.00	Coarse skewed +0.43 – +1.30
Poorly sorted	2.00 – 4.00	Very coarse skewed > +1.30
Very poorly sorted	4.00 – 16.00	
Extremely poorly sorted	> 16.00	

(c) Logarithmic Method of Moments

Mean	Standard Deviation	Skewness	Kurtosis
$\bar{x}_f = \frac{\sum f m_f}{100}$	$S_f = \sqrt{\frac{\sum f(m_f - \bar{x}_f)^2}{100}}$	$Sk_f = \frac{\sum f(m_f - \bar{x}_f)^3}{100S_f^3}$	$K_f = \frac{\sum f(m_f - \bar{x}_f)^4}{100S_f^4}$

Sorting (S_f)	Skewness (Sk_f)	Kurtosis (K_f)
Very well sorted	< 0.35	Very fine skewed > +1.30
Well sorted	0.35 – 0.50	Fine skewed +0.43 – +1.30
Moderately well sorted	0.50 – 0.70	Symmetrical -0.43 – +0.43
Moderately sorted	0.70 – 1.00	Coarse skewed -0.43 – -1.30
Poorly sorted	1.00 – 2.00	Very coarse skewed < -1.30
Very poorly sorted	2.00 – 4.00	
Extremely poorly sorted	> 4.00	

SAMPLE STATISTICS

SAMPLE IDENTITY: **AO-1 9, Unit 1**

ANALYST & DATE: JES,

SAMPLE TYPE: Unimodal, Well Sorted

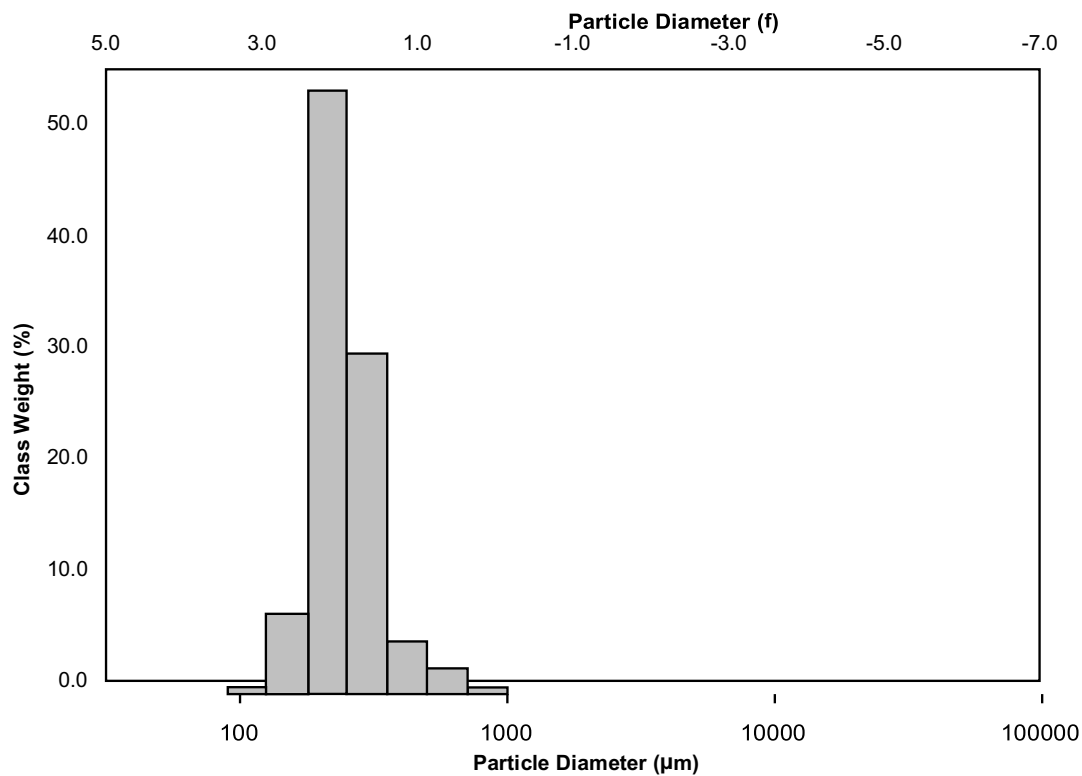
TEXTURAL GROUP: Sand

SEDIMENT NAME: Well Sorted Fine Sand

GPS: 29 32'35" N, 34 58'47" E

	∞ m		ϕ		GRAIN SIZE DISTRIBUTION	
	∞ m	ϕ	∞ m	ϕ	GRAIN SIZE DISTRIBUTION	GRAIN SIZE DISTRIBUTION
MODE 1:	215.0	2.237			GRAVEL: 0.0%	COARSE SAND: 3.0%
MODE 2:					SAND: 100.0%	MEDIUM SAND: 36.3%
MODE 3:					MUD: 0.0%	FINE SAND: 60.1%
D ₁₀ :	181.9	1.530			V FINE SAND: 0.6%	
MEDIAN or D ₅₀ :	233.8	2.097			V COARSE GRAVEL: 0.0%	V COARSE SILT: 0.0%
D ₉₀ :	346.2	2.459			COARSE GRAVEL: 0.0%	COARSE SILT: 0.0%
(D ₉₀ / D ₁₀):	1.903	1.607			MEDIUM GRAVEL: 0.0%	MEDIUM SILT: 0.0%
(D ₉₀ - D ₁₀):	164.3	0.928			FINE GRAVEL: 0.0%	FINE SILT: 0.0%
(D ₇₅ / D ₂₅):	1.466	1.312			V FINE GRAVEL: 0.0%	V FINE SILT: 0.0%
(D ₇₅ - D ₂₅):	93.18	0.552			V COARSE SAND: 0.0%	CLAY: 0.0%
METHOD OF MOMENTS			FOLK & WARD METHOD			
	Arithmetic	Geometric	Logarithmic	Geometric	Logarithmic	Description
	∞ m	∞ m	\square	∞ m	\square	
MEAN (\bar{x}):	260.3	244.4	2.033	242.7	2.043	Fine Sand
SORTING (σ):	94.57	1.344	0.427	1.338	0.420	Well Sorted
SKEWNESS (Sk):	2.729	0.938	-0.938	0.200	-0.200	Coarse Skewed
KURTOSIS (K):	14.21	5.366	5.366	1.106	1.106	Mesokurtic

GRAIN SIZE DISTRIBUTION



SAMPLE STATISTICS

SAMPLE IDENTITY: **AO-1 3, Unit 4**

ANALYST & DATE: JES,

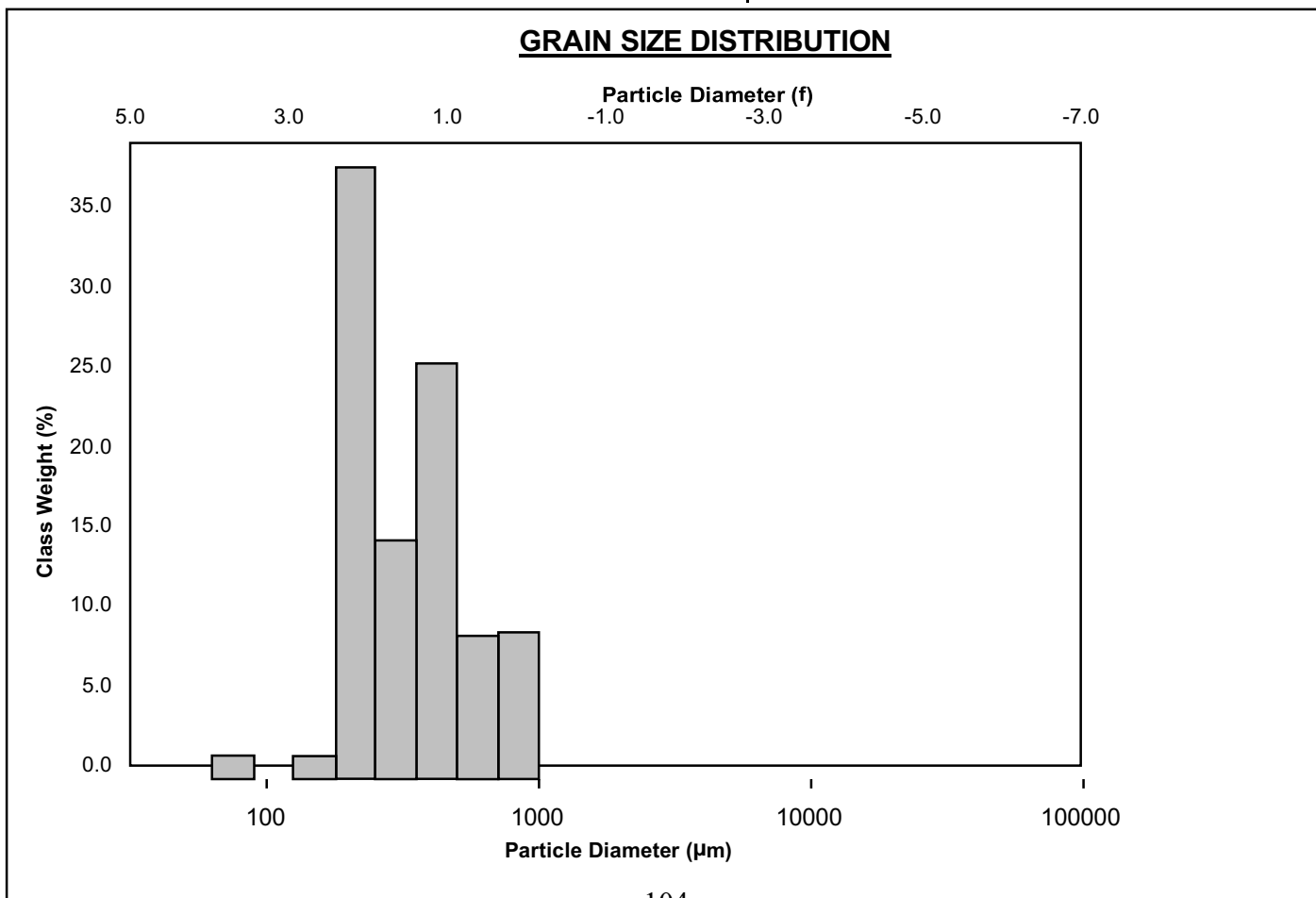
SAMPLE TYPE: Trimodal, Moderately Well Sorted

TEXTURAL GROUP: Sand

SEDIMENT NAME: Moderately Well Sorted Medium Sand

GPS: 29 32'35" N, 34 58'47" E

	∞ m		ϕ		GRAIN SIZE DISTRIBUTION		
	∞ m	ϕ	GRAVEL: 0.0%	COARSE SAND: 18.5%	SAND: 100.0%	MEDIUM SAND: 41.5%	FINE SAND: 38.5%
MODE 1:	215.0	2.237	MUD: 0.0%	V FINE SAND: 1.5%			
MODE 2:	427.5	1.247	V COARSE GRAVEL: 0.0%	V COARSE SILT: 0.0%			
MODE 3:	855.0	0.247	COARSE GRAVEL: 0.0%	COARSE SILT: 0.0%			
D ₁₀ :	191.4	0.536	MEDIUM GRAVEL: 0.0%	MEDIUM SILT: 0.0%			
MEDIAN or D ₅₀ :	314.0	1.671	FINE GRAVEL: 0.0%	FINE SILT: 0.0%			
D ₉₀ :	689.6	2.385	V FINE GRAVEL: 0.0%	V FINE SILT: 0.0%			
(D ₉₀ / D ₁₀):	3.602	4.448	V COARSE SAND: 0.0%	CLAY: 0.0%			
(D ₉₀ - D ₁₀):	498.1	1.849					
(D ₇₅ / D ₂₅):	2.098	1.952					
(D ₇₅ - D ₂₅):	240.2	1.069					
	METHOD OF MOMENTS			FOLK & WARD METHOD			
	Arithmetic	Geometric	Logarithmic	Geometric	Logarithmic	Description	
	∞ m	∞ m	\square	∞ m	\square		
MEAN (\bar{x}):	376.0	327.1	1.612	326.5	1.615	Medium Sand	
SORTING (\square):	198.2	1.642	0.715	1.615	0.691	Moderately Well Sorted	
SKEWNESS (Sk):	1.169	0.133	-0.133	0.202	-0.202	Coarse Skewed	
KURTOSIS (K):	3.586	2.937	2.937	0.836	0.836	Platykurtic	



SAMPLE STATISTICS

SAMPLE IDENTITY: **AO-1 8, Unit 10**

ANALYST & DATE: JES,

SAMPLE TYPE: Unimodal, Moderately Well Sorted

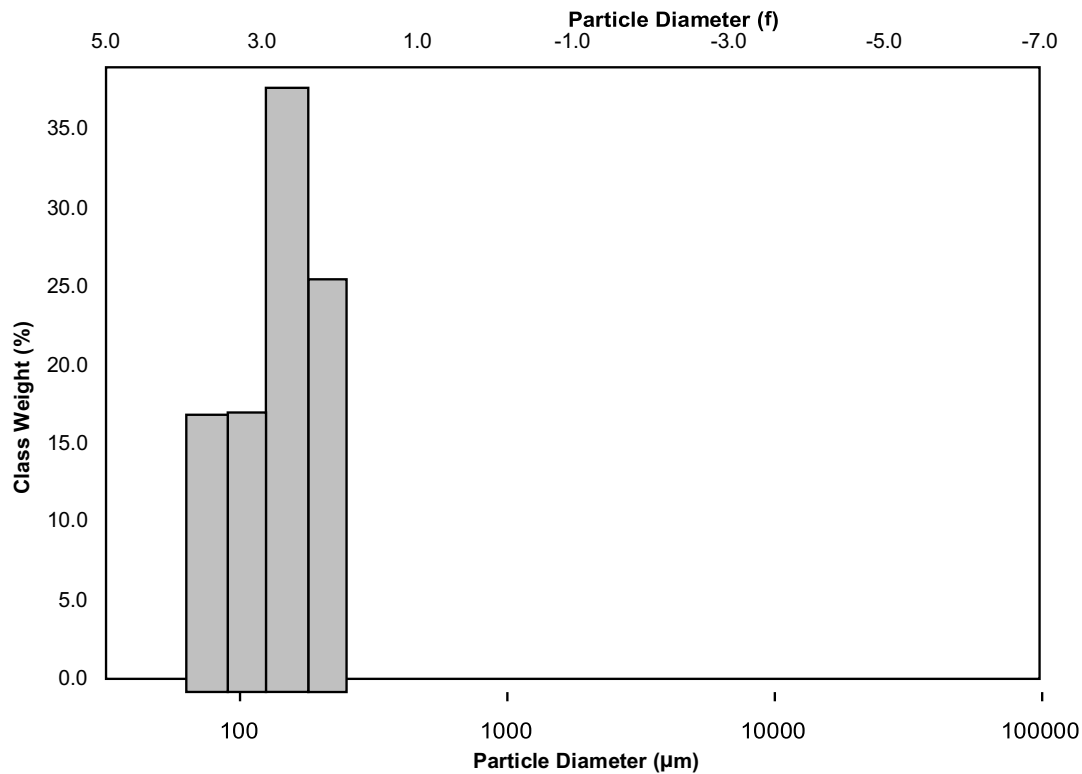
TEXTURAL GROUP: Sand

SEDIMENT NAME: Moderately Well Sorted Fine Sand

GPS: 29 32'35" N, 34 58'47" E

	∞ m		ϕ		GRAIN SIZE DISTRIBUTION	
	∞ m	ϕ	∞ m	ϕ	METHOD OF MOMENTS	FOLK & WARD METHOD
MODE 1:	152.5	2.737			GRAVEL: 0.0%	COARSE SAND: 0.0%
MODE 2:					SAND: 100.0%	MEDIUM SAND: 0.0%
MODE 3:					MUD: 0.0%	FINE SAND: 65.1%
D ₁₀ :	76.73	2.191				V FINE SAND: 34.9%
MEDIAN or D ₅₀ :	143.3	2.803			V COARSE GRAVEL: 0.0%	V COARSE SILT: 0.0%
D ₉₀ :	219.0	3.704			COARSE GRAVEL: 0.0%	COARSE SILT: 0.0%
(D ₉₀ / D ₁₀):	2.854	1.691			MEDIUM GRAVEL: 0.0%	MEDIUM SILT: 0.0%
(D ₉₀ - D ₁₀):	142.3	1.513			FINE GRAVEL: 0.0%	FINE SILT: 0.0%
(D ₇₅ / D ₂₅):	1.744	1.324			V FINE GRAVEL: 0.0%	V FINE SILT: 0.0%
(D ₇₅ - D ₂₅):	76.66	0.802			V COARSE SAND: 0.0%	CLAY: 0.0%
					METHOD OF MOMENTS	FOLK & WARD METHOD
	Arithmetic	Geometric	Logarithmic	Geometric	Logarithmic	Description
	∞ m	∞ m	\square	∞ m	\square	
MEAN (\bar{x}):	146.7	136.1	2.877	135.8	2.881	Fine Sand
SORTING (σ):	48.17	1.427	0.513	1.487	0.572	Moderately Well Sorted
SKEWNESS (Sk):	0.058	-0.404	0.404	-0.191	0.191	Fine Skewed
KURTOSIS (K):	1.892	2.034	2.034	0.894	0.894	Platykurtic

GRAIN SIZE DISTRIBUTION



SAMPLE STATISTICS

SAMPLE IDENTITY: **AO-1 5-1, Unit 18**

ANALYST & DATE: JES,

SAMPLE TYPE: Unimodal, Well Sorted

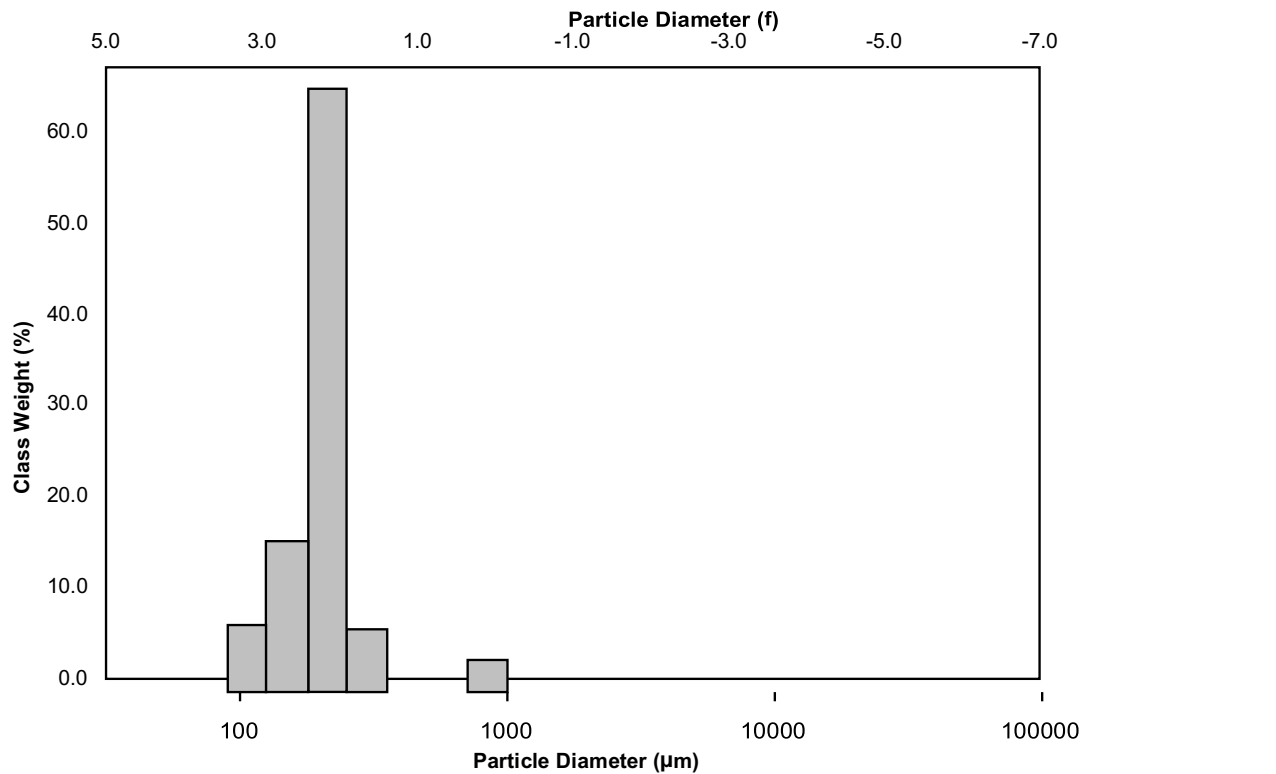
TEXTURAL GROUP: Sand

SEDIMENT NAME: Well Sorted Fine Sand

GPS: 29 32'35" N, 34 58'47" E

	∞ m		ϕ		GRAIN SIZE DISTRIBUTION	
	∞ m	ϕ	∞ m	ϕ		
MODE 1:	215.0	2.237			GRAVEL: 0.0%	COARSE SAND: 3.6%
MODE 2:					SAND: 100.0%	MEDIUM SAND: 7.1%
MODE 3:					MUD: 0.0%	FINE SAND: 82.2%
D ₁₀ :	132.5	1.950				V FINE SAND: 7.1%
MEDIAN or D ₅₀ :	204.5	2.290			V COARSE GRAVEL: 0.0%	V COARSE SILT: 0.0%
D ₉₀ :	258.9	2.916			COARSE GRAVEL: 0.0%	COARSE SILT: 0.0%
(D ₉₀ / D ₁₀):	1.953	1.495			MEDIUM GRAVEL: 0.0%	MEDIUM SILT: 0.0%
(D ₉₀ - D ₁₀):	126.4	0.966			FINE GRAVEL: 0.0%	FINE SILT: 0.0%
(D ₇₅ / D ₂₅):	1.291	1.175			V FINE GRAVEL: 0.0%	V FINE SILT: 0.0%
(D ₇₅ - D ₂₅):	52.39	0.369			V COARSE SAND: 0.0%	CLAY: 0.0%
	METHOD OF MOMENTS			FOLK & WARD METHOD		
	Arithmetic	Geometric	Logarithmic	Geometric	Logarithmic	Description
	∞ m	∞ m	\square	∞ m	\square	
MEAN (\bar{x}):	225.3	204.2	2.292	195.4	2.356	Fine Sand
SORTING (σ):	128.8	1.435	0.521	1.328	0.409	Well Sorted
SKEWNESS (Sk):	4.102	1.701	-1.701	-0.193	0.193	Fine Skewed
KURTOSIS (K):	20.49	9.414	9.414	1.720	1.720	Very Leptokurtic

GRAIN SIZE DISTRIBUTION



SAMPLE STATISTICS

SAMPLE IDENTITY: **AO-1 11, Unit 19**

ANALYST & DATE: JES,

SAMPLE TYPE: Unimodal, Well Sorted

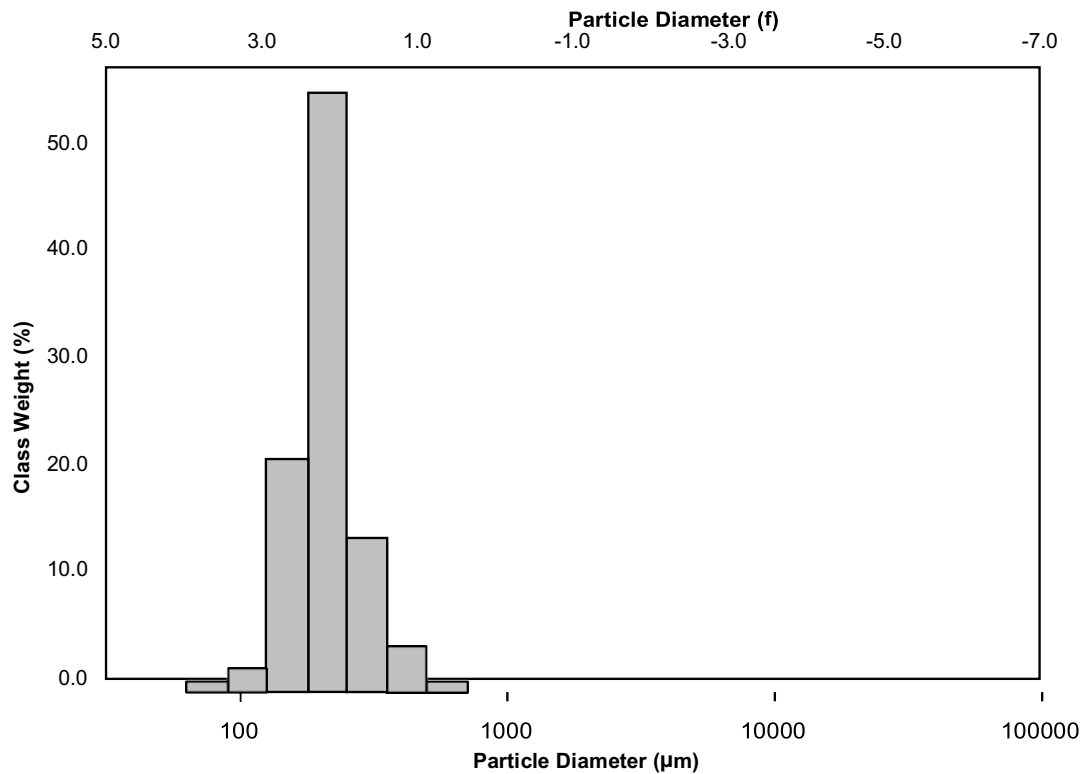
TEXTURAL GROUP: Sand

SEDIMENT NAME: Well Sorted Fine Sand

GPS: 29 32'35" N, 34 58'47" E

	∞m ϕ		GRAIN SIZE DISTRIBUTION			
	MODE 1:	215.0	2.237	GRAVEL: 0.0%	COARSE SAND: 1.1%	
MODE 2:			SAND: 100.0%	MEDIUM SAND: 18.9%		
MODE 3:			MUD: 0.0%	FINE SAND: 76.8%		
D ₁₀ :	139.2	1.657		V FINE SAND: 3.2%		
MEDIAN or D ₅₀ :	208.1	2.265	V COARSE GRAVEL: 0.0%	V COARSE SILT: 0.0%		
D ₉₀ :	317.1	2.845	COARSE GRAVEL: 0.0%	COARSE SILT: 0.0%		
(D ₉₀ / D ₁₀):	2.278	1.717	MEDIUM GRAVEL: 0.0%	MEDIUM SILT: 0.0%		
(D ₉₀ - D ₁₀):	177.9	1.188	FINE GRAVEL: 0.0%	FINE SILT: 0.0%		
(D ₇₅ / D ₂₅):	1.375	1.225	V FINE GRAVEL: 0.0%	V FINE SILT: 0.0%		
(D ₇₅ - D ₂₅):	66.16	0.460	V COARSE SAND: 0.0%	CLAY: 0.0%		
	METHOD OF MOMENTS		FOLK & WARD METHOD			
	Arithmetic	Geometric	Logarithmic	Geometric	Logarithmic	Description
	∞m	∞m	\square	∞m	\square	
MEAN (\bar{x}):	222.7	208.8	2.260	206.1	2.279	Fine Sand
SORTING (σ):	76.92	1.365	0.449	1.355	0.438	Well Sorted
SKEWNESS (Sk):	1.928	0.241	-0.241	0.012	-0.012	Symmetrical
KURTOSIS (K):	9.095	4.663	4.663	1.332	1.332	Leptokurtic

GRAIN SIZE DISTRIBUTION



SAMPLE STATISTICS

SAMPLE IDENTITY: **AO-1 12, Unit 19**

ANALYST & DATE: JES,

SAMPLE TYPE: Unimodal, Moderately Well Sorted

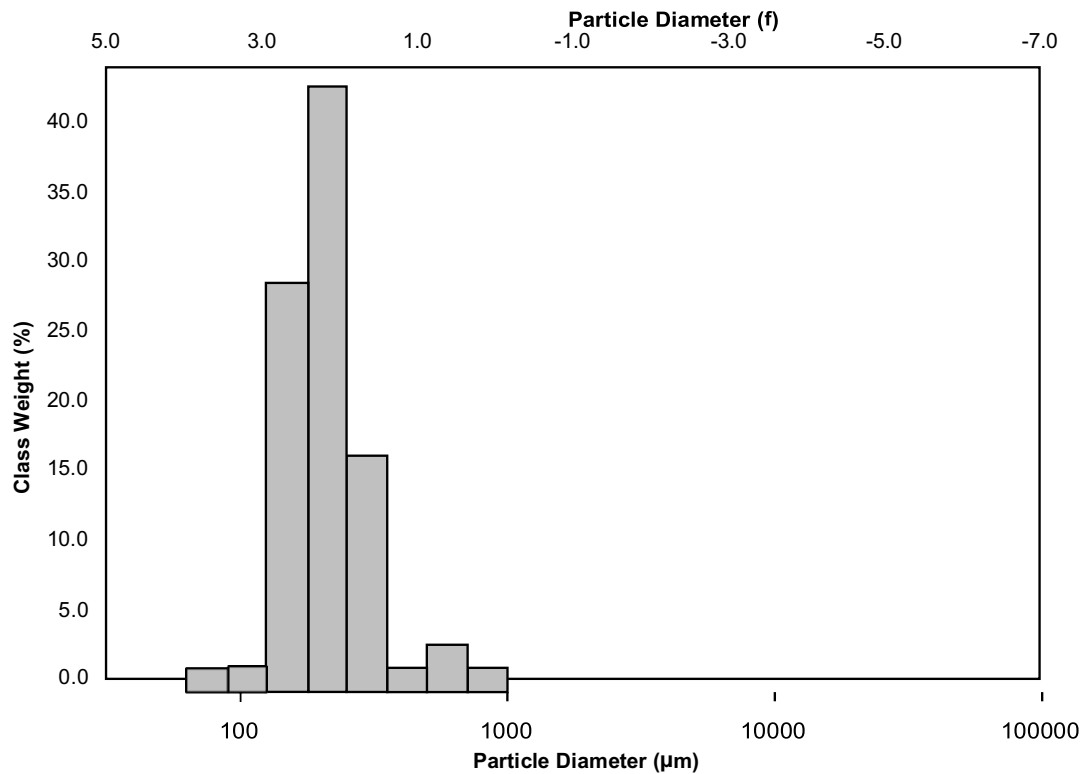
TEXTURAL GROUP: Sand

SEDIMENT NAME: Moderately Well Sorted Fine Sand

GPS: 29 32'35" N, 34 58'47" E

	∞ m		ϕ		GRAIN SIZE DISTRIBUTION		
MODE 1:	215.0		2.237		GRAVEL: 0.0%		COARSE SAND: 5.2%
MODE 2:					SAND: 100.0%		MEDIUM SAND: 19.0%
MODE 3:					MUD: 0.0%		FINE SAND: 72.4%
D ₁₀ :	135.0		1.585				V FINE SAND: 3.4%
MEDIAN or D ₅₀ :	203.6		2.296		V COARSE GRAVEL: 0.0%		V COARSE SILT: 0.0%
D ₉₀ :	333.3		2.889		COARSE GRAVEL: 0.0%		COARSE SILT: 0.0%
(D ₉₀ / D ₁₀):	2.468		1.822		MEDIUM GRAVEL: 0.0%		MEDIUM SILT: 0.0%
(D ₉₀ - D ₁₀):	198.2		1.304		FINE GRAVEL: 0.0%		FINE SILT: 0.0%
(D ₇₅ / D ₂₅):	1.542		1.311		V FINE GRAVEL: 0.0%		V FINE SILT: 0.0%
(D ₇₅ - D ₂₅):	87.26		0.625		V COARSE SAND: 0.0%		CLAY: 0.0%
					METHOD OF MOMENTS		FOLK & WARD METHOD
		Arithmetic	Geometric	Logarithmic	Geometric	Logarithmic	Description
		∞ m	∞ m	\square	∞ m	\square	
MEAN (\bar{x}):		234.6	210.5	2.248	205.7	2.282	Fine Sand
SORTING (σ):		125.5	1.495	0.580	1.474	0.559	Moderately Well Sorted
SKEWNESS (Sk):		2.915	0.946	-0.946	0.182	-0.182	Coarse Skewed
KURTOSIS (K):		13.12	5.281	5.281	1.311	1.311	Leptokurtic

GRAIN SIZE DISTRIBUTION



SAMPLE STATISTICS

SAMPLE IDENTITY: **AO-1 2, Unit 20**

ANALYST & DATE: JES,

SAMPLE TYPE: Unimodal, Very Well Sorted

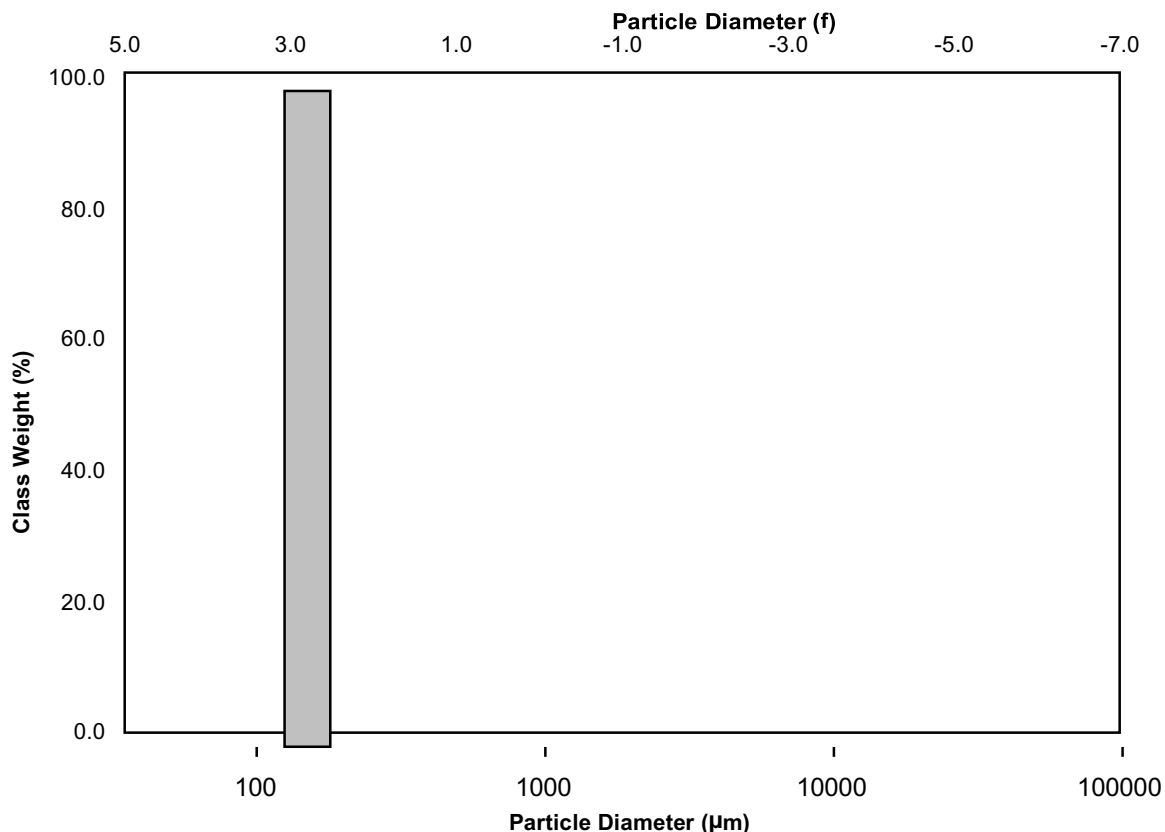
TEXTURAL GROUP:

SEDIMENT NAME:

GPS: 29 32'35" N, 34 58'47" E

		∞ m	ϕ	GRAIN SIZE DISTRIBUTION		
MODE 1:		152.5	2.737	GRAVEL:		COARSE SAND:
MODE 2:				SAND:		MEDIUM SAND:
MODE 3:				MUD:		FINE SAND:
D ₁₀ :		129.6	2.527			V FINE SAND:
MEDIAN or D ₅₀ :		150.0	2.737	V COARSE GRAVEL:		V COARSE SILT:
D ₉₀ :		173.6	2.947	COARSE GRAVEL:		COARSE SILT:
(D ₉₀ / D ₁₀):		1.339	1.167	MEDIUM GRAVEL:		MEDIUM SILT:
(D ₉₀ - D ₁₀):		43.91	0.421	FINE GRAVEL:		FINE SILT:
(D ₇₅ / D ₂₅):		1.200	1.101	V FINE GRAVEL:		V FINE SILT:
(D ₇₅ - D ₂₅):		27.39	0.263	V COARSE SAND:		CLAY:
METHOD OF MOMENTS				FOLK & WARD METHOD		
	Arithmetic	Geometric	Logarithmic	Geometric	Logarithmic	Description
	∞ m	∞ m	ϕ	∞ m	ϕ	
MEAN (\bar{x}):	152.5	150.0	2.737	150.0	2.737	Fine Sand
SORTING (σ):	0.000	1.000	0.000	1.118	0.161	Very Well Sorted
SKEWNESS (Sk):	#DIV/0!	-0.781	#DIV/0!	0.000	0.000	Symmetrical
KURTOSIS (K):	#DIV/0!	0.720	#DIV/0!	0.738	0.738	Platykurtic

GRAIN SIZE DISTRIBUTION



SAMPLE STATISTICS

SAMPLE IDENTITY: **AO-1 13, Unit 22**

ANALYST & DATE: JES,

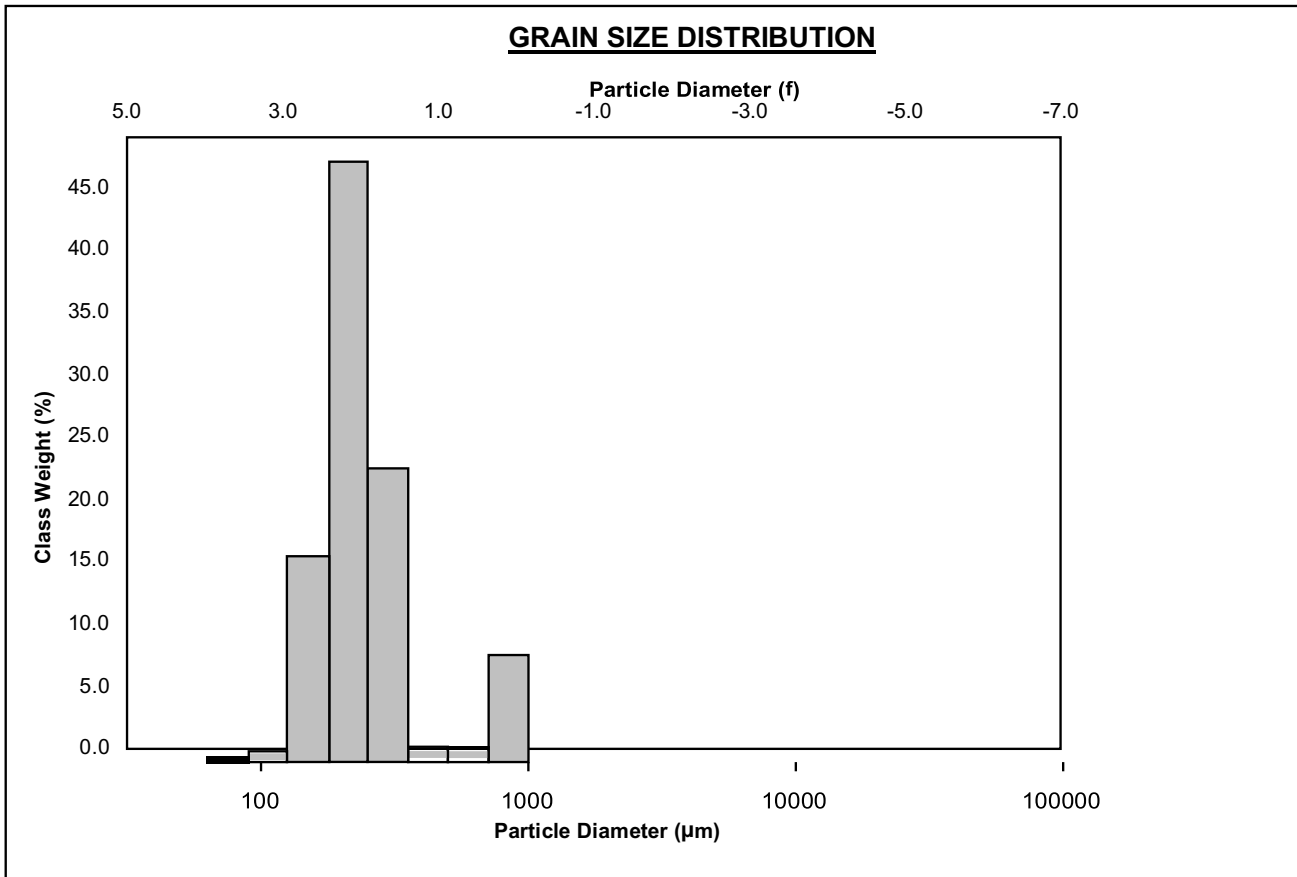
SAMPLE TYPE: Bimodal, Moderately Well Sorted

TEXTURAL GROUP: Sand

SEDIMENT NAME: Moderately Well Sorted Fine Sand

GPS: 29 32'35" N, 34 58'47" E

	αm ϕ		GRAIN SIZE DISTRIBUTION			
	MODE 1:	215.0	2.237	GRAVEL: 0.0%	COARSE SAND: 9.8%	
MODE 2:	855.0	0.247	SAND: 100.0%	MEDIUM SAND: 25.3%		
MODE 3:			MUD: 0.0%	FINE SAND: 63.7%		
D ₁₀ :	150.0	1.085		V FINE SAND: 1.2%		
MEDIAN or D ₅₀ :	224.8	2.153	V COARSE GRAVEL: 0.0%	V COARSE SILT: 0.0%		
D ₉₀ :	471.5	2.737	COARSE GRAVEL: 0.0%	COARSE SILT: 0.0%		
(D ₉₀ / D ₁₀):	3.144	2.524	MEDIUM GRAVEL: 0.0%	MEDIUM SILT: 0.0%		
(D ₉₀ - D ₁₀):	321.5	1.652	FINE GRAVEL: 0.0%	FINE SILT: 0.0%		
(D ₇₅ / D ₂₅):	1.539	1.348	V FINE GRAVEL: 0.0%	V FINE SILT: 0.0%		
(D ₇₅ - D ₂₅):	101.4	0.622	V COARSE SAND: 0.0%	CLAY: 0.0%		
	METHOD OF MOMENTS			FOLK & WARD METHOD		
	Arithmetic αm	Geometric αm	Logarithmic ϕ	Geometric αm	Logarithmic ϕ	Description
MEAN (\bar{x}):	285.9	246.5	2.020	232.8	2.103	Fine Sand
SORTING (σ):	187.6	1.592	0.671	1.551	0.633	Moderately Well Sorted
SKEWNESS (Sk):	2.358	1.353	-1.353	0.296	-0.296	Coarse Skewed
KURTOSIS (K):	7.434	4.856	4.856	1.712	1.712	Very Leptokurtic



SAMPLE STATISTICS

SAMPLE IDENTITY: **AO-1 10, Unit 26**

ANALYST & DATE: JES,

SAMPLE TYPE: Unimodal, Well Sorted

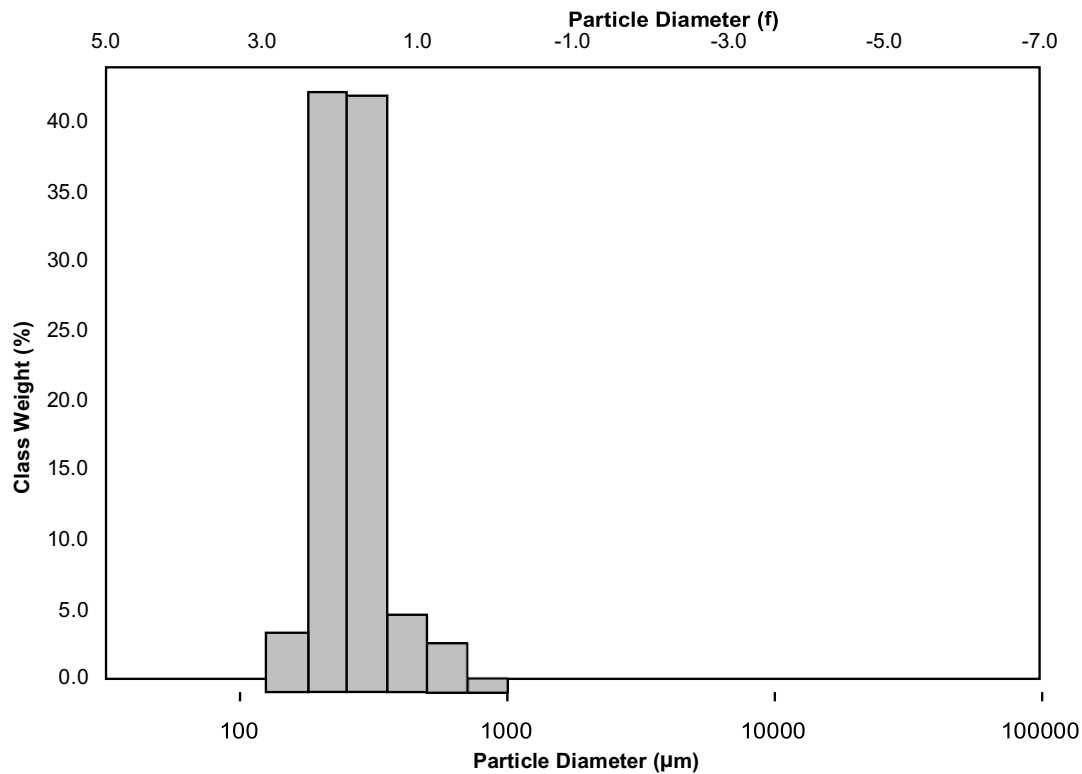
TEXTURAL GROUP: Sand

SEDIMENT NAME: Well Sorted Medium Sand

GPS: 29 32'35" N, 34 58'47" E

	∞m ϕ		GRAIN SIZE DISTRIBUTION			
	MODE 1:	215.0	2.237	GRAVEL: 0.0%	COARSE SAND: 4.6%	
MODE 2:			SAND: 100.0%	MEDIUM SAND: 49.5%		
MODE 3:			MUD: 0.0%	FINE SAND: 46.0%		
D ₁₀ :	188.0	1.484		V FINE SAND: 0.0%		
MEDIAN or D ₅₀ :	258.2	1.953	V COARSE GRAVEL: 0.0%	V COARSE SILT: 0.0%		
D ₉₀ :	357.4	2.411	COARSE GRAVEL: 0.0%	COARSE SILT: 0.0%		
(D ₉₀ / D ₁₀):	1.901	1.625	MEDIUM GRAVEL: 0.0%	MEDIUM SILT: 0.0%		
(D ₉₀ - D ₁₀):	169.4	0.927	FINE GRAVEL: 0.0%	FINE SILT: 0.0%		
(D ₇₅ / D ₂₅):	1.489	1.345	V FINE GRAVEL: 0.0%	V FINE SILT: 0.0%		
(D ₇₅ - D ₂₅):	103.5	0.574	V COARSE SAND: 0.0%	CLAY: 0.0%		
	METHOD OF MOMENTS		FOLK & WARD METHOD			
	Arithmetic	Geometric	Logarithmic	Geometric	Logarithmic	Description
	∞m	∞m	\square	∞m	\square	
MEAN (\bar{x}):	282.7	264.9	1.917	258.3	1.953	Medium Sand
SORTING (σ):	104.8	1.350	0.433	1.330	0.412	Well Sorted
SKEWNESS (Sk):	2.623	1.034	-1.034	0.141	-0.141	Coarse Skewed
KURTOSIS (K):	12.51	5.170	5.170	1.020	1.020	Mesokurtic

GRAIN SIZE DISTRIBUTION



SAMPLE STATISTICS

SAMPLE IDENTITY: **AO-1 7, Unit 27**

ANALYST & DATE: JES,

SAMPLE TYPE: Unimodal, Well Sorted

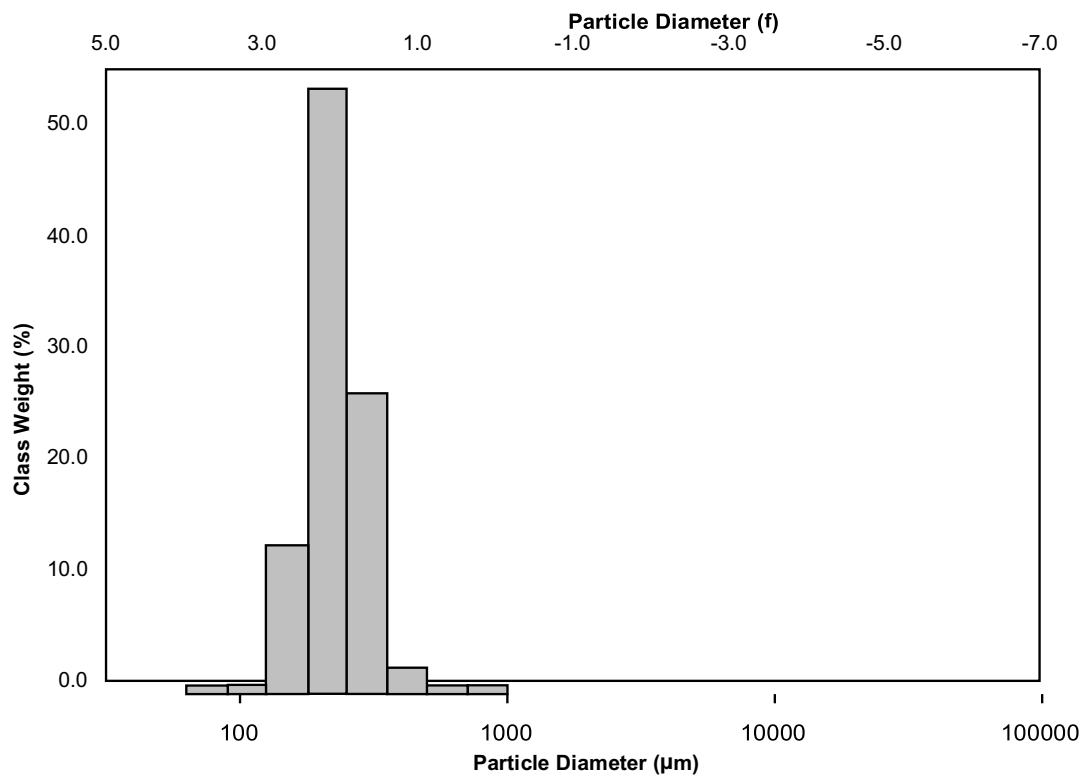
TEXTURAL GROUP: Sand

SEDIMENT NAME: Well Sorted Fine Sand

GPS: 29 32'35" N, 34 58'47" E

	∞ m		ϕ		GRAIN SIZE DISTRIBUTION	
	∞ m	ϕ	∞ m	ϕ	METHOD OF MOMENTS	FOLK & WARD METHOD
MODE 1:	215.0	2.237			GRAVEL: 0.0%	COARSE SAND: 1.6%
MODE 2:					SAND: 100.0%	MEDIUM SAND: 30.2%
MODE 3:					MUD: 0.0%	FINE SAND: 66.7%
D ₁₀ :	155.0	1.604				V FINE SAND: 1.6%
MEDIAN or D ₅₀ :	223.0	2.165			V COARSE GRAVEL: 0.0%	V COARSE SILT: 0.0%
D ₉₀ :	328.9	2.690			COARSE GRAVEL: 0.0%	COARSE SILT: 0.0%
(D ₉₀ / D ₁₀):	2.123	1.677			MEDIUM GRAVEL: 0.0%	MEDIUM SILT: 0.0%
(D ₉₀ - D ₁₀):	174.0	1.086			FINE GRAVEL: 0.0%	FINE SILT: 0.0%
(D ₇₅ / D ₂₅):	1.428	1.274			V FINE GRAVEL: 0.0%	V FINE SILT: 0.0%
(D ₇₅ - D ₂₅):	81.60	0.514			V COARSE SAND: 0.0%	CLAY: 0.0%
					METHOD OF MOMENTS	FOLK & WARD METHOD
	Arithmetic	Geometric	Logarithmic	Geometric	Logarithmic	Description
	∞ m	∞ m	\square	∞ m	\square	
MEAN (\bar{x}):	241.6	226.7	2.141	230.5	2.117	Fine Sand
SORTING (σ):	87.93	1.354	0.437	1.316	0.396	Well Sorted
SKEWNESS (Sk):	3.313	0.434	-0.434	0.074	-0.074	Symmetrical
KURTOSIS (K):	21.85	6.405	6.405	1.085	1.085	Mesokurtic

GRAIN SIZE DISTRIBUTION



SAMPLE STATISTICS

SAMPLE IDENTITY: **AO-1 4, Unit 31**

ANALYST & DATE: JES,

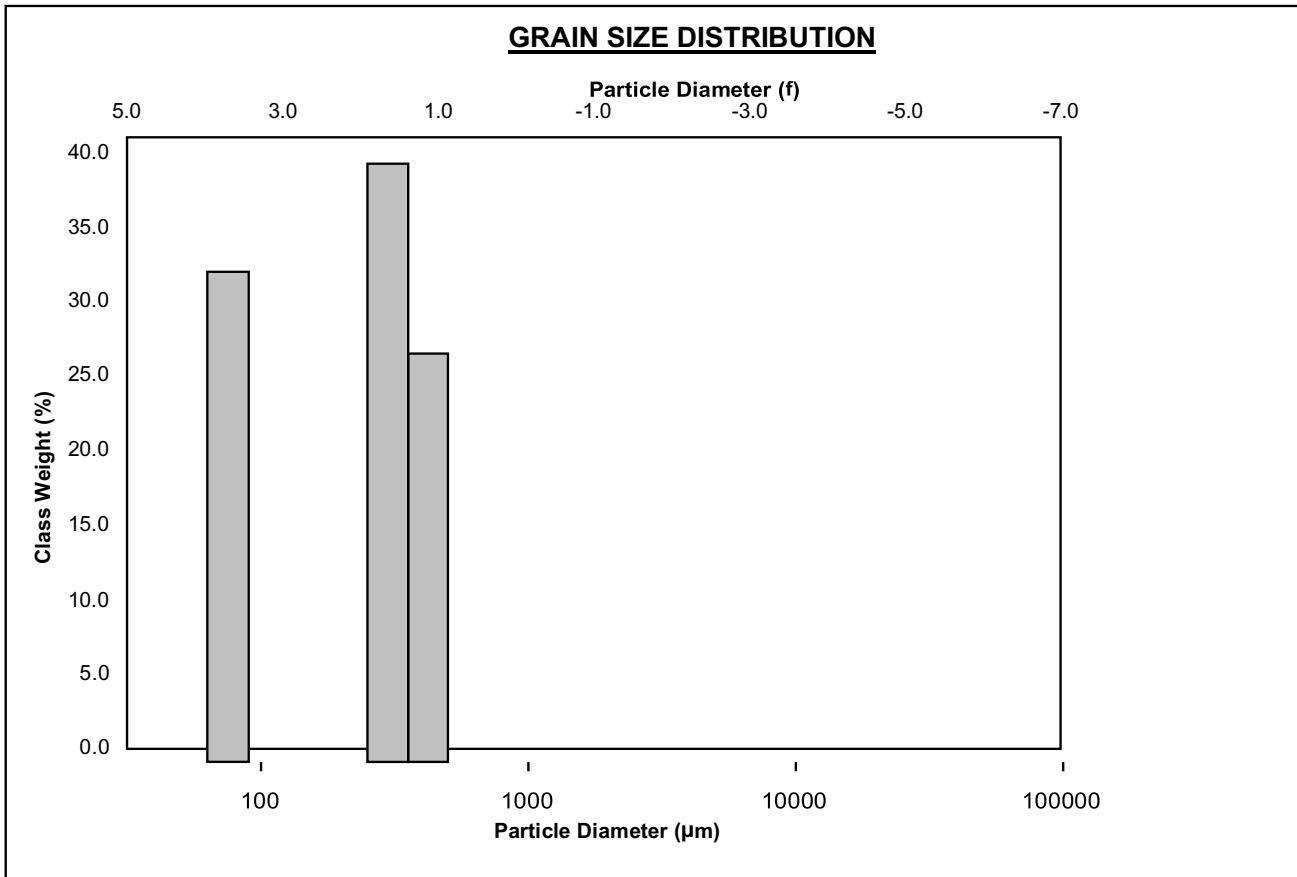
SAMPLE TYPE: Bimodal, Poorly Sorted

TEXTURAL GROUP: Sand

SEDIMENT NAME: Poorly Sorted Medium Sand

GPS: 29 32'35" N, 34 58'47" E

	αm ϕ		GRAIN SIZE DISTRIBUTION			
	MODE 1:	302.5	1.747	GRAVEL: 0.0%	COARSE SAND: 0.0%	
MODE 2:	76.50	3.731	SAND: 100.0%	MEDIUM SAND: 66.7%		
MODE 3:			MUD: 0.0%	FINE SAND: 0.0%		
D ₁₀ :	70.12	1.185		V FINE SAND: 33.3%		
MEDIAN or D ₅₀ :	289.3	1.789	V COARSE GRAVEL: 0.0%	V COARSE SILT: 0.0%		
D ₉₀ :	439.7	3.834	COARSE GRAVEL: 0.0%	COARSE SILT: 0.0%		
(D ₉₀ / D ₁₀):	6.272	3.235	MEDIUM GRAVEL: 0.0%	MEDIUM SILT: 0.0%		
(D ₉₀ - D ₁₀):	369.6	2.649	FINE GRAVEL: 0.0%	FINE SILT: 0.0%		
(D ₇₅ / D ₂₅):	4.406	2.462	V FINE GRAVEL: 0.0%	V FINE SILT: 0.0%		
(D ₇₅ - D ₂₅):	280.4	2.139	V COARSE SAND: 0.0%	CLAY: 0.0%		
	METHOD OF MOMENTS			FOLK & WARD METHOD		
	Arithmetic αm	Geometric αm	Logarithmic ϕ	Geometric αm	Logarithmic ϕ	Description
MEAN (\bar{x}):	260.5	206.6	2.275	206.5	2.276	Fine Sand
SORTING (σ):	139.4	2.069	1.049	2.054	1.038	Poorly Sorted
SKEWNESS (Sk):	-0.297	-0.590	0.590	-0.551	0.551	Very Fine Skewed
KURTOSIS (K):	1.565	1.510	1.510	0.540	0.540	Very Platykurtic



SAMPLE STATISTICS

SAMPLE IDENTITY: **AO 2 - Unit 4**

ANALYST & DATE: JES

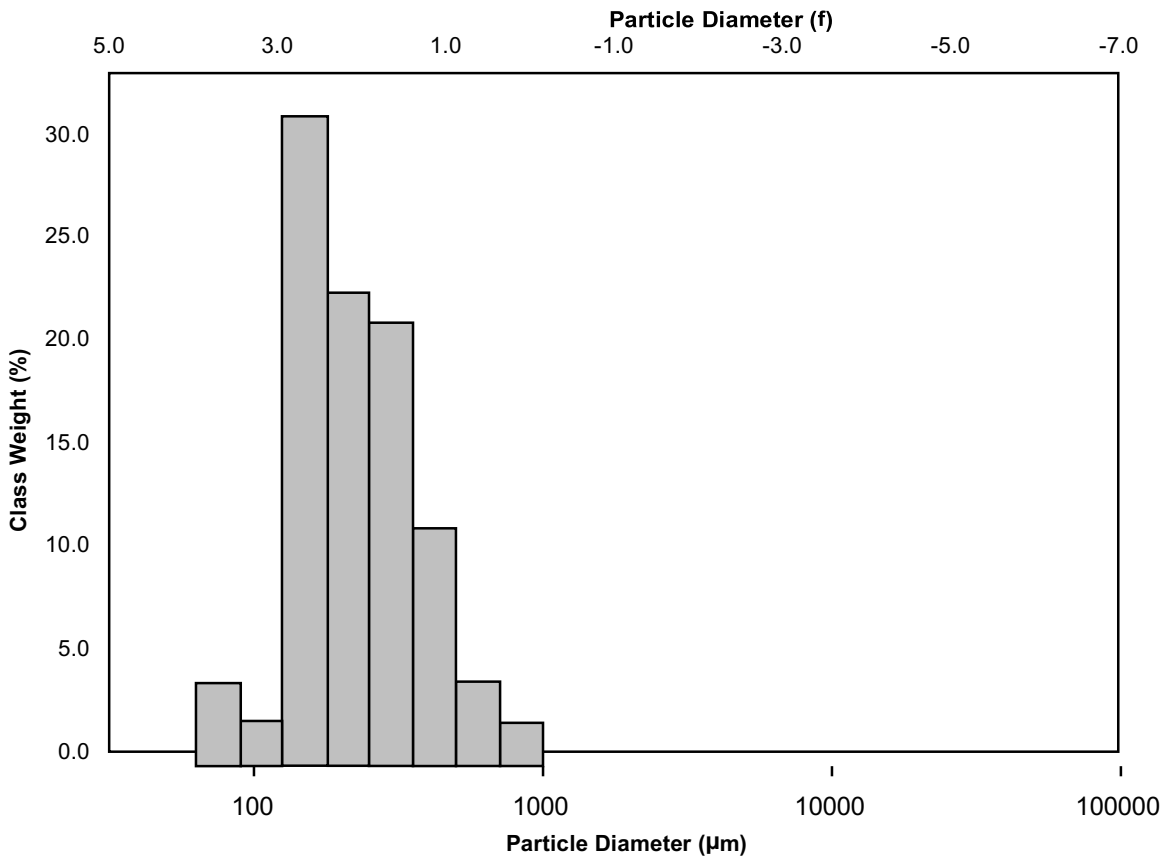
SAMPLE TYPE: Unimodal, Moderately Sorted
 SEDIMENT NAME: Moderately Sorted Fine Sand

TEXTURAL GROUP: Sand
 GPS: 29.3240N, 34.5851E
 Depth: 1.30m

	∞ m	ϕ	GRAIN SIZE DISTRIBUTION			
MODE 1:	152.5	2.737	GRAVEL: 0.0%	COARSE SAND: 6.2%		
MODE 2:			SAND: 100.0%	MEDIUM SAND: 33.0%		
MODE 3:			MUD: 0.0%	FINE SAND: 54.6%		
D ₁₀ :	130.4	1.166	V COARSE GRAVEL: 0.0%	V FINE SAND: 6.2%		
MEDIAN or D ₅₀ :	212.1	2.237	COARSE GRAVEL: 0.0%	V COARSE SILT: 0.0%		
D ₉₀ :	445.5	2.939	MEDIUM GRAVEL: 0.0%	COARSE SILT: 0.0%		
(D ₉₀ / D ₁₀):	3.417	2.520	FINE GRAVEL: 0.0%	MEDIUM SILT: 0.0%		
(D ₉₀ - D ₁₀):	315.1	1.773	V FINE GRAVEL: 0.0%	FINE SILT: 0.0%		
(D ₇₅ / D ₂₅):	2.044	1.618	V COARSE SAND: 0.0%	V FINE SILT: 0.0%		
(D ₇₅ - D ₂₅):	160.6	1.031		CLAY: 0.0%		

	METHOD OF MOMENTS			FOLK & WARD METHOD		
	Arithmetic	Geometric	Logarithmic	Geometric	Logarithmic	Description
	∞ m	∞ m	\square	∞ m	\square	
MEAN (\bar{x}):	258.8	223.2	2.163	222.3	2.169	Fine Sand
SORTING (\square):	147.9	1.653	0.725	1.647	0.720	Moderately Sorted
SKEWNESS (Sk):	1.824	0.310	-0.310	0.143	-0.143	Coarse Skewed
KURTOSIS (K):	7.072	3.046	3.046	0.961	0.961	Mesokurtic

GRAIN SIZE DISTRIBUTION



SAMPLE STATISTICS

SAMPLE IDENTITY: **AO 2 - 5**

ANALYST & DATE: JES,

SAMPLE TYPE: Unimodal, Well Sorted

TEXTURAL GROUP: Sand

SEDIMENT NAME: Well Sorted Fine Sand

GPS: 29 32' 40" N, 34 58' 51" E

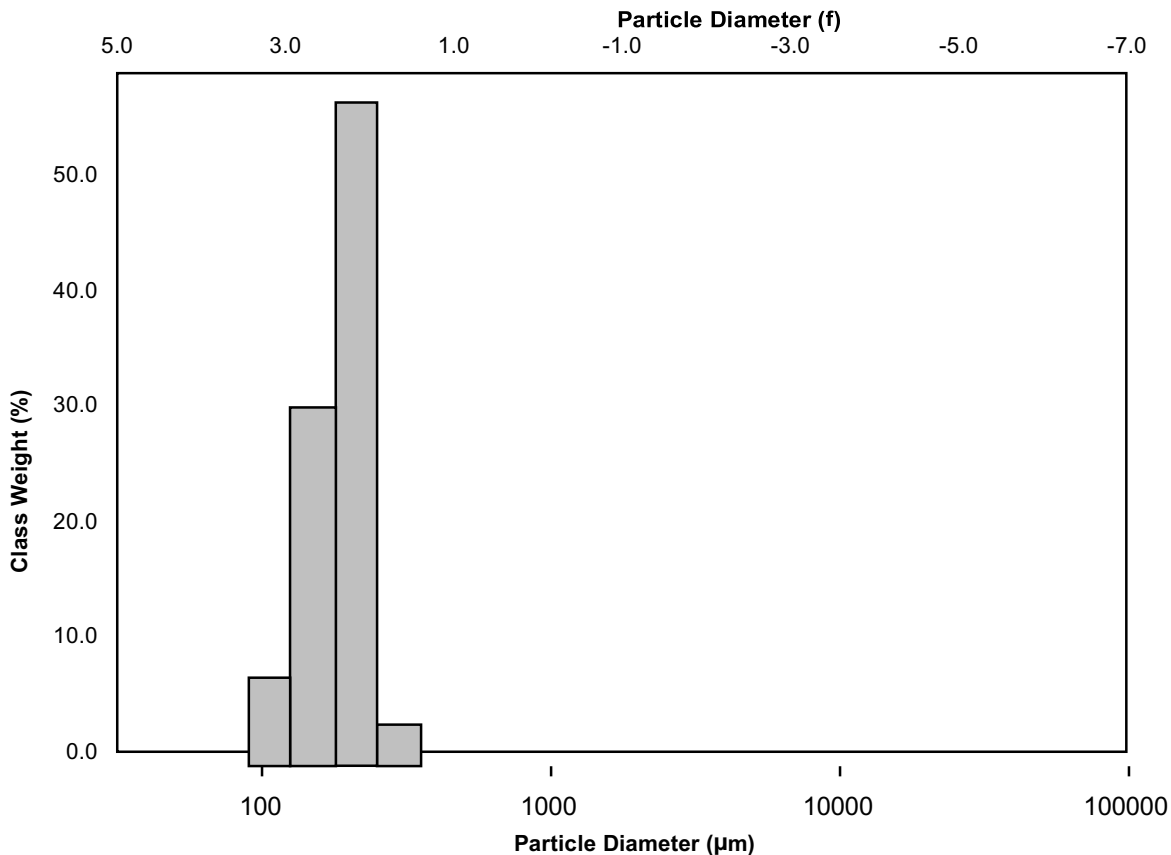
Depth: 2.18m

	∞ m	ϕ
MODE 1:	215.0	2.237
MODE 2:		
MODE 3:		
D ₁₀ :	128.6	2.054
MEDIAN or D ₅₀ :	190.1	2.395
D ₉₀ :	240.9	2.959
(D ₉₀ / D ₁₀):	1.873	1.441
(D ₉₀ - D ₁₀):	112.3	0.905
(D ₇₅ / D ₂₅):	1.455	1.248
(D ₇₅ - D ₂₅):	68.88	0.541

GRAIN SIZE DISTRIBUTION	
GRAVEL: 0.0%	COARSE SAND: 0.0%
SAND: 100.0%	MEDIUM SAND: 3.7%
MUD: 0.0%	FINE SAND: 88.9%
	V FINE SAND: 7.4%
V COARSE GRAVEL: 0.0%	V COARSE SILT: 0.0%
COARSE GRAVEL: 0.0%	COARSE SILT: 0.0%
MEDIUM GRAVEL: 0.0%	MEDIUM SILT: 0.0%
FINE GRAVEL: 0.0%	FINE SILT: 0.0%
V FINE GRAVEL: 0.0%	V FINE SILT: 0.0%
V COARSE SAND: 0.0%	CLAY: 0.0%

	METHOD OF MOMENTS			FOLK & WARD METHOD		Description
	Arithmetic	Geometric	Logarithmic	Geometric	Logarithmic	
MEAN (\bar{x}):	189.4	181.8	2.460	182.4	2.455	Fine Sand
SORTING (σ):	42.28	1.267	0.342	1.286	0.363	Well Sorted
SKEWNESS (S_k):	0.069	-0.562	0.562	-0.282	0.282	Fine Skewed
KURTOSIS (K):	3.204	2.931	2.931	0.866	0.866	Platykurtic

GRAIN SIZE DISTRIBUTION



SAMPLE STATISTICS

SAMPLE IDENTITY: **AO 2 - Unit 6**

ANALYST & DATE: JES,

SAMPLE TYPE: Unimodal, Very Well Sorted

TEXTURAL GROUP: Sand

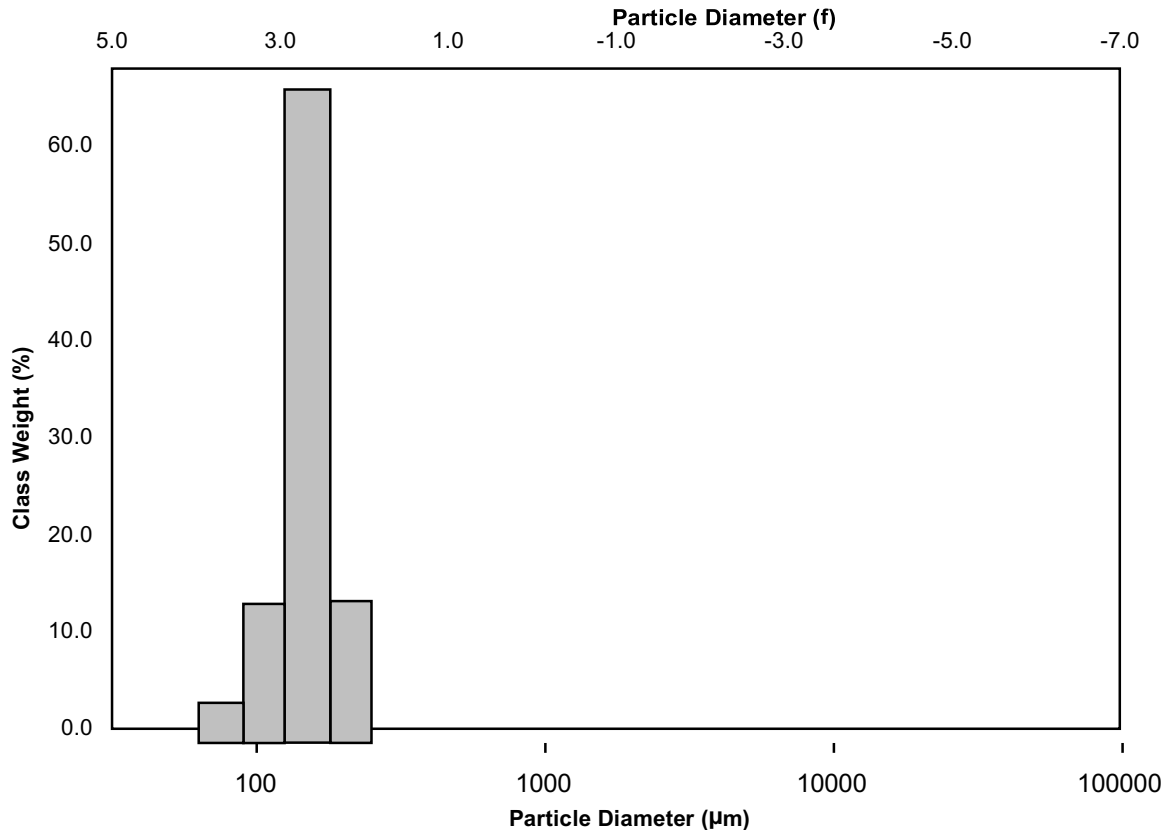
SEDIMENT NAME: Very Well Sorted Fine Sand

GPS: 29.3240N, 34.5851E

Depth: 2.67m

			GRAIN SIZE DISTRIBUTION			
MODE 1:	∞ m	ϕ	GRAVEL:	0.0%	COARSE SAND:	0.0%
MODE 2:			SAND:	100.0%	MEDIUM SAND:	0.0%
MODE 3:			MUD:	0.0%	FINE SAND:	82.6%
D ₁₀ :	104.1	2.351	V COARSE GRAVEL:	0.0%	V COARSE SILT:	0.0%
MEDIAN or D ₅₀ :	148.5	2.752	COARSE GRAVEL:	0.0%	COARSE SILT:	0.0%
D ₉₀ :	196.0	3.265	MEDIUM GRAVEL:	0.0%	MEDIUM SILT:	0.0%
(D ₉₀ / D ₁₀):	1.884	1.389	FINE GRAVEL:	0.0%	FINE SILT:	0.0%
(D ₉₀ - D ₁₀):	91.98	0.914	V FINE GRAVEL:	0.0%	V FINE SILT:	0.0%
(D ₇₅ / D ₂₅):	1.302	1.149	V COARSE SAND:	0.0%	CLAY:	0.0%
(D ₇₅ - D ₂₅):	39.29	0.381				
			METHOD OF MOMENTS			
	∞ m	ϕ	\square	FOLK & WARD METHOD		
	∞ m	ϕ	\square	∞ m	ϕ	Description
MEAN (\bar{x}):	151.8	145.9	2.777	147.1	2.765	Fine Sand
SORTING (σ):	32.17	1.254	0.326	1.258	0.331	Very Well Sorted
SKEWNESS (S_k):	0.144	-0.798	0.798	-0.081	0.081	Symmetrical
KURTOSIS (K):	3.732	4.586	4.586	1.365	1.365	Leptokurtic

GRAIN SIZE DISTRIBUTION



SAMPLE STATISTICS

SAMPLE IDENTITY: **AO 2 - 7**

ANALYST & DATE: JES,

SAMPLE TYPE: Bimodal, Moderately Well Sorted

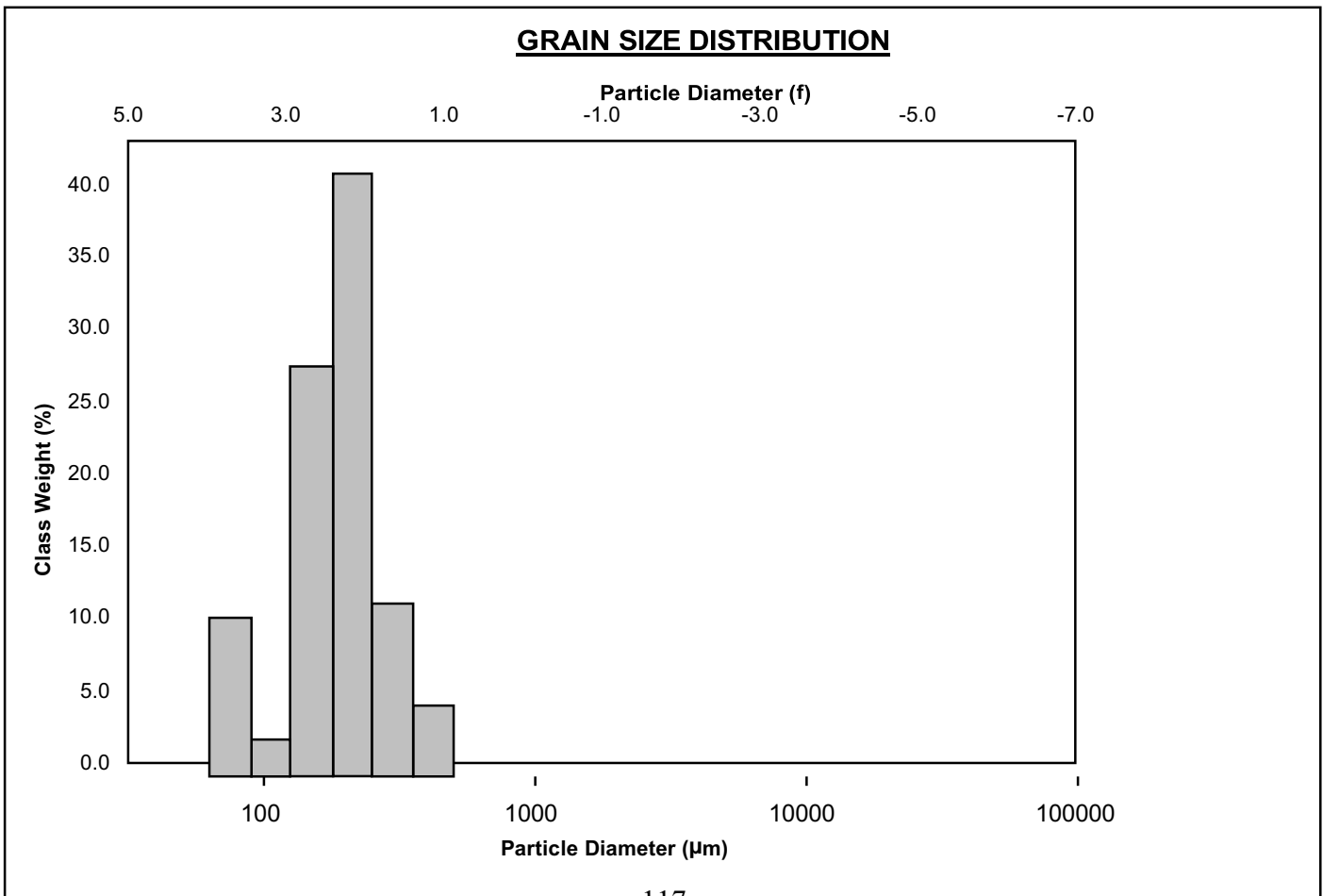
TEXTURAL GROUP: Sand

SEDIMENT NAME: Moderately Well Sorted Fine Sand

GPS: 29 32' 40" N, 34 58' 51" E

Depth: 2.85m

	α m		ϕ		GRAIN SIZE DISTRIBUTION	
	α m	ϕ	GRAVEL: 0.0%	COARSE SAND: 0.0%	SAND: 100.0%	MEDIUM SAND: 16.9%
MODE 1:	215.0	2.237	MUD: 0.0%	FINE SAND: 69.4%		
MODE 2:	76.50	3.731		V FINE SAND: 13.7%		
MODE 3:			V COARSE GRAVEL: 0.0%	V COARSE SILT: 0.0%		
D ₁₀ :	86.41	1.710	COARSE GRAVEL: 0.0%	COARSE SILT: 0.0%		
MEDIAN or D ₅₀ :	189.9	2.397	MEDIUM GRAVEL: 0.0%	MEDIUM SILT: 0.0%		
D ₉₀ :	305.7	3.533	FINE GRAVEL: 0.0%	FINE SILT: 0.0%		
(D ₉₀ / D ₁₀):	3.538	2.066	V FINE GRAVEL: 0.0%	V FINE SILT: 0.0%		
(D ₉₀ - D ₁₀):	219.3	1.823	V COARSE SAND: 0.0%	CLAY: 0.0%		
(D ₇₅ / D ₂₅):	1.629	1.336				
(D ₇₅ - D ₂₅):	90.30	0.704				
	METHOD OF MOMENTS		EQUILIBRIUM METHOD		Description	
	Arithmetic α m	Geometric α m	Normal σ	Geometric α m	Equilibrium σ	
MEAN (\bar{x}):	199.0	180.3	2.472	184.4	2.439	Fine Sand
SORTING ($\bar{\sigma}$):	80.41	1.526	0.610	1.507	0.592	Moderately Well Sorted
SKEWNESS (S_k):	0.880	-0.448	0.448	-0.167	0.167	Fine Skewed
KURTOSIS (K):	4.171	3.157	3.157	1.315	1.315	Leptokurtic



SAMPLE STATISTICS

SAMPLE IDENTITY: **AO 2 - Unit 8**

ANALYST & DATE: JES,

SAMPLE TYPE: Bimodal, Moderately Well Sorted

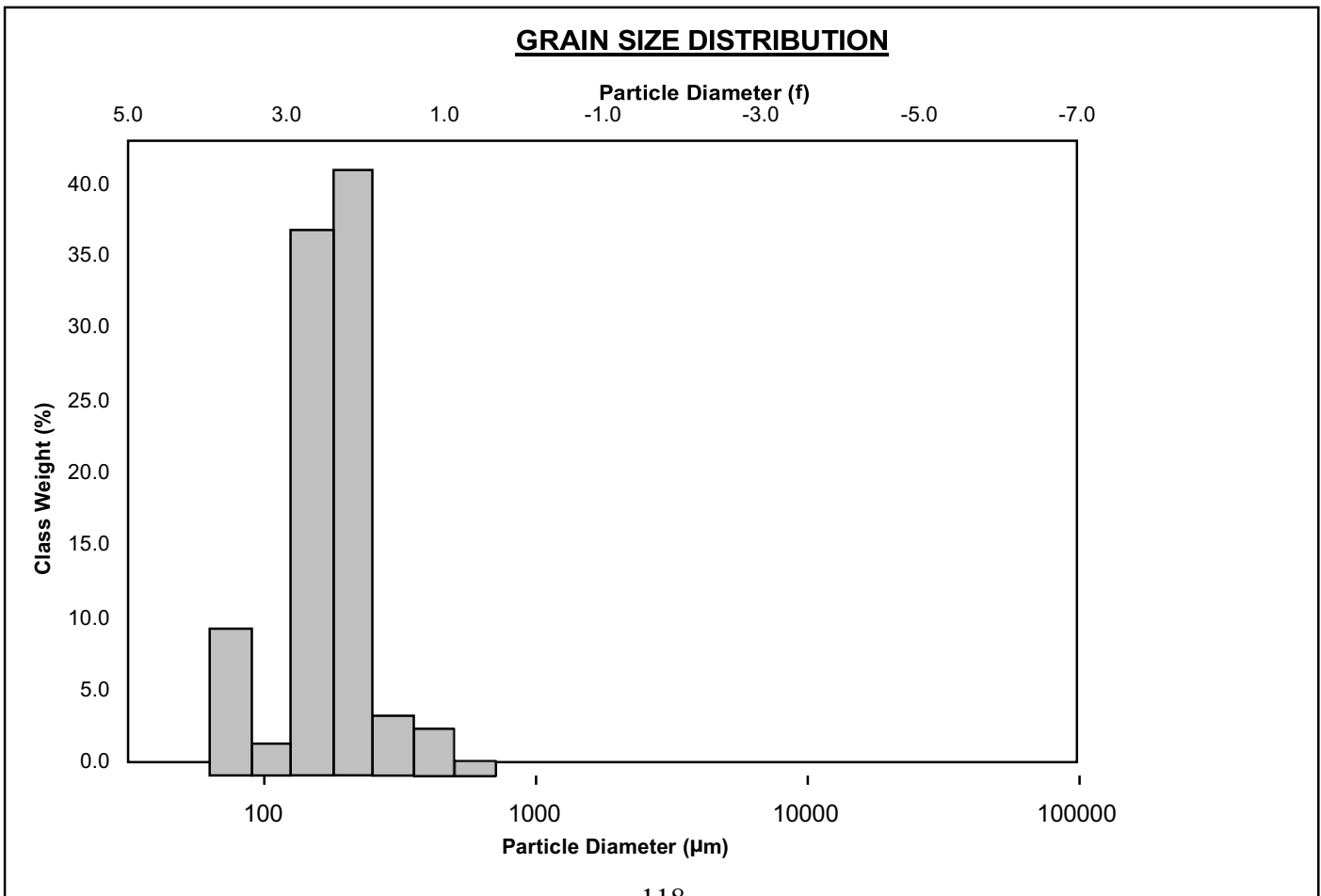
TEXTURAL GROUP: Sand

SEDIMENT NAME: Moderately Well Sorted Fine Sand

GPS: 29.3240N, 34.5851E

Depth: 3.25m

	∞ m		ϕ		GRAIN SIZE DISTRIBUTION		
	∞ m	ϕ	GRAVEL: 0.0%	COARSE SAND: 1.0%	SAND: 100.0%	MEDIUM SAND: 7.3%	FINE SAND: 79.2%
MODE 1:	215.0	2.237	MUD: 0.0%	V FINE SAND: 12.5%			
MODE 2:	76.50	3.731	V COARSE GRAVEL: 0.0%	V COARSE SILT: 0.0%			
MODE 3:			COARSE GRAVEL: 0.0%	COARSE SILT: 0.0%			
D ₁₀ :	88.72	2.020	MEDIUM GRAVEL: 0.0%	MEDIUM SILT: 0.0%			
MEDIAN or D ₅₀ :	176.6	2.502	FINE GRAVEL: 0.0%	FINE SILT: 0.0%			
D ₉₀ :	246.6	3.495	V FINE GRAVEL: 0.0%	V FINE SILT: 0.0%			
(D ₉₀ / D ₁₀):	2.779	1.730	V COARSE SAND: 0.0%	CLAY: 0.0%			
(D ₉₀ - D ₁₀):	157.9	1.475					
(D ₇₅ / D ₂₅):	1.552	1.288					
(D ₇₅ - D ₂₅):	77.46	0.634					
	METHOD OF MOMENTS			FOLK & WARD METHOD			
	Arithmetic	Geometric	Logarithmic	Geometric	Logarithmic	Description	
	∞ m	∞ m	\square	∞ m	\square		
MEAN (\bar{x}):	188.0	171.4	2.544	174.9	2.516	Fine Sand	
SORTING (\square):	79.80	1.482	0.567	1.455	0.541	Moderately Well Sorted	
SKEWNESS (Sk):	2.130	-0.123	0.123	-0.102	0.102	Fine Skewed	
KURTOSIS (K):	10.92	4.154	4.154	1.387	1.387	Leptokurtic	



SAMPLE STATISTICS

SAMPLE IDENTITY: **AO 2 - Unit 9**

ANALYST & DATE: JES,

SAMPLE TYPE: Bimodal, Moderately Sorted

TEXTURAL GROUP: Sand

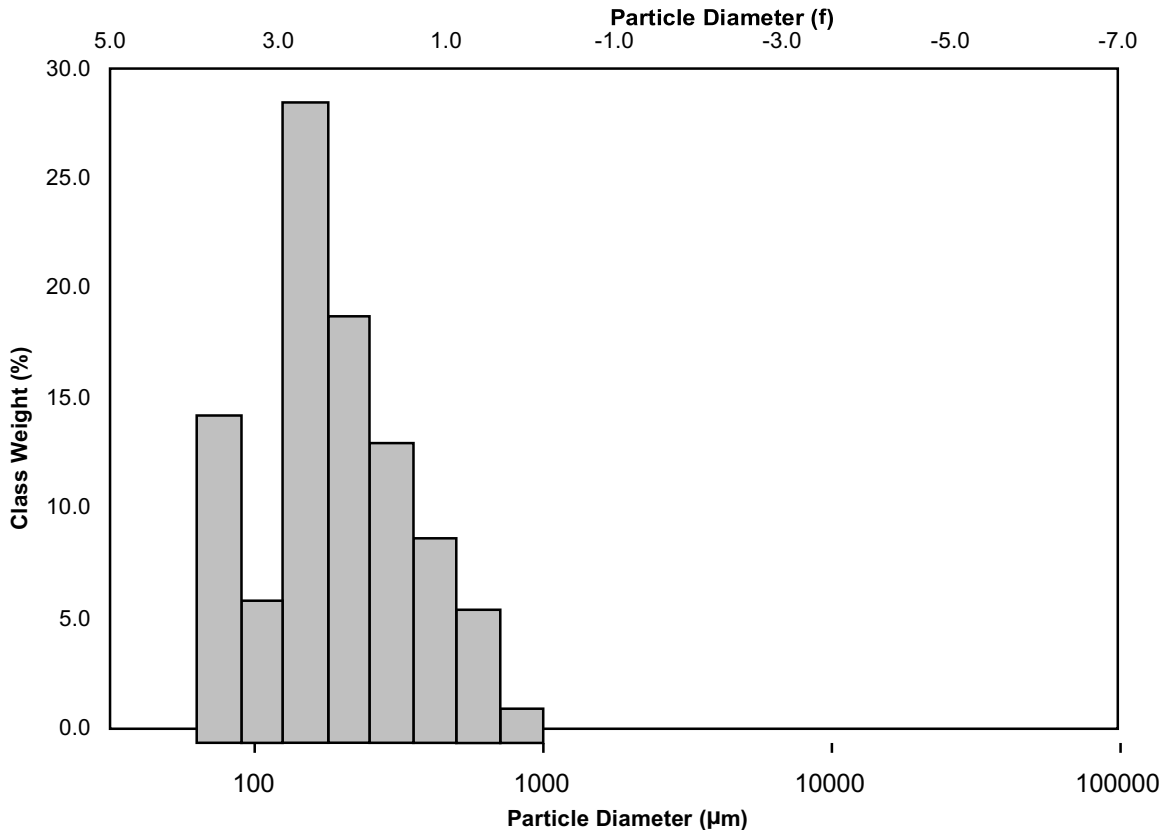
SEDIMENT NAME: Moderately Sorted Fine Sand

GPS: 29.3240N, 34.5851E

Depth: 3.7m

	σ_m ϕ		GRAIN SIZE DISTRIBUTION			
	σ_m	ϕ	GRAVEL: 0.0%	COARSE SAND: 7.6%		
MODE 1:	152.5	2.737	SAND: 100.0%	MEDIUM SAND: 22.7%		
MODE 2:	76.50	3.731	MUD: 0.0%	FINE SAND: 48.5%		
MODE 3:				V FINE SAND: 21.2%		
D ₁₀ :	79.72	1.132	V COARSE GRAVEL: 0.0%	V COARSE SILT: 0.0%		
MEDIAN or D ₅₀ :	176.8	2.500	COARSE GRAVEL: 0.0%	COARSE SILT: 0.0%		
D ₉₀ :	456.4	3.649	MEDIUM GRAVEL: 0.0%	MEDIUM SILT: 0.0%		
(D ₉₀ / D ₁₀):	5.725	3.225	FINE GRAVEL: 0.0%	FINE SILT: 0.0%		
(D ₉₀ - D ₁₀):	376.7	2.517	V FINE GRAVEL: 0.0%	V FINE SILT: 0.0%		
(D ₇₅ / D ₂₅):	2.190	1.627	V COARSE SAND: 0.0%	CLAY: 0.0%		
(D ₇₅ - D ₂₅):	155.7	1.131				
			METHOD OF MOMENTS FOLK & WARD METHOD			
	Arithmetic	Geometric	Logarithmic	Geometric	Logarithmic	Description
	σ_m	σ_m	σ_m	σ_m	σ_m	
MEAN (\bar{x}):	233.2	189.7	2.398	182.4	2.455	Fine Sand
SORTING (σ):	158.3	1.834	0.875	1.928	0.947	Moderately Sorted
SKEWNESS (Sk):	1.669	0.291	-0.291	0.100	-0.100	Coarse Skewed
KURTOSIS (K):	5.868	2.515	2.515	1.099	1.099	Mesokurtic

GRAIN SIZE DISTRIBUTION



SAMPLE STATISTICS

SAMPLE IDENTITY: **AO 2 - Unit 10**

ANALYST & DATE: JES,

SAMPLE TYPE: Unimodal, Moderately Well Sorted

TEXTURAL GROUP: Sand

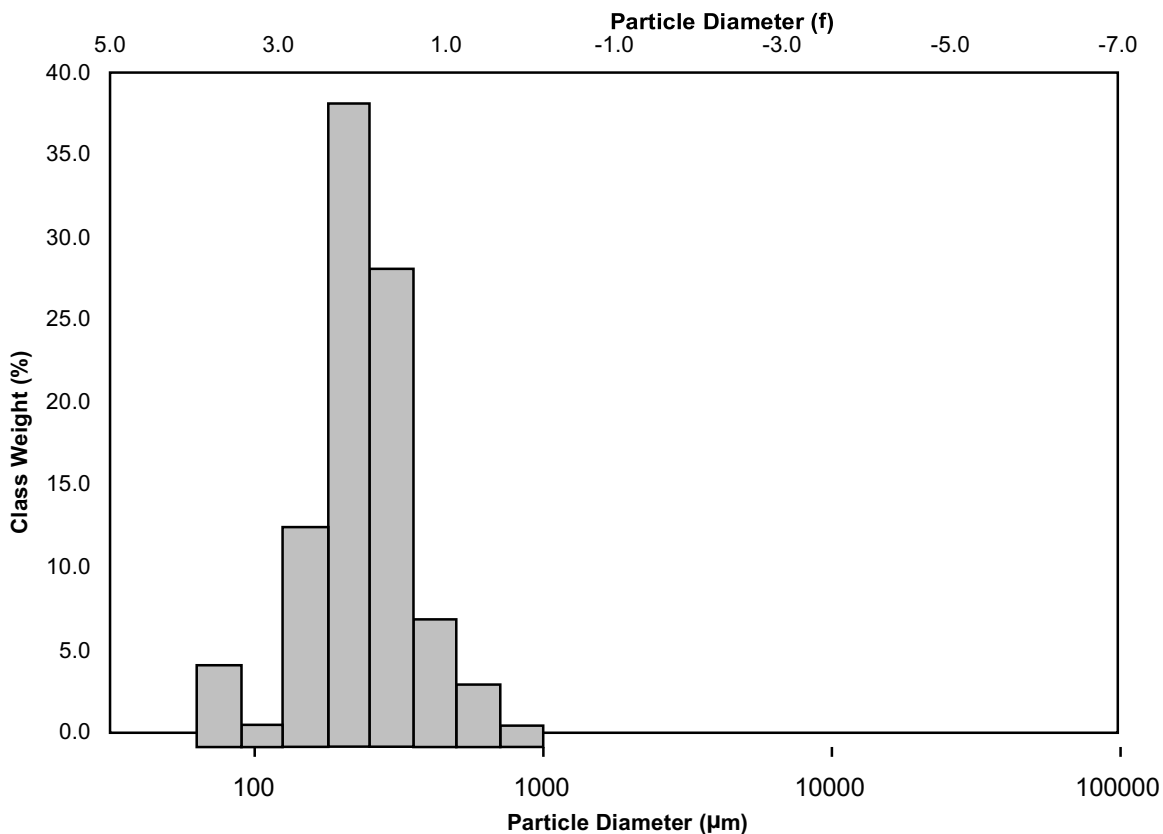
SEDIMENT NAME: Moderately Well Sorted Fine Sand

GPS: 29.3240N, 34.5851E

Depth: 4.05m

	∞m		ϕ		GRAIN SIZE DISTRIBUTION			
	∞m	ϕ						
MODE 1:	215.0	2.237			GRAVEL: 0.0%		COARSE SAND: 5.1%	
MODE 2:					SAND: 100.0%		MEDIUM SAND: 37.2%	
MODE 3:					MUD: 0.0%		FINE SAND: 51.3%	
D ₁₀ :	137.2	1.313					V FINE SAND: 6.4%	
MEDIAN or D ₅₀ :	233.6	2.098			V COARSE GRAVEL: 0.0%		V COARSE SILT: 0.0%	
D ₉₀ :	402.5	2.866			COARSE GRAVEL: 0.0%		COARSE SILT: 0.0%	
(D ₉₀ / D ₁₀):	2.935	2.183			MEDIUM GRAVEL: 0.0%		MEDIUM SILT: 0.0%	
(D ₉₀ - D ₁₀):	265.3	1.553			FINE GRAVEL: 0.0%		FINE SILT: 0.0%	
(D ₇₅ / D ₂₅):	1.640	1.419			V FINE GRAVEL: 0.0%		V FINE SILT: 0.0%	
(D ₇₅ - D ₂₅):	119.9	0.714			V COARSE SAND: 0.0%		CLAY: 0.0%	
			METHOD OF MOMENTS		FOLK & WARD METHOD			
			Arithmetic	Geometric	Logarithmic	Geometric	Logarithmic	Description
	∞m	∞m			\square	∞m	\square	
MEAN (\bar{x}):	263.1	234.3			2.093	233.9	2.096	Fine Sand
SORTING (σ):	127.3	1.571			0.651	1.572	0.653	Moderately Well Sorted
SKEWNESS (S_k):	1.911	-0.180			0.180	-0.052	0.052	Symmetrical
KURTOSIS (K):	8.562	4.079			4.079	1.438	1.438	Leptokurtic

GRAIN SIZE DISTRIBUTION



SAMPLE STATISTICS

SAMPLE IDENTITY: **AO 2 - Unit 12b**

ANALYST & DATE: JES,

SAMPLE TYPE: Bimodal, Moderately Well Sorted

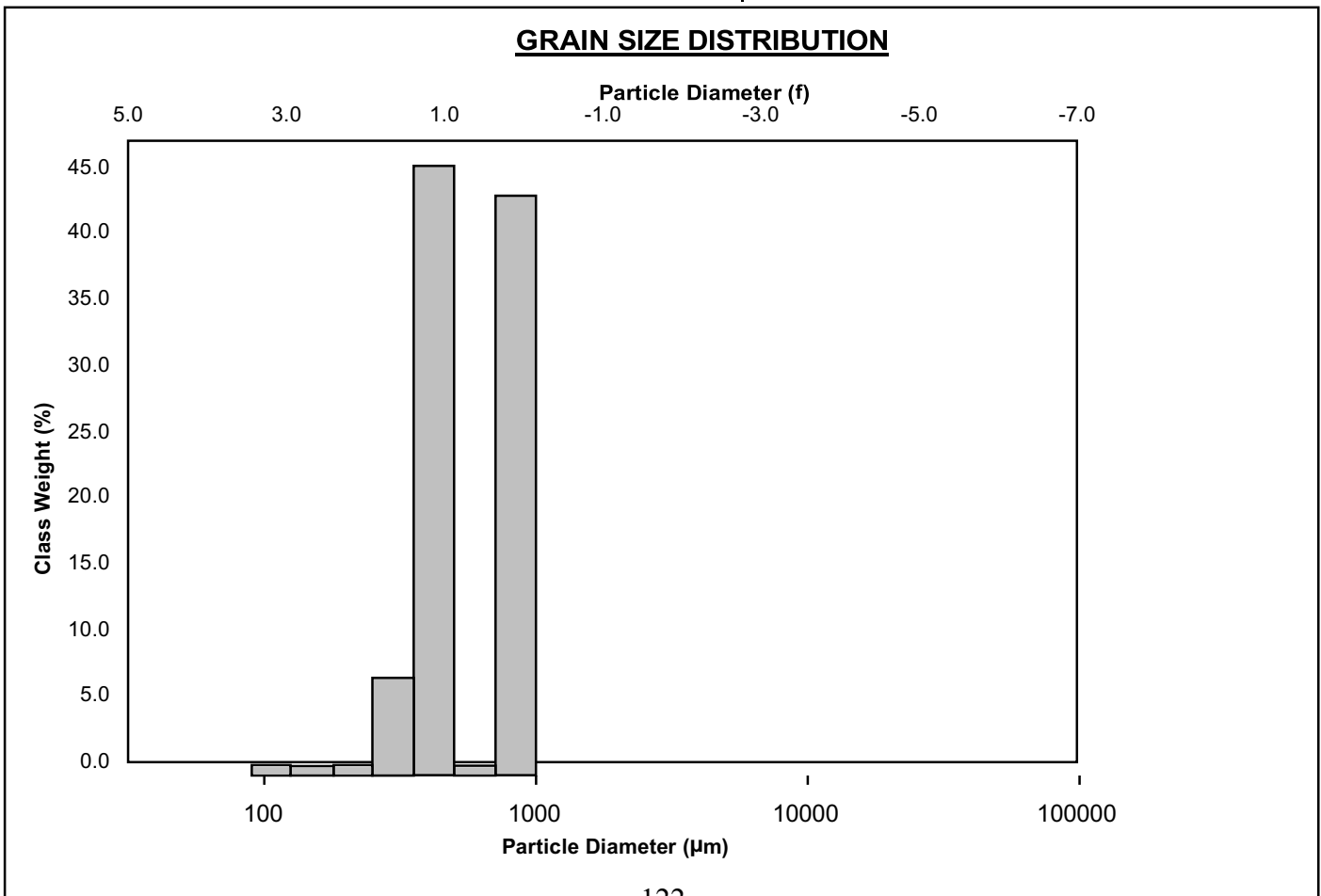
TEXTURAL GROUP: Sand

SEDIMENT NAME: Moderately Well Sorted Medium Sand

GPS: 29.3240N, 34.5851E

Depth: 5.4m

	μm		ϕ		GRAIN SIZE DISTRIBUTION		
	μm	ϕ					
MODE 1:	427.5	1.247			GRAVEL: 0.0%		COARSE SAND: 44.4%
MODE 2:	855.0	0.247			SAND: 100.0%		MEDIUM SAND: 53.4%
MODE 3:					MUD: 0.0%		FINE SAND: 1.5%
D ₁₀ :	355.6	0.113					V FINE SAND: 0.8%
MEDIAN or D ₅₀ :	479.4	1.061			V COARSE GRAVEL: 0.0%		V COARSE SILT: 0.0%
D ₉₀ :	924.5	1.492			COARSE GRAVEL: 0.0%		COARSE SILT: 0.0%
(D ₉₀ / D ₁₀):	2.600	13.17			MEDIUM GRAVEL: 0.0%		MEDIUM SILT: 0.0%
(D ₉₀ - D ₁₀):	568.9	1.378			FINE GRAVEL: 0.0%		FINE SILT: 0.0%
(D ₇₅ / D ₂₅):	2.066	4.696			V FINE GRAVEL: 0.0%		V FINE SILT: 0.0%
(D ₇₅ - D ₂₅):	424.0	1.047			V COARSE SAND: 0.0%		CLAY: 0.0%
	METHOD OF MOMENTS			FOLK & WARD METHOD			
	Arithmetic	Geometric	Logarithmic	Geometric	Logarithmic	Description	
	μm	μm	ϕ	μm	ϕ		
MEAN (\bar{x}):	599.8	544.0	0.878	539.7	0.890	Coarse Sand	
SORTING (σ):	230.4	1.528	0.612	1.493	0.578	Moderately Well Sorted	
SKEWNESS (Sk):	0.076	-0.558	0.558	0.277	-0.277	Coarse Skewed	
KURTOSIS (K):	1.329	3.335	3.335	0.688	0.688	Platykurtic	



SAMPLE STATISTICS

SAMPLE IDENTITY: **AO 3-11, Unit 5**

ANALYST & DATE: JES,

SAMPLE TYPE: Unimodal, Well Sorted

TEXTURAL GROUP: Sand

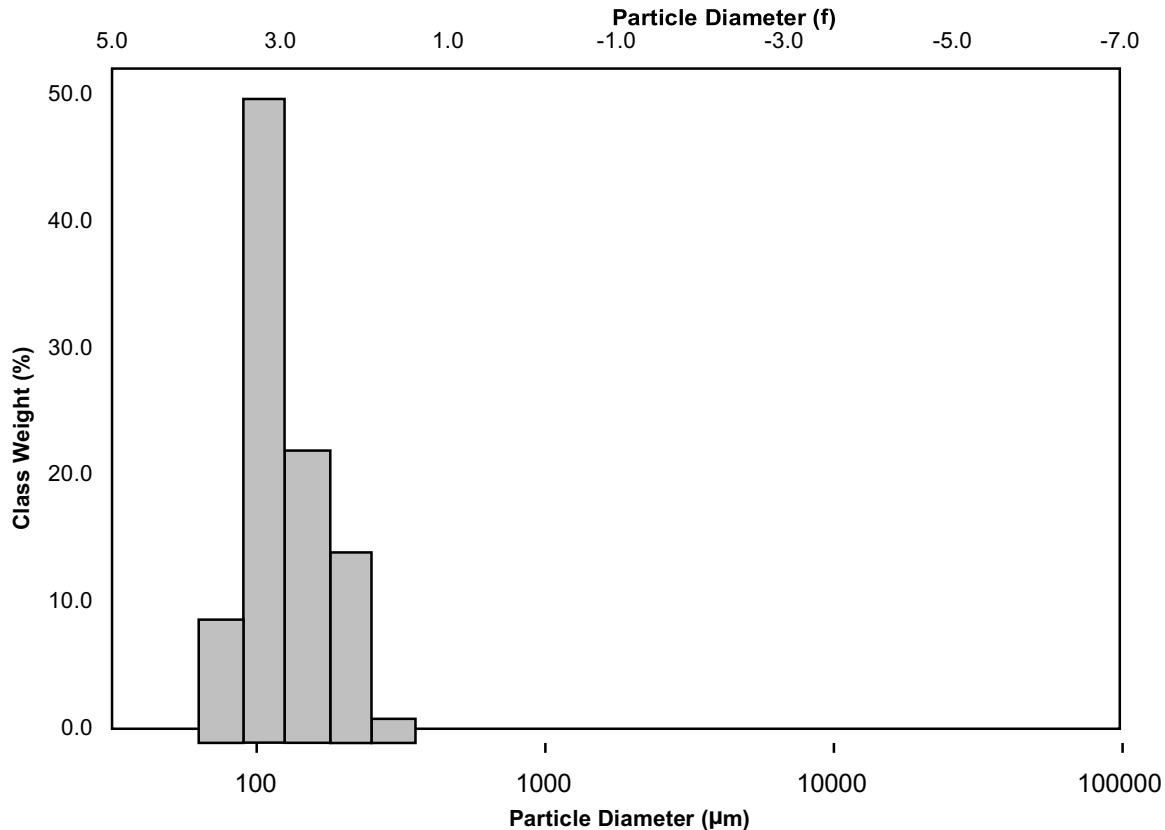
SEDIMENT NAME: Well Sorted Very Fine Sand

GPS: 29 32'43" N, 34 58'53" E

Depth: 3.2 m

			GRAIN SIZE DISTRIBUTION			
MODE 1:	∞ m	ϕ	GRAVEL:	0.0%	COARSE SAND:	0.0%
MODE 2:			SAND:	100.0%	MEDIUM SAND:	2.0%
MODE 3:			MUD:	0.0%	FINE SAND:	39.1%
D ₁₀ :	89.52	2.264	V COARSE GRAVEL:	0.0%	V COARSE SILT:	0.0%
MEDIAN or D ₅₀ :	117.7	3.087	COARSE GRAVEL:	0.0%	COARSE SILT:	0.0%
D ₉₀ :	208.2	3.482	MEDIUM GRAVEL:	0.0%	MEDIUM SILT:	0.0%
(D ₉₀ / D ₁₀):	2.326	1.538	FINE GRAVEL:	0.0%	FINE SILT:	0.0%
(D ₉₀ - D ₁₀):	118.7	1.218	V FINE GRAVEL:	0.0%	V FINE SILT:	0.0%
(D ₇₅ / D ₂₅):	1.593	1.253	V COARSE SAND:	0.0%	CLAY:	0.0%
(D ₇₅ - D ₂₅):	59.02	0.672				
⋮						
			METHOD OF MOMENTS		FOLK & WARD METHOD	
	∞ m		∞ m		∞ m	\square
MEAN (\bar{x})	134.8		125.8		126.0	2.988
SORTING (\square)	47.58		1.377		1.401	0.487
SKEWNESS (Sk)	1.282		0.556		0.259	-0.259
KURTOSIS (K)	4.465		2.780		0.997	0.997
						Description
						Fine Sand
						Well Sorted
						Coarse Skewed
						Mesokurtic

GRAIN SIZE DISTRIBUTION



SAMPLE STATISTICS

SAMPLE IDENTITY: **AO 3-5, Unit 6**

ANALYST & DATE: JES,

SAMPLE TYPE: Unimodal, Moderately Well Sorted

TEXTURAL GROUP: Sand

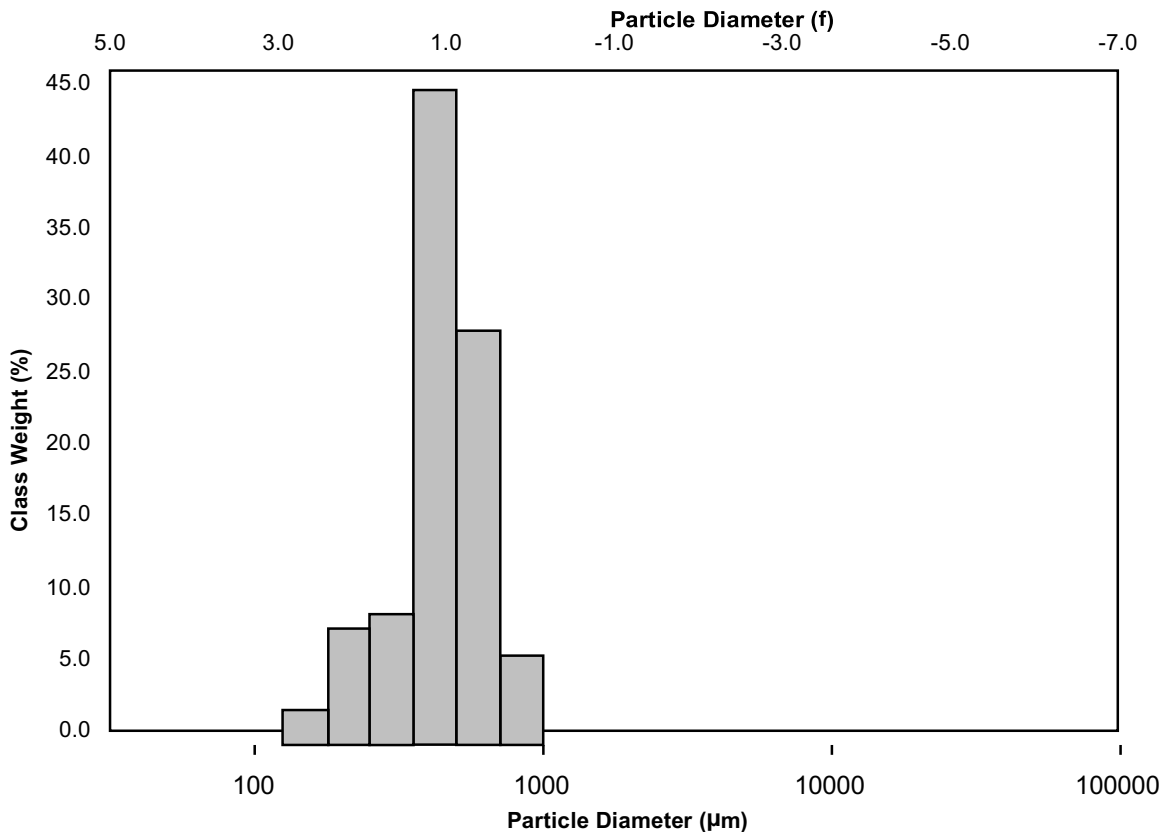
SEDIMENT NAME: Moderately Well Sorted Medium Sand

GPS: 29 32'43" N, 34 58'53" E

Depth: 3.4 m

	∞ m		ϕ		GRAIN SIZE DISTRIBUTION			
	∞ m	ϕ	GRAVEL:	COARSE SAND:	SAND:	MEDIUM SAND:	FINE SAND:	
MODE 1:	427.5	1.247	0.0%	35.4%	100.0%	54.4%	10.3%	
MODE 2:			0.0%	0.0%	0.0%	0.0%	0.0%	
MODE 3:			0.0%	0.0%	0.0%	0.0%	0.0%	
D ₁₀ :	247.3	0.561	V COARSE GRAVEL:	0.0%	V COARSE SILT:	0.0%	0.0%	
MEDIAN or D ₅₀ :	447.5	1.160	COARSE GRAVEL:	0.0%	COARSE SILT:	0.0%	0.0%	
D ₉₀ :	678.0	2.015	MEDIUM GRAVEL:	0.0%	MEDIUM SILT:	0.0%	0.0%	
(D ₉₀ / D ₁₀):	2.741	3.594	FINE GRAVEL:	0.0%	FINE SILT:	0.0%	0.0%	
(D ₉₀ - D ₁₀):	430.6	1.455	V FINE GRAVEL:	0.0%	V FINE SILT:	0.0%	0.0%	
(D ₇₅ / D ₂₅):	1.530	1.748	V COARSE SAND:	0.0%	CLAY:	0.0%	0.0%	
(D ₇₅ - D ₂₅):	196.1	0.613						
			METHOD OF MOMENTS		FOLK & WARD METHOD			
			Arithmetic	Geometric	Logarithmic	Geometric	Logarithmic	Description
	∞ m	∞ m	\square	∞ m	\square			
MEAN (\bar{x}):	470.8	435.3	1.200	444.5	1.170			Medium Sand
SORTING (σ):	159.5	1.450	0.536	1.460	0.546			Moderately Well Sorted
SKEWNESS (S_k):	0.397	-0.737	0.737	-0.120	0.120			Fine Skewed
KURTOSIS (K):	3.252	3.665	3.665	1.284	1.284			Leptokurtic

GRAIN SIZE DISTRIBUTION



SAMPLE STATISTICS

SAMPLE IDENTITY: **AO 3-4, Unit 7**

ANALYST & DATE: JES,

SAMPLE TYPE: Bimodal, Moderately Well Sorted

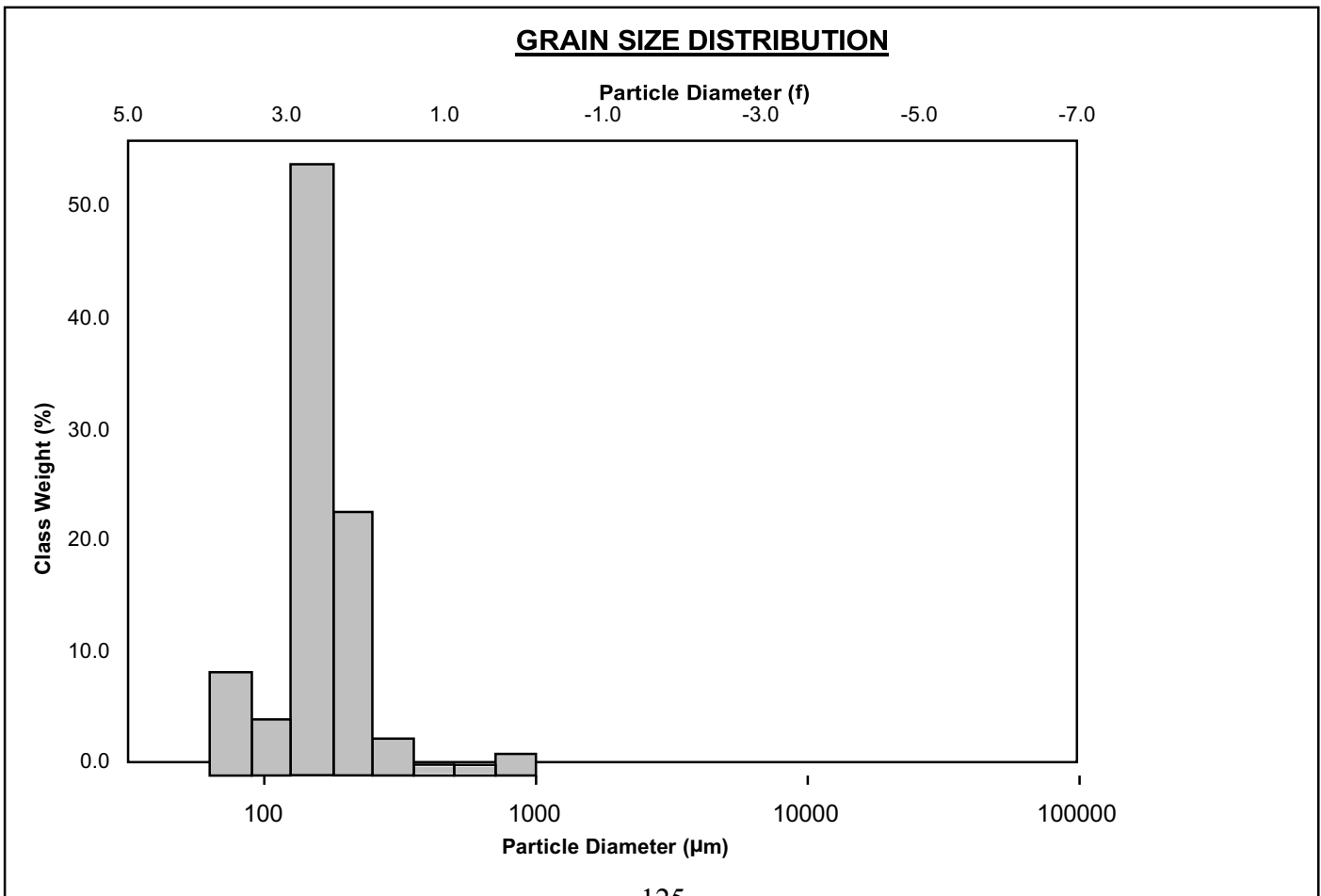
TEXTURAL GROUP: Sand

SEDIMENT NAME: Moderately Well Sorted Fine Sand

GPS: 29 32'43" N, 34 58'53" E

Depth: 3.42 m

	∞ m	ϕ	GRAIN SIZE DISTRIBUTION			
	MODE 1:	152.5	2.737	GRAVEL: 0.0%	COARSE SAND: 2.8%	
MODE 2:	76.50	3.731	SAND: 100.0%	MEDIUM SAND: 4.2%		
MODE 3:			MUD: 0.0%	FINE SAND: 78.9%		
D ₁₀ :	93.93	2.063		V FINE SAND: 14.1%		
MEDIAN or D ₅₀ :	157.4	2.667	V COARSE GRAVEL: 0.0%	V COARSE SILT: 0.0%		
D ₉₀ :	239.3	3.412	COARSE GRAVEL: 0.0%	COARSE SILT: 0.0%		
(D ₉₀ / D ₁₀):	2.547	1.654	MEDIUM GRAVEL: 0.0%	MEDIUM SILT: 0.0%		
(D ₉₀ - D ₁₀):	145.3	1.349	FINE GRAVEL: 0.0%	FINE SILT: 0.0%		
(D ₇₅ / D ₂₅):	1.427	1.215	V FINE GRAVEL: 0.0%	V FINE SILT: 0.0%		
(D ₇₅ - D ₂₅):	57.28	0.513	V COARSE SAND: 0.0%	CLAY: 0.0%		
.....						
	METHOD OF MOMENTS		EQUATION		Description	
	Arithmetic	Geometric	Arithmetic	Geometric		
	∞ m	∞ m	\square	∞ m	\square	
MEAN (x):	182.0	161.4	2.631	163.4	2.614	Fine Sand
SORTING (\square):	115.2	1.512	0.596	1.419	0.505	Moderately Well Sorted
SKEWNESS (Sk):	4.248	1.146	-1.146	0.086	-0.086	Symmetrical
KURTOSIS (K):	23.88	7.361	7.361	1.621	1.621	Very Leptokurtic



SAMPLE STATISTICS

SAMPLE IDENTITY: **AO 3-7, Unit 7**

ANALYST & DATE: JES,

SAMPLE TYPE: Bimodal, Well Sorted

TEXTURAL GROUP: Sand

SEDIMENT NAME: Well Sorted Fine Sand

GPS: 29 32'43" N, 34 58'53" E

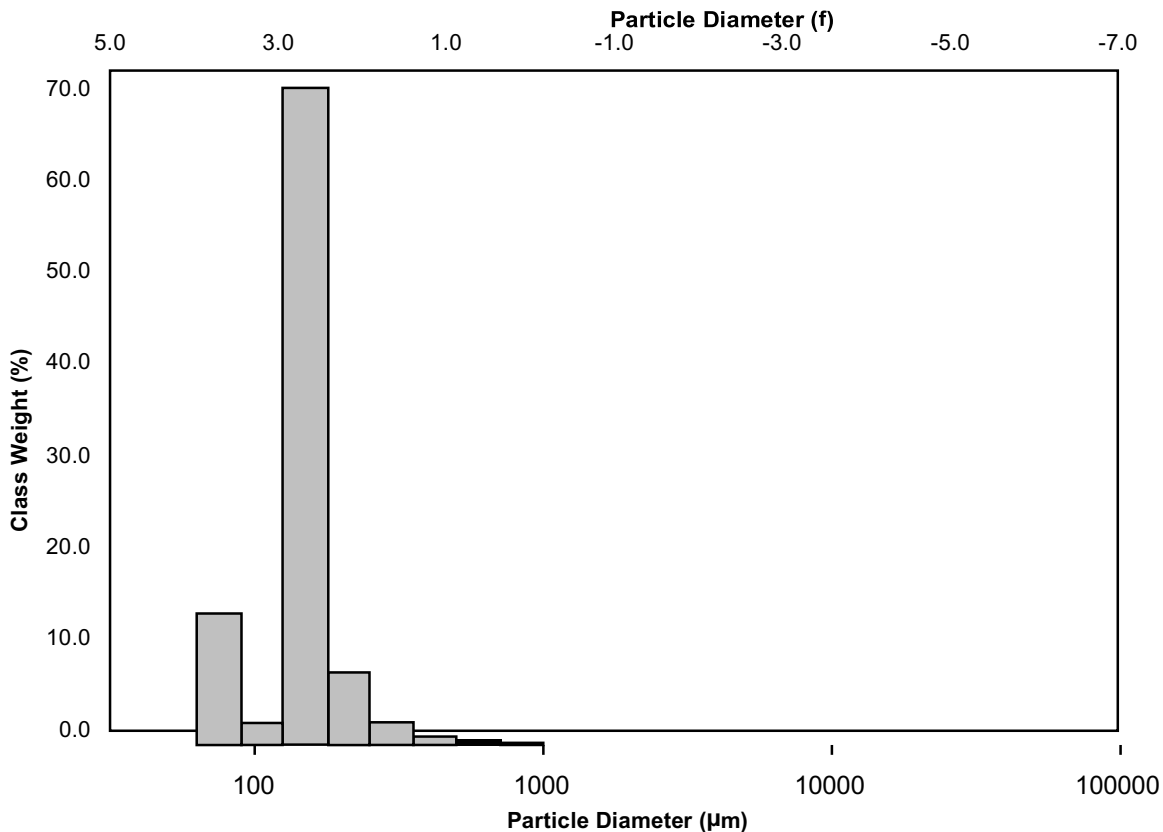
Depth: 3.5 m

	∞ m	ϕ
MODE 1:	152.5	2.737
MODE 2:	76.50	3.731
MODE 3:		
D ₁₀ :	81.00	2.399
MEDIAN or D ₅₀ :	148.0	2.756
D ₉₀ :	189.6	3.626
(D ₉₀ / D ₁₀):	2.341	1.511
(D ₉₀ - D ₁₀):	108.6	1.227
(D ₇₅ / D ₂₅):	1.286	1.141
(D ₇₅ - D ₂₅):	37.33	0.363

GRAIN SIZE DISTRIBUTION	
GRAVEL: 0.0%	COARSE SAND: 0.7%
SAND: 100.0%	MEDIUM SAND: 3.3%
MUD: 0.0%	FINE SAND: 79.7%
	V FINE SAND: 16.4%
V COARSE GRAVEL: 0.0%	V COARSE SILT: 0.0%
COARSE GRAVEL: 0.0%	COARSE SILT: 0.0%
MEDIUM GRAVEL: 0.0%	MEDIUM SILT: 0.0%
FINE GRAVEL: 0.0%	FINE SILT: 0.0%
V FINE GRAVEL: 0.0%	V FINE SILT: 0.0%
V COARSE SAND: 0.0%	CLAY: 0.0%

	METHOD OF MOMENTS			FOLK & WARD METHOD		Description
	Arithmetic	Geometric	Logarithmic	Geometric	Logarithmic	
MEAN (\bar{x}):	154.8	143.4	2.802	145.4	2.782	Fine Sand
SORTING (σ):	65.76	1.398	0.483	1.325	0.406	Well Sorted
SKEWNESS (S_k):	4.768	0.295	-0.295	-0.173	0.173	Fine Skewed
KURTOSIS (K^1):	41.47	6.731	6.731	1.962	1.962	Very Leptokurtic

GRAIN SIZE DISTRIBUTION



SAMPLE STATISTICS

SAMPLE IDENTITY: **AO 3-10, Unit 8**

ANALYST & DATE: JES,

SAMPLE TYPE: Bimodal, Moderately Well Sorted

TEXTURAL GROUP: Sand

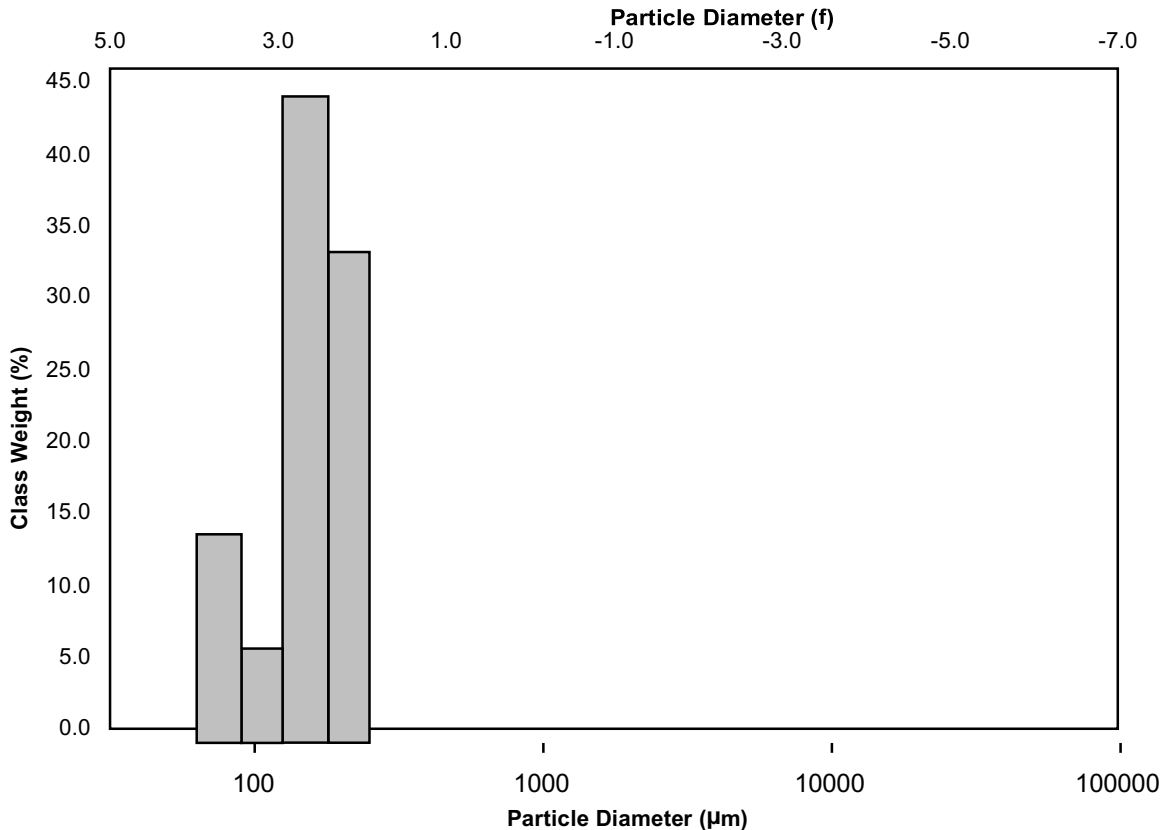
SEDIMENT NAME: Moderately Well Sorted Fine Sand

GPS: 29 32'43" N, 34 58'53" E

Depth: 3.6m

	∞ m		ϕ		GRAIN SIZE DISTRIBUTION		Description
	∞ m	ϕ	∞ m	ϕ	∞ m	ϕ	
MODE 1:	152.5	2.737			GRAVEL: 0.0%	COARSE SAND: 0.0%	
MODE 2:	76.50	3.731			SAND: 100.0%	MEDIUM SAND: 0.0%	
MODE 3:					MUD: 0.0%	FINE SAND: 79.0%	
D ₁₀ :	80.15	2.148				V FINE SAND: 21.0%	
MEDIAN or D ₅₀ :	156.6	2.675			V COARSE GRAVEL: 0.0%	V COARSE SILT: 0.0%	
D ₉₀ :	225.7	3.641			COARSE GRAVEL: 0.0%	COARSE SILT: 0.0%	
(D ₉₀ / D ₁₀):	2.816	1.695			MEDIUM GRAVEL: 0.0%	MEDIUM SILT: 0.0%	
(D ₉₀ - D ₁₀):	145.5	1.493			FINE GRAVEL: 0.0%	FINE SILT: 0.0%	
(D ₇₅ / D ₂₅):	1.501	1.247			V FINE GRAVEL: 0.0%	V FINE SILT: 0.0%	
(D ₇₅ - D ₂₅):	64.60	0.586			V COARSE SAND: 0.0%	CLAY: 0.0%	
	Arithmetic		Geometric		Logarithmic		
	METHOD OF MOMENTS		EQUATION		EQUATION		
	∞ m		∞ m		\square		
MEAN (\bar{x}):	158.5	148.2	2.755	147.2	2.765		Fine Sand
SORTING ($\bar{\sigma}$):	46.88	1.406	0.492	1.465	0.550		Moderately Well Sorted
SKEWNESS (S_k):	-0.313	-0.844	0.844	-0.272	0.272		Fine Skewed
KURTOSIS (K):	2.150	2.756	2.756	1.218	1.218		Leptokurtic

GRAIN SIZE DISTRIBUTION



SAMPLE STATISTICS

SAMPLE IDENTITY: **AO 3-3, Unit 8**

ANALYST & DATE: JES,

SAMPLE TYPE: Bimodal, Poorly Sorted

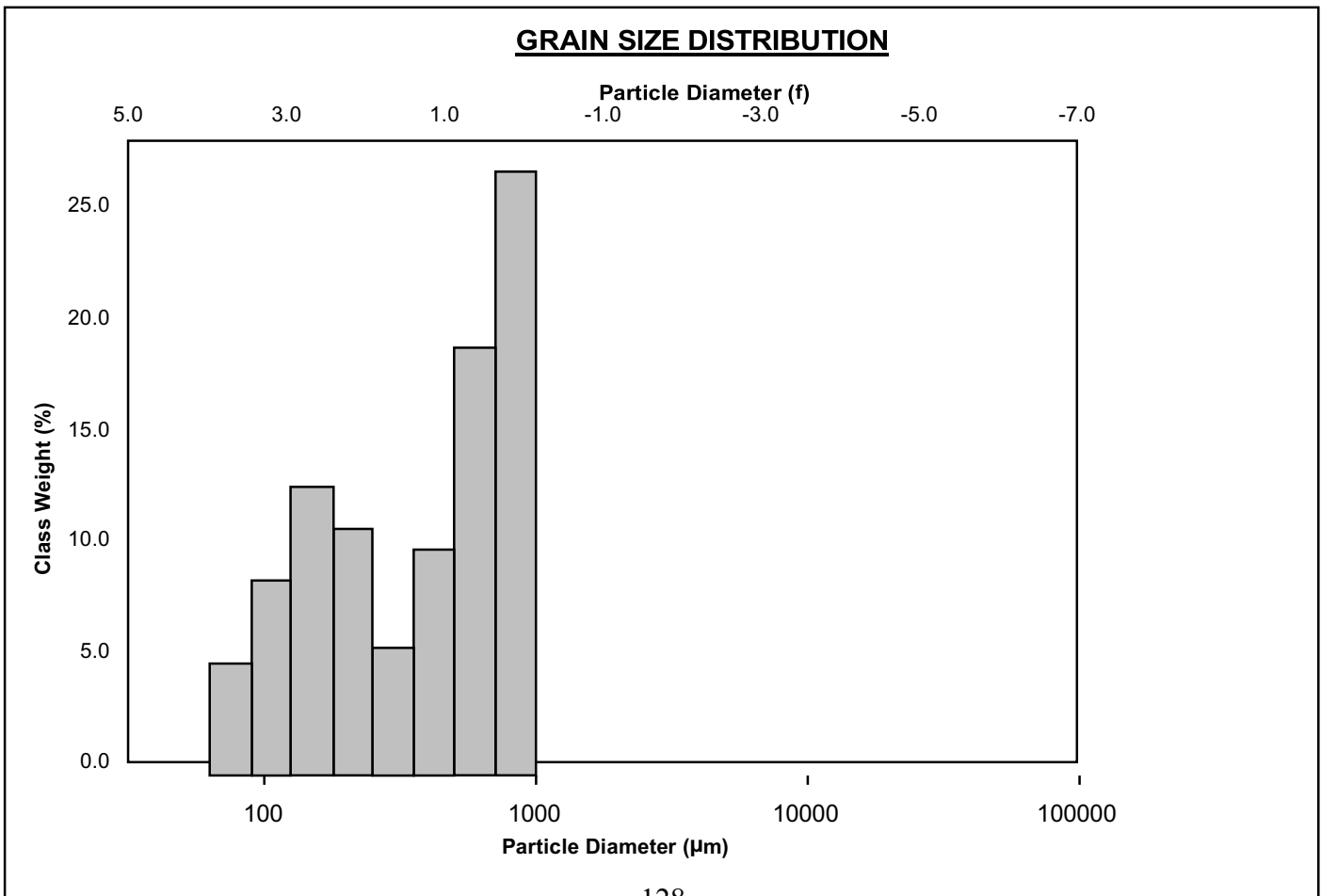
TEXTURAL GROUP: Sand

SEDIMENT NAME: Poorly Sorted Coarse Sand

GPS: 29 32'43" N, 34 58'53" E

Depth: 3.70m

	∞ m ϕ		GRAIN SIZE DISTRIBUTION			
	MODE 1:	855.0	0.247	GRAVEL: 0.0%	COARSE SAND: 46.4%	
MODE 2:	152.5	2.737	SAND: 100.0%	MEDIUM SAND: 15.9%		
MODE 3:			MUD: 0.0%	FINE SAND: 24.2%		
D ₁₀ :	108.8	0.184		V FINE SAND: 13.5%		
MEDIAN or D ₅₀ :	442.2	1.177	V COARSE GRAVEL: 0.0%	V COARSE SILT: 0.0%		
D ₉₀ :	880.4	3.200	COARSE GRAVEL: 0.0%	COARSE SILT: 0.0%		
(D ₉₀ / D ₁₀):	8.092	17.42	MEDIUM GRAVEL: 0.0%	MEDIUM SILT: 0.0%		
(D ₉₀ - D ₁₀):	771.6	3.017	FINE GRAVEL: 0.0%	FINE SILT: 0.0%		
(D ₇₅ / D ₂₅):	4.285	5.570	V FINE GRAVEL: 0.0%	V FINE SILT: 0.0%		
(D ₇₅ - D ₂₅):	557.6	2.099	V COARSE SAND: 0.0%	CLAY: 0.0%		
⋮						
	METHOD OF MOMENTS			FOLK & WARD METHOD		
	Arithmetic	Geometric	Logarithmic	Geometric	Logarithmic	Description
	∞ m	∞ m	□	∞ m	□	
MEAN (\bar{x}):	464.9	350.5	1.512	363.8	1.459	Medium Sand
SORTING (□):	291.2	2.217	1.148	2.247	1.168	Poorly Sorted
SKEWNESS (S_k):	0.145	-0.430	0.430	-0.342	0.342	Very Fine Skewed
KURTOSIS (K):	1.473	1.776	1.776	0.664	0.664	Very Platykurtic



SAMPLE STATISTICS

SAMPLE IDENTITY: **AO 3-12, Unit 9**

ANALYST & DATE: JES,

SAMPLE TYPE: Bimodal, Moderately Sorted

TEXTURAL GROUP: Sand

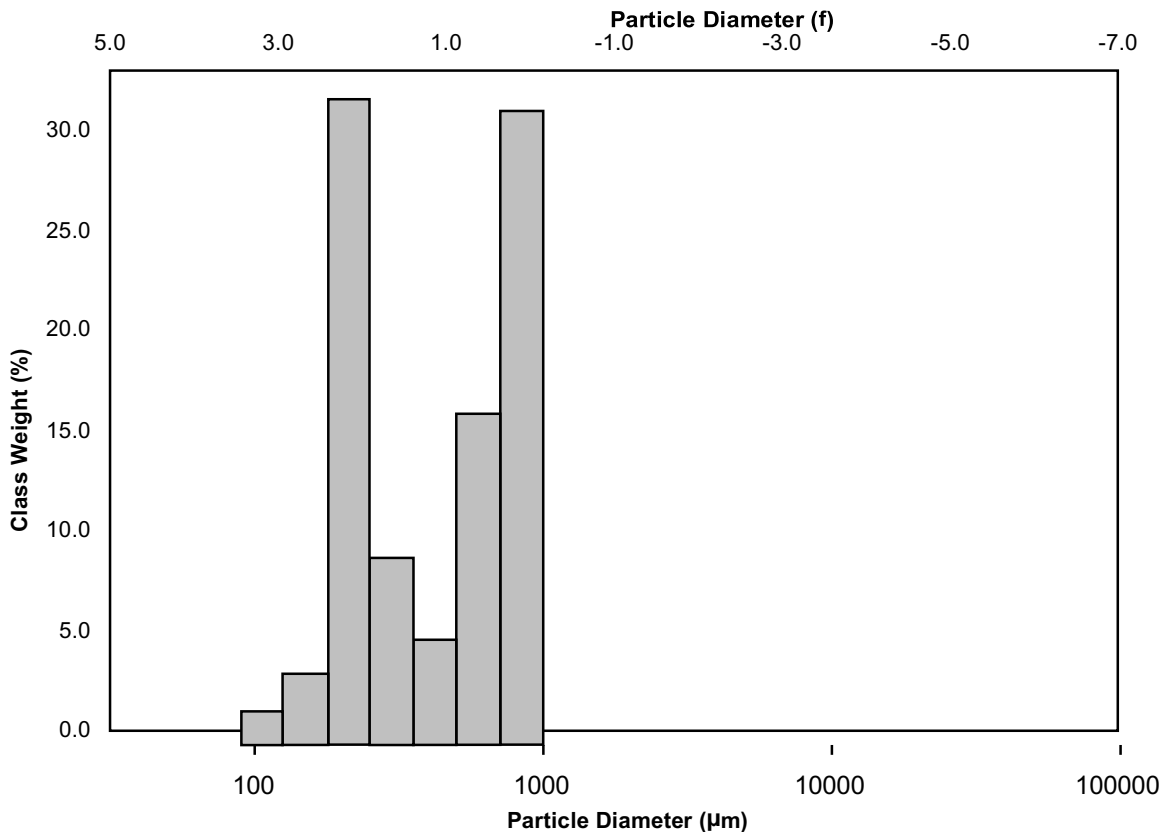
SEDIMENT NAME: Moderately Sorted Coarse Sand

GPS: 29 32'43" N, 34 58'53" E

Depth: 4.0 m

	∞ m ϕ		GRAIN SIZE DISTRIBUTION			
	∞ m	ϕ	GRAVEL: 0.0%	COARSE SAND: 48.7%	SAND: 100.0%	MEDIUM SAND: 14.9%
MODE 1:	215.0	2.237	MUD: 0.0%	FINE SAND: 34.8%		
MODE 2:	855.0	0.247			V FINE SAND: 1.6%	
MODE 3:					V COARSE SILT: 0.0%	
D ₁₀ :	189.0	0.156	V COARSE GRAVEL: 0.0%	COARSE SILT: 0.0%		
MEDIAN or D ₅₀ :	460.2	1.120	COARSE GRAVEL: 0.0%	COARSE SILT: 0.0%		
D ₉₀ :	897.7	2.404	MEDIUM GRAVEL: 0.0%	MEDIUM SILT: 0.0%		
(D ₉₀ / D ₁₀):	4.751	15.44	FINE GRAVEL: 0.0%	FINE SILT: 0.0%		
(D ₉₀ - D ₁₀):	708.8	2.248	V FINE GRAVEL: 0.0%	V FINE SILT: 0.0%		
(D ₇₅ / D ₂₅):	3.447	5.588	V COARSE SAND: 0.0%	CLAY: 0.0%		
(D ₇₅ - D ₂₅):	542.1	1.785				
	METHOD OF MOMENTS		FOLK & WARD METHOD			
	Arithmetic	Geometric	Logarithmic	Geometric	Logarithmic	Description
	∞ m	∞ m	\square	∞ m	\square	
MEAN (\bar{x}):	499.9	409.4	1.288	427.2	1.227	Medium Sand
SORTING (σ):	279.6	1.883	0.913	1.850	0.887	Moderately Sorted
SKEWNESS (Sk):	0.180	-0.162	0.162	-0.153	0.153	Fine Skewed
KURTOSIS (K):	1.342	1.499	1.499	0.563	0.563	Very Platykurtic

GRAIN SIZE DISTRIBUTION



SAMPLE STATISTICS

SAMPLE IDENTITY: **AO 3-8, Unit 10**

ANALYST & DATE: JES,

SAMPLE TYPE: Unimodal, Well Sorted

TEXTURAL GROUP: Sand

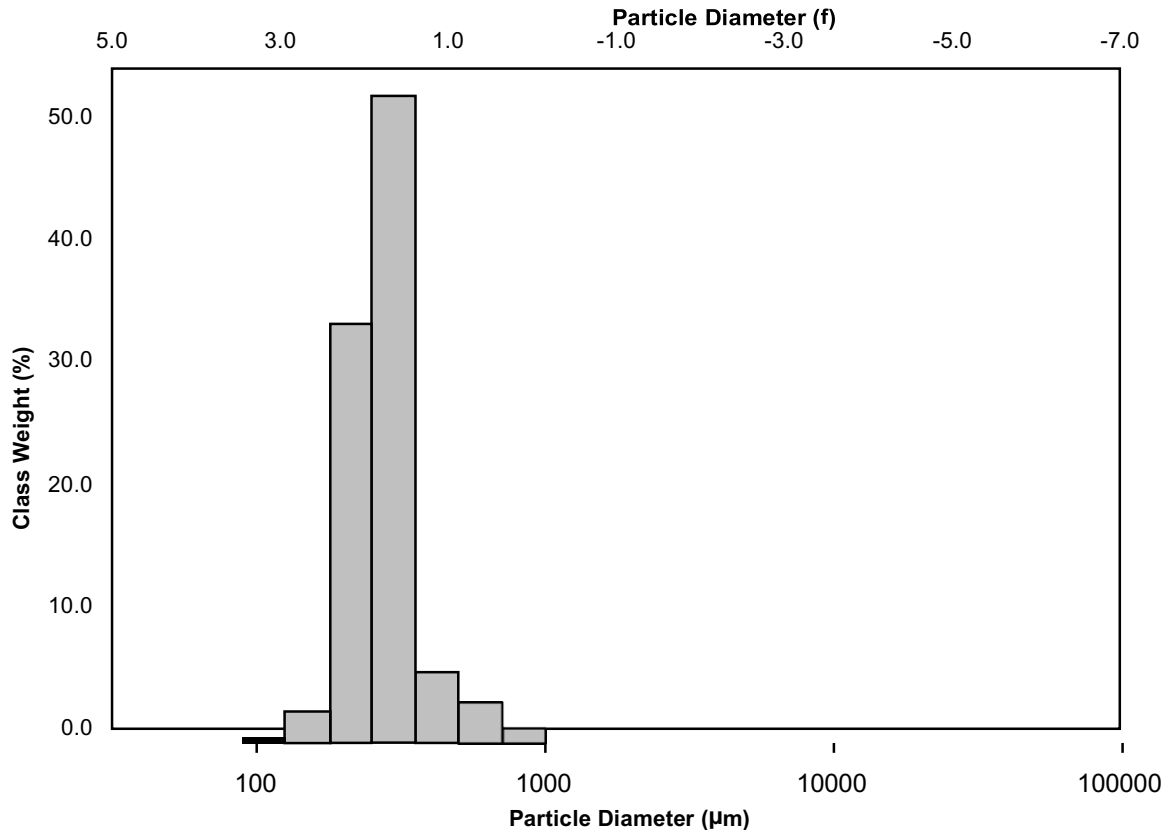
SEDIMENT NAME: Well Sorted Medium Sand

GPS: 29 32'43" N, 34 58'53" E

Depth: 3.9 m

		GRAIN SIZE DISTRIBUTION				
MODE 1:	∞ m	ϕ	GRAVEL:	0.0%	COARSE SAND:	4.5%
MODE 2:			SAND:	100.0%	MEDIUM SAND:	59.7%
MODE 3:			MUD:	0.0%	FINE SAND:	35.5%
D ₁₀ :	193.0	1.468	V COARSE GRAVEL:	0.0%	V COARSE SILT:	0.0%
MEDIAN or D ₅₀ :	274.2	1.866	COARSE GRAVEL:	0.0%	COARSE SILT:	0.0%
D ₉₀ :	361.4	2.373	MEDIUM GRAVEL:	0.0%	MEDIUM SILT:	0.0%
(D ₉₀ / D ₁₀):	1.872	1.616	FINE GRAVEL:	0.0%	FINE SILT:	0.0%
(D ₉₀ - D ₁₀):	168.3	0.905	V FINE GRAVEL:	0.0%	V FINE SILT:	0.0%
(D ₇₅ / D ₂₅):	1.438	1.321	V COARSE SAND:	0.0%	CLAY:	0.0%
(D ₇₅ - D ₂₅):	98.24	0.524				
⋮						
METHOD OF MOMENTS			FOLK & WARD METHOD			
	Arithmetic	Geometric	Logarithmic	Geometric	Logarithmic	Description
	∞ m	∞ m	\square	∞ m	\square	
MEAN (\bar{x}):	293.1	275.7	1.859	267.9	1.900	Medium Sand
SORTING (σ):	103.9	1.336	0.418	1.317	0.398	Well Sorted
SKEWNESS (Sk):	2.718	0.909	-0.909	0.020	-0.020	Symmetrical
KURTOSIS (K):	13.46	5.731	5.731	1.100	1.100	Mesokurtic

GRAIN SIZE DISTRIBUTION



SAMPLE STATISTICS

SAMPLE IDENTITY: **AO 3-9, Unit 10**

ANALYST & DATE: JES,

SAMPLE TYPE: Bimodal, Moderately Sorted

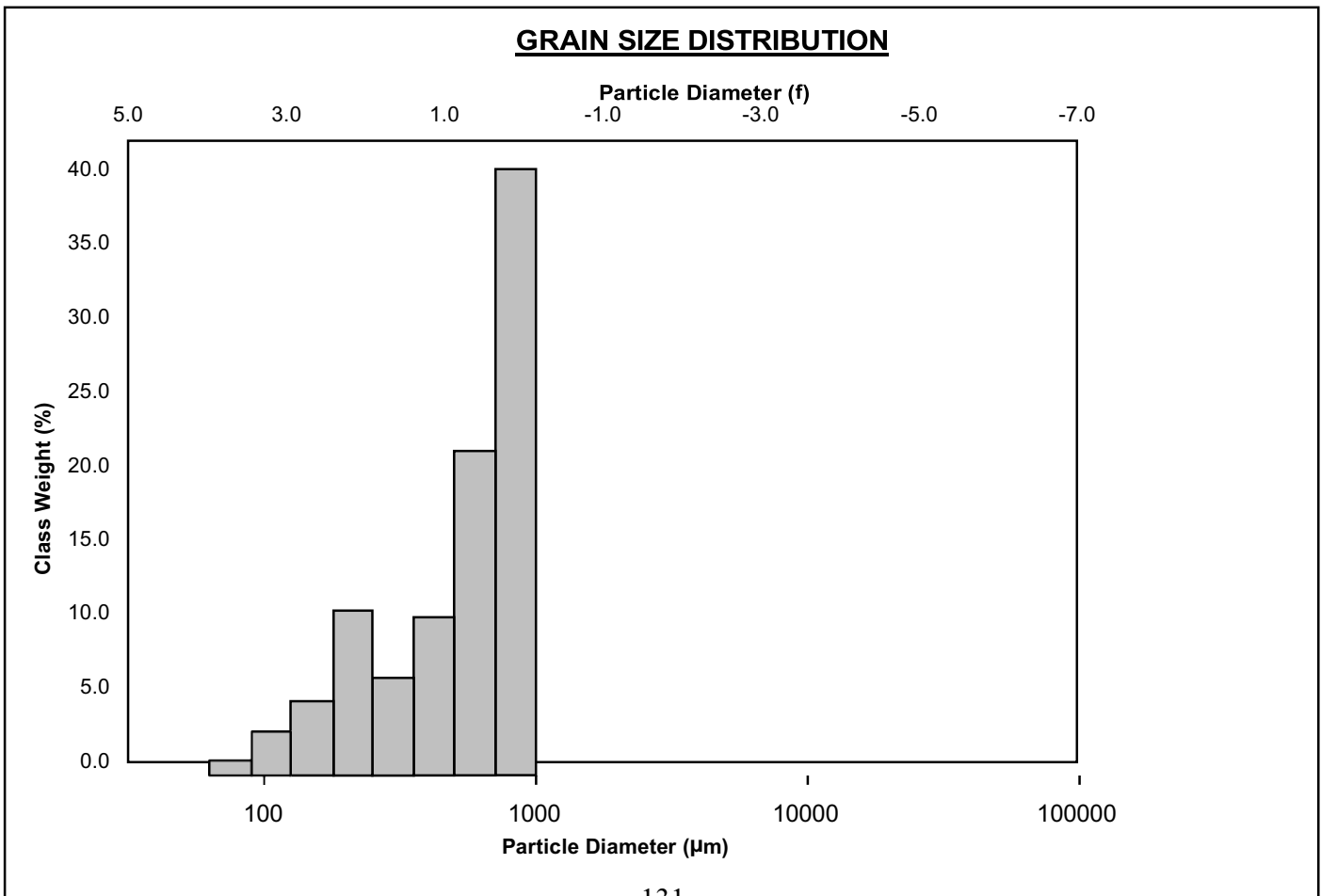
TEXTURAL GROUP: Sand

SEDIMENT NAME: Moderately Sorted Coarse Sand

GPS: 29 32'43" N, 34 58'53" E

Depth: 3.8m

	∞ m		ϕ		GRAIN SIZE DISTRIBUTION		
	∞ m	ϕ	Arithmetic	Geometric	Logarithmic	Geometric	Logarithmic
MODE 1:	855.0	0.247					
MODE 2:	215.0	2.237					
MODE 3:							
D ₁₀ :	184.6	0.122					
MEDIAN or D ₅₀ :	612.7	0.707					
D ₉₀ :	919.2	2.437					
(D ₉₀ / D ₁₀):	4.979	20.05					
(D ₉₀ - D ₁₀):	734.6	2.316					
(D ₇₅ / D ₂₅):	2.467	5.285					
(D ₇₅ - D ₂₅):	481.6	1.302					
			METHOD OF MOMENTS		FOLK & WARD METHOD		
			Arithmetic	Geometric	Logarithmic	Geometric	Logarithmic
			∞ m	∞ m	\square	∞ m	\square
MEAN (\bar{x}):			582.5	490.0	1.029	491.9	1.023
SORTING (\square):			267.0	1.880	0.911	1.895	0.922
SKEWNESS (Sk):			-0.395	-1.044	1.044	-0.512	0.512
KURTOSIS (K):			1.690	3.023	3.023	0.890	0.890
							Description
							Medium Sand
							Moderately Sorted
							Very Fine Skewed
							Platykurtic



SAMPLE STATISTICS

SAMPLE IDENTITY: **AO 3-13, Unit 11**

ANALYST & DATE: JES,

SAMPLE TYPE: Unimodal, Well Sorted

TEXTURAL GROUP: Sand

SEDIMENT NAME: Well Sorted Fine Sand

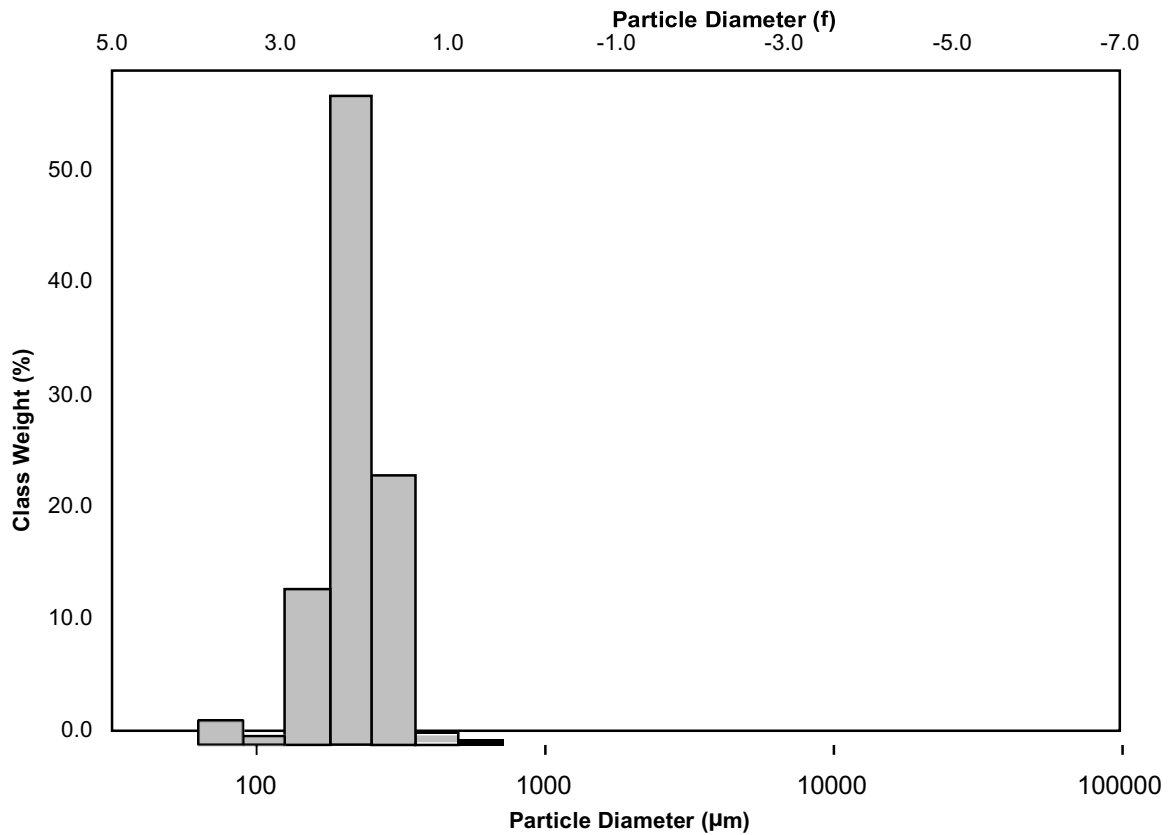
GPS: 29 32'43" N, 34 58'53" E

Depth: 4.30 m

	∞ m	ϕ	GRAIN SIZE DISTRIBUTION			
MODE 1:	215.0	2.237	GRAVEL: 0.0%	COARSE SAND: 0.4%		
MODE 2:			SAND: 100.0%	MEDIUM SAND: 25.9%		
MODE 3:			MUD: 0.0%	FINE SAND: 70.8%		
D ₁₀ :	148.5	1.668	V COARSE GRAVEL: 0.0%	V COARSE SILT: 0.0%		
MEDIAN or D ₅₀ :	217.4	2.201	COARSE GRAVEL: 0.0%	COARSE SILT: 0.0%		
D ₉₀ :	314.6	2.751	MEDIUM GRAVEL: 0.0%	MEDIUM SILT: 0.0%		
(D ₉₀ / D ₁₀):	2.118	1.649	FINE GRAVEL: 0.0%	FINE SILT: 0.0%		
(D ₉₀ - D ₁₀):	166.1	1.083	V FINE GRAVEL: 0.0%	V FINE SILT: 0.0%		
(D ₇₅ / D ₂₅):	1.356	1.222	V COARSE SAND: 0.0%	CLAY: 0.0%		
(D ₇₅ - D ₂₅):	66.75	0.439				

	METHOD OF MOMENTS			FOLK & WARD METHOD		
	Arithmetic	Geometric	Logarithmic	Geometric	Logarithmic	Description
	∞ m	∞ m	\square	∞ m	\square	
MEAN (\bar{x})	227.3	215.5	2.214	221.1	2.177	Fine Sand
SORTING (\square)	62.44	1.333	0.415	1.314	0.393	Well Sorted
SKEWNESS (Sk)	0.989	-0.837	0.837	0.015	-0.015	Symmetrical
KURTOSIS (K)	7.800	5.917	5.917	1.272	1.272	Leptokurtic

GRAIN SIZE DISTRIBUTION



SAMPLE STATISTICS

SAMPLE IDENTITY: **TK 4-1**

ANALYST & DATE: JES,

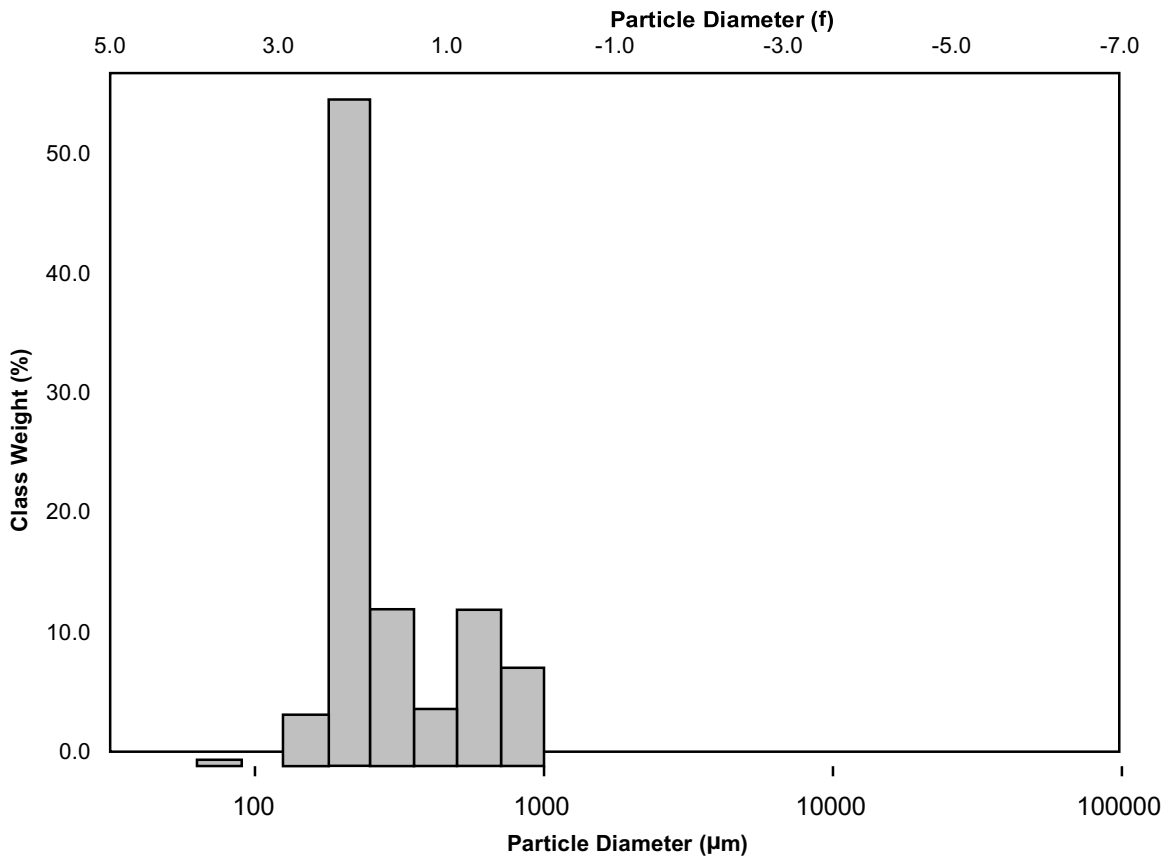
SAMPLE TYPE: Bimodal, Moderately Sorted

TEXTURAL GROUP: Sand

SEDIMENT NAME: Moderately Sorted Fine Sand

	∞ m ϕ		GRAIN SIZE DISTRIBUTION			
	∞ m	ϕ	GRAVEL: 0.0%	COARSE SAND: 22.0%	SAND: 100.0%	MEDIUM SAND: 18.5%
MODE 1:	215.0	2.237	MUD: 0.0%	FINE SAND: 59.0%		
MODE 2:	605.0	0.747			V FINE SAND: 0.5%	
MODE 3:					V COARSE GRAVEL: 0.0%	V COARSE SILT: 0.0%
D ₁₀ :	185.3	0.555	COARSE GRAVEL: 0.0%	COARSE SILT: 0.0%	MEDIUM GRAVEL: 0.0%	MEDIUM SILT: 0.0%
MEDIAN or D ₅₀ :	236.0	2.083	FINE GRAVEL: 0.0%	FINE SILT: 0.0%	V FINE GRAVEL: 0.0%	V FINE SILT: 0.0%
D ₉₀ :	680.4	2.432			V COARSE SAND: 0.0%	CLAY: 0.0%
(D ₉₀ / D ₁₀):	3.672	4.378				
(D ₉₀ - D ₁₀):	495.1	1.877				
(D ₇₅ / D ₂₅):	1.987	1.756				
(D ₇₅ - D ₂₅):	200.2	0.991				
⋮						
	METHOD OF MOMENTS			FOLK & WARD METHOD		
	Arithmetic	Geometric	Logarithmic	Geometric	Logarithmic	Description
	∞ m	∞ m	ϕ	∞ m	ϕ	
MEAN (\bar{x}):	340.1	290.2	1.785	297.9	1.747	Medium Sand
SORTING (σ):	206.8	1.658	0.730	1.663	0.734	Moderately Sorted
SKEWNESS (S_k):	1.412	0.855	-0.855	0.627	-0.627	Very Coarse Skewed
KURTOSIS (K):	3.696	2.713	2.713	0.911	0.911	Mesokurtic

GRAIN SIZE DISTRIBUTION



SAMPLE STATISTICS

SAMPLE IDENTITY: **TK 4-2**

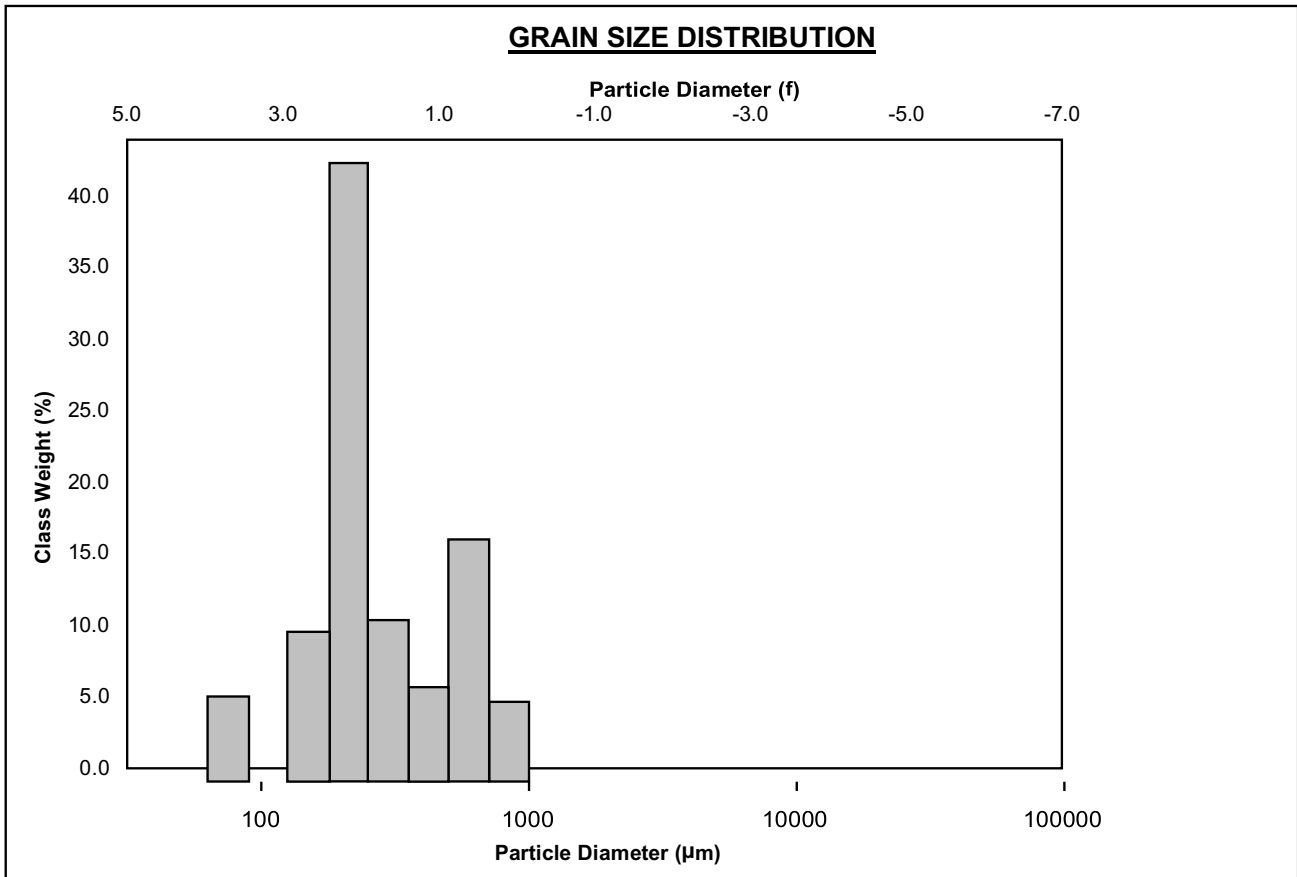
ANALYST & DATE: JES,

SAMPLE TYPE: Bimodal, Moderately Sorted

TEXTURAL GROUP: Sand

SEDIMENT NAME: Moderately Sorted Fine Sand

	ϕ		GRAIN SIZE DISTRIBUTION			
	ϕ	m				
MODE 1:	215.0	2.237	GRAVEL: 0.0%		COARSE SAND: 22.9%	
MODE 2:	605.0	0.747	SAND: 100.0%		MEDIUM SAND: 18.2%	
MODE 3:			MUD: 0.0%		FINE SAND: 52.7%	
D ₁₀ :	141.5	0.623			V FINE SAND: 6.2%	
MEDIAN or D ₅₀ :	233.0	2.101	V COARSE GRAVEL: 0.0%		V COARSE SILT: 0.0%	
D ₉₀ :	649.3	2.821	COARSE GRAVEL: 0.0%		COARSE SILT: 0.0%	
(D ₉₀ / D ₁₀):	4.588	4.528	MEDIUM GRAVEL: 0.0%		MEDIUM SILT: 0.0%	
(D ₉₀ - D ₁₀):	507.8	2.198	FINE GRAVEL: 0.0%		FINE SILT: 0.0%	
(D ₇₅ / D ₂₅):	2.349	2.067	V FINE GRAVEL: 0.0%		V FINE SILT: 0.0%	
(D ₇₅ - D ₂₅):	257.9	1.232	V COARSE SAND: 0.0%		CLAY: 0.0%	
	METHOD OF MOMENTS		FOLK & WARD METHOD			
	Arithmetic	Geometric	Logarithmic	Geometric	Logarithmic	Description
	m	m	ϕ	m	ϕ	
MEAN (\bar{x}):	327.0	269.1	1.894	284.7	1.812	Medium Sand
SORTING (σ):	205.4	1.821	0.864	1.878	0.909	Moderately Sorted
SKEWNESS (Sk):	1.137	0.094	-0.094	0.279	-0.279	Coarse Skewed
KURTOSIS (K):	3.253	2.670	2.670	1.041	1.041	Mesokurtic



SAMPLE STATISTICS

SAMPLE IDENTITY: **TK 4-3**

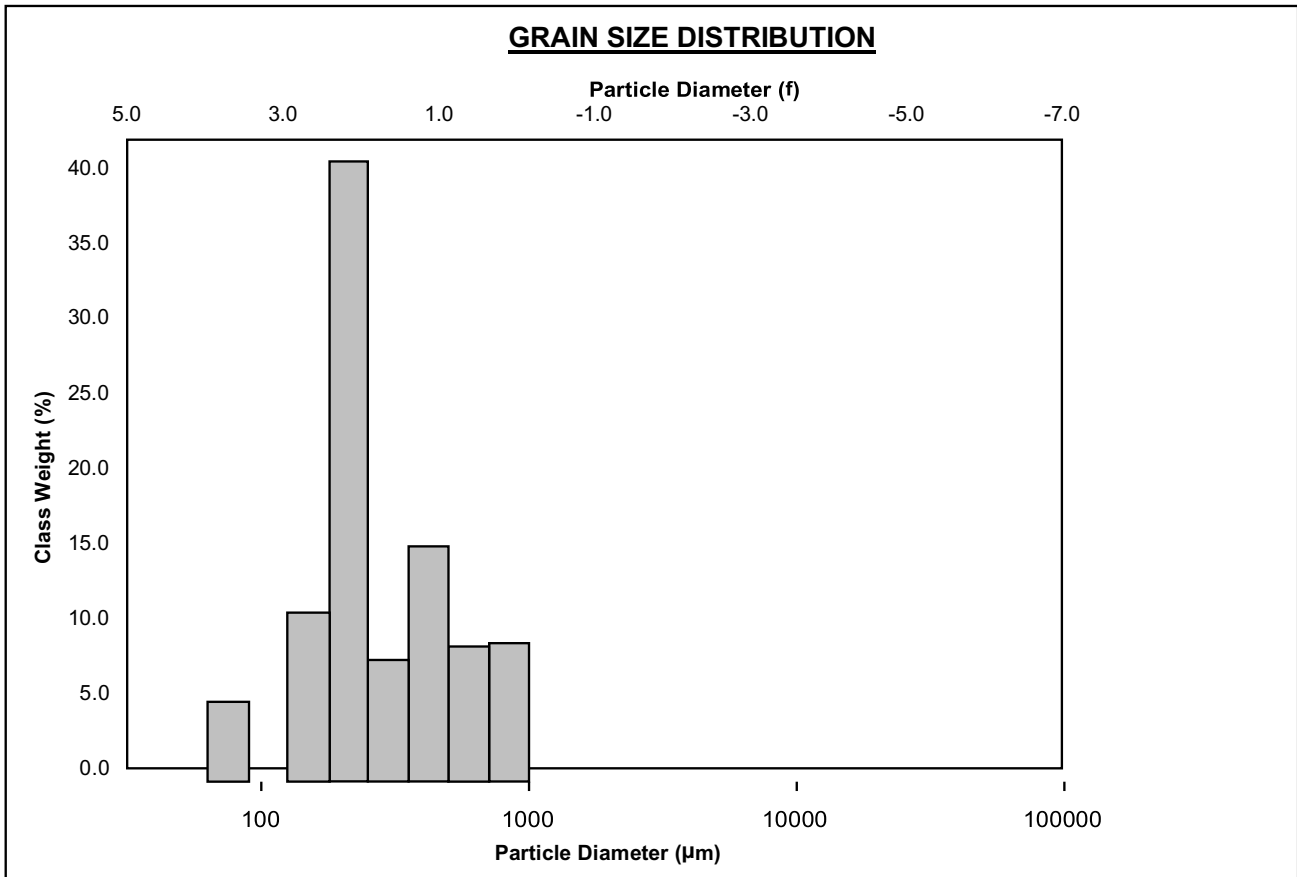
ANALYST & DATE: JES,

SAMPLE TYPE: Trimodal, Moderately Sorted

TEXTURAL GROUP: Sand

SEDIMENT NAME: Moderately Sorted Fine Sand

	∞m	ϕ	GRAIN SIZE DISTRIBUTION			
	MODE 1:	215.0	2.237	GRAVEL: 0.0%	COARSE SAND: 18.5%	
MODE 2:	427.5	1.247	SAND: 100.0%	MEDIUM SAND: 24.1%		
MODE 3:	855.0	0.247	MUD: 0.0%	FINE SAND: 51.9%		
D ₁₀ :	143.0	0.535		V FINE SAND: 5.6%		
MEDIAN or D ₅₀ :	235.2	2.088	V COARSE GRAVEL: 0.0%	V COARSE SILT: 0.0%		
D ₉₀ :	690.4	2.806	COARSE GRAVEL: 0.0%	COARSE SILT: 0.0%		
(D ₉₀ / D ₁₀):	4.828	5.249	MEDIUM GRAVEL: 0.0%	MEDIUM SILT: 0.0%		
(D ₉₀ - D ₁₀):	547.4	2.271	FINE GRAVEL: 0.0%	FINE SILT: 0.0%		
(D ₇₅ / D ₂₅):	2.270	1.983	V FINE GRAVEL: 0.0%	V FINE SILT: 0.0%		
(D ₇₅ - D ₂₅):	242.9	1.182	V COARSE SAND: 0.0%	CLAY: 0.0%		
	METHOD OF MOMENTS		FOLK & WARD METHOD			
	Arithmetic ∞m	Geometric ∞m	Logarithmic \square	Geometric ∞m	Logarithmic \square	Description
MEAN (\bar{x}):	335.9	275.2	1.861	281.0	1.831	Medium Sand
SORTING (\square):	216.1	1.830	0.872	1.884	0.914	Moderately Sorted
SKEWNESS (Sk):	1.235	0.134	-0.134	0.288	-0.288	Coarse Skewed
KURTOSIS (K):	3.531	2.690	2.690	1.130	1.130	Leptokurtic



SAMPLE STATISTICS

SAMPLE IDENTITY: **TK 4-4**

ANALYST & DATE: JES,

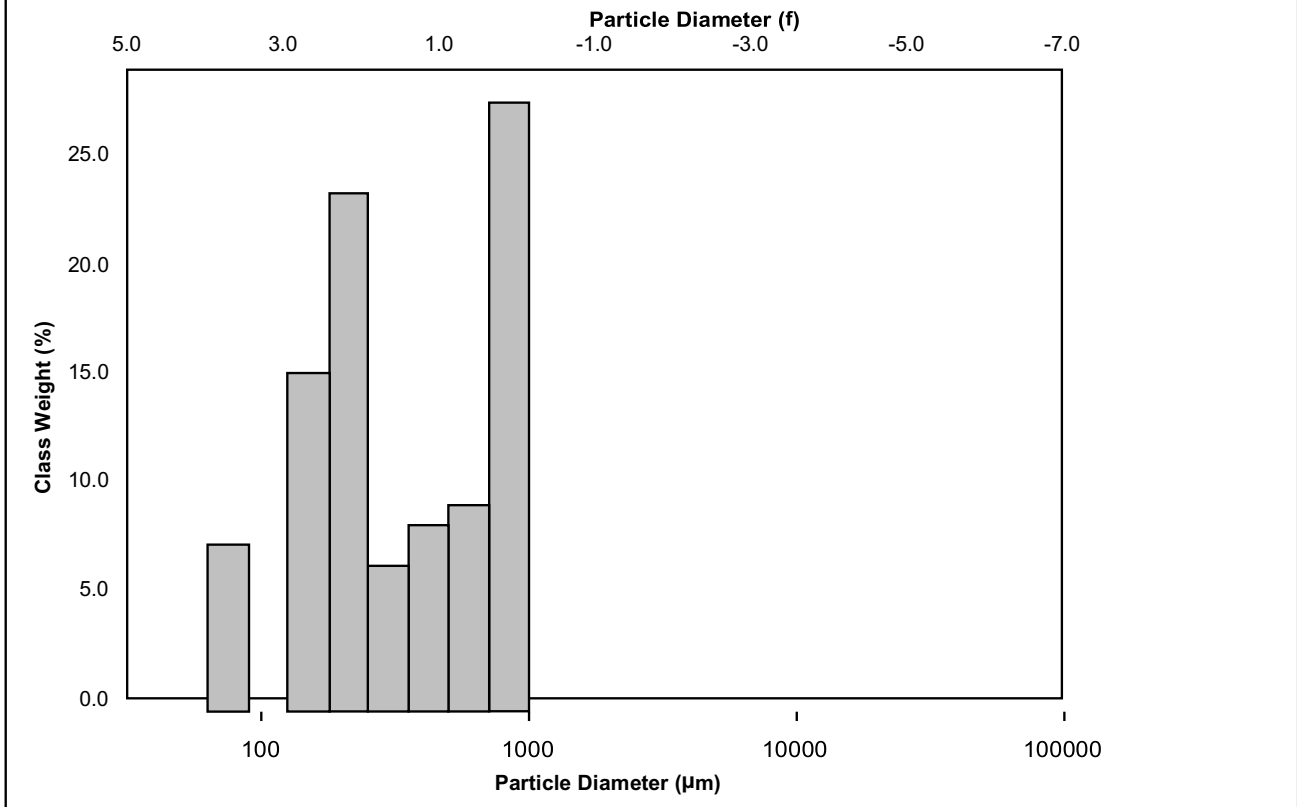
SAMPLE TYPE: Trimodal, Poorly Sorted

TEXTURAL GROUP: Sand

SEDIMENT NAME: Poorly Sorted Fine Sand

	αm	ϕ	GRAIN SIZE DISTRIBUTION			
MODE 1:	855.0	0.247	GRAVEL: 0.0%		COARSE SAND: 37.5%	
MODE 2:	215.0	2.237	SAND: 100.0%		MEDIUM SAND: 15.3%	
MODE 3:	76.50	3.731	MUD: 0.0%		FINE SAND: 39.2%	
D ₁₀ :	130.8	0.177			V FINE SAND: 8.0%	
MEDIAN or D ₅₀ :	289.3	1.789	V COARSE GRAVEL: 0.0%		V COARSE SILT: 0.0%	
D ₉₀ :	884.2	2.935	COARSE GRAVEL: 0.0%		COARSE SILT: 0.0%	
(D ₉₀ / D ₁₀):	6.760	16.53	MEDIUM GRAVEL: 0.0%		MEDIUM SILT: 0.0%	
(D ₉₀ - D ₁₀):	753.4	2.757	FINE GRAVEL: 0.0%		FINE SILT: 0.0%	
(D ₇₅ / D ₂₅):	4.051	5.549	V FINE GRAVEL: 0.0%		V FINE SILT: 0.0%	
(D ₇₅ - D ₂₅):	553.8	2.018	V COARSE SAND: 0.0%		CLAY: 0.0%	
⋮						
	METHOD OF MOMENTS			FOLK & WARD METHOD		
	Arithmetic αm	Geometric αm	Logarithmic \square	Geometric αm	Logarithmic \square	Description
MEAN (\bar{x}):	433.6	324.8	1.622	328.6	1.605	Medium Sand
SORTING (\square):	295.8	2.176	1.122	2.229	1.157	Poorly Sorted
SKEWNESS (Sk):	0.445	-0.165	0.165	0.088	-0.088	Symmetrical
KURTOSIS (K):	1.532	1.842	1.842	0.726	0.726	Platykurtic

GRAIN SIZE DISTRIBUTION



SAMPLE STATISTICS

SAMPLE IDENTITY: **TK 4-5a**

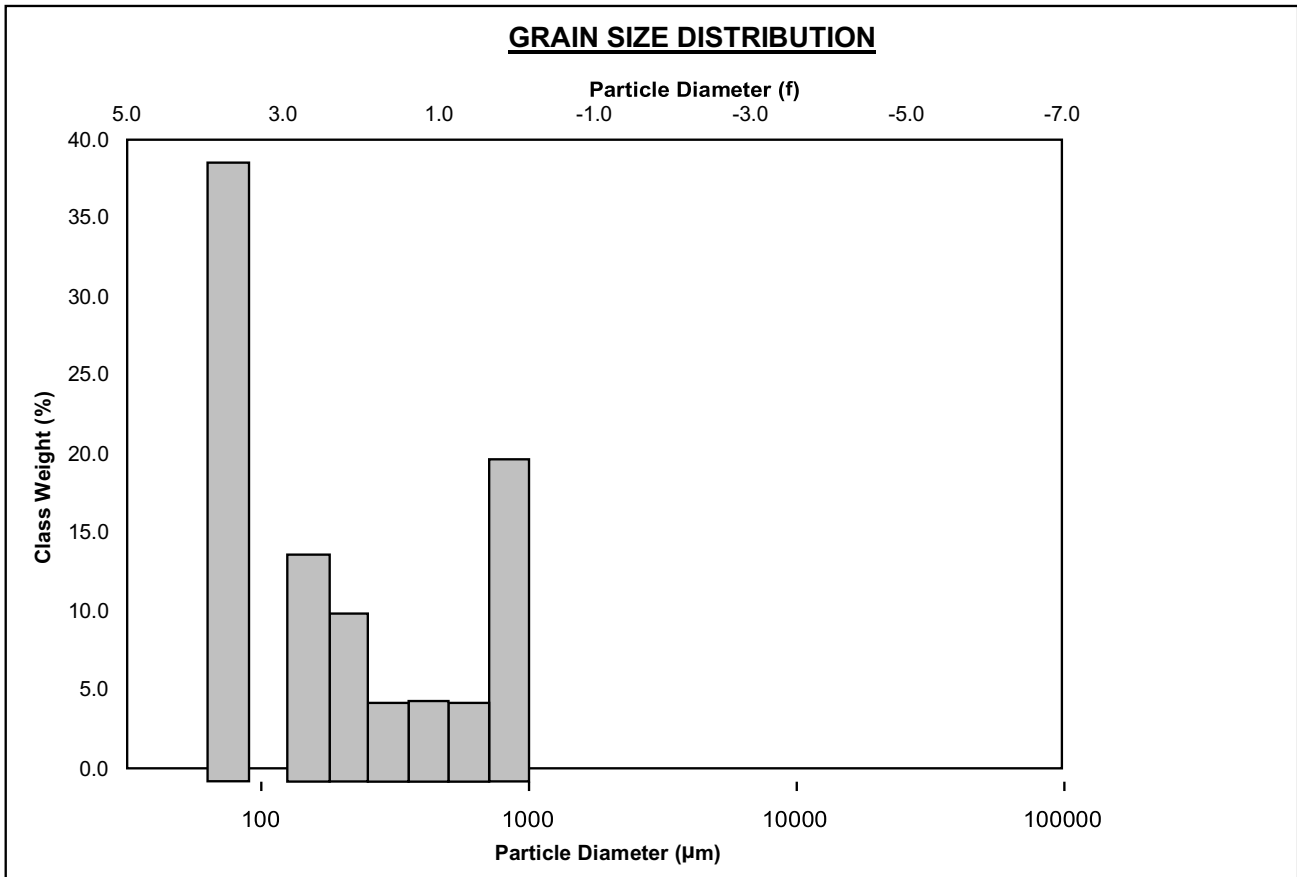
ANALYST & DATE: JES,

SAMPLE TYPE: Trimodal, Poorly Sorted

TEXTURAL GROUP: Sand

SEDIMENT NAME: Poorly Sorted Very Fine Sand

	αm	ϕ	GRAIN SIZE DISTRIBUTION			
MODE 1:	76.50	3.731	GRAVEL: 0.0%		COARSE SAND: 25.0%	
MODE 2:	855.0	0.247	SAND: 100.0%		MEDIUM SAND: 10.0%	
MODE 3:	152.5	2.737	MUD: 0.0%		FINE SAND: 25.0%	
D ₁₀ :	68.88	0.247			V FINE SAND: 40.0%	
MEDIAN or D ₅₀ :	159.4	2.649	V COARSE GRAVEL: 0.0%		V COARSE SILT: 0.0%	
D ₉₀ :	842.6	3.860	COARSE GRAVEL: 0.0%		COARSE SILT: 0.0%	
(D ₉₀ / D ₁₀):	12.23	15.62	MEDIUM GRAVEL: 0.0%		MEDIUM SILT: 0.0%	
(D ₉₀ - D ₁₀):	773.7	3.613	FINE GRAVEL: 0.0%		FINE SILT: 0.0%	
(D ₇₅ / D ₂₅):	6.351	3.667	V FINE GRAVEL: 0.0%		V FINE SILT: 0.0%	
(D ₇₅ - D ₂₅):	421.3	2.667	V COARSE SAND: 0.0%		CLAY: 0.0%	
	METHOD OF MOMENTS		FOLK & WARD METHOD			
	Arithmetic αm	Geometric αm	Logarithmic \square	Geometric αm	Logarithmic \square	Description
MEAN (\bar{x}):	312.7	194.4	2.363	206.5	2.276	Fine Sand
SORTING (\square):	301.5	2.586	1.371	2.681	1.423	Poorly Sorted
SKEWNESS (Sk):	0.994	0.449	-0.449	0.330	-0.330	Very Coarse Skewed
KURTOSIS (K):	2.303	1.655	1.655	0.584	0.584	Very Platykurtic



SAMPLE STATISTICS

SAMPLE IDENTITY: **TK 4-8**

ANALYST & DATE: JES,

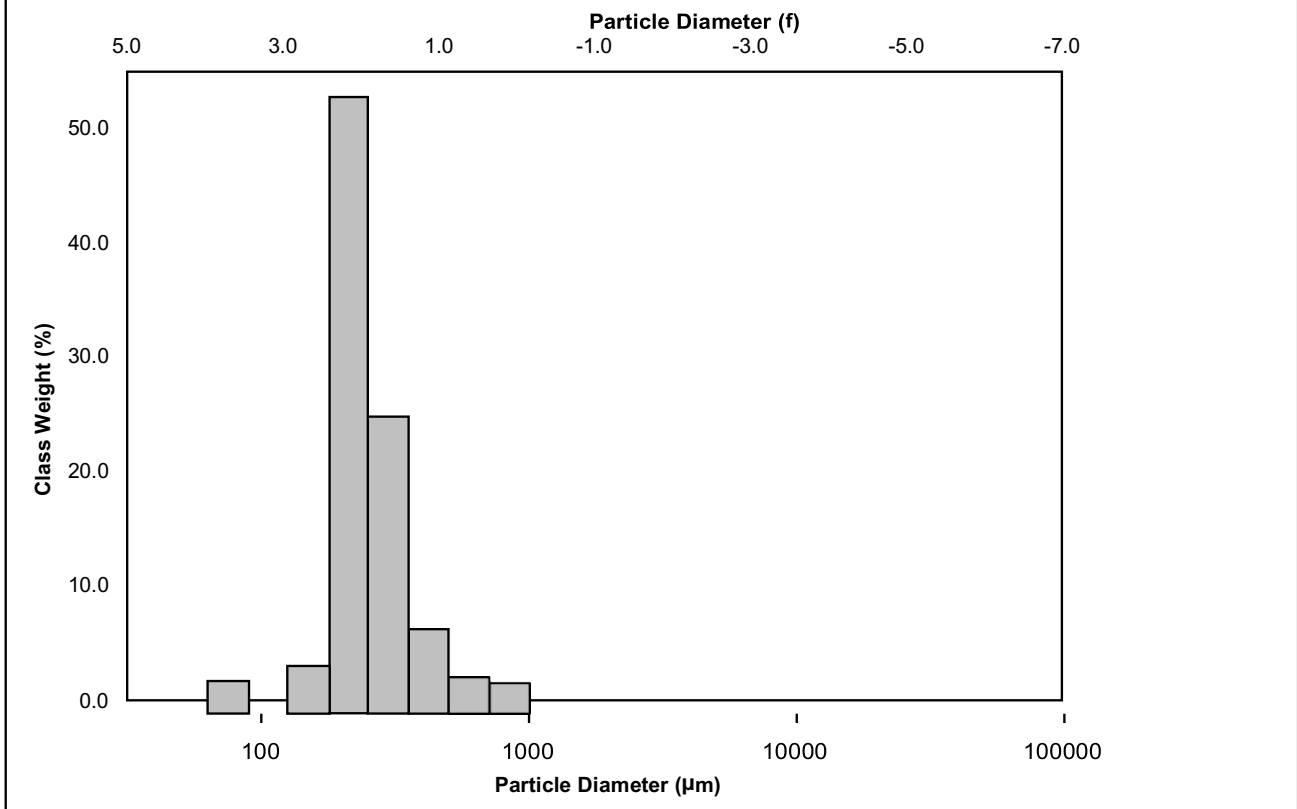
SAMPLE TYPE: Unimodal, Moderately Well Sorted

TEXTURAL GROUP: Sand

SEDIMENT NAME: Moderately Well Sorted Fine Sand

	αm	ϕ	GRAIN SIZE DISTRIBUTION			
	MODE 1:	215.0	2.237	GRAVEL: 0.0%	COARSE SAND: 6.0%	
MODE 2:			SAND: 100.0%	MEDIUM SAND: 34.3%		
MODE 3:			MUD: 0.0%	FINE SAND: 56.7%		
D ₁₀ :	182.9	1.267		V FINE SAND: 3.0%		
MEDIAN or D ₅₀ :	235.2	2.088	V COARSE GRAVEL: 0.0%	V COARSE SILT: 0.0%		
D ₉₀ :	415.5	2.451	COARSE GRAVEL: 0.0%	COARSE SILT: 0.0%		
(D ₉₀ / D ₁₀):	2.272	1.935	MEDIUM GRAVEL: 0.0%	MEDIUM SILT: 0.0%		
(D ₉₀ - D ₁₀):	232.7	1.184	FINE GRAVEL: 0.0%	FINE SILT: 0.0%		
(D ₇₅ / D ₂₅):	1.519	1.352	V FINE GRAVEL: 0.0%	V FINE SILT: 0.0%		
(D ₇₅ - D ₂₅):	104.3	0.603	V COARSE SAND: 0.0%	CLAY: 0.0%		
⋮						
	METHOD OF MOMENTS			FOLK & WARD METHOD		
	Arithmetic αm	Geometric αm	Logarithmic \square	Geometric αm	Logarithmic \square	Description
MEAN (\bar{x}):	277.4	250.7	1.996	248.4	2.009	Fine Sand
SORTING (\square):	135.2	1.495	0.580	1.418	0.503	Moderately Well Sorted
SKEWNESS (Sk):	2.482	0.316	-0.316	0.286	-0.286	Coarse Skewed
KURTOSIS (K):	10.40	5.660	5.660	1.301	1.301	Leptokurtic

GRAIN SIZE DISTRIBUTION



SAMPLE STATISTICS

SAMPLE IDENTITY: **TK 4-9**

ANALYST & DATE: JES,

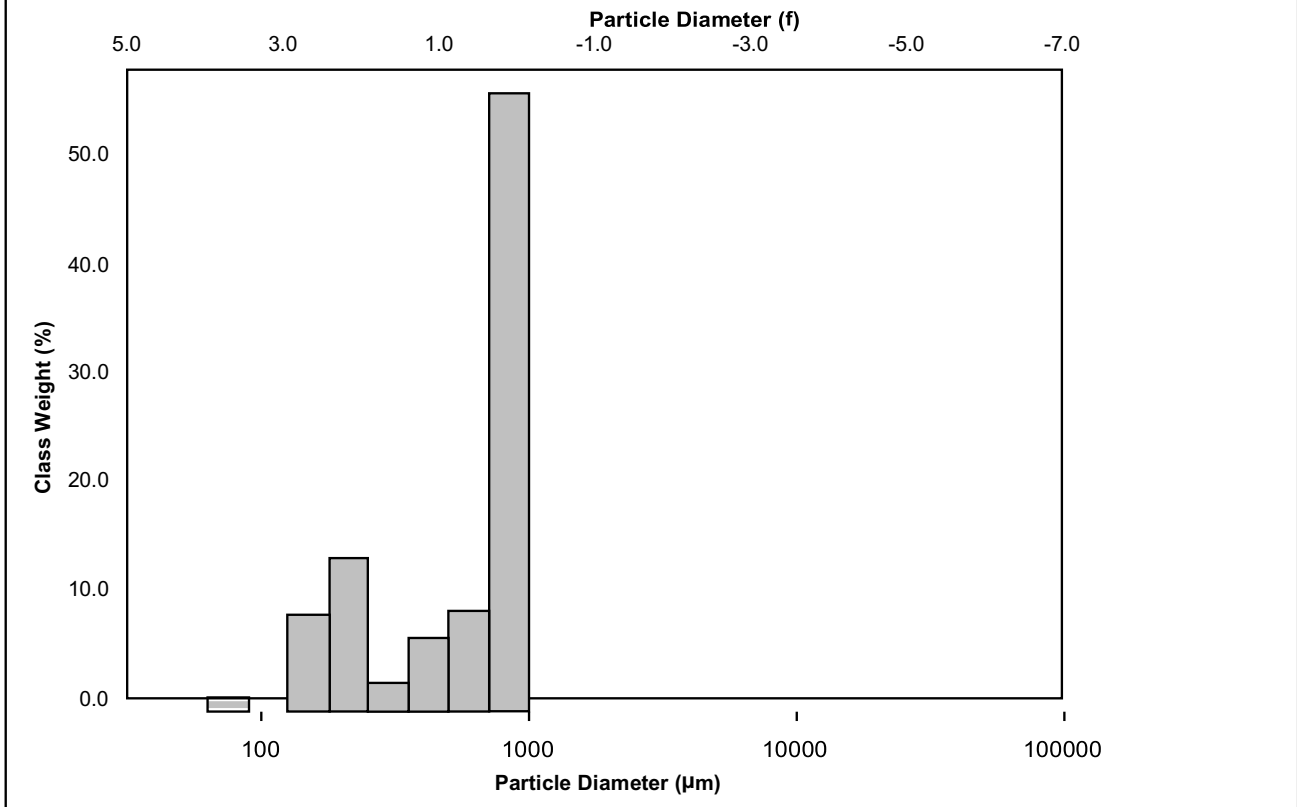
SAMPLE TYPE: Bimodal, Moderately Sorted

TEXTURAL GROUP: Sand

SEDIMENT NAME: Moderately Sorted Coarse Sand

	αm ϕ		GRAIN SIZE DISTRIBUTION			
	MODE 1:	855.0	0.247	GRAVEL: 0.0%	COARSE SAND: 66.2%	
MODE 2:	215.0	2.237	SAND: 100.0%	MEDIUM SAND: 9.5%		
MODE 3:			MUD: 0.0%	FINE SAND: 23.0%		
D ₁₀ :	174.5	0.087		V FINE SAND: 1.3%		
MEDIAN or D ₅₀ :	739.6	0.435	V COARSE GRAVEL: 0.0%	V COARSE SILT: 0.0%		
D ₉₀ :	941.4	2.519	COARSE GRAVEL: 0.0%	COARSE SILT: 0.0%		
(D ₉₀ / D ₁₀):	5.396	28.94	MEDIUM GRAVEL: 0.0%	MEDIUM SILT: 0.0%		
(D ₉₀ - D ₁₀):	767.0	2.432	FINE GRAVEL: 0.0%	FINE SILT: 0.0%		
(D ₇₅ / D ₂₅):	3.149	8.604	V FINE GRAVEL: 0.0%	V FINE SILT: 0.0%		
(D ₇₅ - D ₂₅):	586.9	1.655	V COARSE SAND: 0.0%	CLAY: 0.0%		
⋮						
	METHOD OF MOMENTS			FOLK & WARD METHOD		
	Arithmetic αm	Geometric αm	Logarithmic ϕ	Geometric αm	Logarithmic ϕ	Description
MEAN (\bar{x}):	624.1	516.2	0.954	515.7	0.955	Coarse Sand
SORTING (σ):	288.8	1.957	0.968	1.939	0.955	Moderately Sorted
SKEWNESS (Sk):	-0.657	-1.018	1.018	-0.720	0.720	Very Fine Skewed
KURTOSIS (K):	1.679	2.591	2.591	0.682	0.682	Platykurtic

GRAIN SIZE DISTRIBUTION



SAMPLE STATISTICS

SAMPLE IDENTITY: **TK 4-10**

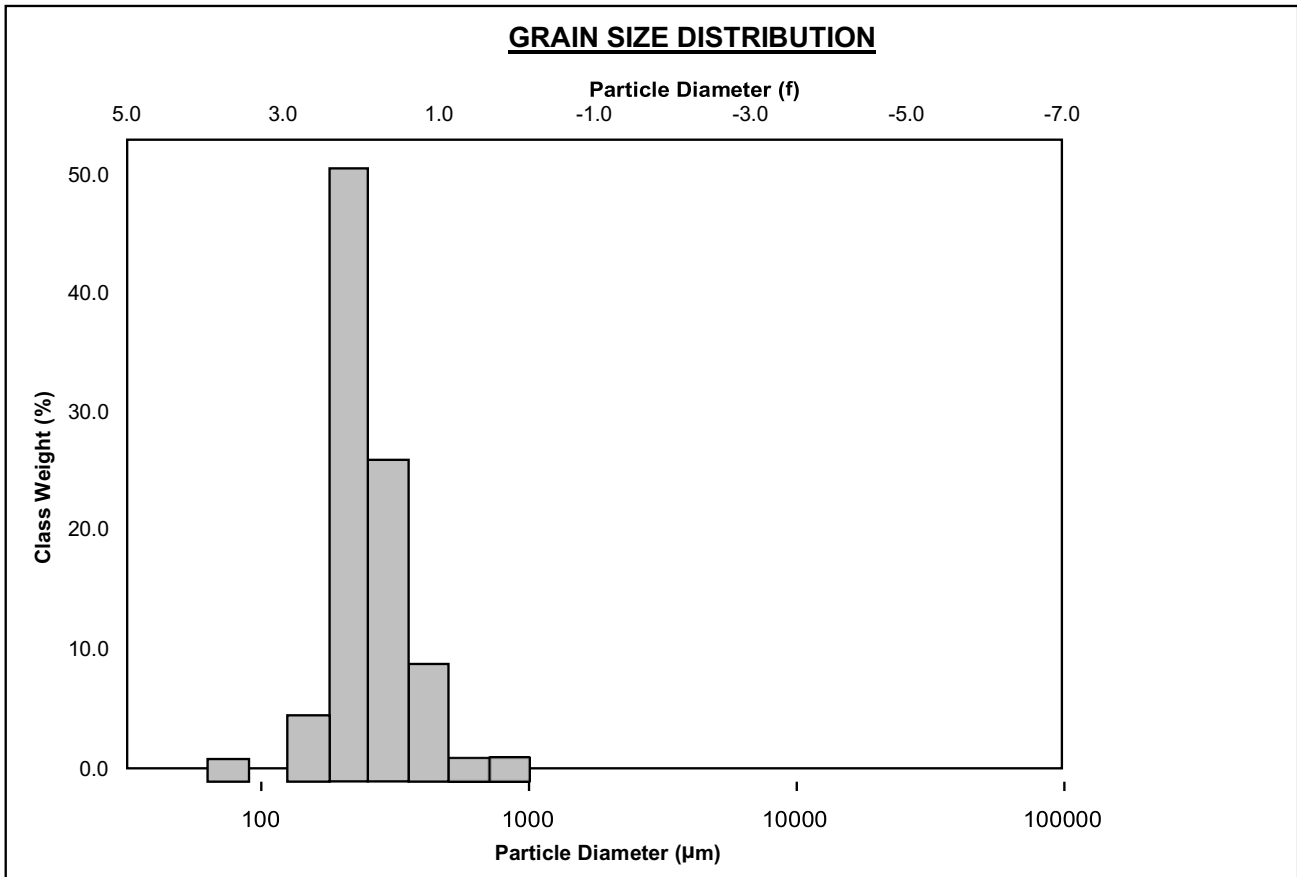
ANALYST & DATE: JES,

SAMPLE TYPE: Unimodal, Well Sorted

TEXTURAL GROUP: Sand

SEDIMENT NAME: Well Sorted Fine Sand

	αm ϕ		GRAIN SIZE DISTRIBUTION			
	MODE 1:	215.0	2.237	GRAVEL: 0.0%	COARSE SAND: 4.0%	
MODE 2:			SAND: 100.0%	MEDIUM SAND: 38.0%		
MODE 3:			MUD: 0.0%	FINE SAND: 56.0%		
D ₁₀ :	182.4	1.296		V FINE SAND: 2.0%		
MEDIAN or D ₅₀ :	237.2	2.076	V COARSE GRAVEL: 0.0%	V COARSE SILT: 0.0%		
D ₉₀ :	407.1	2.455	COARSE GRAVEL: 0.0%	COARSE SILT: 0.0%		
(D ₉₀ / D ₁₀):	2.232	1.894	MEDIUM GRAVEL: 0.0%	MEDIUM SILT: 0.0%		
(D ₉₀ - D ₁₀):	224.7	1.159	FINE GRAVEL: 0.0%	FINE SILT: 0.0%		
(D ₇₅ / D ₂₅):	1.537	1.366	V FINE GRAVEL: 0.0%	V FINE SILT: 0.0%		
(D ₇₅ - D ₂₅):	108.0	0.620	V COARSE SAND: 0.0%	CLAY: 0.0%		
⋮						
	METHOD OF MOMENTS			FOLK & WARD METHOD		
	Arithmetic αm	Geometric αm	Logarithmic ϕ	Geometric αm	Logarithmic ϕ	Description
MEAN (\bar{x}):	274.8	251.5	1.991	249.8	2.001	Fine Sand
SORTING (σ):	122.2	1.451	0.537	1.388	0.473	Well Sorted
SKEWNESS (Sk):	2.529	0.337	-0.337	0.237	-0.237	Coarse Skewed
KURTOSIS (K):	11.70	5.647	5.647	1.116	1.116	Leptokurtic



SAMPLE STATISTICS

SAMPLE IDENTITY: **TK 4-11**

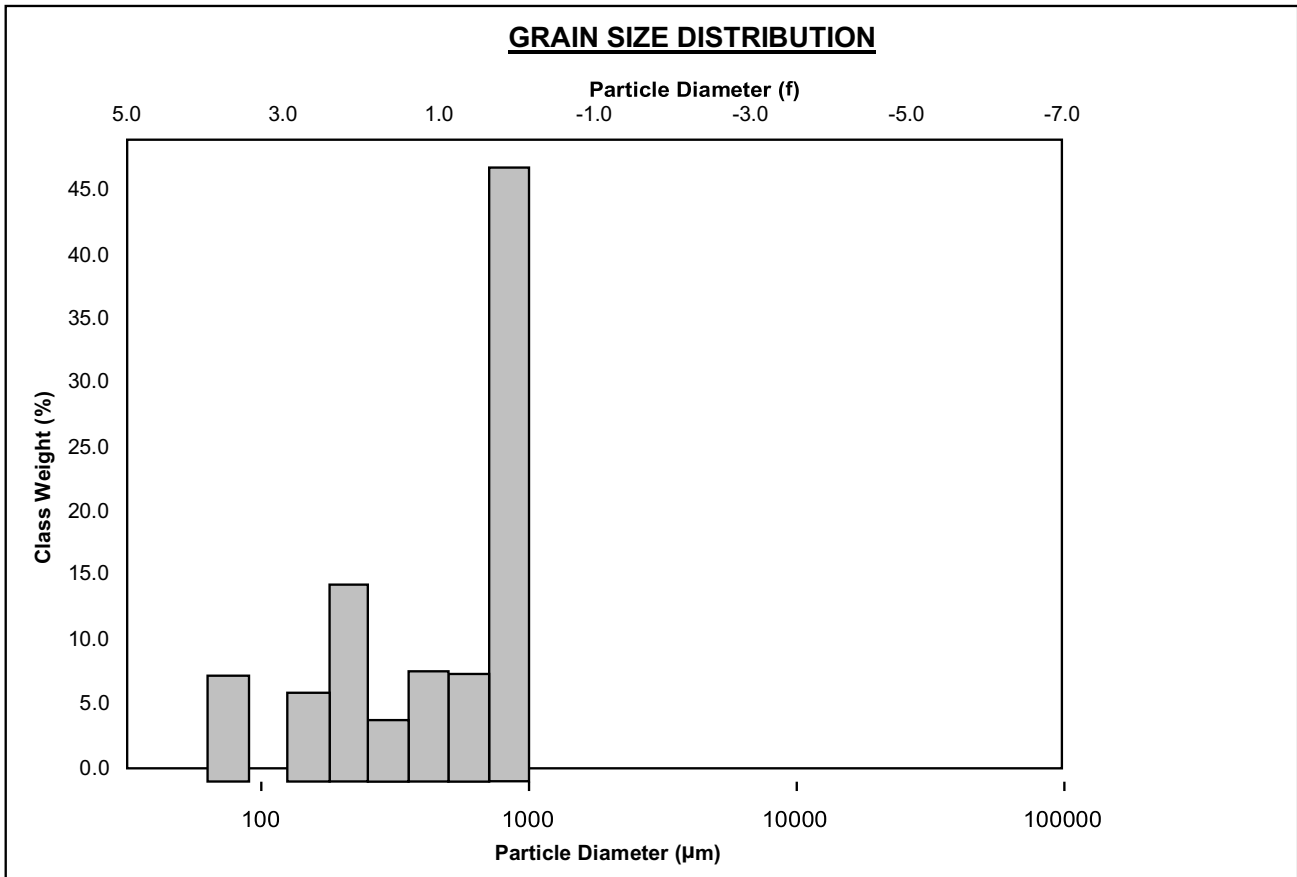
ANALYST & DATE: JES,

SAMPLE TYPE: Polymodal, Poorly Sorted

TEXTURAL GROUP: Sand

SEDIMENT NAME: Poorly Sorted Coarse Sand

	αm ϕ		GRAIN SIZE DISTRIBUTION			
	MODE 1:	855.0	0.247	GRAVEL: 0.0%	COARSE SAND: 56.1%	
MODE 2:	215.0	2.237	SAND: 100.0%	MEDIUM SAND: 13.4%		
MODE 3:	427.5	1.247	MUD: 0.0%	FINE SAND: 21.9%		
D ₁₀ :	134.4	0.104		V FINE SAND: 8.5%		
MEDIAN or D ₅₀ :	642.2	0.639	V COARSE GRAVEL: 0.0%	V COARSE SILT: 0.0%		
D ₉₀ :	930.5	2.895	COARSE GRAVEL: 0.0%	COARSE SILT: 0.0%		
(D ₉₀ / D ₁₀):	6.922	27.86	MEDIUM GRAVEL: 0.0%	MEDIUM SILT: 0.0%		
(D ₉₀ - D ₁₀):	796.1	2.791	FINE GRAVEL: 0.0%	FINE SILT: 0.0%		
(D ₇₅ / D ₂₅):	3.779	8.384	V FINE GRAVEL: 0.0%	V FINE SILT: 0.0%		
(D ₇₅ - D ₂₅):	614.2	1.918	V COARSE SAND: 0.0%	CLAY: 0.0%		
	METHOD OF MOMENTS			FOLK & WARD METHOD		
	Arithmetic αm	Geometric αm	Logarithmic ϕ	Geometric αm	Logarithmic ϕ	Description
MEAN (\bar{x}):	558.7	429.5	1.219	469.3	1.092	Medium Sand
SORTING (σ):	309.5	2.232	1.158	2.183	1.127	Poorly Sorted
SKEWNESS (Sk):	-0.305	-0.853	0.853	-0.633	0.633	Very Fine Skewed
KURTOSIS (K):	1.367	2.434	2.434	0.777	0.777	Platykurtic



SAMPLE STATISTICS

SAMPLE IDENTITY: **TK 4-12**

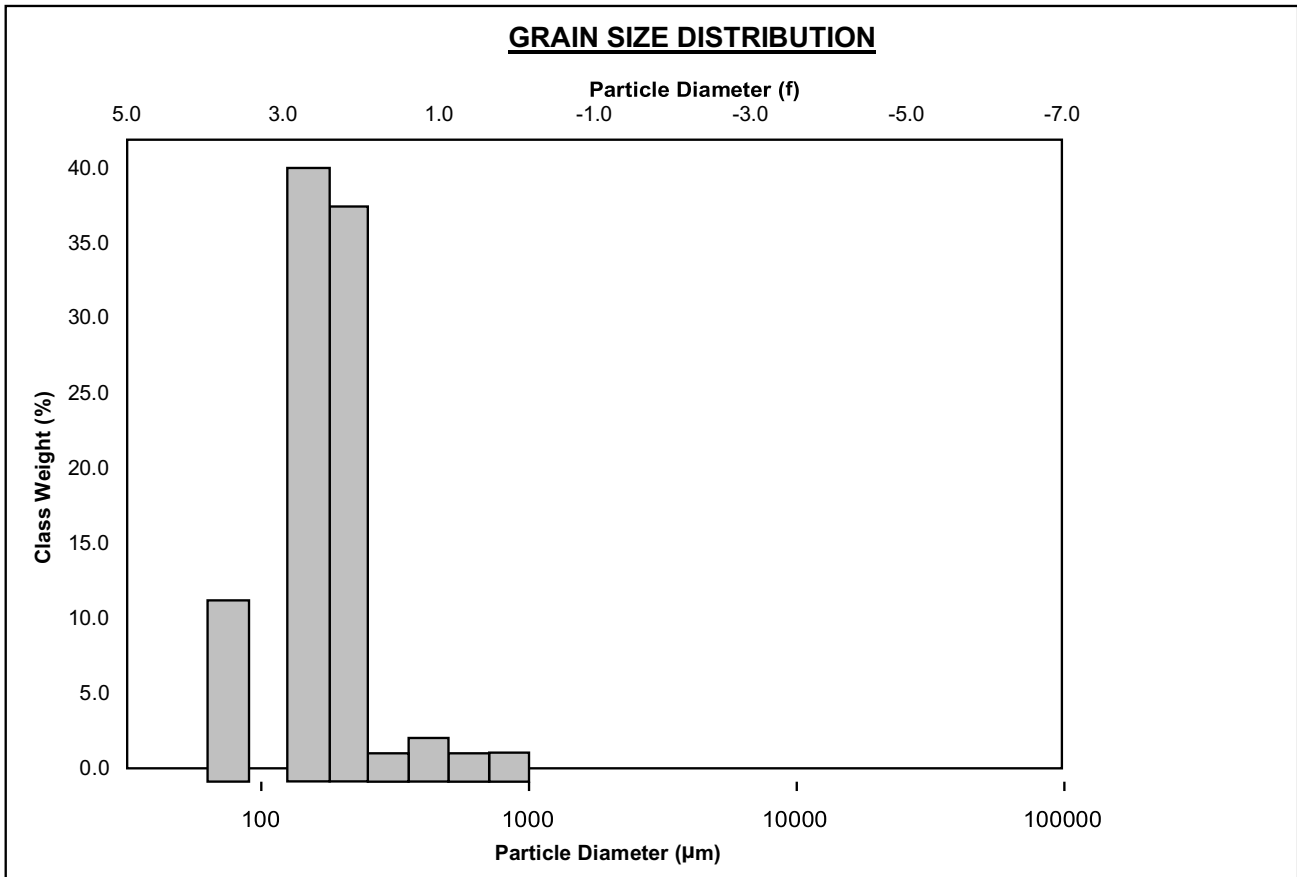
ANALYST & DATE: JES,

SAMPLE TYPE: Bimodal, Moderately Well Sorted

TEXTURAL GROUP: Sand

SEDIMENT NAME: Moderately Well Sorted Fine Sand

	∞m ϕ		GRAIN SIZE DISTRIBUTION			
	MODE 1:	152.5	2.737	GRAVEL: 0.0%	COARSE SAND: 3.8%	
MODE 2:	76.50	3.731	SAND: 100.0%	MEDIUM SAND: 4.8%		
MODE 3:			MUD: 0.0%	FINE SAND: 79.1%		
D ₁₀ :	84.03	2.019		V FINE SAND: 12.4%		
MEDIAN or D ₅₀ :	172.1	2.538	V COARSE GRAVEL: 0.0%	V COARSE SILT: 0.0%		
D ₉₀ :	246.8	3.573	COARSE GRAVEL: 0.0%	COARSE SILT: 0.0%		
(D ₉₀ / D ₁₀):	2.936	1.770	MEDIUM GRAVEL: 0.0%	MEDIUM SILT: 0.0%		
(D ₉₀ - D ₁₀):	162.7	1.554	FINE GRAVEL: 0.0%	FINE SILT: 0.0%		
(D ₇₅ / D ₂₅):	1.547	1.284	V FINE GRAVEL: 0.0%	V FINE SILT: 0.0%		
(D ₇₅ - D ₂₅):	76.18	0.630	V COARSE SAND: 0.0%	CLAY: 0.0%		
METHOD OF MOMENTS FOLK & WARD METHOD						
	Arithmetic	Geometric	Logarithmic	Geometric	Logarithmic	Description
	∞m	∞m	\square	∞m	\square	
MEAN (\bar{x}):	198.4	172.8	2.533	173.1	2.530	Fine Sand
SORTING (\square):	126.0	1.589	0.668	1.520	0.604	Moderately Well Sorted
SKEWNESS (Sk):	3.376	0.662	-0.662	0.031	-0.031	Symmetrical
KURTOSIS (K):	16.50	5.303	5.303	1.674	1.674	Very Leptokurtic



SAMPLE STATISTICS

SAMPLE IDENTITY: **TK 4-13**

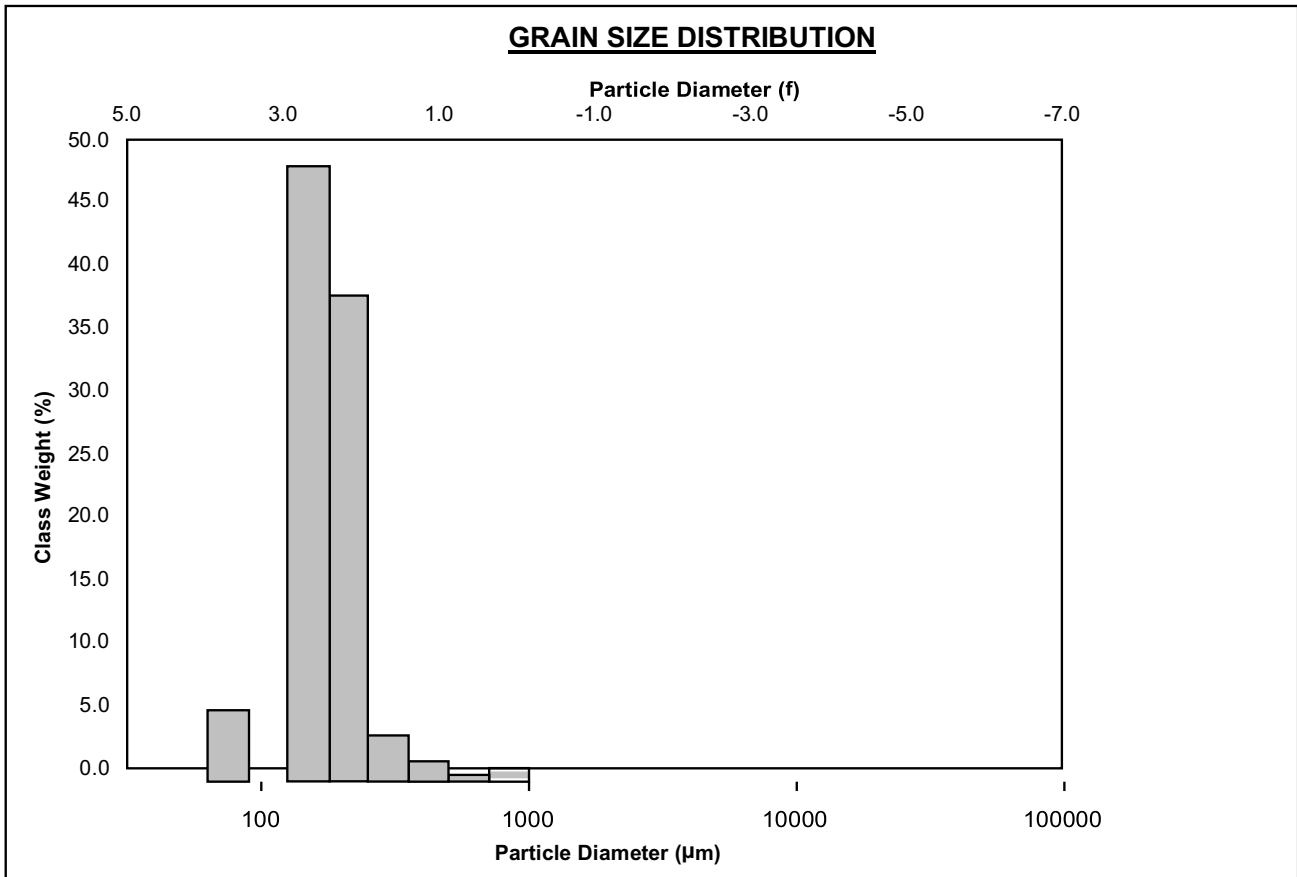
ANALYST & DATE: JES,

SAMPLE TYPE: Unimodal, Well Sorted

TEXTURAL GROUP: Sand

SEDIMENT NAME: Well Sorted Fine Sand

	αm ϕ		GRAIN SIZE DISTRIBUTION			
	MODE 1:	152.5	2.737	GRAVEL: 0.0%	COARSE SAND: 1.6%	
MODE 2:			SAND: 100.0%	MEDIUM SAND: 5.3%		
MODE 3:			MUD: 0.0%	FINE SAND: 87.4%		
D ₁₀ :	128.8	2.041		V FINE SAND: 5.8%		
MEDIAN or D ₅₀ :	171.4	2.544	V COARSE GRAVEL: 0.0%	V COARSE SILT: 0.0%		
D ₉₀ :	243.0	2.957	COARSE GRAVEL: 0.0%	COARSE SILT: 0.0%		
(D ₉₀ / D ₁₀):	1.886	1.448	MEDIUM GRAVEL: 0.0%	MEDIUM SILT: 0.0%		
(D ₉₀ - D ₁₀):	114.1	0.915	FINE GRAVEL: 0.0%	FINE SILT: 0.0%		
(D ₇₅ / D ₂₅):	1.479	1.253	V FINE GRAVEL: 0.0%	V FINE SILT: 0.0%		
(D ₇₅ - D ₂₅):	68.75	0.565	V COARSE SAND: 0.0%	CLAY: 0.0%		
	METHOD OF MOMENTS			FOLK & WARD METHOD		
	Arithmetic αm	Geometric αm	Logarithmic \square	Geometric αm	Logarithmic \square	Description
MEAN (\bar{x}):	190.4	174.8	2.516	174.4	2.520	Fine Sand
SORTING (\square):	92.76	1.421	0.507	1.381	0.466	Well Sorted
SKEWNESS (Sk):	4.528	0.767	-0.767	-0.008	0.008	Symmetrical
KURTOSIS (K):	30.68	7.807	7.807	1.303	1.303	Leptokurtic



SAMPLE STATISTICS

SAMPLE IDENTITY: **TK 4-14**

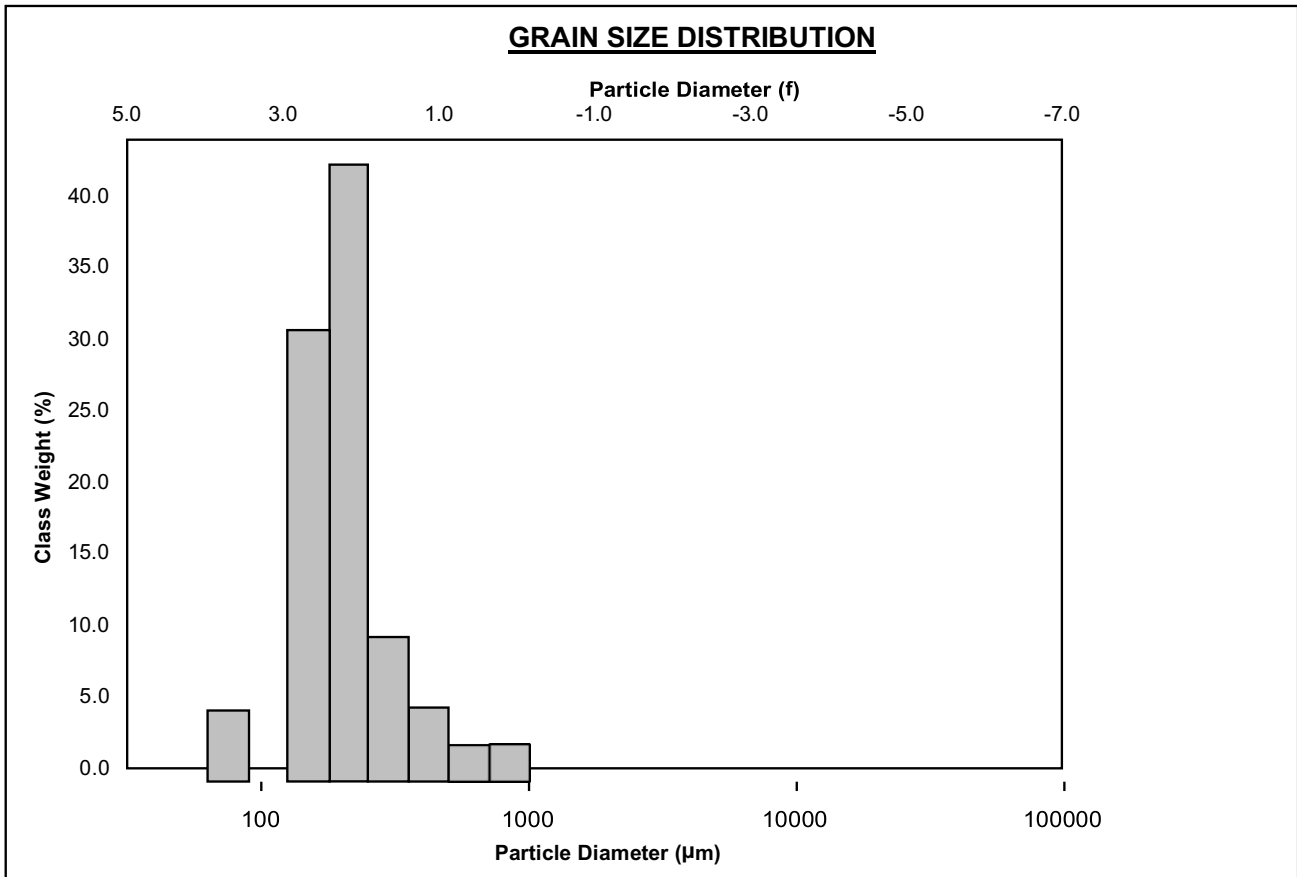
ANALYST & DATE: JES,

SAMPLE TYPE: Unimodal, Moderately Well Sorted

TEXTURAL GROUP: Sand

SEDIMENT NAME: Moderately Well Sorted Fine Sand

	αm ϕ		GRAIN SIZE DISTRIBUTION			
	MODE 1:	215.0	2.237	GRAVEL: 0.0%	COARSE SAND: 5.1%	
MODE 2:			SAND: 100.0%	MEDIUM SAND: 15.4%		
MODE 3:			MUD: 0.0%	FINE SAND: 74.4%		
D ₁₀ :	131.8	1.470		V FINE SAND: 5.1%		
MEDIAN or D ₅₀ :	197.4	2.341	V COARSE GRAVEL: 0.0%	V COARSE SILT: 0.0%		
D ₉₀ :	361.0	2.923	COARSE GRAVEL: 0.0%	COARSE SILT: 0.0%		
(D ₉₀ / D ₁₀):	2.738	1.988	MEDIUM GRAVEL: 0.0%	MEDIUM SILT: 0.0%		
(D ₉₀ - D ₁₀):	229.1	1.453	FINE GRAVEL: 0.0%	FINE SILT: 0.0%		
(D ₇₅ / D ₂₅):	1.552	1.309	V FINE GRAVEL: 0.0%	V FINE SILT: 0.0%		
(D ₇₅ - D ₂₅):	85.82	0.635	V COARSE SAND: 0.0%	CLAY: 0.0%		
	METHOD OF MOMENTS		FOLK & WARD METHOD			
	Arithmetic αm	Geometric αm	Logarithmic \square	Geometric αm	Logarithmic \square	Description
MEAN (\bar{x}):	233.3	204.5	2.290	200.9	2.316	Fine Sand
SORTING (σ):	139.4	1.574	0.654	1.562	0.643	Moderately Well Sorted
SKEWNESS (Sk):	2.768	0.728	-0.728	0.079	-0.079	Symmetrical
KURTOSIS (K):	11.74	4.885	4.885	1.622	1.622	Very Leptokurtic



APPENDIX D

Radiocarbon Calibration Data

**Appendix D Radiocarbon Data
D.1 Ayla Oasis Samples**

CALIB REV7.1.0 RADIOCARBON CALIBRATION PROGRAM*

Copyright 1986-2018 M Stuiver and PJ Reimer

*To be used in conjunction with:

Stuiver, M., and Reimer, P.J., 1993, Radiocarbon, 35, 215-230.

AO-2-15

Lab Code CAMS 163766

Sample Description : wood

Radiocarbon Age BP 3060 +/- 30

Calibration data set: intcal13.14c

% area enclosed cal AD age ranges

68.3 (1 sigma) cal BC 1389- 1337

1321- 1277

95.4 (2 sigma) cal BC 1410- 1257

1249- 1232

Median Probability: -1329

Reimer et al. 2013
relative area under
probability distribution

0.548

0.452

0.958

0.042

AO-2-15

Lab Code CAMS 163766

Sample Description : wood

Radiocarbon Age BP 3060 +/- 30

Calibration data set: intcal13.14c

% area enclosed cal BP age ranges

68.3 (1 sigma) cal BP 3226 - 3270

3286 - 3338

95.4 (2 sigma) cal BP 3181 - 3198

3206 - 3359

Median Probability: 3278

Reimer et al. 2013
relative area under
probability distribution

0.452

0.548

0.042

0.958

AO-2-18

Lab Code CAMS 163767

Sample Description charcoal

Radiocarbon Age BP 2935 +/- 30

Calibration data set: intcal13.14c

% area enclosed cal AD age ranges

68.3 (1 sigma) cal BC 1209- 1109

1098- 1089

95.4 (2 sigma) cal BC 1224- 1030

Median Probability: -1143

Reimer et al. 2013
relative area under
probability distribution

0.938

0.062

1.000

AO-2-18

Lab Code CAMS 163767

Sample Description charcoal

Radiocarbon Age BP 2935 +/- 30

Calibration data set: intcal13.14c

% area enclosed cal BP age ranges

68.3 (1 sigma) cal BP 3038 - 3047

3058 - 3158

95.4 (2 sigma) cal BP 2979 - 3173

Reimer et al. 2013
relative area under
probability distribution

0.062

0.938

1.000

Median Probability: 3092

AO-3-1

Lab Code CAMS 162768
Sample Description wood
Radiocarbon Age BP 3435 +/- 30
Calibration data set: intcal13.14c # Reimer et al. 2013
% area enclosed cal AD age ranges relative area under
probability distribution

68.3 (1 sigma)	cal BC 1859- 1854	0.028
	1771- 1689	0.972
95.4 (2 sigma)	cal BC 1877- 1839	0.132
	1827- 1794	0.069
	1784- 1660	0.798

Median Probability: -1739

AO-3-1

Lab Code CAMS 162768
Sample Description wood
Radiocarbon Age BP 3435 +/- 30
Calibration data set: intcal13.14c # Reimer et al. 2013
% area enclosed cal BP age ranges relative area under
probability distribution

68.3 (1 sigma)	cal BP 3638 - 3720	0.972
	3803 - 3808	0.028
95.4 (2 sigma)	cal BP 3609 - 3733	0.798
	3743 - 3776	0.069
	3788 - 3826	0.132

Median Probability: 3688

AO-7b-1

Lab Code CAMS 163769
Sample Description wood
Radiocarbon Age BP 5690 +/- 30
Calibration data set: intcal13.14c # Reimer et al. 2013
% area enclosed cal AD age ranges relative area under
probability distribution

68.3 (1 sigma)	cal BC 4548- 4486	0.953
	4471- 4466	0.047
95.4 (2 sigma)	cal BC 4600- 4457	1.000

Median Probability: -4519

AO-7b-1

Lab Code CAMS 163769
Sample Description wood
Radiocarbon Age BP 5690 +/- 30
Calibration data set: intcal13.14c # Reimer et al. 2013
% area enclosed cal BP age ranges relative area under
probability distribution

68.3 (1 sigma)	cal BP 6415 - 6420	0.047
	6435 - 6497	0.953
95.4 (2 sigma)	cal BP 6406 - 6549	1.000

Median Probability: 6468

References for calibration datasets:

D.2 Brückner (1999) Radiocarbon Data

RADIOCARBON CALIBRATION PROGRAM*

CALIB REV7.1.0

Copyright 1986-2018 M Stuiver and PJ Reimer

*To be used in conjunction with:

Stuiver, M., and Reimer, P.J., 1993, Radiocarbon, 35, 215-230.

AQ 5/11F

Lab Code Beta 121046
Sample Description *Codakia punctata* (LINNE 1767)
Radiocarbon Age BP 3740 +/- 50
Delta R = 165.0 +/- 72.0
Calibration data set: marine13.14c # Reimer et al. 2013
% area enclosed cal AD age ranges relative area under
probability distribution
68.3 (1 sigma) cal BC 1620- 1416 1.000
95.4 (2 sigma) cal BC 1738- 1300 1.000
Median Probability: -1523

AQ 5/11F

Lab Code Beta 121046
Sample Description *Codakia punctata* (LINNE 1767)
Radiocarbon Age BP 3740 +/- 50
Delta R = 165.0 +/- 72.0
Calibration data set: marine13.14c # Reimer et al. 2013
% area enclosed cal BP age ranges relative area under
probability distribution
68.3 (1 sigma) cal BP 3365 - 3569 1.000
95.4 (2 sigma) cal BP 3249 - 3687 1.000
Median Probability: 3472

AQ 6/15F

Lab Code Beta 121047
Sample Description clam shell fragment
Radiocarbon Age BP 6200 +/- 60
Delta R = 165.0 +/- 72.0
Calibration data set: marine13.14c # Reimer et al. 2013
% area enclosed cal AD age ranges relative area under
probability distribution
68.3 (1 sigma) cal BC 4612- 4395 1.000
95.4 (2 sigma) cal BC 4716- 4319 1.000
Median Probability: -4510

AQ 6/15F

Lab Code Beta 121047
Sample Description clam shell fragment
Radiocarbon Age BP 6200 +/- 60
Delta R = 165.0 +/- 72.0
Calibration data set: marine13.14c # Reimer et al. 2013
% area enclosed cal BP age ranges relative area under
probability distribution
68.3 (1 sigma) cal BP 6344 - 6561 1.000
95.4 (2 sigma) cal BP 6268 - 6665 1.000
Median Probability: 6459

D.3 Friedman (1965) Radiocarbon Data

RADIOCARBON CALIBRATION PROGRAM*

CALIB REV7.1.0

Copyright 1986-2018 M Stuiver and PJ Reimer

*To be used in conjunction with:

Stuiver, M., and Reimer, P.J., 1993, Radiocarbon, 35, 215-230.

Friedman C

Lab Code

Friedman Coral Ages (1965)

Radiocarbon Age BP 4770 +/- 140

Delta R = 165.0 +/- 72.0

Calibration data set: marine13.14c

% area enclosed cal BP age ranges

Reimer et al. 2013
relative area under
probability distribution

68.3 (1 sigma) cal BP 4585 - 5029

1.000

95.4 (2 sigma) cal BP 4421 - 5261

1.000

Median Probability: 4824

References for calibration datasets:

Reimer PJ, Bard E, Bayliss A, Beck JW, Blackwell PG, Bronk Ramsey C, Buck CE, Cheng H, Edwards RL, Friedrich M, Grootes PM, Guilderson TP, Haflidason H, Hajdas I, Hatté C, Heaton TJ, Hogg AG, Hughen KA, Kaiser KF, Kromer B, Manning SW, Niu M, Reimer RW, Richards DA, Scott EM, Southon JR, Turney CSM, van der Plicht J.

IntCal13 and MARINE13 radiocarbon age calibration curves 0-50000 years calBP Radiocarbon 55(4). DOI: 10.2458/azu_js_rc.55.16947

Comments:

* This standard deviation (error) includes a lab error multiplier.

** 2 sigma = 2 x square root of (sample std. dev.^2 + Delta R uncertainty ^2)

where ^2 = quantity squared.

[] = calibrated range impinges on end of calibration data set

0* = cannot calibrate due to nuclear testing C-14.

1955* or 1960* denote influence of nuclear testing C-14

NOTE: Cal ages and ranges are rounded to the nearest year which may be too precise in many instances. Users are advised to round results to the nearest 10 yr for samples with standard deviation in the radiocarbon age greater than 50 yr.

D.4 Moustafa (2000) Radiocarbon Calibration

RADIOCARBON CALIBRATION PROGRAM*

CALIB REV7.1.0

Copyright 1986-2018 M Stuiver and PJ Reimer

*To be used in conjunction with:

Stuiver, M., and Reimer, P.J., 1993, Radiocarbon, 35, 215-230.

H2 Lab KI

Lab Code

Moustafa Corals (2000)

Radiocarbon Age BP 4600 +/- 50

Delta R = 165.0 +/- 72.0

Calibration data set: marine13.14c

% area enclosed cal BP age ranges

Reimer et al. 2013

relative area under
probability distribution

68.3 (1 sigma) cal BP 4503 - 4730
4747 - 4770

0.923

0.077

95.4 (2 sigma) cal BP 4395 - 4823

1.000

Median Probability: 4611

F3 Lab KI

Lab Code

Moustafa Corals (2000)

Radiocarbon Age BP 4890 +/- 40

Delta R = 165.0 +/- 72.0

Calibration data set: marine13.14c

% area enclosed cal BP age ranges

Reimer et al. 2013

relative area under
probability distribution

68.3 (1 sigma) cal BP 4836 - 5072

1.000

95.4 (2 sigma) cal BP 4807 - 5243

1.000

Median Probability: 4982

H5 GrA 78

Lab Code

Moustafa Corals (2000)

Radiocarbon Age BP 4600 +/- 60

Delta R = 165.0 +/- 72.0

Calibration data set: marine13.14c

% area enclosed cal BP age ranges

Reimer et al. 2013

relative area under
probability distribution

68.3 (1 sigma) cal BP 4503 - 4735
4745 - 4771

0.917

0.083

95.4 (2 sigma) cal BP 4375 - 4834

1.000

Median Probability: 4610

F6 GrA 78

Lab Code

Moustafa Corals (2000)

Radiocarbon Age BP 4960 +/- 60

Delta R = 165.0 +/- 72.0

Calibration data set: marine13.14c

% area enclosed cal BP age ranges

Reimer et al. 2013

relative area under
probability distribution

68.3 (1 sigma) cal BP 4953 - 5228

1.000

95.4 (2 sigma) cal BP 4835 - 5296

1.000

Median Probability: 5076

F7 GrA 78
 Lab Code
 Moustafa Corals (2000)
 Radiocarbon Age BP 5140 +/- 60
 Delta R = 165.0 +/- 72.0
 Calibration data set: marine13.14c # Reimer et al. 2013
 % area enclosed cal BP age ranges relative area under
 probability distribution
 68.3 (1 sigma) cal BP 5208 - 5459 1.000
 95.4 (2 sigma) cal BP 5041 - 5550 1.000
 Median Probability: 5317

F8 GrA 78
 Lab Code
 Moustafa Corals (2000)
 Radiocarbon Age BP 5750 +/- 60
 Delta R = 165.0 +/- 72.0
 Calibration data set: marine13.14c # Reimer et al. 2013
 % area enclosed cal BP age ranges relative area under
 probability distribution
 68.3 (1 sigma) cal BP 5883 - 6107 1.000
 95.4 (2 sigma) cal BP 5747 - 6197 1.000
 Median Probability: 5986

F9 GrA 78
 Lab Code
 Moustafa Corals (2000)
 Radiocarbon Age BP 5100 +/- 60
 Delta R = 165.0 +/- 72.0
 Calibration data set: marine13.14c # Reimer et al. 2013
 % area enclosed cal BP age ranges relative area under
 probability distribution
 68.3 (1 sigma) cal BP 5131 - 5417 1.000
 95.4 (2 sigma) cal BP 4963 - 5490 1.000
 Median Probability: 5257

F11 GrA 7
 Lab Code
 Moustafa Corals (2000)
 Radiocarbon Age BP 5370 +/- 60
 Delta R = 165.0 +/- 72.0
 Calibration data set: marine13.14c # Reimer et al. 2013
 % area enclosed cal BP age ranges relative area under
 probability distribution
 68.3 (1 sigma) cal BP 5456 - 5658 1.000
 95.4 (2 sigma) cal BP 5314 - 5763 1.000
 Median Probability: 5564

F23 GrA 7
 Lab Code
 Moustafa Corals (2000)
 Radiocarbon Age BP 4920 +/- 90
 Delta R = 165.0 +/- 72.0
 Calibration data set: marine13.14c # Reimer et al. 2013
 % area enclosed cal BP age ranges relative area under
 probability distribution

68.3 (1 sigma)	cal BP 4861 - 5137	0.892
	5152 - 5191	0.108
95.4 (2 sigma)	cal BP 4717 - 4755	0.011
	4765 - 5317	0.989
Median Probability: 5028		

F24 GrA 7

Lab Code

Moustafa Corals (2000)

Radiocarbon Age BP 4450 +/- 90

Delta R = 165.0 +/- 72.0

Calibration data set: marine13.14c

% area enclosed cal BP age ranges

Reimer et al. 2013
relative area under
probability distribution

68.3 (1 sigma)	cal BP 4229 - 4560	1.000
95.4 (2 sigma)	cal BP 4085 - 4730	0.989
	4747 - 4770	0.011

Median Probability: 4402

References for calibration datasets:

Reimer PJ, Bard E, Bayliss A, Beck JW, Blackwell PG, Bronk Ramsey C, Buck CE, Cheng H, Edwards RL, Friedrich M, Grootes PM, Guilderson TP, Haflidason H, Hajdas I, Hatté C, Heaton TJ, Hogg AG, Hughen KA, Kaiser KF, Kromer B, Manning SW, Niu M, Reimer RW, Richards DA, Scott EM, Southon JR, Turney CSM, van der Plicht J.

IntCal13 and MARINE13 radiocarbon age calibration curves 0-50000 years calBP Radiocarbon 55(4). DOI: 10.2458/azu_js_rc.55.16947

Comments:

* This standard deviation (error) includes a lab error multiplier.

** 2 sigma = 2 x square root of (sample std. dev.^2 + Delta R uncertainty ^2)

where ^2 = quantity squared.

[] = calibrated range impinges on end of calibration data set

0* = cannot calibrate due to nuclear testing C-14.

1955* or 1960* denote influence of nuclear testing C-14

NOTE: Cal ages and ranges are rounded to the nearest year which may be too precise in many instances. Users are advised to round results to the nearest 10 yr for samples with standard deviation in the radiocarbon age greater than 50 yr.

The median probability is calculated as a weighted mean given the following equation:

$$\text{weighted mean of } \Delta R = \mu = \frac{\sum_i \frac{\Delta R_i}{\sigma_i^2}}{\sum_i \frac{1}{\sigma_i^2}}$$

where σ_i = uncertainty in ΔR_i

$$\text{variance of } \Delta R = \frac{\frac{1}{n-1} \cdot \sum_i \left(\frac{\Delta R_i - \mu}{\sigma_i} \right)^2}{\frac{1}{n} \cdot \sum_i \frac{1}{\sigma_i^2}}$$

Standard Deviation of $\Delta R = \sqrt{\text{variance}}$

References for calibration datasets:

Reimer PJ, Bard E, Bayliss A, Beck JW, Blackwell PG, Bronk Ramsey C, Buck CE, Cheng H, Edwards RL, Friedrich M, Grootes PM, Guilderson TP, Haflidason H, Hajdas I, Hatté C, Heaton TJ, Hogg AG, Hughen KA, Kaiser KF, Kromer B, Manning SW, Niu M, Reimer RW, Richards DA, Scott EM, Southon JR, Turney CSM, van der Plicht J.

IntCal13 and MARINE13 radiocarbon age calibration curves 0-50000 years calBP Radiocarbon 55(4). DOI: 10.2458/azu_js_rc.55.16947

Comments:

* This standard deviation (error) includes a lab error multiplier.
 ** 2 sigma = 2 x square root of (sample std. dev.^2 + Delta R uncertainty

^2)

where ^2 = quantity squared.

[] = calibrated range impinges on end of calibration data set
 0* = cannot calibrate due to nuclear testing C-14.

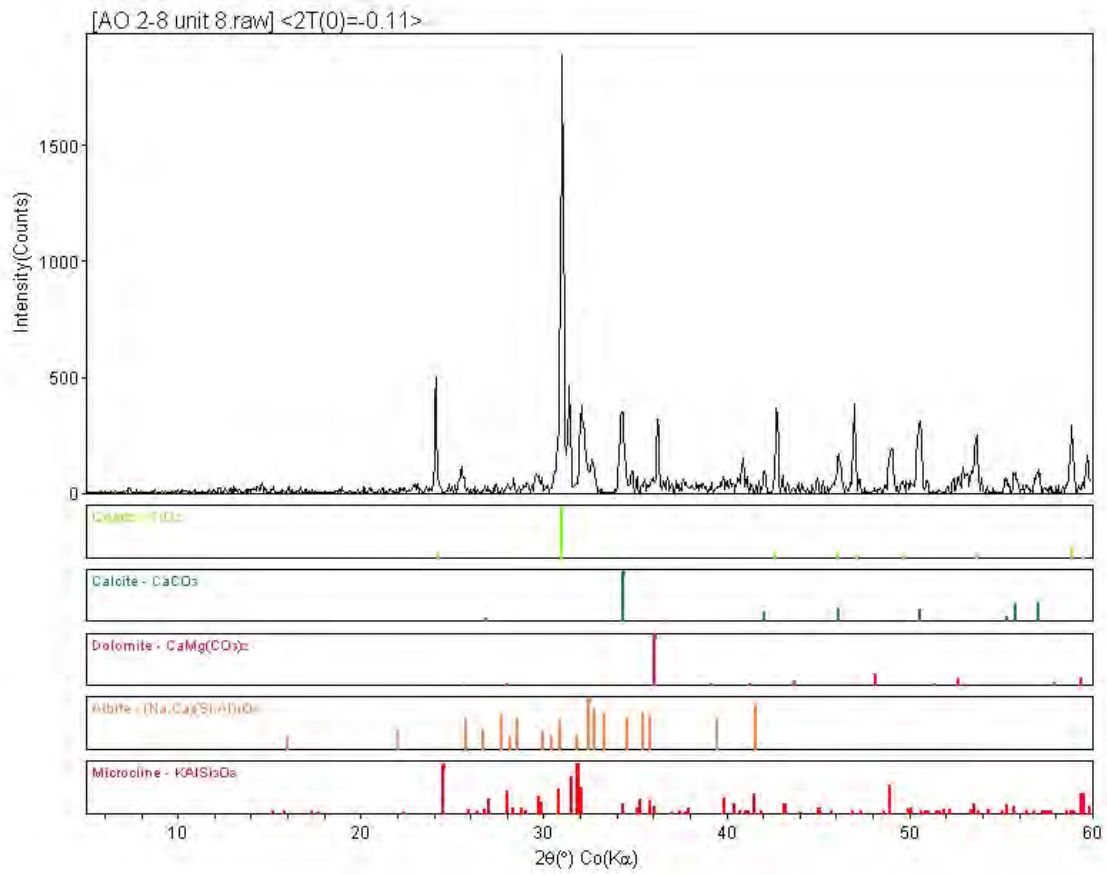
1955* or 1960* denote influence of nuclear testing C-14

NOTE: Cal ages and ranges are rounded to the nearest year which may be too precise in many instances. Users are advised to round results to the nearest 10 yr for samples with standard deviation in the radiocarbon age greater than 50 yr.

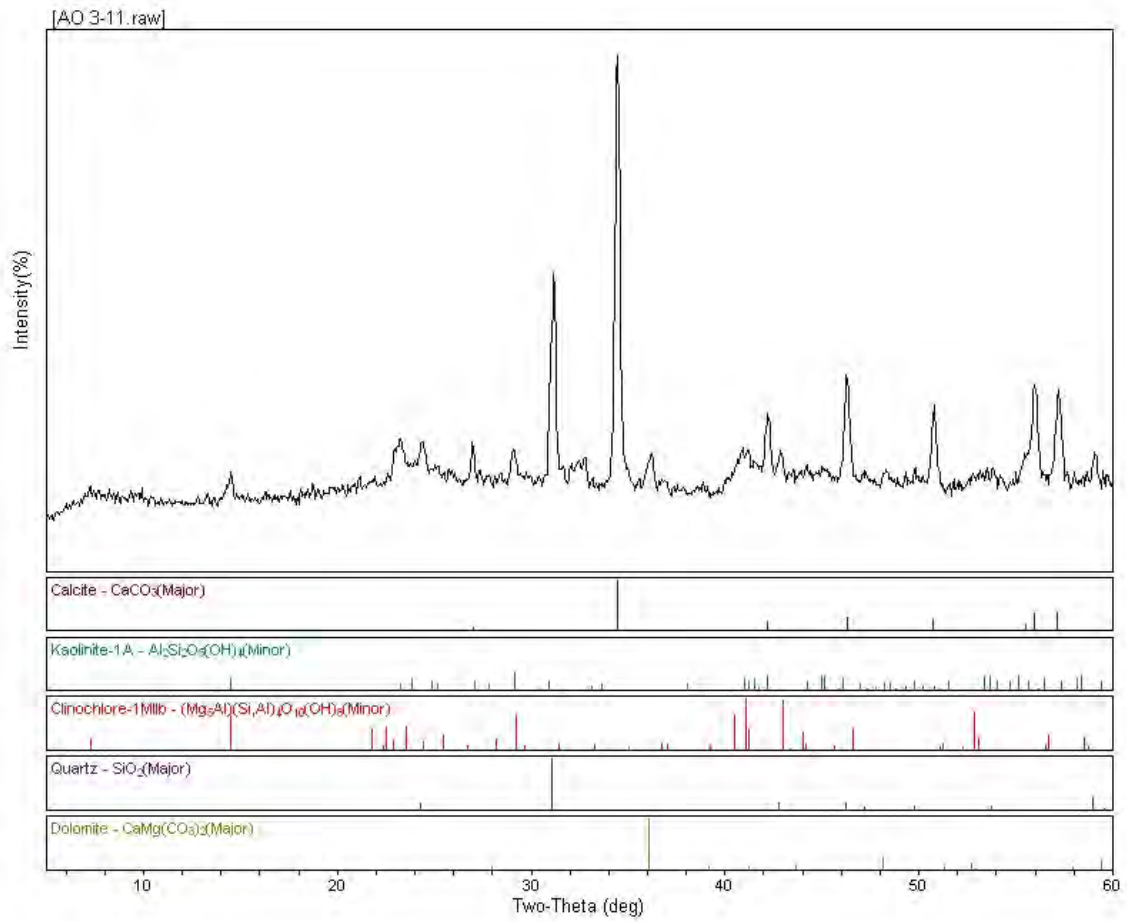
APPENDIX E

XRD, SEM, and EDS Data

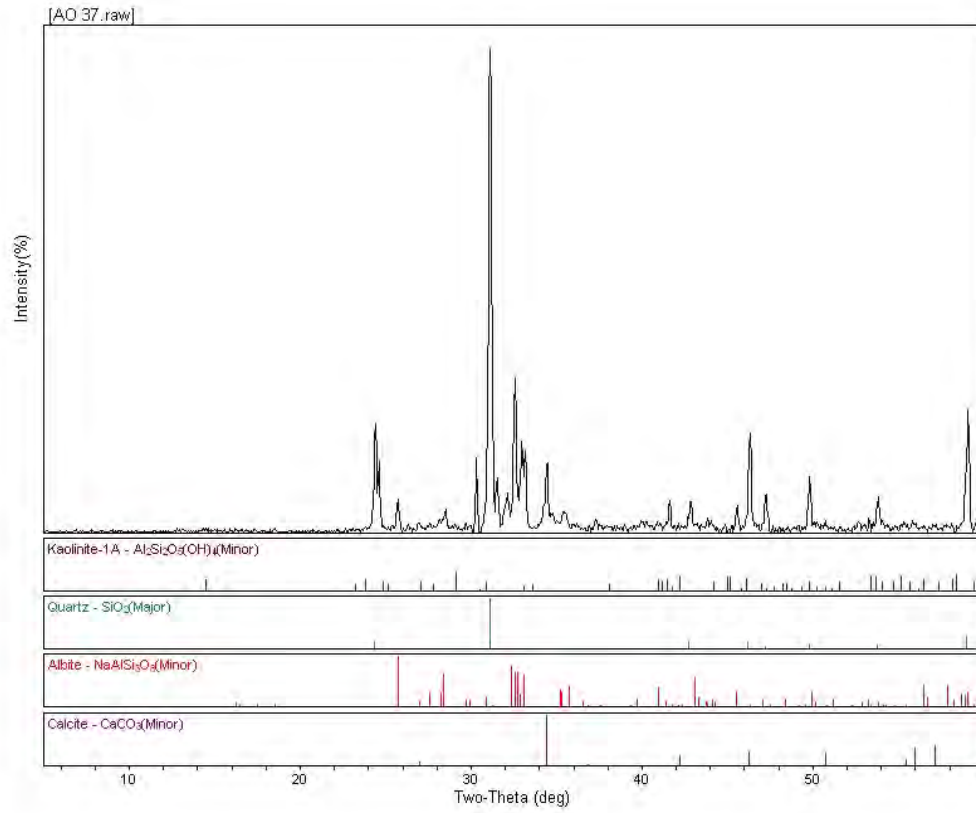
XRD AO-2 8, Unit 8



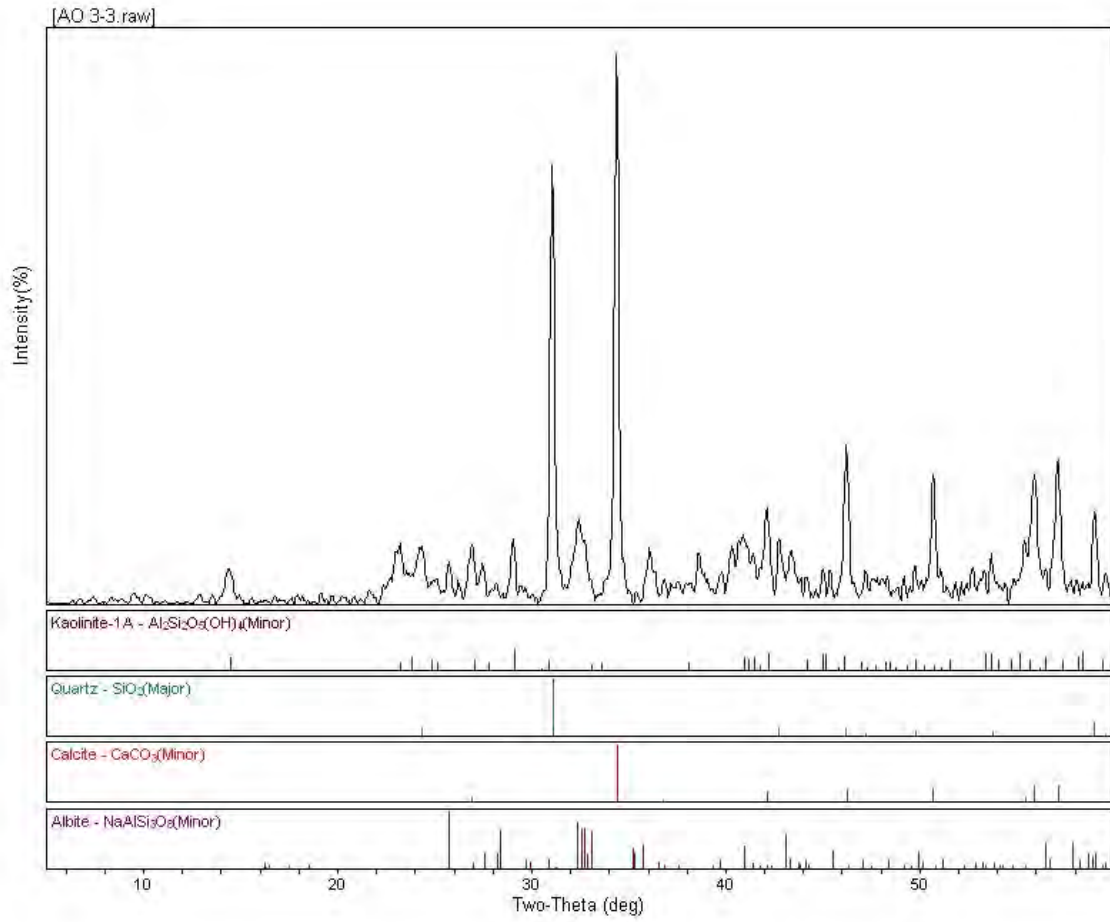
XRD AO-3 11, Unit 5



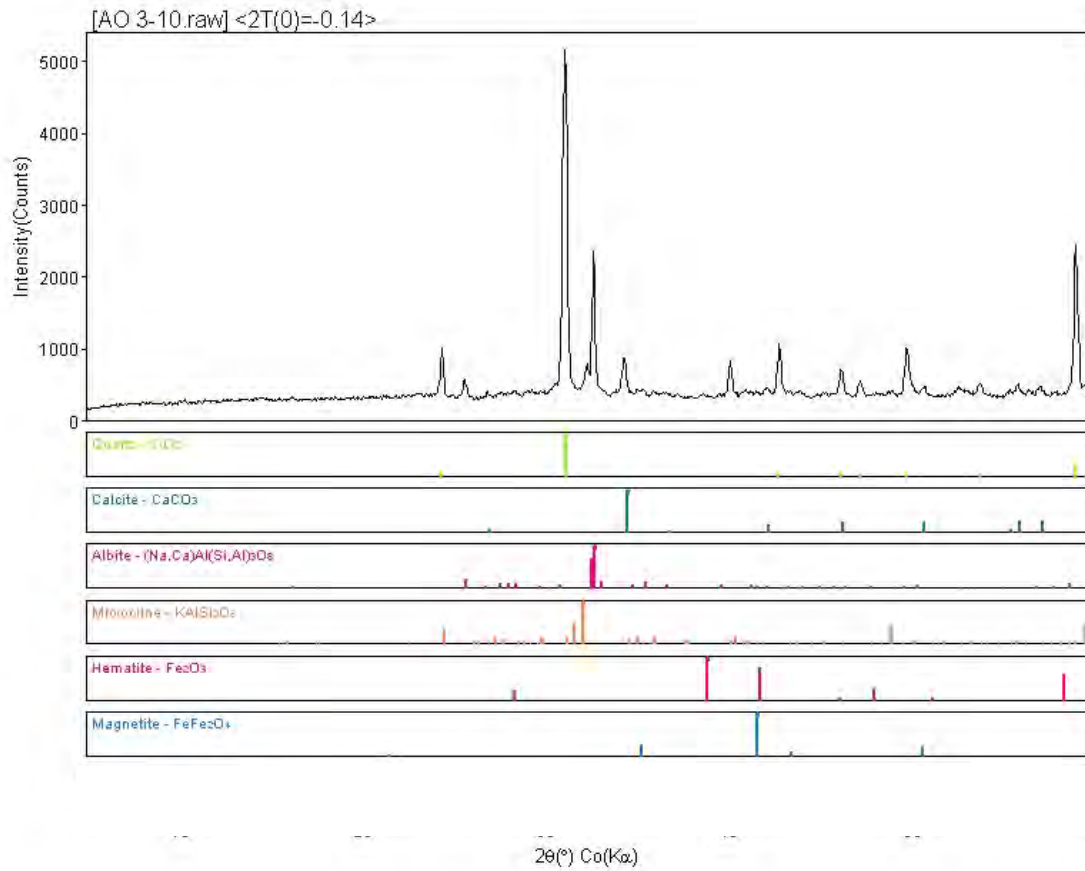
XRD AO-3 7, Unit 7



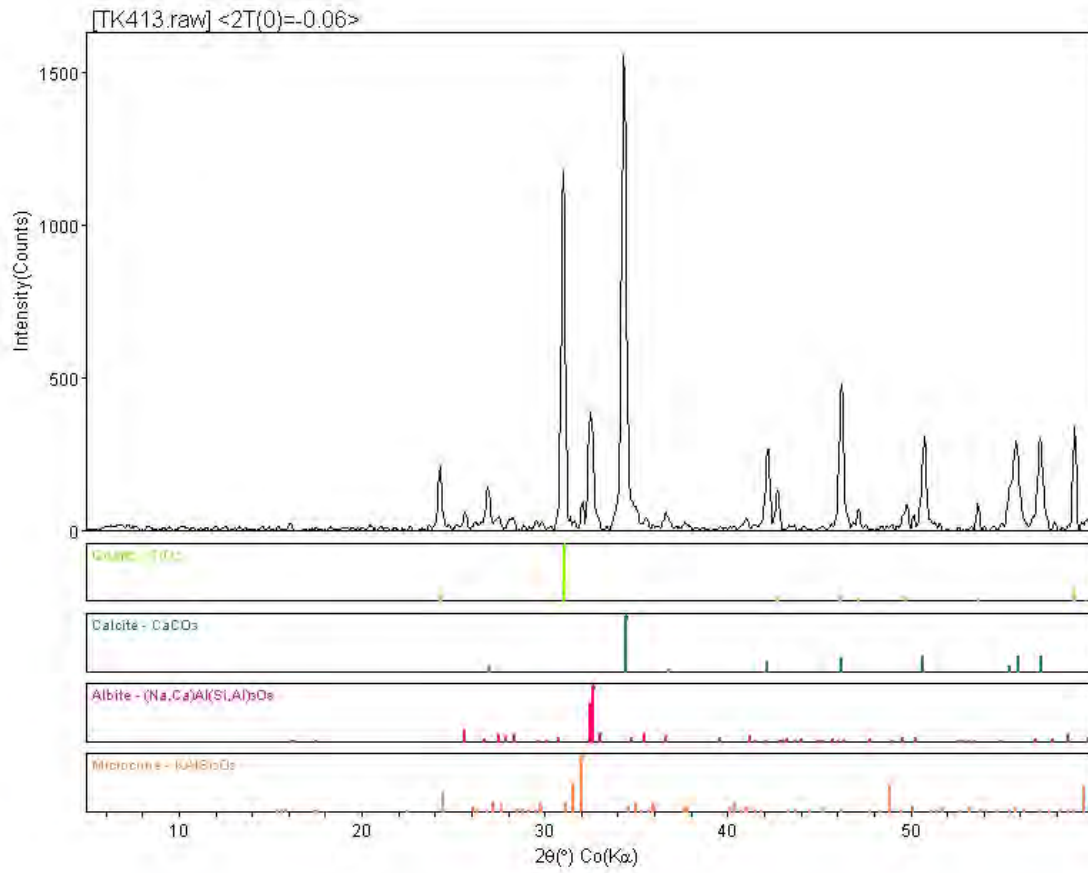
XRD AO-3 3, Unit 8



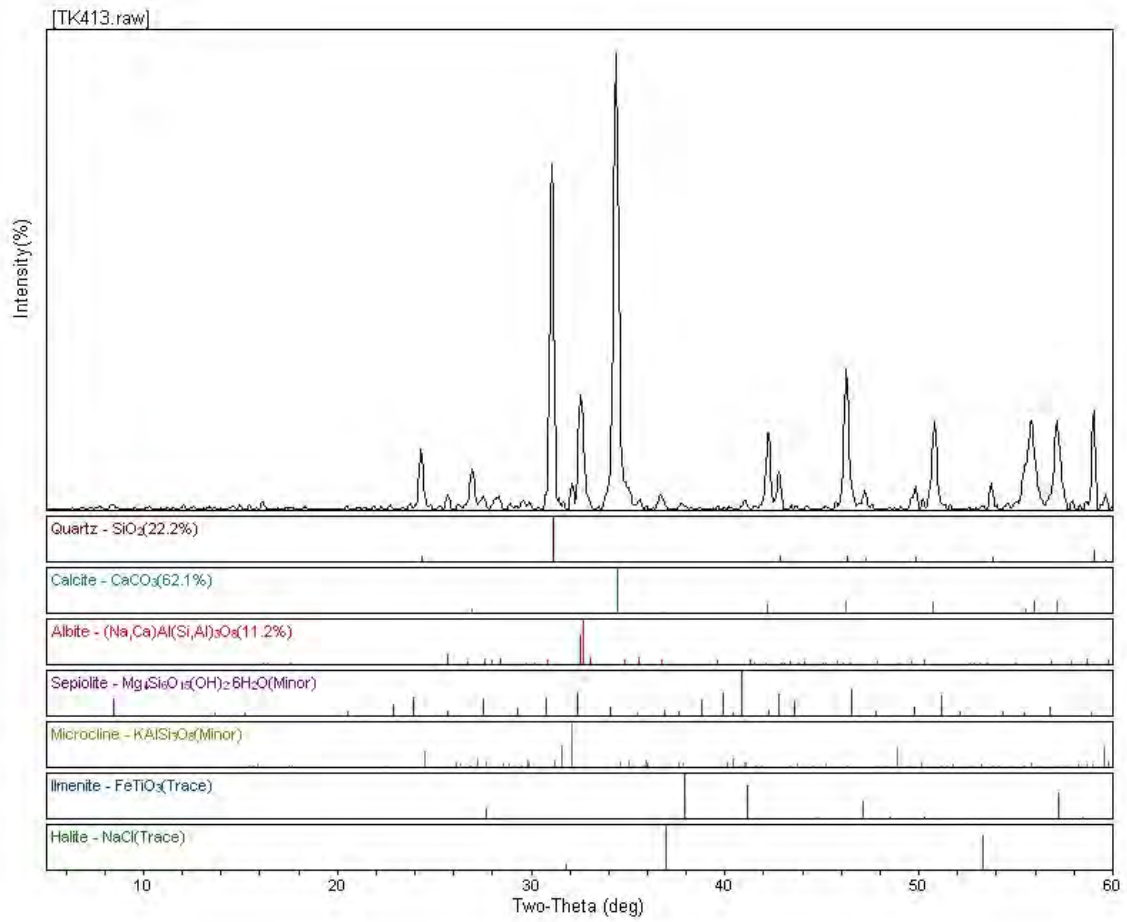
XRD AO-3 10, Unit 8



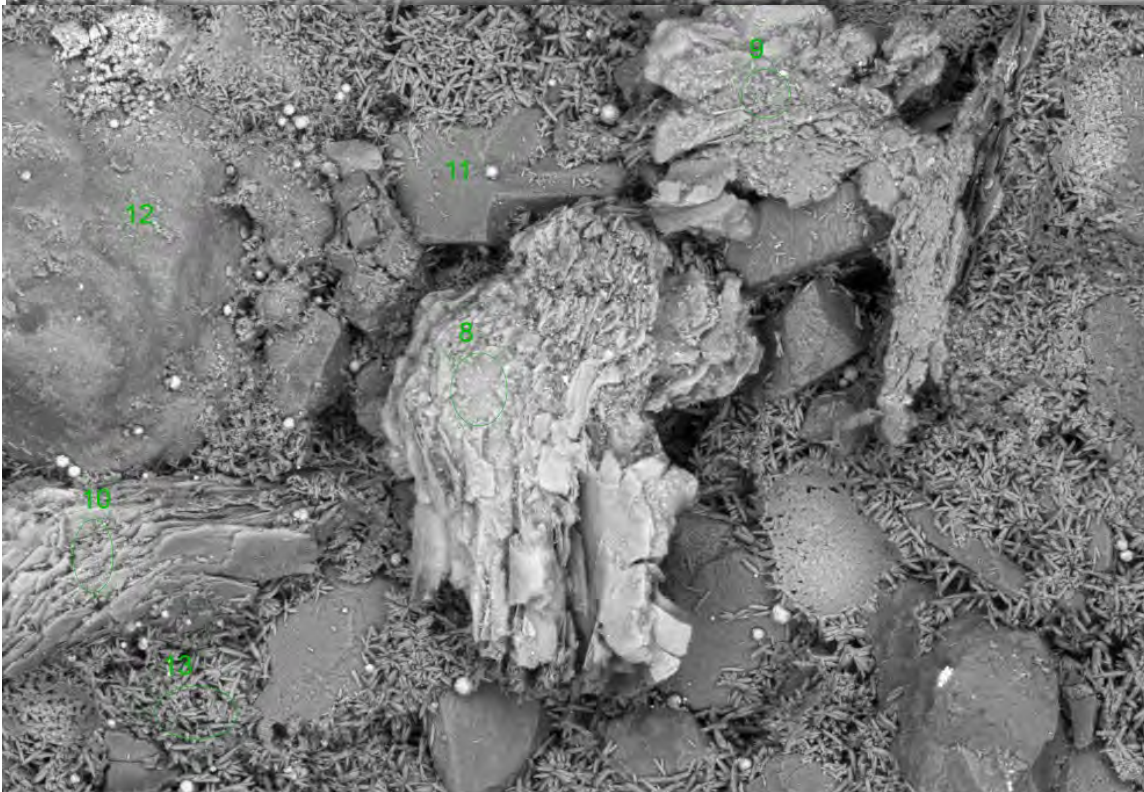
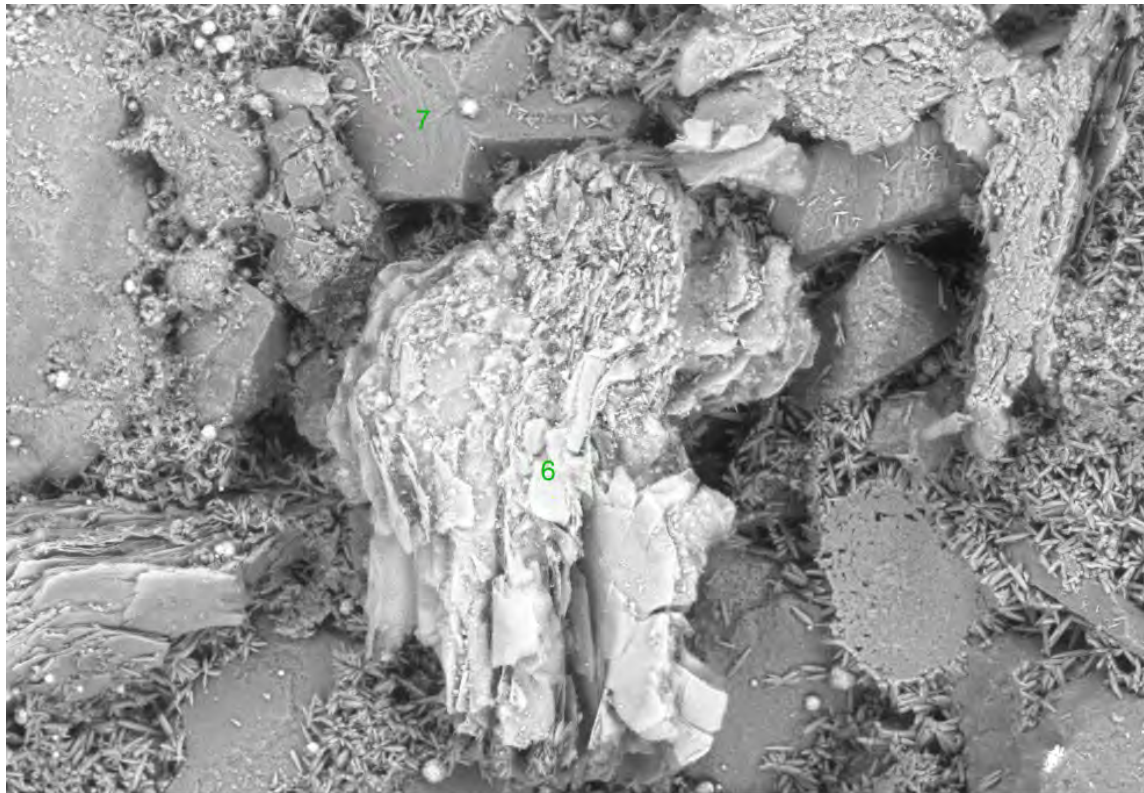
XRD TK-4, Unit 13 Bulk Sample



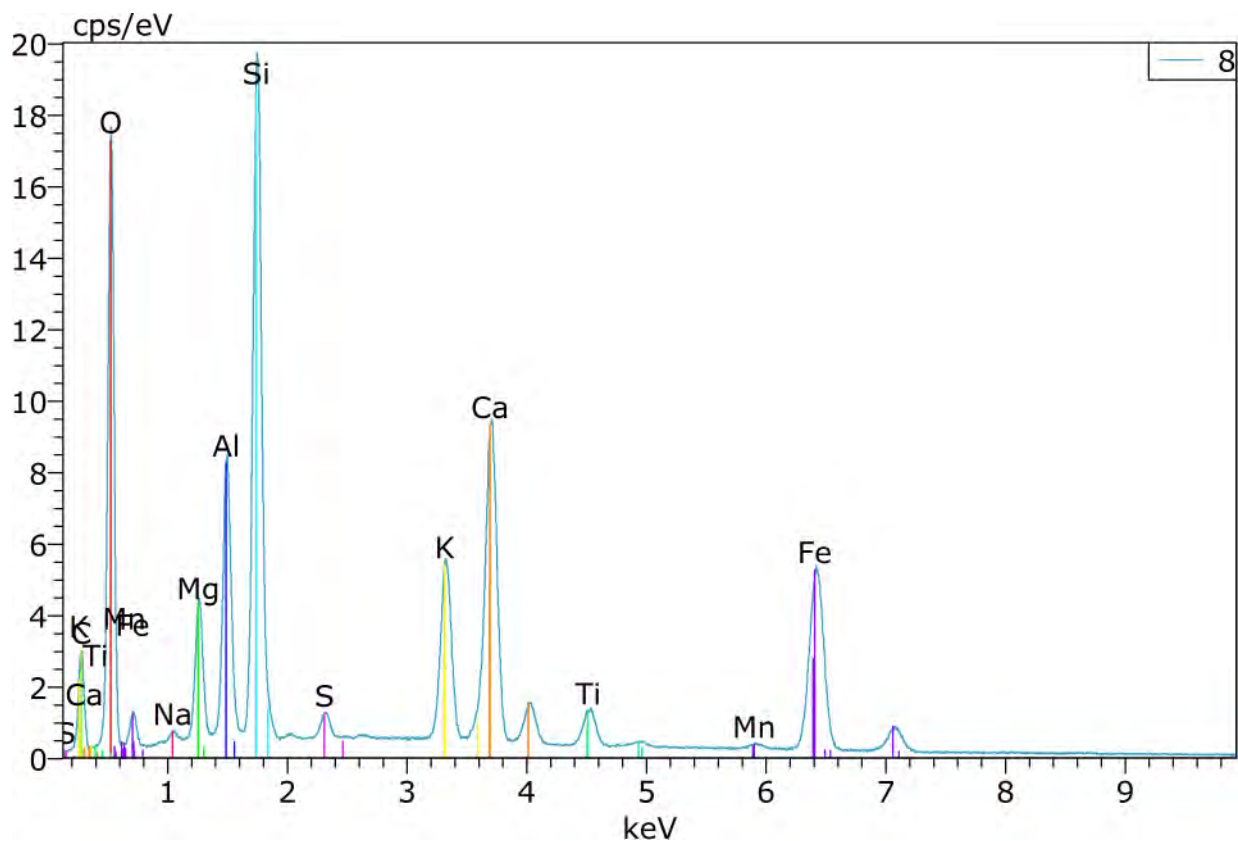
XRD TK-4, Unit 13 Concretion Sample



TK 4-13 SEM

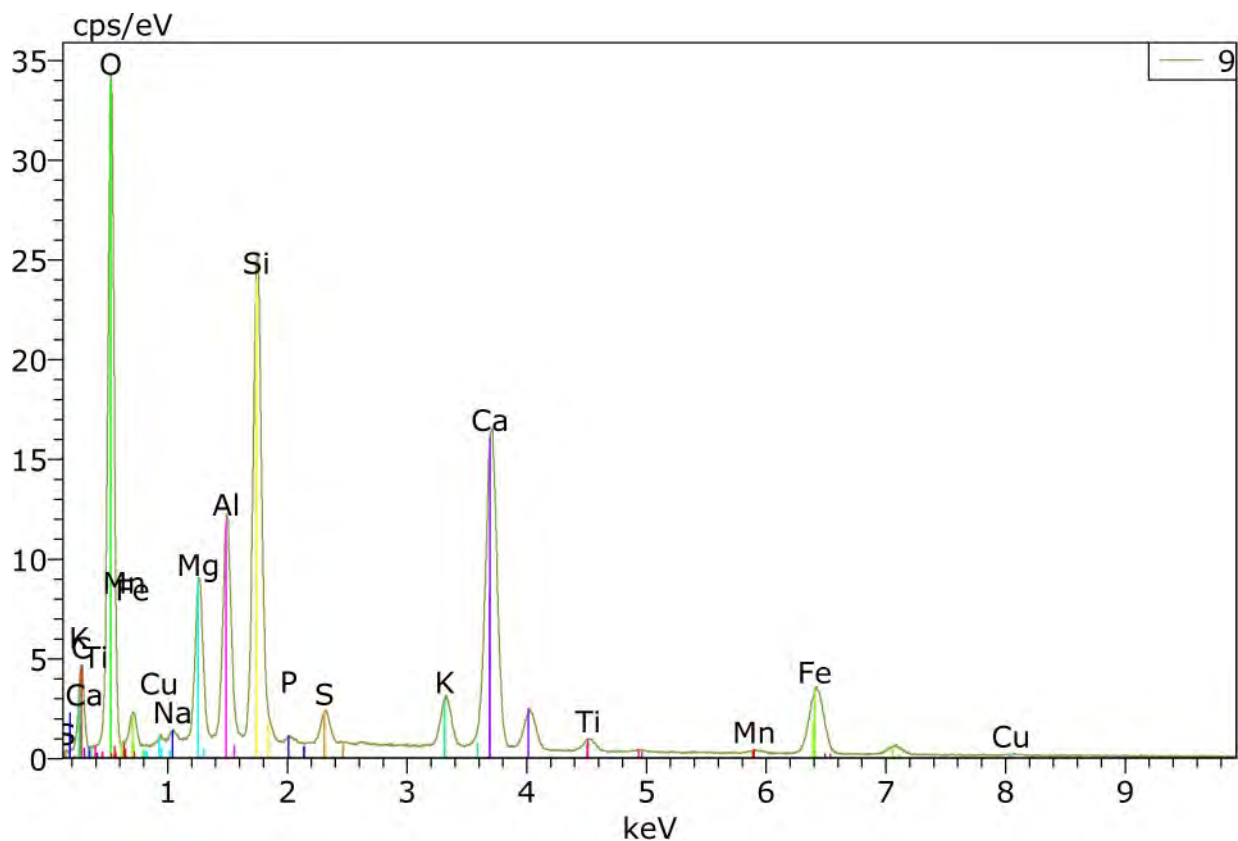


TK413 11 Mapping
BSE MAG: 243 x HV: 20.0 kV WD: 15.0 mm Px: 0.85 μ m
200 μ m



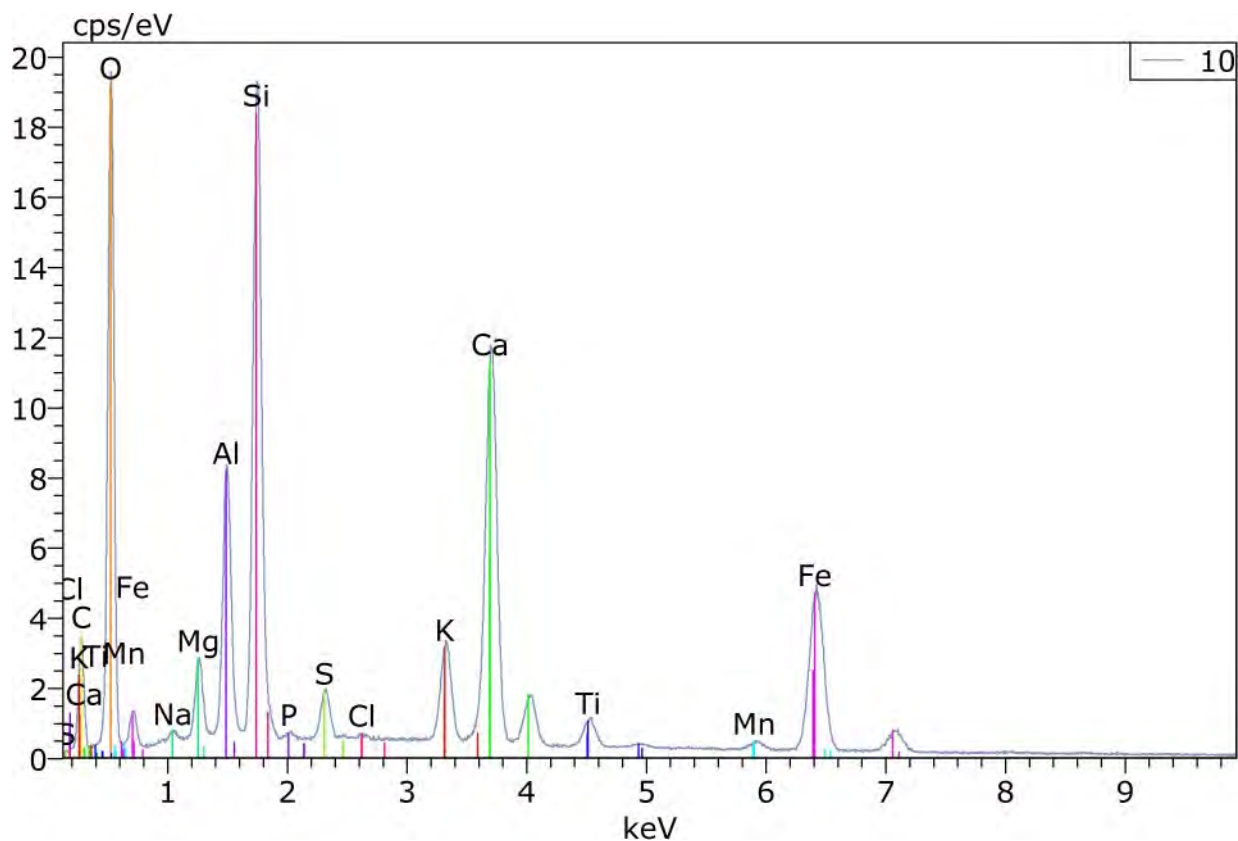
Spectrum: 8

El	AN	Series	unn. C [wt.%]	norm. C [wt.%]	Atom. C [at.%]	Error	(1 Sigma) [wt.%]
C	6	K-series	11.15	11.02	18.84		1.39
O	8	K-series	42.58	42.09	54.03		4.64
Na	11	K-series	0.44	0.44	0.39		0.06
Mg	12	K-series	3.17	3.13	2.65		0.20
Al	13	K-series	5.44	5.37	4.09		0.29
Si	14	K-series	11.00	10.87	7.95		0.49
S	16	K-series	0.49	0.49	0.31		0.04
K	19	K-series	3.85	3.81	2.00		0.14
Ca	20	K-series	8.86	8.76	4.49		0.28
Ti	22	K-series	1.45	1.43	0.61		0.07
Mn	25	K-series	0.52	0.52	0.19		0.04
Fe	26	K-series	12.22	12.08	4.44		0.35
Total:			101.17	100.00	100.00		



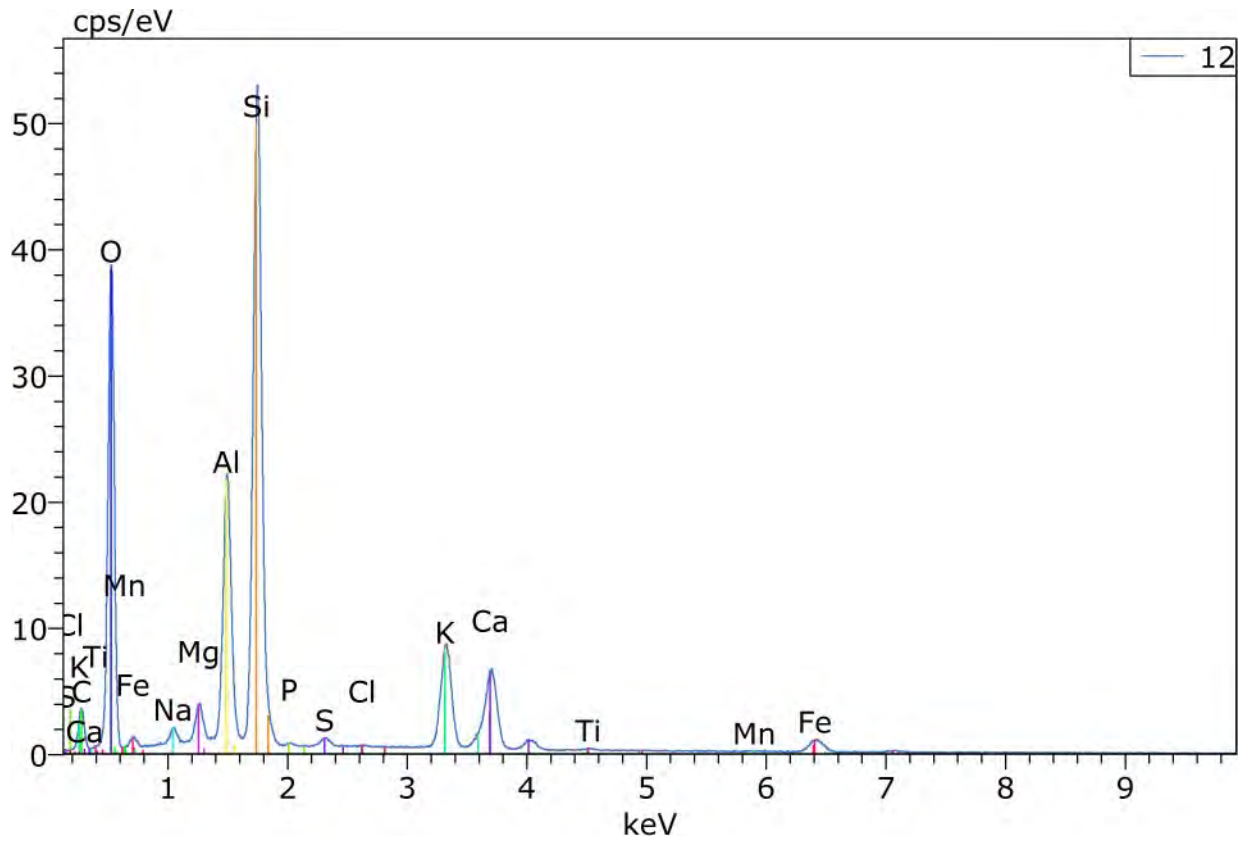
Spectrum: 9

El	AN	Series	unn. C [wt.%]	norm. C [wt.%]	Atom. C [at.%]	Error	(1 Sigma) [wt.%]
C	6	K-series	11.65	10.99	17.56		1.47
O	8	K-series	55.00	51.90	62.22		5.97
Na	11	K-series	0.34	0.32	0.27		0.05
Mg	12	K-series	3.14	2.96	2.34		0.20
Al	13	K-series	3.92	3.69	2.63		0.21
Si	14	K-series	7.79	7.35	5.02		0.36
P	15	K-series	0.11	0.10	0.06		0.03
S	16	K-series	0.75	0.71	0.42		0.05
K	19	K-series	1.52	1.43	0.70		0.07
Ca	20	K-series	13.24	12.49	5.98		0.41
Ti	22	K-series	0.76	0.72	0.29		0.05
Mn	25	K-series	0.40	0.38	0.13		0.04
Fe	26	K-series	7.18	6.77	2.33		0.22
Cu	29	K-series	0.19	0.18	0.05		0.03
Total:			105.99	100.00	100.00		



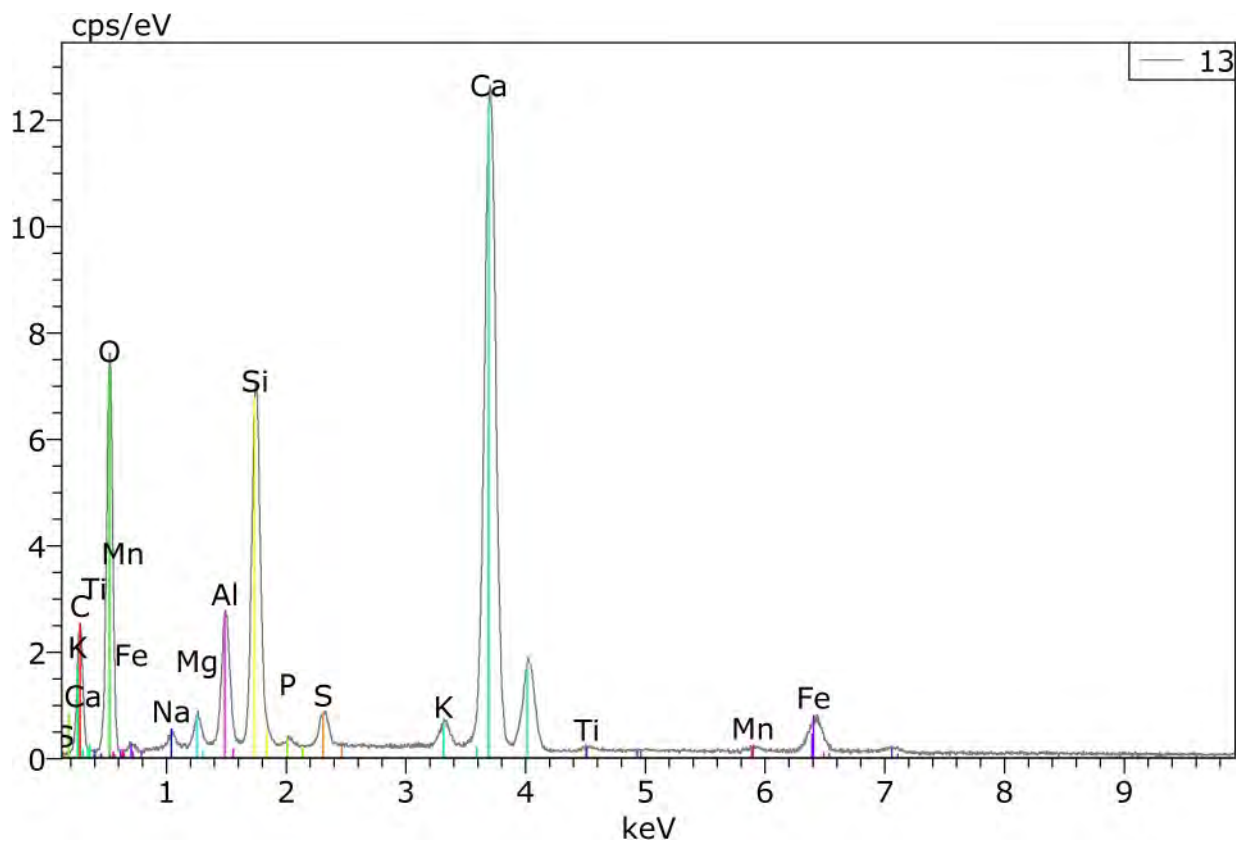
Spectrum: 10

El	AN	Series	unn. C [wt.%]	norm. C [wt.%]	Atom. C [at.%]	Error	(1 Sigma) [wt.%]
C	6	K-series	12.45	11.81	19.68		1.59
O	8	K-series	47.27	44.84	56.10		5.22
Na	11	K-series	0.51	0.48	0.42		0.06
Mg	12	K-series	1.88	1.79	1.47		0.13
Al	13	K-series	5.29	5.02	3.72		0.28
Si	14	K-series	10.44	9.90	7.06		0.47
P	15	K-series	0.12	0.11	0.07		0.03
S	16	K-series	0.95	0.90	0.56		0.06
Cl	17	K-series	0.08	0.08	0.04		0.03
K	19	K-series	2.15	2.04	1.04		0.09
Ca	20	K-series	11.20	10.63	5.31		0.35
Ti	22	K-series	1.08	1.02	0.43		0.06
Mn	25	K-series	0.67	0.64	0.23		0.05
Fe	26	K-series	11.34	10.75	3.86		0.33
Total:			105.41	100.00	100.00		



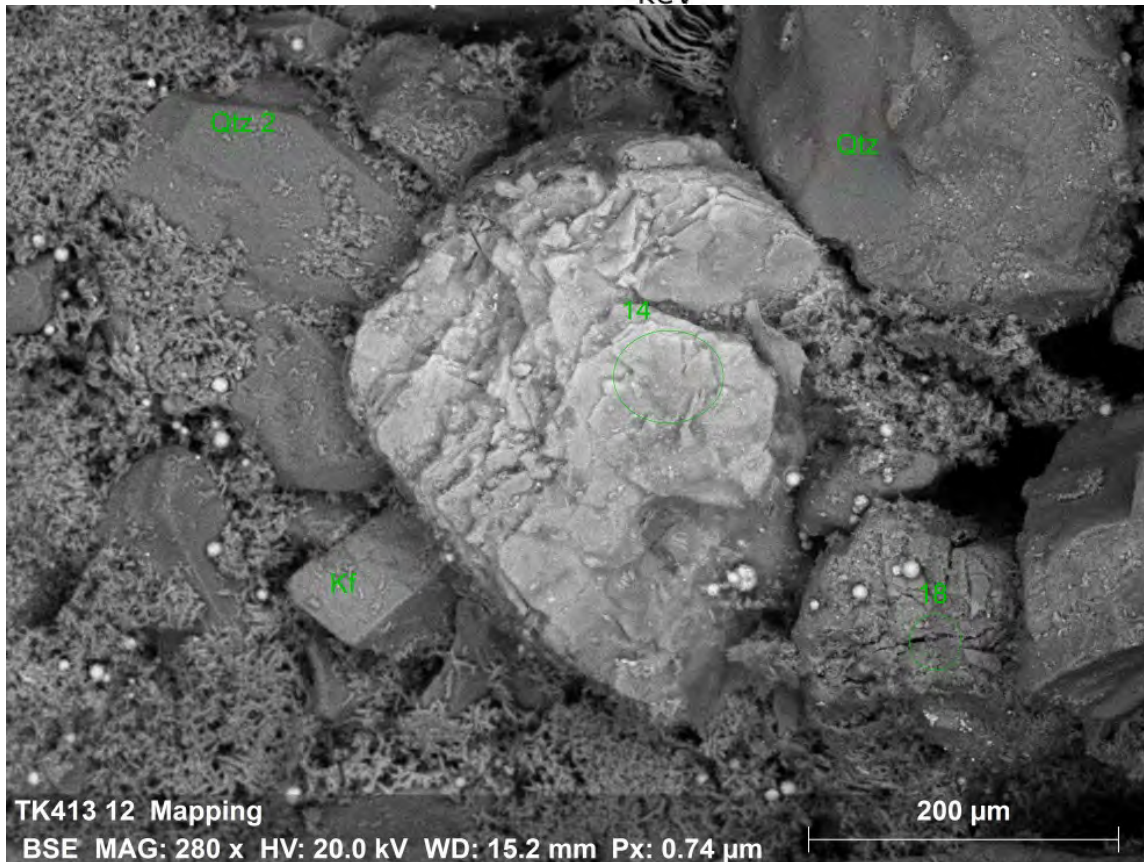
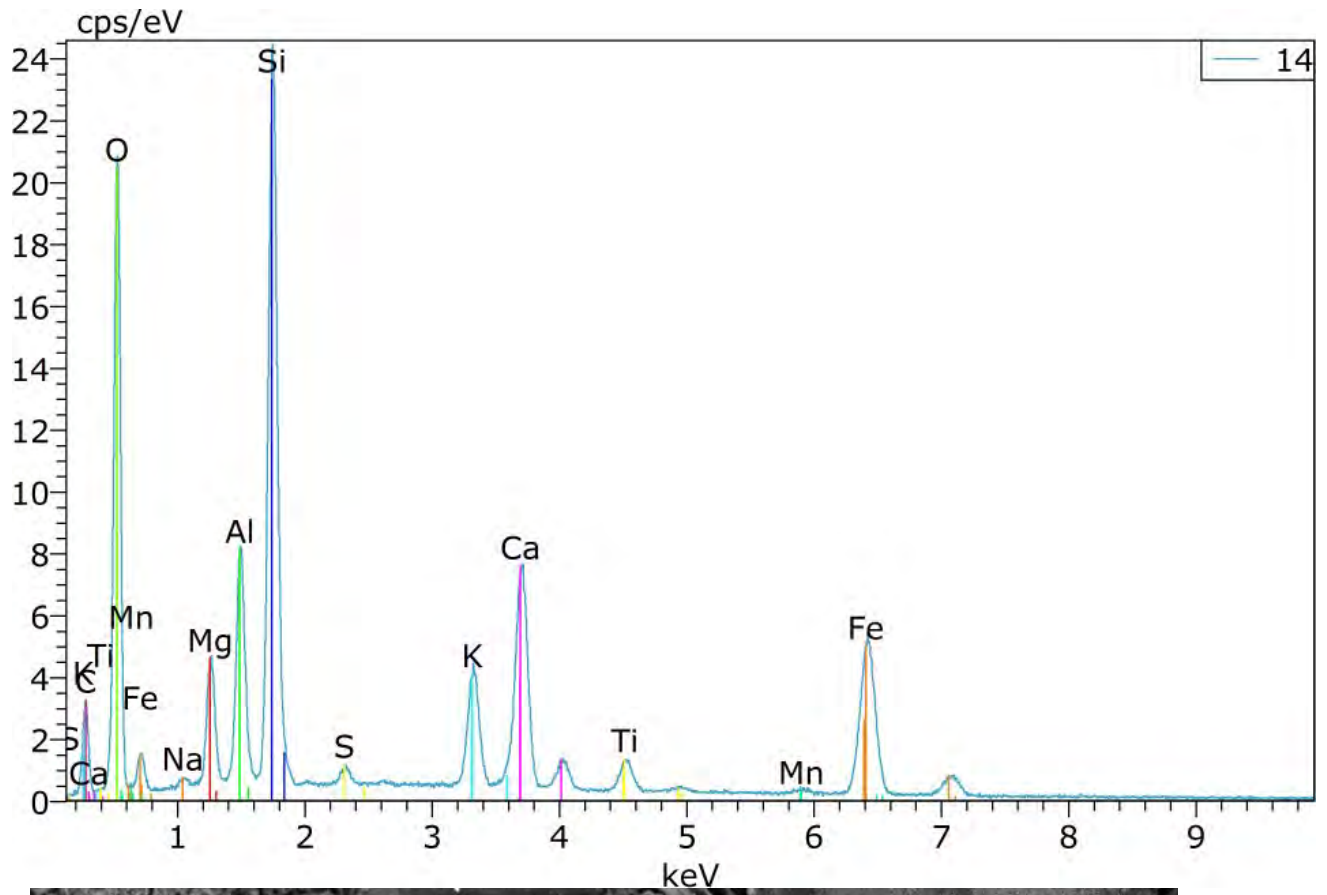
Spectrum: 12

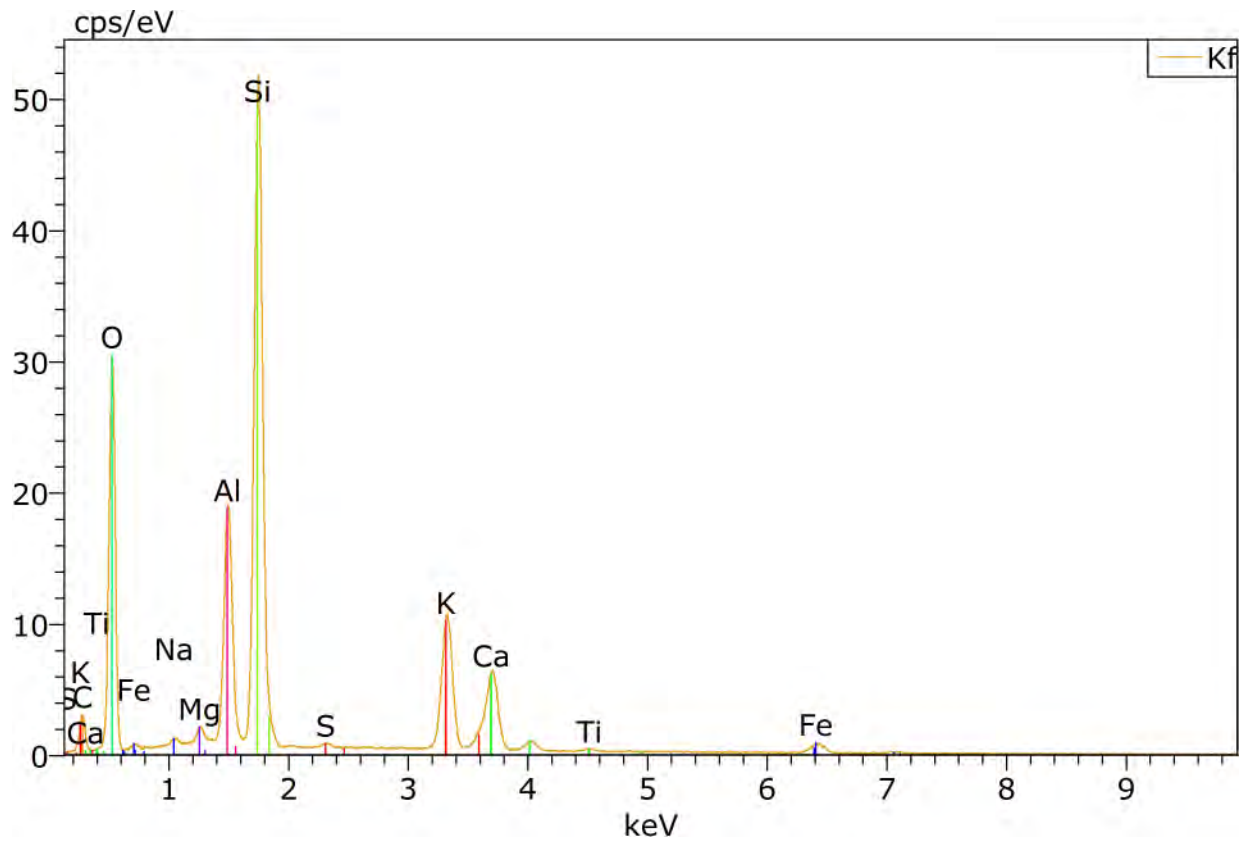
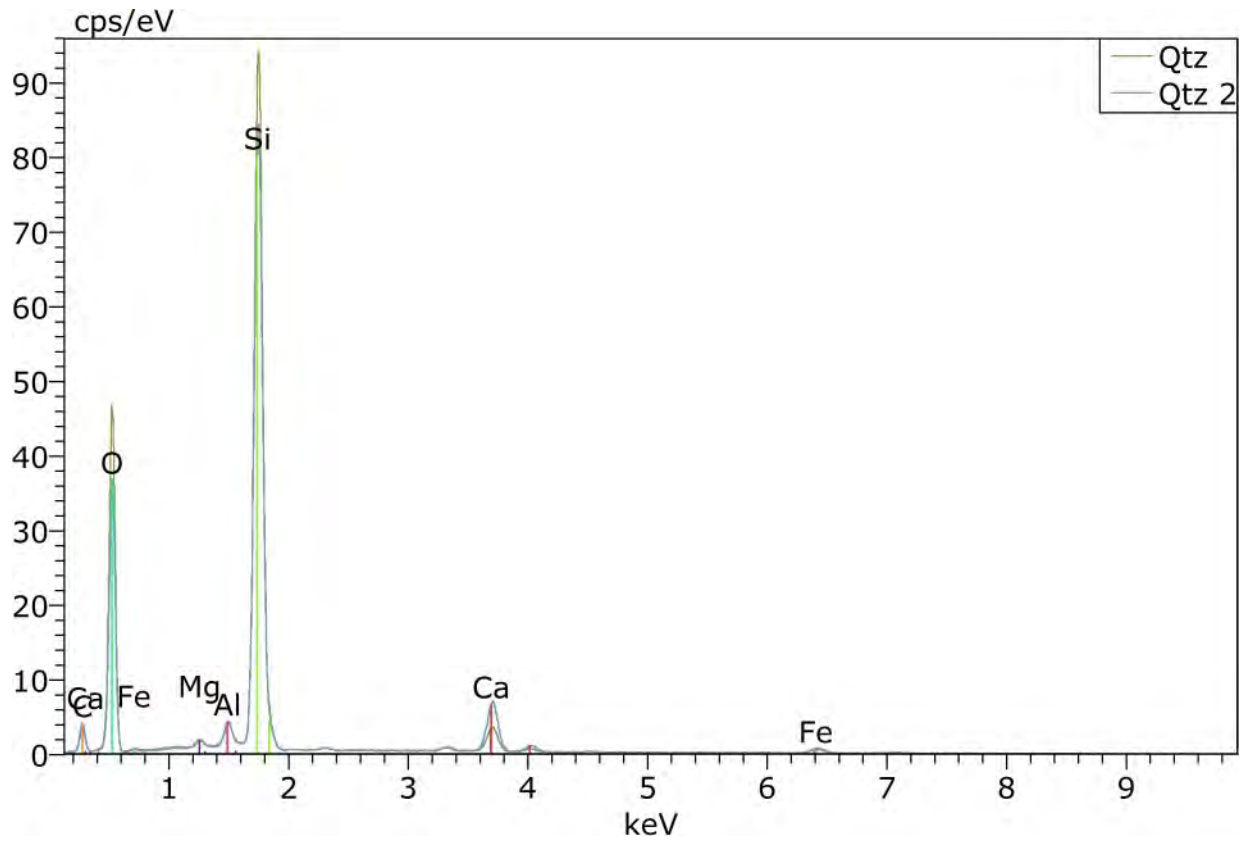
El	AN	Series	unn. C [wt.%]	norm. C [wt.%]	Atom. C [at.%]	Error	(1 Sigma) [wt.%]
C	6	K-series	11.98	9.83	15.34		1.63
O	8	K-series	63.48	52.07	61.03		6.95
Na	11	K-series	1.22	1.00	0.81		0.11
Mg	12	K-series	1.76	1.45	1.12		0.12
Al	13	K-series	9.56	7.84	5.45		0.48
Si	14	K-series	20.45	16.77	11.20		0.90
P	15	K-series	0.13	0.11	0.07		0.03
S	16	K-series	0.34	0.28	0.16		0.04
Cl	17	K-series	0.05	0.04	0.02		0.03
K	19	K-series	5.48	4.49	2.16		0.19
Ca	20	K-series	5.37	4.41	2.06		0.18
Ti	22	K-series	0.12	0.10	0.04		0.03
Mn	25	K-series	0.03	0.03	0.01		0.03
Fe	26	K-series	1.95	1.60	0.54		0.08
Total:			121.92	100.00	100.00		

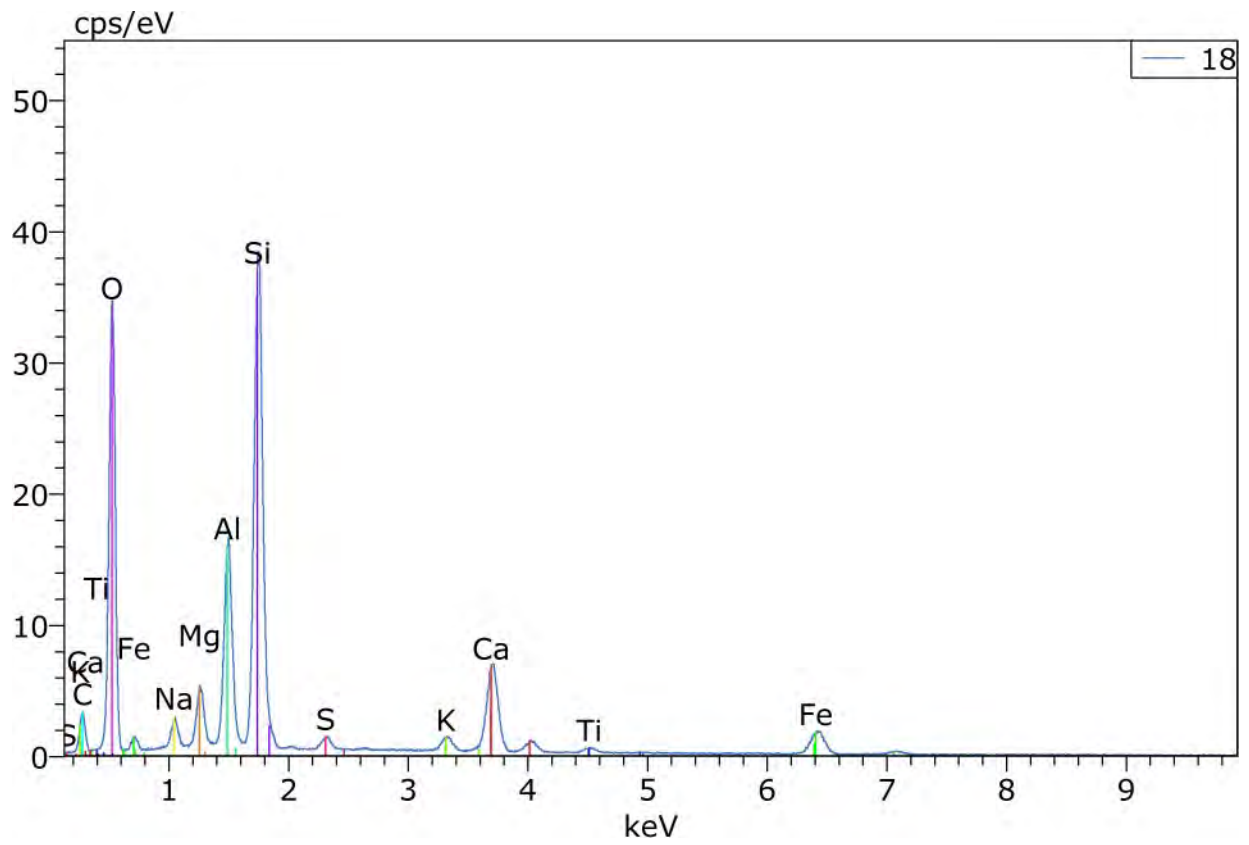


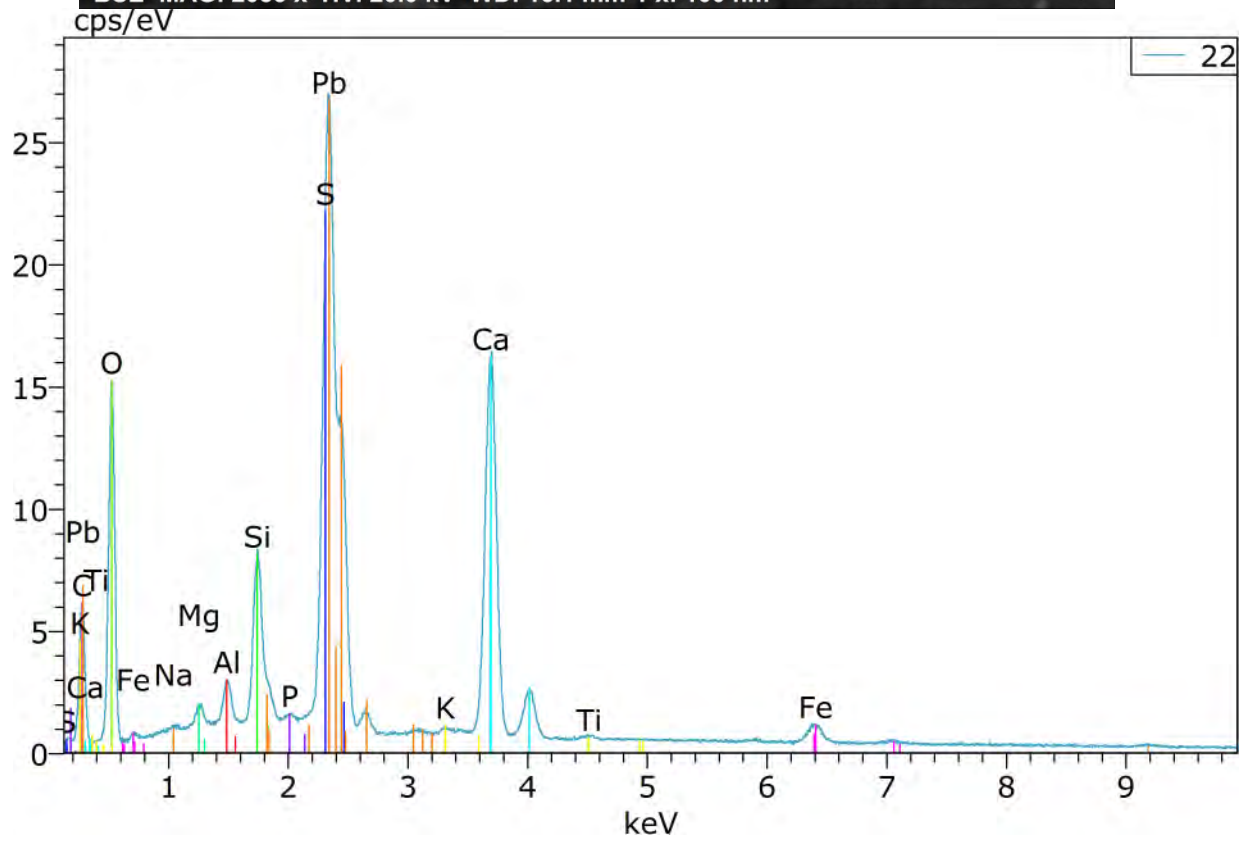
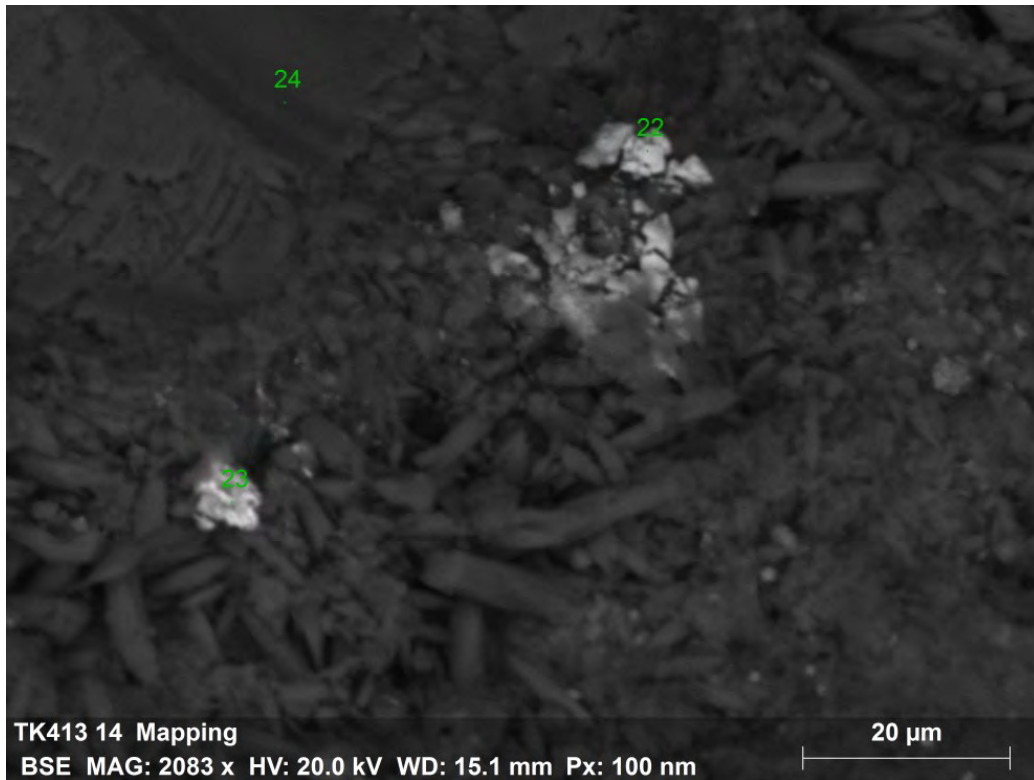
Spectrum: 13

El	AN	Series	unn. C [wt.%]	norm. C [wt.%]	Atom. C [at.%]	Error	(1 Sigma) [wt.%]
C	6	K-series	16.94	14.31	22.85		2.39
O	8	K-series	54.98	46.46	55.69		6.67
Na	11	K-series	0.91	0.77	0.64		0.09
Mg	12	K-series	1.12	0.95	0.75		0.09
Al	13	K-series	4.03	3.40	2.42		0.22
Si	14	K-series	8.78	7.42	5.07		0.40
P	15	K-series	0.21	0.18	0.11		0.04
S	16	K-series	1.04	0.88	0.52		0.07
K	19	K-series	0.64	0.54	0.27		0.05
Ca	20	K-series	26.85	22.69	10.86		0.81
Ti	22	K-series	0.17	0.14	0.06		0.03
Mn	25	K-series	0.32	0.27	0.09		0.04
Fe	26	K-series	2.36	2.00	0.69		0.09
Total:			118.35	100.00	100.00		



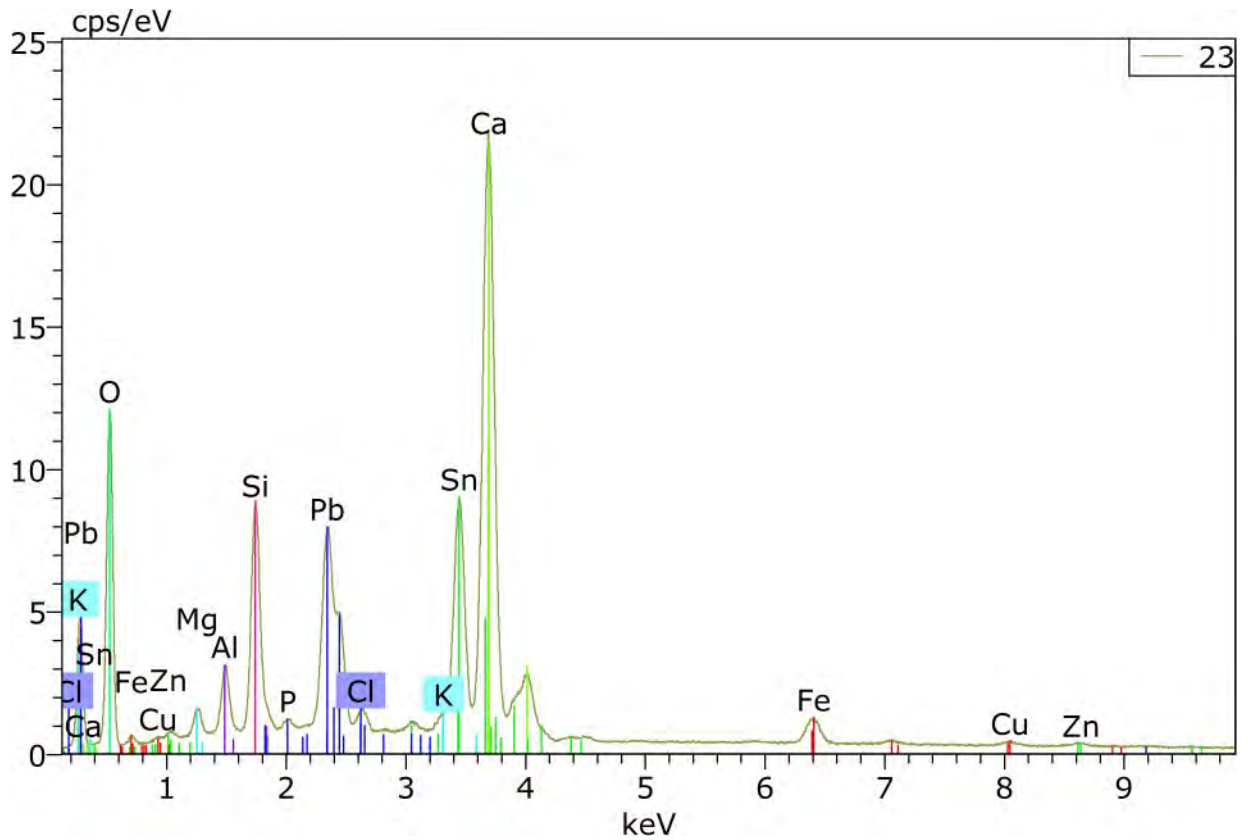






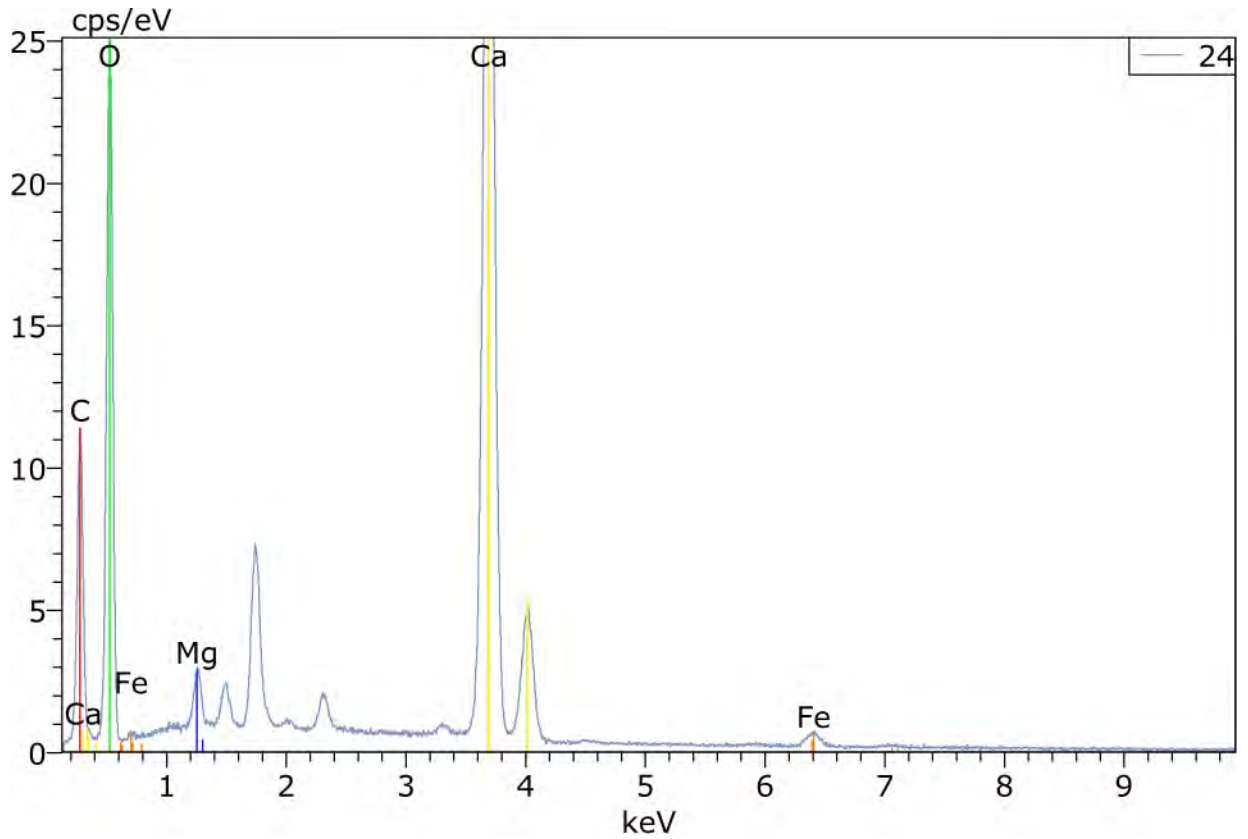
Spectrum: 22

El	AN	Series	unn. C [wt.%]	norm. C [wt.%]	Atom. C [at.%]	Error	(1 Sigma) [wt.%]
C	6	K-series	9.66	10.79	23.73		1.23
O	8	K-series	28.35	31.64	52.26		3.25
Na	11	K-series	0.05	0.05	0.06		0.03
Mg	12	K-series	0.31	0.34	0.37		0.04
Al	13	K-series	0.59	0.66	0.64		0.05
Si	14	K-series	2.24	2.50	2.35		0.12
P	15	K-series	0.05	0.06	0.05		0.03
S	16	K-series	4.07	4.54	3.74		0.17
K	19	K-series	0.26	0.29	0.19		0.03
Ca	20	K-series	16.21	18.10	11.93		0.50
Ti	22	K-series	0.16	0.18	0.10		0.03
Fe	26	K-series	1.62	1.80	0.85		0.07
Pb	82	L-series	26.03	29.06	3.71		0.82
Total:			89.59	100.00	100.00		



Spectrum: 23

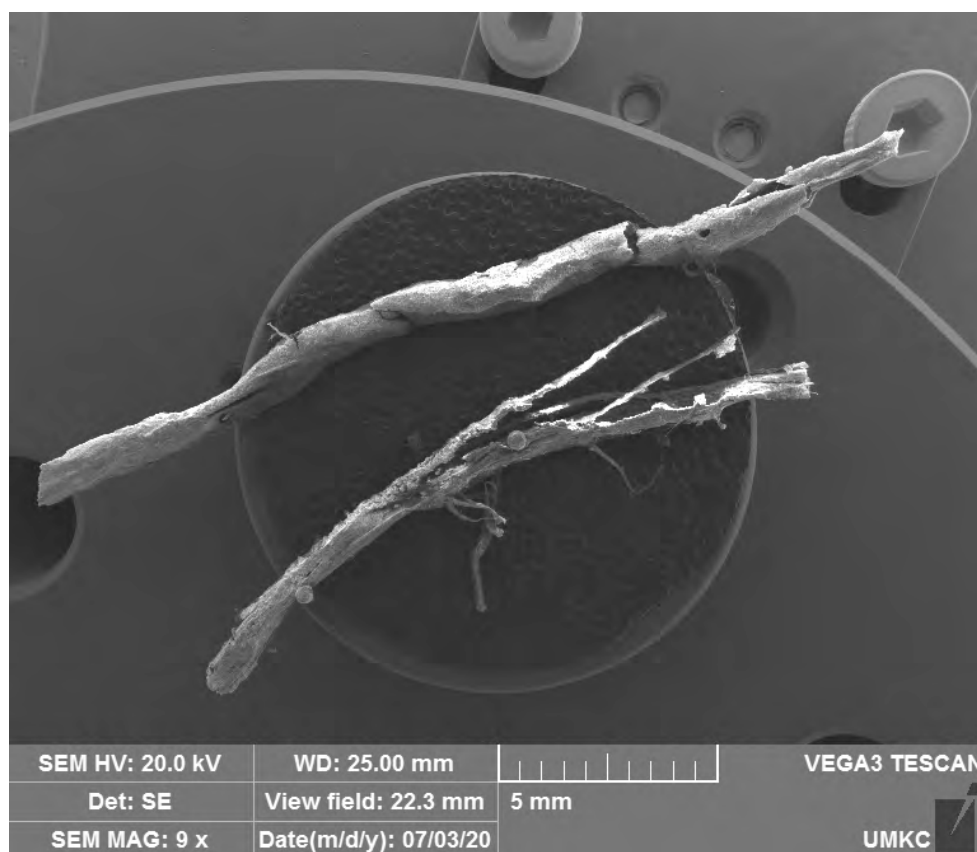
El	AN	Series	unn. C [wt.%]	norm. C [wt.%]	Atom. C [at.%]	Error (1 Sigma) [wt.%]
C	6	K-series	10.19	9.78	21.41	1.23
O	8	K-series	33.42	32.08	52.71	3.71
Mg	12	K-series	0.75	0.72	0.78	0.07
Al	13	K-series	1.54	1.48	1.44	0.10
Si	14	K-series	4.72	4.53	4.24	0.23
P	15	K-series	0.21	0.20	0.17	0.03
Cl	17	K-series	0.34	0.33	0.24	0.04
K	19	K-series	0.54	0.52	0.35	0.04
Ca	20	K-series	19.05	18.29	12.00	0.58
Fe	26	K-series	2.03	1.95	0.92	0.08
Cu	29	K-series	0.44	0.42	0.17	0.04
Zn	30	K-series	0.33	0.32	0.13	0.04
Sn	50	L-series	18.92	18.16	4.02	0.58
Pb	82	L-series	11.71	11.24	1.43	0.38
Total:			104.18	100.00	100.00	



Spectrum: 24

El	AN	Series	unn. C [wt.%]	norm. C [wt.%]	Atom. C [at.%]	Error	(1 Sigma) [wt.%]
C	6	K-series	18.54	15.23	22.92		2.35
O	8	K-series	69.54	57.14	64.53		8.06
Mg	12	K-series	0.88	0.72	0.54		0.08
Ca	20	K-series	31.66	26.02	11.73		0.95
Fe	26	K-series	1.08	0.89	0.29		0.06
Total:			121.70	100.00	100.00		

Rootlets AO-2, Unit 6



VITA

After a career in finance which took her from Little Rock, Arkansas to Dallas, Texas, New York City, Washington DC, and finally to Kansas City Janet Smith changed her career path. After leaving the brokerage industry, Janet spent a few years in radio as a producer and on-air talent at a local radio station. Then after her second child was born, she became a stay-at-home mom for several years before deciding to go back to school to earn her second bachelor's degree.

She began her degree pursuit at the University of Missouri – Kansas City in the summer of 2012 and graduated in the summer of 2015 with a B.S. in Geology. As an undergraduate at UMKC, she was active in Geology Club. She received scholarships and an undergraduate research grant. She traveled Jordan and the Bahamas to assist in fieldwork for graduate research for UMKC students. Janet analyzed clay minerals and geochronology from the cosmogenic nuclide Beryllium-10 of a sediment core taken from the Al-Jafr basin in Jordan. She presented posters at the American Association of Geographers' (AAG) annual meeting and at the Geological Society of America's (GSA) annual meeting. Janet also gave a talk at the AAG annual meeting on her research the following year.

She began her master's studies in the fall of 2015. Janet taught Environmental Science lab for four semesters. She is a student member of the Geological Society of America and Sigma Xi. Janet is married to Douglas Smith, a public defender for the state of Missouri and they have three children.